



**Environmental and Material Controls on  
Desiccation Cracking in Engineered Clay  
Embankments**

**Oboho Okon Eminue**

**A thesis submitted for the degree of Doctor of Philosophy**

**School of Civil Engineering and Geosciences**

**Newcastle University**

**January 2018**



## **Abstract**

Desiccation cracking is a natural phenomenon commonly associated with drying of expansive soils. The role of cracks in surface permeability increase and overall deterioration of infrastructure slopes makes it a key factor in climate-related slope instability processes. Despite this significance, the controls on soil cracking in engineered slopes still represent a poorly understood area. In this study, soil cracking behaviour in clay embankments exposed to cyclic wetting and drying was investigated to improve understanding of this phenomenon for application in geotechnical practice. A complimentary field and laboratory study was undertaken, approaches commonly conducted in isolation in the literature. The field program involved direct investigation of natural crack development in a heavily instrumented, clay embankment (BIONICS, Newcastle University). Crack morphology parameters were quantified under engineering, meteorological and near surface soil hydrological conditions to understand how temporal change influences these. Laboratory experimentation was carried out on materials representative of typical embankment fills and construction methods in the UK in a bespoke climate control system. Time series photographs of the crack networks were analysed using image processing technique to compare their intensities across the experimental conditions.

Syntheses of field and laboratory results show the influence of factors related to the embankment geometry (i.e. slope aspect, layer thickness), material properties (i.e. soil density and plasticity) and environmental condition (i.e. wetting and drying cycles) on the cracking behaviour in engineered clay slopes. The sensitivity of cracking intensity under given climate conditions critically relates to the rate of moisture loss and the material strength. Overall, this research presents how newly gained understanding of cracking can potentially impact upon improved construction techniques of engineered clay embankments and the susceptibility of historic embankments constructed to lower densities to climatic changes, including how drying/wetting cycles can exacerbate crack development.

## **Dedication**

To my dear wife, Mabel

And

My gifted children: Excel, Edwardo, Stesha and Jeff.

## **Acknowledgements**

My PhD work was a worthwhile undertaking. I got to the pinnacle of it seemingly alone, but undoubtedly with support and collaboration of esteemed individuals. Through the love of my Lord Jesus Christ, I use this page to acknowledge all who contributed to bringing this work to great success.

My special gratitude and deepest respect go to my first supervisor, Dr Colin Davie. From the conception until completion, you zealously assisted in engineering the context and content of this work to its best academic and professional form. Your apt guidance and generous support provided tremendous enthusiasm throughout the mission. I learned a lot from your conscientious working style which in my career would be amplified. My much deserved thanks go to my second supervisor, Dr Ross Stirling. I sincerely appreciate your proactive discussions and many fruitful comments that have substantially helped to improve the research value of this work. Quite an accomplished scholar, I am indeed privileged to work with you. I also extend my appreciation to Dr Paul Hughes who was part of the supervisory team at the early stage. Paul introduced me to important aspects of the current research and gave useful advice on time management. Not forgetting Professor Esu Esu who encouraged me to undertake my PhD study in the UK.

Many thanks to the staff of Geotechnical laboratory, CEG admin and IT and my fellow researchers in the GEST group. A big thank you to Akwa Ibom State University, TETFUND and the ever-loving Eminue family for their different financial support.

Finally, my endless thanks go to my Wife, Barr (Mrs) Mabel Eminue, for warmly being beside me while I toiled the years. Your unfeigned belief in me gave me the courage to go through it all excitingly. And to my lovely kids, thanks for enduring thousands of hours without Daddy's full attention. I share the crown with you guys.



## Table of Contents

Abstract.....	iii
Dedication.....	iv
Acknowledgement.....	v
Table of Contents.....	vii
List of Figures .....	xiii
List of Table .....	xxiv
Chapter 1 General Introduction .....	1
1.1 Background .....	1
1.2 The Problem: Failures of infrastructure embankments.....	1
1.2.1 Climate and the processes of deterioration in infrastructure slopes.....	4
1.3 Project definition.....	9
1.3.1 Aim .....	9
1.3.2 Objectives.....	9
1.4 Applications .....	10
1.5 Thesis structure.....	10
Chapter 2 Literature review .....	12
2.1 Introduction.....	12
2.2 Causes and types of soil cracking .....	12
2.2.1 Characteristics of desiccation cracking in soil .....	14
2.2.2 Significance of soil cracking .....	22
2.3 Theory of desiccation cracking.....	23
2.3.1 Drying and Shrinkage Phenomena in unsaturated soil.....	24
2.3.2 Shrinkage cracking.....	30
2.3.3 Air entry value and crack initiation: Soil water retention curve..	33
2.3.4 Fracture theory and crack propagation in soil.....	36
2.3.5 Field and laboratory methods in the study of desiccation cracks .....	39

2.3.6	Influencing factors in desiccation cracking of soil .....	42
2.3.7	Quantification of cracking in soil .....	53
2.4	Clay soils and performance of clay earth slopes .....	57
2.4.1	Clay mineralogy .....	57
2.4.2	Structure and Fabric of clay soil.....	60
2.4.3	Clay fills and construction of infrastructure embankment.....	61
2.4.4	Performance of clay embankments in the UK.....	63
2.4.5	Volume change analysis and effects of cracking in drying soil	66
2.4.6	Role of desiccation cracks in pore water pressure response in soil .....	69
2.4.7	Methods of analysis of slopes with cracks .....	70
2.4.8	Influence of vegetation on clay slope deformation .....	74
2.4.9	Estimation of soil evapotranspiration .....	77
2.4.10	Estimation of suction developed in unsaturated soil .....	80
2.4.11	Soil water retention curve .....	81
2.5	Research gaps.....	84
2.6	Summary and Conclusion.....	85
Chapter 3	Methodology.....	87
3.1	Introduction.....	87
3.2	Field procedures .....	87
3.2.1	The BIONICS experimental embankment.....	88
3.2.2	Crack Survey .....	94
3.2.3	Method to measure cracks .....	96
3.2.4	Method of estimation of volume of a crack section .....	97
3.2.5	Measurement of soil moisture and suction changes in the field .....	101
3.2.6	Evaluation of climatic parameters .....	102
3.2.7	Influence of vegetation on soil cracking .....	103
3.2.8	Summary of field study .....	103

3.3	Methodological development for laboratory testing .....	104
3.3.1	Design and construction of soil mould .....	105
3.3.2	Design of climate control unit .....	107
3.3.3	Instrumentation and measurements .....	109
3.3.4	Validation of laboratory experimental system .....	112
3.4	Soil Materials.....	113
3.4.1	Material preparation and testing .....	114
3.4.2	Simulation of a very high plasticity clay material .....	114
3.4.3	Materials Property .....	117
3.4.4	Sample preparation for desiccation experiment .....	118
3.4.5	Compaction of soil for desiccation experiment .....	119
3.4.6	Method for estimation of soil suction in desiccated soil .....	120
3.4.7	Method for crack image analysis .....	124
3.4.8	Three-dimensional crack model .....	125
3.4.9	Control variables and laboratory testing programs .....	126
3.5	Summary on laboratory methodology and testing .....	127
3.6	Conclusion on study approach and methodology .....	128
Chapter 4	Hydrology characteristics of desiccation cracking in soil.....	129
4.1	Introduction.....	129
4.2	Moisture characteristics and suction development on clay embankment .....	129
4.2.1	Moisture profiles in engineered clay fills .....	133
4.2.2	Development of soil suction in drying dense soil .....	140
4.2.3	Cyclical characteristics of soil moisture and suction.....	146
4.3	Hydrodynamic controls in desiccation cracking of soil.....	147
4.3.1	Occurrence and distribution of cracks in the embankment.....	148
4.3.2	Crack morphological development .....	151
4.3.3	Characterisation of cracking with changes in near surface soil moisture.....	158

4.3.4	Significance of volume of crack in slopes water regime.....	161
4.4	Quantifying crack intensity in drying soil .....	162
4.4.1	Moisture changes in initial stage of crack development.....	168
4.4.2	Moisture changes in active stage of crack development.....	170
4.4.3	Moisture changes in steady stage of crack development .....	171
4.4.4	Critical cracking moisture and suction in soil .....	175
4.4.5	Properties of cracks under cyclic moisture behaviour in soil..	179
4.4.6	Rate of desiccation and residual moisture .....	187
4.5	Summary and conclusion .....	190
Chapter 5	Role of material properties in desiccation crack behavior ..	194
5.1	Introduction.....	194
5.2	Influence of plasticity on desiccation behavior of compacted soils	195
5.2.1	The role of plasticity in soil-water retention during desiccation	200
5.2.2	Suction development in drying plastic soils .....	201
5.3	Desiccation cracking behavior of compacted plastic soils .....	204
5.3.1	Comparison of cracking moisture and suction in three plastic	205
5.3.2	Crack intensity in the compacted plastic soils.....	206
5.3.3	Assessment of the potential of soil cracking across the UK... 210	
5.4	Factors influencing crack propagation and formation of network	211
5.4.1	Moisture changes and crack propagation in soil.....	212
5.4.2	Soil texture and desiccation cracks network characteristics ..	217
5.4.3	Influence of vegetation in crack network formation .....	221
5.4.4	Mechanisms of crack intersection and orientation in soil	228
5.4.5	Effect of wetting and drying cycle on cracks outline.....	234

5.4.6	Cross-section of cracks .....	239
5.4.7	Surface processes and the modification of cracks geometry..	240
5.4.8	Relationship between crack geometry properties.....	244
5.5	Summary.....	248
5.6	Conclusion.....	251
Chapter 6	General summary, conclusions and recommendations .....	252
6.1	Introduction.....	252
6.1.1	Research approach and methods of analysis.....	252
6.2	Hydromechanical response in engineered clay embankment ...	253
6.2.1	Moisture behaviour in engineered clay embankment .....	253
6.2.2	Suction profiles in the near surface clay layer .....	255
6.2.3	Desiccation cracking and hydrologic changes in clay embankment.....	256
6.3	Influencing factors of cracking in engineered clay embankment	257
6.3.1	Influence of soil density .....	257
6.3.2	Effect of embankment geometry.....	258
6.3.3	Effect of soil plasticity .....	259
6.3.4	Role of vegetation in cracking of clay embankment .....	260
6.3.5	Crack intensity under cyclic wetting and drying .....	261
6.4	Mechanisms of cracks orientation and modification .....	261
6.4.1	Influence of soil texture.....	261
6.4.2	Surface processes and crack morphology changes in a grass covered embankment.....	262
6.5	Conclusions.....	262
6.5.1	Soil moisture movement and crack development .....	263
6.5.2	Factors affecting intensity of cracking in engineered clay slope .....	263
6.6	Recommendations for further study .....	265
References.....		266

Appendix ..... 287

## List of Figures

Figure 1.1: The problem: Different events and magnitude of earth slope failures affecting railways and highways transport corridor in the UK (photo a, b & c from ICE archives/Network rail; d & e from Briggs <i>et al.</i> (2016); from Electrokinetic Ltd, Newcastle University).....	2
Figure 1.2: Rainfall and landslide data for the UK between 2012 and 2017 (British Geological Survey report, February 2017).....	6
Figure 1.3: Earthworks failures by type and year (adapted from Wilks, 2015) .....	8
Figure 2.1: (a) Orthogonal crack pattern (b) Hexagonal crack pattern (adapted from Kodikara <i>et al.</i> , 2000) .....	14
Figure 2.2: Stress distribution and crack intersection (from Walker, 1986) .....	15
Figure 2.3: Crack Spacing. $S_0$ is the mean spacing between primary cracks at the soil surface, and $h$ is the depth of the primary crack (Chertkov, 2000).....	16
Figure 2.4: Approximation of a crack dimensions (Li and Zhang, 2010)...	18
Figure 2.5: Vertical cross-section through a crack, showing the triangular, square root and rectangular shapes (adapted from Ringrose-Voase and Sanidad (1996) .....	19
Figure 2.6: Capillary phenomena in drying soil. Adapted from Holtz and Kovacs (1981) and Péron <i>et al.</i> (2009b).....	25
Figure 2.7: Drying shrinkage and tensile stress development in expansive soil from (Laloui and Nuth, 2009).....	25
Figure 2.8: Interaction between the components of unsaturated soil .....	27
Figure 2.9: Typical shrinkage curve for clay soils (Tang <i>et al.</i> , 2011a).....	28
Figure 2.10: Soil hydro-structure during shrinkage (from Bensallam <i>et al.</i> (2012)).....	29

Figure 2.11: Shrinking clay bars (Left) Fixed at both ends, (Right) Fixed at one end. From Towner 1987.....	31
Figure 2.12: Idealised tensile failure in soil (from Kodikara and Choi 2006) .....	32
Figure 2.13: Crack initiation near Air entry value at saturation (from Peron <i>et al.</i> , 2009b).....	33
Figure 2.14: Air-water interface in porous media (a) drainage during drying processes and (b) advancing drying front. From (Fredlund and Rahardjo, 1993) and (Péron <i>et al.</i> , 2009a) .....	34
Figure 2.15: Schematic drawing of soil crack initiation process under saturation (a) Initial fully saturated soil; (b) water–air interface meniscus developed between soil particles; (c) capillary suction between soil particles; (d) tensile stress developed in the upper layer; and surface crack initiated (from Tang <i>et al.</i> 2013).....	35
Figure 2.16: Combine influence of stress and flaws in crack initiation (from Costa <i>et al.</i> , 2013). .....	36
Figure 2.17: Crack in an infinite plate subject to a remote tensile stress. “infinite” practically means the width of the plate is $\gg 2a$ . From (Anderson and Anderson, 2005) .....	37
Figure 2.18: Stresses near the tip of a crack in an elastic material. (Anderson and Anderson, 2005).....	38
Figure 2.19: Fracture failure modes. From Pook (2007) .....	39
Figure 2.20: Bespoke soil tensile strength test apparatus (from Stirling 2014).....	43
Figure 2.21: Desiccation Box/Tensile load device. From Varsei <i>et al.</i> (2014) .....	44
Figure 2.22: Schematic of the effect of soil structures on cracking patterns. (a) Flocculated structure, and (b) Dispersed structure (from Fang and Daniels, 2006).....	46

Figure 2.23: Changes in water content with time under different temperatures (from Tang <i>et al.</i> , 2010) .....	48
Figure 2.24: Stages of evaporation during soil desiccation (a) Slurry soil (b) Compacted soil (from Tang <i>et al.</i> 2011, Nalhawi and Kodikara, 2006)	49
Figure 2.25: Profiles of desiccation in soils; cracking water content indicated by vertical arrows (from Kodikara <i>et al.</i> 2000) .....	49
Figure 2.26: Homogenous to aggregated structure (Left to right) and volume change in a soil after 3 wet-dry cycles. From (Tang <i>et al.</i> , 2016).	52
Figure 2.27: Digital image processing procedure. (a) Initial grey level image, (b) binary black and white image, and (c) skeleton of crack network (from Tang <i>et al.</i> , 2008) .....	55
Figure 2.28: Experimental cracking results (a) CIF and (b) LF as functions of time From Miller <i>et al.</i> (1998) and Trabelsi <i>et al.</i> (2012) .....	56
Figure 2.29: Particle size of sand, silt and clay .....	58
Figure 2.30: Structure of the main clay minerals: (a) kaolinite, (b) illites and (c) montmorillonite, based on combined sheets (Knappett and Craig, 2012) .....	59
Figure 2.31: Shrink–swell potential map of UK (Jones and Jefferson, 2012) .....	62
Figure 2.32: Modern highway embankment (Left) compared with historic rail embankment (Right). From Loveridge <i>et al.</i> (2010). .....	63
Figure 2.33: Schematic diagram of 3-D shrink-swell in soil (the dashed line express the sample in saturated state, while the continuous line express the sample after shrinkage – adapted from Bronswijk, 1990) .....	67
Figure 2.34: Model of rainwater infiltration in a crack soil (from Stirling, 2014) .....	69
Figure 2.35: Finite element mesh of a slope with crack at the crest (from Wang <i>et al.</i> 2011) .....	71

Figure 2.36 : 2D illustration of method of slices in traditional limit equilibrium analysis of slope stability (slip surface = AB).....	72
Figure 2.37: Composite slices with crack at the top of the slope. The crack reduced the slip surface from AB to AB' (adapted from Smith and Smith, 1989).....	72
Figure 2.38: Sketch of regions where cracks do and do not affect slope stability (from Utili, 2013) .....	73
Figure 2.39: Illustration of the effect of wind speed, temperature and humidity on evapotranspiration (from Allen <i>et al.</i> , 1998).....	78
Figure 2.40: Drying curve with a definition of variables for a SWRC (from Fredlund, 2011). .....	82
Figure 2.41: Comparison of suctions obtained from drying moisture paths in soil (from Fredlund <i>et al.</i> , 2011) .....	83
Figure 3.1: Layout and part of physical structure of the embankment. adapted from (Hughes <i>et al.</i> , 2009; Toll <i>et al.</i> , 2012).....	89
Figure 3.2: Some of the monitoring instrument on a section of the embankment.....	92
Figure 3.3: Illustration of instrument plan in the embankment (not to scale) arranged on the lower, middle and upper sections of the slopes .....	93
Figure 3.4: Cross section of embankment showing slope faces and soil probes.....	94
Figure 3.5: Crack survey on Bionics embankment. Crack location marked with red flags.....	95
Figure 3.6: Line gauges and probes for crack geometric measurement ..	97
Figure 3.7: Cross section of a truncated fulcrum (adapted from Holgate, 1901).....	98

Figure 3.8: Geometry of crack section: $w_1$ , $w_2$ are crack width, $d_1$ , $d_2$ are vertical crack depth, $g$ is the gap between the sections (length of crack section), $\iota$ is a hypothetical length of the first pyramid. $V_1$ and $V_2$ are volumes of the first and second pyramid. ....	100
Figure 3.9: Vegetation cover on the embankment (March-September 2014) .....	103
Figure 3.10: Schematic of the experimental system for laboratory desiccation crack experiment .....	105
Figure 3.11: Trial test in the plastic mould .....	106
Figure 3.12: Air conditioning unit.....	108
Figure 3.13: The climate cover fitted with axial fan.....	109
Figure 3.14: Schematic of ML2x Theta probe, actual probe inserts (Miller and Gaskin, 1999) .....	110
Figure 3.15: Laboratory scale soil-atmosphere interaction system.....	112
Figure 3.16: Results of the mix design for material estimate (a) Pre-hydrated, (b) Dry mix .....	115
Figure 3.17: Bentonite-Nafferton clay mixture undergoing drying processes .....	117
Figure 3.18: Dew point potentiometer with soil specimen for measurement of suction .....	121
Figure 3.19: Soil water retention curve for Nafferton Clay.....	123
Figure 3.20: Soil water retention curve for Gault Clay .....	123
Figure 3.21: Automated procedures in the CIAS (from Liu et al., 2013) .	124
Figure 3.22: Crack photo editing (a) painting (b) enhanced grey scale contrast and (c) colour pixels of cracks and clods .....	125
Figure 4.1: Soil temperature with aspect of the BIONICS embankment .	130

Figure 4.2: Wind-rose of the embankment (a) South slope (b) North Slope .....	130
Figure 4.3: Evapotranspiration with aspect of the embankment .....	131
Figure 4.4: Profiles of moisture change with aspect across corresponding sections of the embankment (a) South slope and (b) North Slope.....	132
Figure 4.5: Moisture profiles in well and poorly engineered panels of the BIONICS embankment (a) South slope and (b) North Slope .....	134
Figure 4.6: Moisture loss in a clay soil with different densities.....	135
Figure 4.7: Moisture loss with depth (a) well compacted soil (b) poorly compacted soil.....	137
Figure 4.8: Moisture loss in compacted soils of different thicknesses....	139
Figure 4.9: Profiles of moisture and suction in engineered slope (a) and (b) South slope, (b) and (c) North Slope .....	142
Figure 4.10: SWRC for estimation of soil suctions in drying .....	143
Figure 4.11: Changes in estimated range of suctions in a drying soil ....	144
Figure 4.12: Profiles of moisture and suction with depth in a compacted soil specimen.....	145
Figure 4.13: Relationship between rainfall and hydrology in the embankment.....	147
Figure 4.14: Surface cracks in the embankment and displacement monitor installed in one of the cracks location (d).....	148
Figure 4.15: Illustration of crack distribution in the embankment (May 2014 – February 2016) .....	149
Figure 4.16: Crack Intensity in (a) Low density soil (b) High density soil	150
Figure 4.17: Rainfall intensity of the embankment in 2014 and 2015 ....	152
Figure 4.18: Evapotranspiration on the embankment in 2014 and 2015	153

Figure 4.19: Profiles of crack morphological evolution (a) Well compacted soil (b) Poorly compacted soil.....	154
Figure 4.20: Horizontal ground movement at a crack location in the embankment.....	157
Figure 4.21: (a) Comparison of changes in the volumes of cracks and soil hydrology (b) Distances of cracks 3, 10 and 11 from the soil probe (MPS 2), which recorded the hydrological data in Figure 4.21a. ....	159
Figure 4.22: Photographs of desiccation cracks (a) Well compacted soil Nafferton clay soil (b) Poorly compacted Nafferton clay soil (c) Gault clay soil (d) Bentonite-Nafferton clay soil .....	163
Figure 4.23: Desiccation crack intensity of a clay soil with different compaction quality.....	165
Figure 4.24: Stages of cracking in a drying compacted soil.....	166
Figure 4.25: Profiles of moisture loss in a soil compacted to different densities .....	167
Figure 4.26: Crack intensity with moisture loss in the soil compacted to different densities in the laboratory.....	168
Figure 4.27: Cracking around location of flaws in the soil (top photo) Laboratory (bottom photo) Field .....	169
Figure 4.28: Evaporation characteristics in crack soil (adapted from Li and Zhang, 2011).....	170
Figure 4.29: Laboratory measured suction in compacted soils during crack formation .....	174
Figure 4.30: Effect of total number of cracks on CIF .....	175
Figure 4.31: Estimation of the residual moisture for cracking (RCM).....	176

Figure 4.32: Profiles of moisture loss in 2-wetting and drying cycle (a) well compacted soil (b) moderately compacted soil (c) poorly compacted soil .....	180
Figure 4.33: Moisture profiles in the 6-cycle of wetting and drying test..	182
Figure 4.34: Comparison of cracks parameter in a 2-desiccation test (a) Length (b) width .....	184
Figure 4.35: Change in crack intensity with increasing cycles of wetting and drying .....	185
Figure 4.36: Final crack patterns in 6 progressive cycles of wetting and drying in the soil (number of cycle shown at top right corners) .....	186
Figure 4.37 An exponential graph .....	188
Figure 4.38: Profile of moisture loss in the 2 <sup>nd</sup> drying cycle .....	190
Figure 5.1: Desiccation profiles of three common clay embankment soils in the UK (a) Absolute moisture content (b) Change in moisture .....	196
Figure 5.2: The relationship between soil plasticity and the rate of desiccation in compacted plastic soils .....	197
Figure 5.3: Profiles of moisture loss with depth in the plastic soils .....	199
Figure 5.4: Soil water-retention behaviour of the plastic soils .....	200
Figure 5.5: Profiles of suction with depth (a) Nafferton Clay (b) Gault Clay .....	202
Figure 5.6: Photographs of cracks in plastic soils (a) Before 1 <sup>st</sup> cycle desiccation (Left column) and end of 1 <sup>st</sup> cycle desiccation (right column), (b) After rewetting for 2 <sup>nd</sup> desiccation cycle (right column) and at end of 2 <sup>nd</sup> drying (left column) .....	207
Figure 5.7: Time series crack evolution (a) 1 <sup>st</sup> drying cycle (b) 2 <sup>nd</sup> drying cycle.....	208

Figure 5.8: Change in cracking intensity with soil plasticity and cyclic wetting and drying .....	210
Figure 5.9: Example of progressive development and interaction of cracks in the Nafferton Clay.....	212
Figure 5.10: Direction of cracking in Nafferton Clay soil influenced by orientation of the drying (dashed lines).....	214
Figure 5.11: Profiles of desiccation from 2 opposite sides of a rectangular soil block similar in effect to difference in moisture loss with slope aspect in the embankment.....	215
Figure 5.12: Illustration of stress field around a crack. From Goehring (2013).....	216
Figure 5.13: Schematic of cracking in thin soil of height, $h$ . The crack releases stress preferentially in the direction, $x$ perpendicular to its growth. From Goehring (2013).....	216
Figure 5.14: Comparison of crack outlines in different soil textures (a) Tang <i>et al.</i> (2011a):clay slury (b) Kindle (1917): mudcrack (c) Yesiller <i>et al.</i> (2000): clay liner fill and (d) This study .....	218
Figure 5.15: Crack network affected by texture in a compacted clay fill .	220
Figure 5.16: Characteristics crack patterns (a) Laboratory and (b) Field	222
Figure 5.17: Fibrous grass roots in a test pit section on the embankment .....	224
Figure 5.18: Vegetation influence on crack orientation in the embankment .....	225
Figure 5.19: Crack pattern in experimental rooted soil (a) 1 <sup>st</sup> cycle (b) 2 <sup>nd</sup> cycle .....	226
Figure 5.20: Profile of moisture loss with depth in the vegetated soil mass .....	227

Figure 5.21: Crack patterns in compacted soils.....	229
Figure 5.22: Time series changes in crack orientation and intersection (1 <sup>st</sup> cycle) .....	230
Figure 5.23: Stress concentration and crack intersection model (from Walker 1986) .....	232
Figure 5.24: Textural control of crack orientation and intersections in soils .....	233
Figure 5.25: Polygonal cracks formed around stones and clods in exposed soil surfaces of the embankment .....	234
Figure 5.26: Crack repetition during wetting and drying of Nafferton, Gault and VH plastic Clays soils (a) End of 1 <sup>st</sup> drying cycle, (b) Rewetting and (c) End of 2 <sup>nd</sup> cycle drying cycle.....	235
Figure 5.27: Illustration of changes in crack orientation and intersection in 2-cycle of wetting and drying .....	236
Figure 5.28: Changes in crack orientation and intersection in multiple wetting and drying. Cycle number at bottom left corner .....	237
Figure 5.29: Progression of desiccation crack pattern in compacted clay soil subjected to 6 cycles of wetting and drying. Center image shows prominent fines cloaking old crack surface after rewetting.....	238
Figure 5.30: Crack cast.....	239
Figure 5.31: Schematic of vertical moisture gradient and the development of horizontal cracking in soil. Open crack walls enable secondary evaporation. ....	240
Figure 5.32: Loose and wetted soil particles (arrowed) swells within a crack .....	241
Figure 5.33: Illustration of the process of crack closure (a) Loose material fallen into cracks during dry period (b) crack closing both by swelling of wetted soil block and particles in the crack .....	241

Figure 5.34: Rodent burrows (circled) enhancing crack aperture .....	242
Figure 5.35: Effect of bioturbation on surface cracks: (a) and (b) common worm species in the embankment, (c) and (d) worms-generated mulch swells over cracks outline .....	243
Figure 5.36: Surface crack geometry. Crack length, <b>L</b> is >> width, <b>W</b> ....	244
Figure 5.37: Notation for stresses at the crack tip. The point on the crack tip is the origin of the coordinate system and the z-axis lies along the crack tip. Displacements of points within the crack body when the body is loaded are u, v, and w in the x, y, and z directions. From Frost <i>et al.</i> (1974) and Atkinson (1987) .....	245
Figure 5.38: Correlation between crack width and depth in the embankment (a) Poorly compacted panel (b) Well compacted panel.....	246
Figure 5.39: Correlation of cracks depths and widths in plastic soils.....	247

## List of Table

Table 2.1: Activity of clays .....	59
Table 3.1: Properties of the Nafferton clay of the BIONICS (adapted from Hughes <i>et al.</i> 2009; Toll <i>et al.</i> 2012, and Glendenning <i>et al.</i> 2014) .....	90
Table 3.2: Summary of material property .....	118
Table 4.1: Summary of crack geometry property in the embankment....	155
Table 4.2: Summary of hydrologic conditions for cracking.....	177
Table 4.3: Crack geometric properties in multiple cycles of wetting and drying .....	187
Table 4.4: Summary of rate of moisture loss in three compacted clay soil .....	189
Table 5.1: Atterberg limits of tested soil materials .....	194
Table 5.2: Summary of desiccation parameters in three plastic soils ....	197
Table 5.3: Summary of crack properties for three compacted plastics soil after desiccation.....	207

# Chapter 1 General Introduction

## 1.1 Background

Efficient transportation is a key factor in national development. The transportation network enables free flow of goods and services and transport infrastructure connects other forms of infrastructure. According to report of the UK's transport sector in 2012, roads and rails meet over 90% of transportation needs in the country, with estimated 500 billion motor vehicle kilometers travelled in 2009 and 1.3 billion rail journeys completed in 2009/10. Overall, the transport asset in the country is worth about £100 billion by estimate. However, the construction of the infrastructures involves creation of a vast number of earthworks, mainly embankments and cuttings. In an infrastructural appraisal conducted by Perry *et al.* (2003), embankments and cuttings made up over 60% of the rail and road network, and both formed one-third of the total transport asset value. Embankments, in particular, provide support and alignment for the transportation system and including cuttings, constitute some of the oldest geotechnical structures in the UK.

## 1.2 The Problem: Failures of infrastructure embankments

Clay based geologic materials extensively cover the British Isles. Because of this factor, a significant number of embankments in the UK are made of expansive fills from the local geologies. The fill materials range from intermediate to very high plasticity making them prone to volume change as moisture condition in the surrounding environment changes, of course, driven by weather condition. Therefore, the near surface ground condition of most of the fill materials presents problems in civic construction arising from shrink-swell actions in clay. Global damages caused by expansive soils ranges in billions of dollars. Pritchard *et al.* (2013) noted that shrink-swell action in clays poses the highest cost and risk to infrastructure systems in the UK. Well-known sources of unstable slope materials in the country include London Clay, Gault Clay, and materials of the Lias Group etc. Literatures have extensively discussed the problems with expansive clay in construction. This ranges from minor serviceability to ultimate failure of slopes (Figure 1.1) with implications for high cost of maintenance, service delays, route closures, threat to life and properties

etc. (Perry *et al.*, 2003; Kilsby *et al.*, 2009; Rouainia *et al.*, 2009; Dijkstra and Dixon, 2010). The stability of earthwork slopes and a satisfactory network performance, therefore, forms an important theme among the geotechnical community and asset owners.



Figure 1.1: The problem: Different events and magnitude of earth slope failures affecting railways and highways transport corridor in the UK (photo a, b & c from ICE archives/Network rail; d & e from Briggs *et al.* (2016); from Electrokinetic Ltd, Newcastle University)

Apart from nature of the fills, the method of construction can also affect the performance of earthwork slopes. In the UK, two types of embankments

are common, based on age and method of construction. The methods depended on the available technology. Thus, there are the Victorian or historic embankments and the modern embankments. The former mostly refers to the old railway embankments built in the 19<sup>th</sup> century, while the latter refers to the more recent slopes, mainly modern highways whose construction started in early 50's. The main differences between the two are the texture, density and drainage conditions. Due to lack of proper compaction techniques and standard in the olden times, the Victorian railway embankments were constructed by end tipping method where the fills are tip into position and compacted by movement of the tipping trucks as construction progresses. This method resulted in a loosely compacted, heterogeneous soil structure couple with the weak foundation. On the other hand, the advancement in soil mechanics, advent of Proctor compaction equipment and a better understanding of material properties gained from the experience of past constructions enabled better designs and improved construction technique in later times. Hence, construction of modern embankment involved well-designed foundation, good compaction and good drainage control resulting in consistent soil properties (density, strength, stiffness, permeability etc.). Overall, the embankments of the two eras present different stability characteristics, with widespread instability reported on the historic embankments (Nelder *et al.*, 2006; Loveridge *et al.*, 2010; Briggs *et al.*, 2016).

Pore water pressure is an important parameter commonly involved in assessment of slope stability. This is because fluctuation in the pore water pressure has a major influence in the degradation of shear strength by decreasing the effective stress (Loveridge *et al.*, 2010). Seasonal variability in pore water pressure also leads to opposing potentials, i.e. negative and positive pore water pressure in the summer and winter months respectively. The high negative pore water pressure brought about by net higher evapotranspiration in summer gradually depreciate during winter and can become increasingly positive by heavy rainfall wetting to a proportion that could cause slope failure. Several studies e.g. Kilsby *et al.* (2009), Loveridge *et al.* (2010), Wilks (2015), Briggs *et al.* (2016) etc., have noted that rainfall-induced pore water pressure related problems

occur in modern highway embankments, particularly in high plasticity soils prevalent in the South. Shallow slips of not more than 2m deep characterized the failure mode. In old railway embankments, both pore water pressure and shrink-swell problems are frequent, often resulting in deep-seated shear failures (commonly greater than 2m deep). The difference in the failure modes and mechanisms essentially lies in the quality of construction of embankment of the two eras highlighted above. In addition, cyclic pore water pressure conditions brought about by repeated wetting and drying gives rise to progressive strain softening, another common failure mechanism recognized in the overconsolidated materials in the country. Consequently, modern slope stability and asset management focus on seasonal water demand by vegetation as well as facilities of rainwater infiltration into slopes, principally cracks. The role of vegetation in transient pore water pressure fluctuation on slopes has received significant attention in literature with an adaptation of selected plant species and regulations for the management of modern highway slope stability. Soil cracking, on the other hand, is recognized for its potential to increase the surface permeability (Stirling *et al.*, 2017) hence directly contribute to change in pore water pressure. Among the types of soil cracking identified in nature, desiccation cracking brought about by volume changes in soil material during drying is common in clay slopes with behavior that leaves much to understand their characteristics and controls.

#### **1.2.1 *Climate and the processes of deterioration in infrastructure slopes***

Climate is the prevailing weather conditions of a region characterized by the pattern of average temperature, air pressure, humidity, precipitation, sunshine etc., over a long period. The transient behaviour exhibited in the embankments e.g. fluctuation in pore water pressure, suction gradient, and shear strength etc., is linked to microclimate. Patterns of rainfall and sunshine directly influenced the amount of moisture in the soil, hence the strength characteristics of the embankment fill. However, the current issue in slope-atmosphere interaction is the impact of climate change. Climate change is a large-scale alteration in the earth's climate pattern due to rise in temperature (or global warming). Global warming is mainly attributed to

anthropogenic factors, principally municipal and industrial effluents of greenhouse gases which heats up the atmosphere e.g. carbon dioxide, methane. The subject of climate change is a global reality with evidence showing across the world weather, oceans, ecosystems etc. Similarly, the potential impacts of this phenomenon cut across nearly all sphere of life. Hence, it has triggered interdisciplinary and intergovernmental efforts toward proactive management strategies.

The Met Office Hadley Centre is a leading centre that provides probabilistic climate change projections in the UK. It's United Kingdom climate change projections released in 2009 (UKCP09) is widely used as weather generators in climate change models. Weather generators provide time series meteorological variables for projections of future climate scenarios and their probable impacts. Accordingly, the UKCP09 suggests wetter winters across the UK and drier summers, particularly in the south. Annual and seasonal temperatures, and therefore evaporation, are expected to increase in all parts. The official report from the Department of Business, Energy & Industrial Strategy showed that the average temperature in Britain is 1°C higher than it was 100 years ago and 0.5°C higher than in the 1970s ([www.gov.uk/guidance/climate-change-explained](http://www.gov.uk/guidance/climate-change-explained) 23, Oct 2014). Evidently, there are increasing incidents of heat waves, flooding, landslides etc. reported across the country in recent times, with 2012 adjudged as the wettest year since 1910. Report of National environment research council of the British geological survey (BGS, 2017) also shows a significant increase in the number of landslides and slope failures (mainly railway embankments), particularly between July and December 2012 (Figure 1.2).

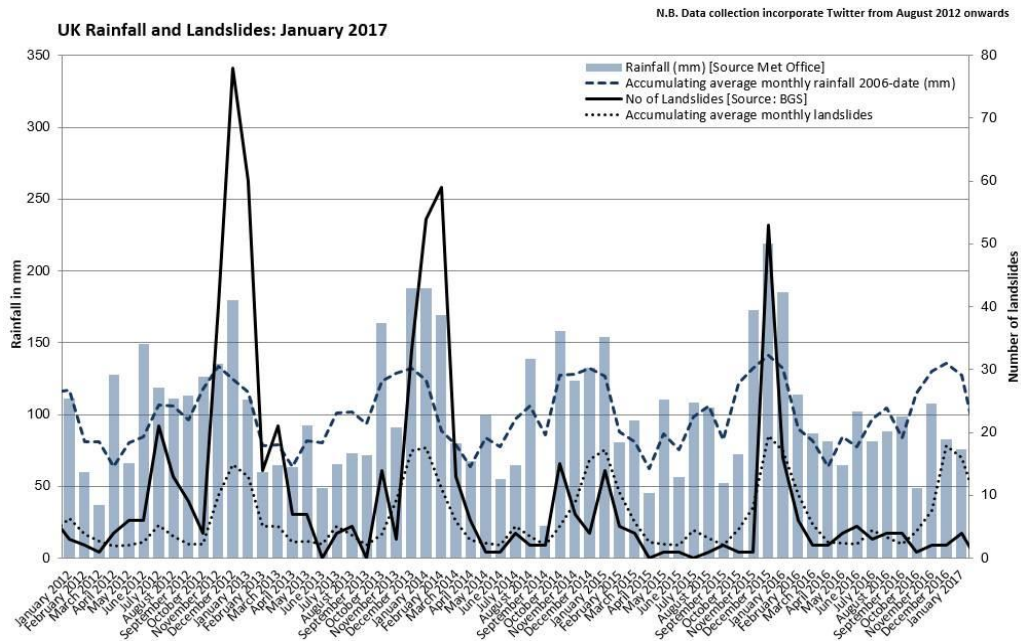


Figure 1.2: Rainfall and landslide data for the UK between 2012 and 2017 (British Geological Survey report, February 2017)

The same BGS report linked extended periods of low rainfall to high levels of shrink-swell subsidence in the clay soils of the South East of the UK. A previous study conducted by Harrison *et al.* (2012) showed that increased precipitation and temperature are coupled factors in increased shrink-swell in the South. The analysis showed that this relationship has potential for increased subsidence-related insurance claims in this region in the near future. A separate report by the office of rail and road (ORR, 2013) indicates that there were 125 earthwork failures between 2012 and 2013 compared to 12, between 2011 and 2012. In a breakdown of landslips data from Network rail assets, Wilks (2015) showed that in the UK, England has the highest record of these weather related events. The evidence is enormous and clearly suggests the vulnerability of the UK's transport infrastructure to climate change with potential for an increase in the cost of maintenance.

With a changing climate towards the extreme, slope responses are likely to change especially with a proliferation of cracking (section 2.4.4 and 4.3.4). Apart from reducing the mechanical integrity of slopes, cracks increase infiltration and this in turn can increase pore water pressure leading to a reduction of the shear resistance in slopes (Baker, 1981; Simoni *et al.*, 2004; Wang *et al.*, 2011). Increased seasonality can increase existing level of shrink-swell deformations in clay based slopes

spread across the country's landmark. Researches therefore, envisaged that higher than average rainfall would likely result in increased earth slope failures because of increased water loading on slopes. Hence, antecedent rainfalls are used for assessment of slope stability in countries such as Hong Kong, New Zealand, Singapore etc. (Rahardjo *et al.*, 2001; Rahardjo *et al.*, 2008). However, more crucial in climate-related slope deterioration mechanisms are the features that accelerate rainwater infiltration in the slope leading to anomalous pore water pressure in the otherwise low permeability engineered fills, which are usually stable for a considerable period after their construction. Overall, the potential impact of climate change on slope put a huge demand on transport geotechnics research and practice to provide adequate understanding and resilient adaptation of infrastructure slopes for acceptable network performance levels in the country.

There is good progress in physical and numerical modelling to understand both the impact of climate and climate change on infrastructure slopes. The studies mainly consider climate variability (using existing weather generators) and material properties to model the hydro-mechanical stability of slopes. However, important issues have arisen from the studies requiring better understanding and these include:

- I. Would climate change lead to increased seasonality hence greater deformations due to increased rates of strength degradation?*
- II. Would the situation lead to greater infiltration hence more ultimate state failures as opposed to superficial failures?*
- III. Would there be a favourable condition for stable slope arising from a possible balance between the envisaged increased rainwater infiltration and high evapotranspiration?*

Some of the studies generally suggest there would be an increase in the shrink-swell deformation including cracking (Kilsby *et al.*, 2009; Dijkstra and Dixon, 2010; Loveridge *et al.*, 2010). These works consider the effect of increase climate seasonality affecting volume sensitive materials in the country. Other outcomes contradict this position by suggesting that the future climate condition is unlikely to have any adverse effect on the

stability of infrastructure slopes (Collison *et al.*, 2000; Davies *et al.*, 2008; Rouainia *et al.*, 2009). The latter group based their conclusions on the fact that increased in evapotranspiration as result of prolong hot weather will balance the high intensity rainfall envisaged, with no net change in the present level of slope deformation. However, the influence of cracks on hydrology is not considered in these works, although recognised and therefore recommended in further studies.

In an analysis of infrastructure records of Network rail, Wilks (2015) showed that presently, desiccation related failures are small compared to other types of slope failure mechanisms (Figure 1.3).

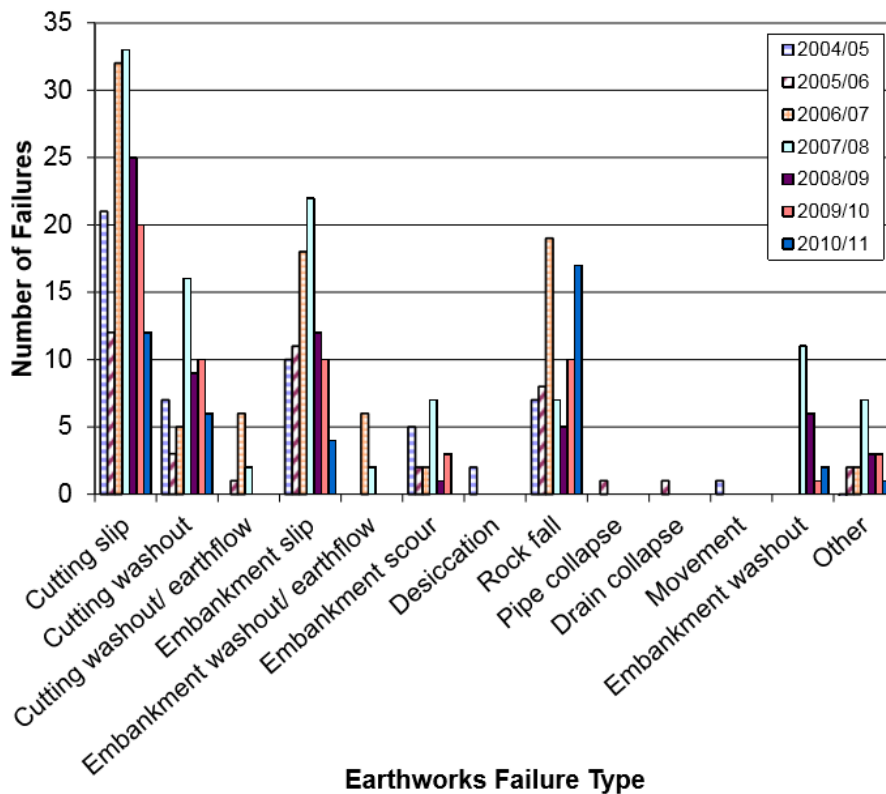


Figure 1.3: Earthworks failures by type and year (adapted from Wilks, 2015)

Notwithstanding, the evolving climate scenario reasonably suggests a condition for increased drying and cracking in the soil. And greater water accumulation could be occurring in slopes. New mechanisms in the slope response can be generated by such conditions including the development of perched water zone, near surface slips etc. Despite this recognition, practical information for understanding of soil cracking in engineered embankment is few. These gaps appear to be connected to the challenge involved in physically monitoring and measuring cracking (Take and

Bolton, 2002), hence lack of quality data and site-base analysis for necessary input. In addition, cracking is a nonlinear process whose changes with time are difficult to model satisfactorily (section 2.4.7). Not only in infrastructure slope stability is desiccation cracks behaviour relevant, impermeable barrier system and a nuclear waste cover are in similar need as they involved construction with clay fills exposed to a temporal environmental condition. Therefore, quality, site-based crack characterization is highly desirable in several practices.

From the preceding, it is clear that crack deteriorate earth slopes. However, just how do cracks occur in engineered slopes and to what extent considering, of course, the quality of construction and material property? Existing knowledge on desiccation cracking involves theories set and mechanism identification. Qualitative descriptions are carried out in small samples and fully saturated soil specimens. To answer the above questions satisfactorily, it is important to exclusively quantify and characterise cracking with the peculiar conditions surrounding the engineered clay embankment.

### **1.3 Project definition**

The general purpose, scope and application of this research are outlined in this section.

#### **1.3.1 Aim**

This project aims to understand desiccation cracking and the controlling factors of its propagation and network formation in engineered clay fills. The study is specifically concerned with the behaviour of desiccation cracks related to near surface moisture changes, suction development and vegetation present in both historic and modern transport embankments in the UK.

#### **1.3.2 Objectives**

In order to achieve this aim, the following specific objectives are set out:

- I. To characterise moisture movement, crack initiation and propagation

- II. To quantify desiccation cracking in clay base infrastructure embankment
- III. To establish the influencing factors in crack orientation and intersections in compacted clay fills
- IV. To determine the influence of vegetation on crack network
- V. To understand the effect of slope geometry on crack occurrence

#### 1.4 Applications

Soil cracking has multidisciplinary significance. However, in infrastructure geotechnics where this study directly applies, environmental impact on near-surface moisture movement have made desiccation cracking important in slope stability problems. This is because cracking of expansive soils is associated with environmental moisture loss. Therefore, in general, the research will contribute to the understanding of desiccation cracking behavior in engineered clay embankment affected by repeated wetting and drying. The results are expected to improve understanding of cracking characteristics and a realistic analysis of clay slopes with cracks. In addition, the study would improve local understanding of the likely behaviour of common volume-sensitive slope materials in the UK as the climate changes, with emphasis on construction techniques of the old and modern infrastructure slopes.

#### 1.5 Thesis structure

This thesis has six chapters. Chapter 1 introduced the general background and outlined the aim and objectives. Chapter 2 reviewed existing theories and significances of cracking in soil across several practices. The various factors and requirements of desiccation cracking, as well as their geotechnical implications, are outlined. In addition, research gaps in the subject are identified. In Chapter 3, field and laboratory methodology of this study is outlined. A full-scale embankment facility used for the field study and an innovative soil-climate interaction system for the laboratory study, are described. The different test programs and methods of quantifying the cracks are also given.

Chapter 4 and 5 provide integrated discussion and presentation of results. The discussions are group into two broad themes, hydrological aspect,

which forms Chapter 4 and material aspect, which forms Chapter 5. Under these themes, time series development of surface cracks in the various test conditions is quantified and characterize to establish the underlying dynamics. Finally, Chapter 6 is a summary of the findings of this research including the conclusions and outlook for future research.

## **Chapter 2 Literature review**

### **2.1 Introduction**

Desiccation cracking occurs mostly in expansive soil as they dry. Due to its significance in a wide range of discipline dealing with soil, the phenomenon has generated much research in the past and is still receiving increasing attention in recent applications. In this chapter, existing knowledge on soil cracking is reviewed and discussed. The review consists of three aspects. The first aspect presents the characteristics and significance of soil cracking. The second deals with the theories of desiccation cracking in soil and the influencing factors. Lastly, the third aspect concerns more specifically with geotechnical implication of soil cracking in infrastructure slopes. Important ideas that relate to present study are highlight as well as the existing research gaps. At the end of the chapter, summary of the review and conclusion are given.

### **2.2 Causes and types of soil cracking**

Cracks in soil are discontinuities or macropores thought to result from stress developed against the soil strength. Stress can arise from several factors in nature including desiccation, wetting and drying, weathering (Konrad & Ayad, 1997; Peron *et al.*, 2009a, Utili, 2004). Fang and Daniels (2006) carried out a broad classification of the common types of cracks based on their primary causes and modes of formation. These include thermal cracks, fracture cracks, tensile cracks and shrinkage cracks. According to Fang and Daniels (2006), thermal cracking occurs due to differences in the soil temperature (or thermal expansion), e.g. cyclic freeze thawing in regions which experience wide temperatures differentials above freezing point during the day or at night. Fracture cracks are micro-cracks resulting from environmentally driven variability in pore water pressures. The variability develops internal cyclic loading in existing void spaces in the soil. Formation of tension cracks is attributed to overburden pressure including structural load, rainwater load, snow load, trees etc. This generally decreases tension and increases compression in the soil mass. Lastly, shrinkage cracks are defined as those formed primarily by shrinkage of clay minerals as the soil mass dries.

The broad classification identifies the different environmental factors associated with crack formation and to some involves weathering. However, from geotechnical point of view, some of the groups appear ambiguous as defined. For instance, there should be no distinction between fracture and shrinkage cracks as both arise from environmentally driven changes in the pore water pressure and capillary tension in soil. Understandably, Fang and Daniel (2006) may have sought to distinguish those effects taking place along pre-existing weakness planes or inherent micro-fractures within soil clods from which shrinkage cracking can preferentially initiate.

Among the different modes of cracking, shrinkage or desiccation cracking, which forms the focus of this study, is acknowledged as the most significant and common in soil (Kodikara *et al.*, 2000). This partly attributes to the abundance and wide application of clay materials, which desiccation crack commonly occur. It also relates with the prevalence of unsaturated soil condition within which moisture changes greatly affect the behaviour of expansive soil. Environmental conditions and nature of the engineered fill are therefore important in their formation. Environmentally driven soil shrinkage can result in complex hydraulic stress field, which require good understanding to explain the different patterns of cracks observed in dry soils. Towner (1987) identified common stress states involved shrinkage cracks formation in different soils. In some cases, shrinkage sets up tensile forces that must exceed the tensile strength of the soil for cracking to occur. In others differential shrinkage through non-uniform drying, sets up complex patterns of shear stress. In other cases e.g. Peds (units of soil separated from each other by surfaces of weakness or incipient cracks), the cracks may be permanent features that simply open and close in response to drying and wetting, and do not involve strength. The first condition is prevalent in isotropic drying in saturated mud and flooded sediment with fine texture while clods and fills with coarse texture can experience tensile and shear stresses. In this study, the term desiccation crack is used rather than shrinkage crack to more directly reflect the primary cause i.e. moisture loss in soil by environmental drying.

### 2.2.1 **Characteristics of desiccation cracking in soil**

Extensive field and laboratory studies have identified the properties of desiccation cracking in a soil, which are useful in characterising the influencing factors of their formation. Important characteristics of desiccation crack highlighted in the literature include crack pattern, width or aperture, depth, spacing and length. The pattern of cracking is the resulting configuration of the crack intersections expressed on the soil surface. It can be considered as the surface expression of the stress field in the soil mass (Lachenbruch, 1961; Konrad and Ayad, 1997a). Although they may appear randomly and complicated, crack patterns developed systematically. In a review of early studies of desiccation cracking, Kodikara *et al.* (2000) defined two categories of commonly observed crack pattern based on their angle of intersections. These are the orthogonal pattern and non-orthogonal pattern. In orthogonal pattern (Figure 2.1a), cracks tend to meet at a right angle while non-orthogonal cracks meet at angles of  $120^\circ$  i.e. hexagonal arrangement (Figure 2.1b).

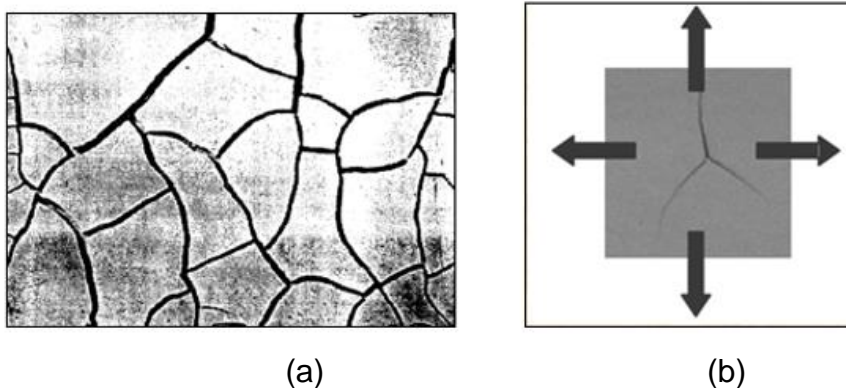


Figure 2.1: (a) Orthogonal crack pattern (b) Hexagonal crack pattern (adapted from Kodikara *et al.*, 2000)

The study also indicates that desiccation cracks occur predominantly in orthogonal and sequential manner. The individual cracks making up the pattern can, therefore, be grouped into Primary cracks, which formed initially, and Secondary cracks, which formed later and further subdivide patterns of the primary cracks into smaller cells. The non-orthogonal category, on the other hand, evolves simultaneously and is common at higher desiccation rate, thin soil layers and low-density soils. The primary cracks also grow relatively faster, wider and longer subsequently allowing the un-cracked areas surrounded by them to shrink.

To explain the dynamics involved in the formation of crack patterns, Walker (1986) illustrated the process of crack intersections in a soil mass (Figure 2.2).

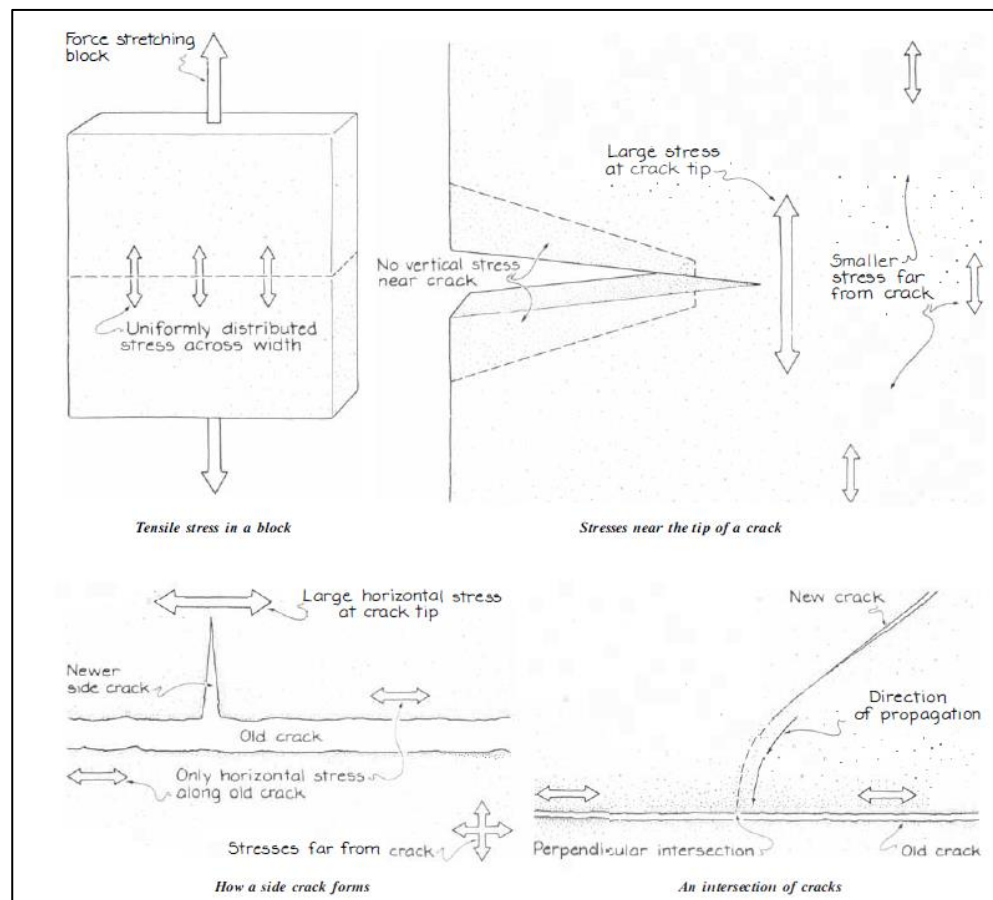


Figure 2.2: Stress distribution and crack intersection (from Walker, 1986)

In this illustration, a block of drying clay is under both vertical and horizontal stresses. While the vertical stress component acts along the surface of the block and is relieved with time to form the initial cracks, the horizontal component propagates parallel to the plane of the initial (or primary) crack, hence persevere longer in the soil mass. It is thought that the horizontal stress is responsible for initiation of side cracks and influences the perpendicular intersection of an approaching new crack. A similar system was also described by Morris *et al.* (1992) and the propagation mechanism at crack tip follows the general theory of fracture energy in elastic materials widely attributed to early work by Griffith (1921).

Crack spacing is the distance between successive cracks in the soil surface. It is a useful parameter which determined other crack properties such as the size of the crack cell (also known as soil clod or soil island -

(Holtz and Kovacs, 1981; Favre *et al.*, 1997)), and intensity of cracking. Because of the complex geometry often exhibited by soil cracking, the distance between any parallel cracks is usually considered for measurement of crack spacing. Lachenbruch (1961), Konrad and Ayad (1997b), Costa *et al.* (2013), Peron *et al.* (2013) etc., noted that crack spacing is highly dependent on local disturbances e.g. inhomogeneous soil strength, flaws and the non-uniform drying conditions etc. These factors essentially influence the pattern of tensile stress field, which governs the sequence. In another study involving analysis of crack features in ten different soils, Chertkov (2000) showed that the depth of primary cracks coincides by order of magnitude with their spacing, which is express as:

$$Z_o \cong S_o \quad 2.1$$

Where  $Z_o$ , is the thickness of an intensive-cracking layer and  $S_o$  is the measurable crack spacing with a surface width between 1.5–3mm. The spacing was considered as the mean between two parallel cracks with a defined depth as illustrated in Figure 2.3.

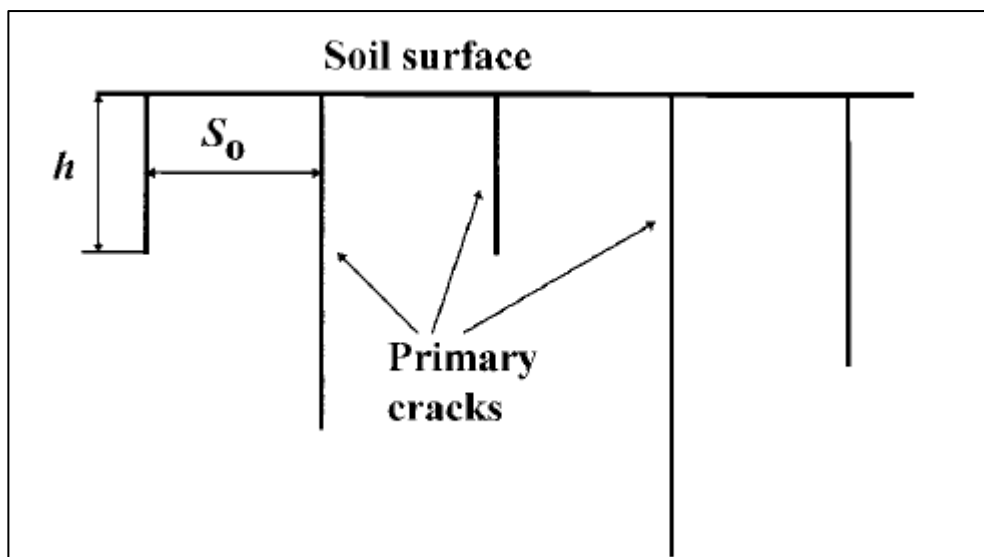


Figure 2.3: Crack Spacing.  $S_o$  is the mean spacing between primary cracks at the soil surface, and  $h$  is the depth of the primary crack (Chertkov, 2000)

Although the above relationship has not been validated, especially with the tortuous nature of common crack outlines and a complex subsurface configuration, a general trend of larger spacing with deeper cracks are reported in the field (Kodikara et al, 2000). This trend can imply that after

initiation, greater energy is spent in deepening and widening the crack (i.e. geometric development). After initiation, crack propagation is believed to be influenced by fracture energy (or strain forces) developing over an effective layer thickness. Costa *et al.* (2013) therefore used the concept of Griffith's fracture energy balance to examine this behaviour and in combination with other soil properties such as effective soil layer thickness,  $t$  and Young's modulus,  $E$ , change in moisture content,  $\Delta\omega$ , the authors established a more encompassing equation for crack spacing,  $S$  as expressed in equations 2.2 to 2.4:

$$\text{For Parallel cracks, } S \approx 2 \frac{G_s}{E(\alpha\Delta\omega)^2} \quad - \quad 2.2$$

$$\text{For Square cracks, } S \approx 4 \frac{G_s}{E(\alpha\Delta\omega)^2} \quad - \quad 2.3$$

$$\text{For Hexagonal cracks, } S \approx 2.31 \frac{G_s}{E(\alpha\Delta\omega)^2} \quad - \quad 2.4$$

Where  $G_s$ , is the strain energy of the material and  $\alpha$ , is a hydraulic constant.

A wide range of crack spacing, from a few millimetres to hundreds of millimetres is reported in field studies. However, the cause of this variation is difficult to explain in field context, rather laboratory studies showed that rapid rates of desiccation tend to produce smaller crack spacing and vice versa. In many cases, additional findings from laboratory investigation give a better understanding of complex field phenomenon. It is considered in the present study that a combination of field and laboratory would produce a coherent understanding of this natural phenomenon.

The width (aperture), depth, length and orientation of a crack are closely related geometric properties and define the surface morphology of the crack (Figure 2.4).

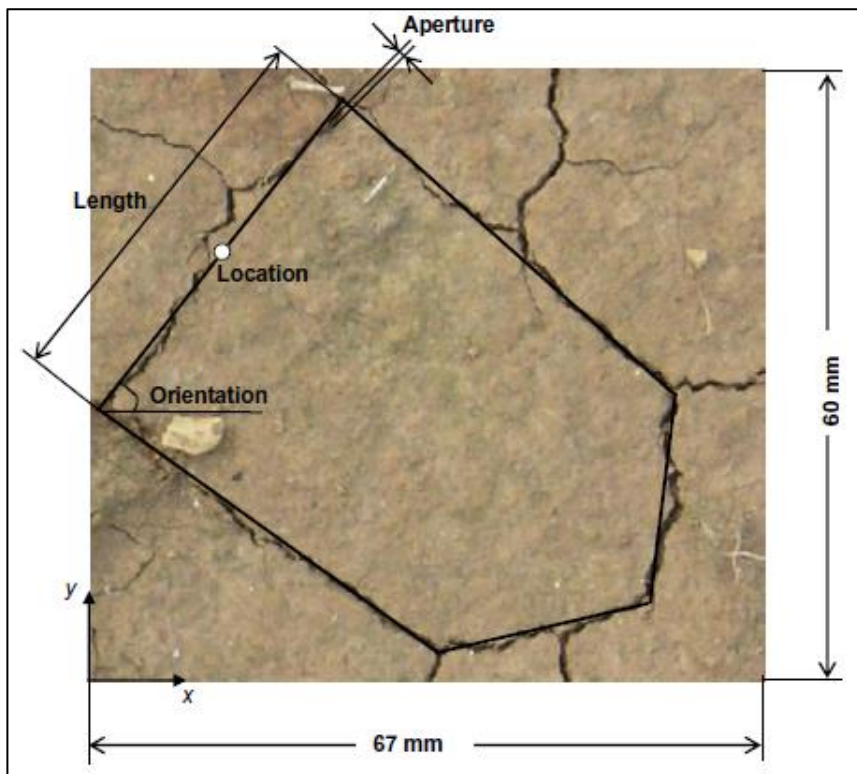


Figure 2.4: Approximation of a crack dimensions (Li and Zhang, 2010)

Crack widths and depths measured in the field are comparable in different observations. Zhan *et al.* (2006) reported width of 10mm and a maximum depth of 1.2m in a clay cutting. In an excavation on a flood embankment, Dyer *et al.* (2009) reported a maximum crack width 8mm which decreases uniformly over 1m depth. Anderson *et al.* (1982) also observed a crack depth of approximately 1m in a motorway embankment. In general, analytical data shows that crack width and depth displays a positive and highly significant correlation (Bandyopadhyay *et al.*, 2003; Kishné *et al.*, 2009). Such relationship suggests a common dynamics of formation a directional implication. Since desiccation cracking is closely associated with shrink-swell action in expansive soils, crack width and depth are useful in the analysis of shrinkage anisotropy. Basically, cracks represent the horizontal plane of the shrink-swell movement (Bronswijk, 1989; Gomboš, 2012). Overall, crack morphology is important in soil water storage and distribution with relevant application in transport phenomena in the soil. Considering their significance in crack characterisation, measurement of the geometric properties of cracks, is important in this study.

Currently, there is little understanding of the cross sectional morphology of a crack in the soil. The crack shape depends on the orientation of the vertical walls. However, three theoretical models are common, namely rectangular, and triangular and square root model. The basic morphology adopted for these models are as illustrated in Figure 2.5.

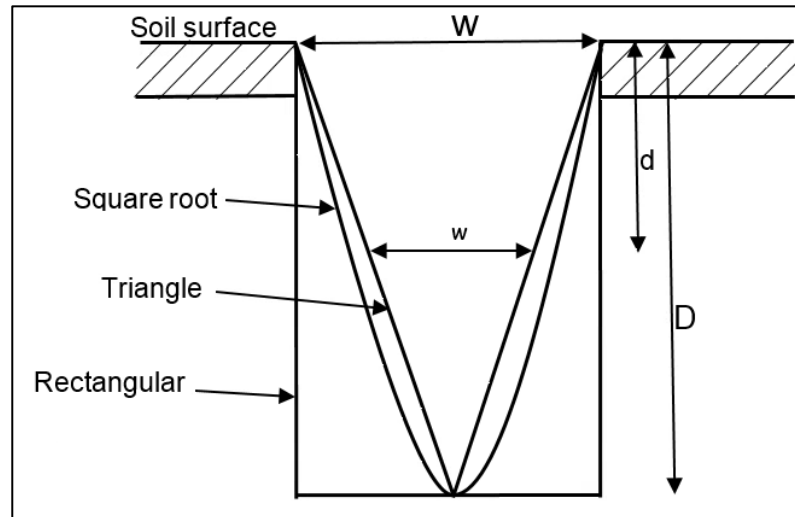


Figure 2.5: Vertical cross-section through a crack, showing the triangular, square root and rectangular shapes (adapted from Ringrose-Voase and Sanidad (1996))

Pioneer work that considered crack subsurface morphology was carried out by El Abedine and Robinson (1971). In order to estimate crack volume, the authors assumed that cracks have a triangular cross-section, which tapers with increasing depth to a point. Therefore the width,  $\omega$  at any depth  $d$ , within a crack of maximum depth  $D$ , and surface width,  $W$ , can be express as:

$$\omega = \frac{W}{D} (D - d) \quad 2.5$$

In a study on Vertisols (i.e. soils with high content of expansive clay minerals such as montmorillonite), Dasog *et al.* (1988) assumed that the crack walls were parallel such that the cross-section becomes rectangular. Then the width is constant throughout its depth and surface area. The triangular and rectangular models are two extremes of the possible shapes, assuming that the walls are parallel (i.e. convex). An intermediate model between this two is sometime assume. This is in situations where the width,  $W$ , follows a square root relationship with depth  $D$ , (i.e. concave walls that bulge outwards) in the form:

$$\omega = \frac{W}{D^{1/2}} (D - d)^{1/2} \quad 2.6$$

Traditionally, the depth of a tension crack is estimated using the equation proposed by Taylor (1948):

$$Z_t = \frac{2c'}{\gamma} \tan \left( 45^\circ + \frac{1}{2} \phi' \right) \quad (\text{For drained condition}) \quad 2.7$$

$$Z_t = \frac{2c_u}{\gamma} \quad (\text{For undrained condition}) \quad 2.8$$

where  $c'$  is the effective cohesion,  $\phi'$  is the effective internal frictional angle,  $C_u$  is the undrained shear strength, and  $\gamma$  is the unit weight of the soil which is affected by pore water pressure (Spencer, 1968). The maximum crack depth corresponds to a point below the ground surface where the horizontal stress equals the tensile strength of the soil (Morris *et al.*, 1992; Wang *et al.*, 2011). Miller *et al.* (2015) assumed such conditions occur at the base of the 'active zone' in unsaturated soils.

Even though there is not yet any valid crack shape, Ringrose-Voase and Sanidad (1996) argued that the rectangular shape is more applicable for large cracks with vertical walls where the width remains fairly constant. Where the surface is still drying and shrinking, it is reasonable to use the triangular model, since deepening of the cracks commonly accompany continued widening near the surface. The latter is justified by a common observation of cracks as an inverted "V-shaped" in excavations in addition to a theoretical supposition that moisture loss in soil presents a decreasing mechanical profile, with a greater concentration of soil-water suction at the surface layer. In order to substantiate the true subsurface morphology of cracks in the soil, a mould cast of crack would be carried out in this study.

An important parameter that involves crack morphology is the estimation of volume of the crack cross-section. Geometric volume is computed from the product of its area and the surface length while the area is computed from a combination of the width (base or breadth in a regular triangular and rectangular shape) and depth (or height). Therefore, in a transect method of a crack survey, Ringrose-Voase and Sanidad (1996), presented

a relation for the mean area, ( $\bar{A}$ ) for a measured number, ( $n$ ) of intersecting cracks as follows:

For a rectangular model,

$$\bar{A} = \frac{1}{n} \cdot \sum_{i=1}^n (W_i \cdot D_i) \quad 2.9$$

For the triangular model,

$$\bar{A} = \frac{1}{2n} \cdot \sum_{i=1}^n (W_i \cdot D_i) \quad 2.10$$

where  $W_i$  and  $D_i$  are width and depth respectively of the individual crack. The approach of computing crack parameters adopted by El Abedine and Robinson (1971) and Ringrose-Voase and Sanidad (1996) are largely applicable to an interconnected network of cracks. Despite their spatial implication, they appear very complex with many assumptions.

Rivera (2008) outlined other field and laboratory methods of estimating crack volume in shrinkage soil. These include the method of the coefficient of linear extensibility (COLE) and relative soil surface subsidence. Both methods relate changes in vertical and horizontal layers of expansive soil to the cross-sectional volume of existing crack. Hence, their results were comparable. However, the methods are not validated. In addition, COLE is solely a laboratory-based measurement, and shrink-swell action is difficult to observe in the field.

Crack geometric properties have also been measured directly with line instrument and depth probes. Although cumbersome and spatially restricted, the method is considered relatively precise and more practical representation of field situations. Dasog *et al.* (1988) reported that the volume of a crack section computed by direct measurement approximate that obtained by sand in-filling. In any case, the volume is a holistic parameter to characterise crack development with changes in soil hydrology. Rivera (2008) used a geometric equation for estimation of the volume of a crack cross-section. However, some terms in the mathematical derivation were wrongly defined leading to significant error in the computation. In the present study, the mathematical derivation is

reviewed in section 3.2.4 to obtain a valid version of the equation to estimate the cross sectional volume of the cracks (4.3.2).

### 2.2.2 **Significance of soil cracking**

Soil cracking is problematic in many practices. The problems were first documented in soil science and agricultural disciplines. In agriculture, the need to improve soil structure for maximum crop yield provided the impetus for crack studies as cracks could either beneficially rejuvenate machine-compacted soils or adversely cause the by-pass flow of gases, moisture, and nutrients beyond the reach of plant roots. The presence of cracks reduces the amount of surface runoff through increased infiltration and, simultaneously water content at deeper soil layer. In addition, surface cracks can enhance soil moisture deficit through accelerated evaporation. Environmental engineering problems associated with soil cracking mainly bordered on the potential of cracks to compromise and mobilize water and leachate in impermeable clay soil barrier e.g. soil liners for landfill and waste covers. A significant increase in permeability has been reported in cracked clay liners (Anderson *et al.*, 1982; Albrecht and Benson, 2001). Cracking, therefore, have greater significance in fine-textured expansive soils due to increase permeability. The presence of cracks often reduces surface runoff by increase infiltration and, simultaneously the water accumulation at deeper soil layers. It is commonly observed that some cracks created during dry period do not completely close in wet periods, thus infiltration rate remain higher in such soils throughout the year with a net increase in the hydraulic conductivity (Novak *et al.*, 2000). In geotechnical practice, where compacted clay soils are widely used in earthworks, the increase in soil hydrology properties by cracking often results in overall degradation of the mechanical property of engineered fills with implication for increased susceptibility to slope failure. This is a common issue in instability of earthwork slopes summarized by Baker (1981) as follows:

1. Shorten the length of potential slip surface, hence facilitate shear movement
2. Hydrostatic pressure within cracks constitute additional driving force which contribute to failure

### 3. Water in the cracks softens the soil and degrades its strength properties

It is recognized that rapid pore water pressure change plays a significant role in clay slope deformation and this is linked to water infiltration in cracks (Potts *et al.*, 1997; Clarke and Smethurst, 2007; Glendinning *et al.*, 2009; Take and Bolton, 2011; Lees *et al.*, 2013). The rapid pore water pressure essentially reduces the effective stress, which tends to stabilize the slope against shear movement. Consequently, quantification of cracks occurring in slopes is an essential step in monitoring the well-being of slopes. Considering these potentials, the occurrence of cracks and increased in their rate of development can serve as an indicator of slope deterioration. Health monitoring of slope and early warning system for failures is essential to mitigate effective management strategy (Smith *et al.*, 2017).

#### 2.3 Theory of desiccation cracking

Several studies have been conducted to understand cracking in soil. Common materials used include soil slurry, gels, suspensions etc., with at least four theories of desiccation popular in literature. These are (1) Air entry (2) Packing collapse (3) Irregular drying front (4) Tensile failure. In the air entry theory, crack initiation occurs through menisci invasion on the liquid-air-solid interface due to increased capillary tension during drying (Herrera *et al.*, 2007; Brinker and Scherer, 2013). The packing collapse theory was used by Holmes *et al.* (2006) to explain desiccation cracking in alumina strip. In this case, the driving force for cracking arises from a misfit strain that occurs when repulsive layers between the particles collapse by capillary suction. The Irregular drying front theory suggests that cracking occurs in the form of failure of pore walls arising from the difference in capillary pressures from irregular drying at different points in glass gel (Zarzycki *et al.*, 1982). The tensile stress theory considers critical drying stress in soil and suggests that cracking would occur in a drying soil material when the resultant tensile stress is greater than material tensile strength. Presently, these theories are either incomplete or cannot be validated. The studies with gels, in particular, cannot be verified against the behaviour of granular materials. However, the tensile stress criterion is the most assumed model in geotechnical and related publications.

(Lachenbruch, 1961; Morris *et al.*, 1992; Abu-Hejleh and Znidarčić, 1995; Konrad and Ayad, 1997b; Kodikara *et al.*, 2000; Hallett and Newson, 2005; Péron *et al.*, 2009b). This is because it involves analysis of stress state variables enshrined in soil mechanics, with consideration of matrix suction in unsaturated soil behaviour. Important aspects of the tensile stress theory of desiccation cracking are presented in the following sub-sections. In addition, crack propagation and spacing are also discussed within the framework of fracture mechanics.

### **2.3.1 *Drying and Shrinkage Phenomena in unsaturated soil***

Drying in soil material is commonly linked to the thermodynamic imbalance between the soil moisture and the surrounding atmosphere. This condition causes transfer of fluids from the soil to the atmosphere by evaporation. During evaporation, moisture moves both in liquid and gaseous phases. The process generates a suction gradient or a negative pore water pressure in the soil surface relative to the atmosphere. The difference in head causes a capillary uplift in the liquid, which is condensed into vapour for evaporation into the atmosphere (Peron *et al.*, 2009b). Several studies involving soil evaporation have shown that water content of a soil profile decreases with depth leading to the widely acknowledged fact that evaporation proceeds from the soil surface. As evaporation proceeds, the profile of the soil show decrease in moisture with depth.

Theoretically, as vapour pressure lowers in the surrounding of the liquid in the soil, capillary pressures develop, which tend to attract soil particles. This condition results in interfacial tension across the developed meniscus. The contact phase of the pore fluids with a plane of the soil grains is shown in Figure 2.6, where  $\Theta$  is the angle between the solid surface and the fluids' interface and  $r_c$ , is the capillary menisci.

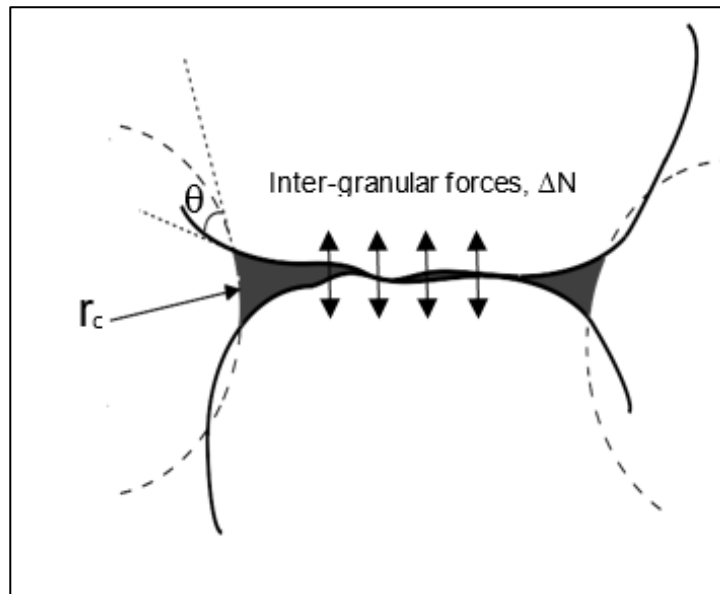


Figure 2.6: Capillary phenomena in drying soil. Adapted from Holtz and Kovacs (1981) and Péron *et al.* (2009b)

The negative pore water pressure developed around the interphase menisci is believed to act as an attractive force between the components of the matrix thereby increasing the inter-granular or effective stress compression,  $\Delta N$  in the soil mass. These conditions result in shrinkage of the soil mass with rearrangement of the particles and the aggregates as moisture evaporates. Reactive tensile stresses also develop to oppose the compressional shrinkage as illustrated in Figure 2.7.

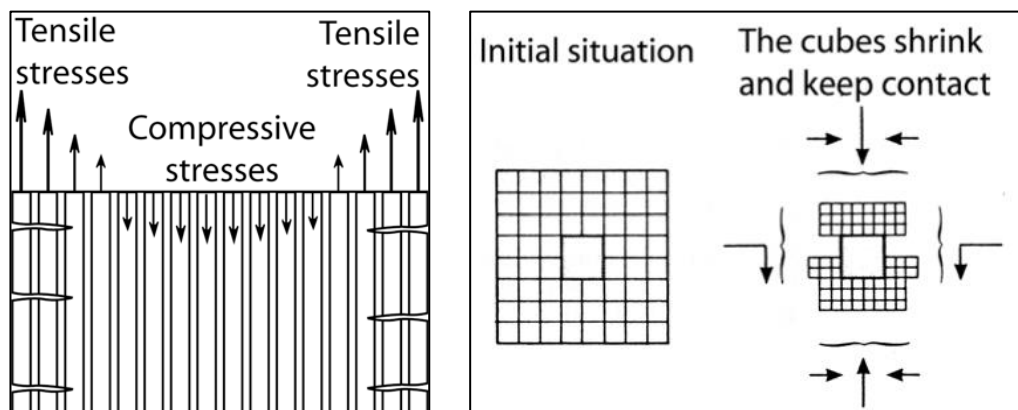


Figure 2.7: Drying shrinkage and tensile stress development in expansive soil from (Laloui and Nuth, 2009)

Croney and Coleman (1953) and Aitchison and Woodburn (1969) reported that within reasonable limits, most soils decrease in volume and water content as suction-induced shrinkage increases. Since matrix suction generally increases as soil volume and water content decreases, the tensile stress developed can be considered as proportional to the state of

soil-water suction. The magnitude of capillary pressure developed during this process depends on the pore size (effective diameter) rather than the grain size (Holtz and Kovacs, 1981). This is because capillary menisci in soil is inversely related to grain sizes. In general, the capillary pressure increases as the interfacial surface area decreases, which explains the development of very large effective stress in partially saturated clay soil. This hydro-mechanical dynamics is often treated under unsaturated soil mechanics (Fredlund and Rahardjo, 1993; Toll, 2001; Fredlund *et al.*, 2012; Sheng *et al.*, 2013).

Soil mechanics involves a combination of engineering mechanics, soil behavior, and the properties of soils. The classification is broad and embraces a wide range of soils (Fredlund, 2006). However, soils could be saturated with water or have other fluids in the voids (e.g., air). Classical soil mechanics emphasis on saturated soils whose voids are fill with water or air. This has led to a description of a single-phase stress state first introduced by Terzaghi (1943). Terzaghi's effective stress theory define stresses in any point of a section through a saturated soil mass in terms of total principal stresses, and the pore water pressure (i.e. filled with water) as shown in equation 2.11.

$$\sigma' = \sigma - u_w \quad 2.11$$

where  $\sigma'$  = effective normal stress,  $\sigma$  = total normal stress, and  $u_w$  = pore-water pressure.

There are however, several soil materials encountered in engineering practice whose behaviour is not consistent with the principles and concepts of classical saturated soil mechanics. The presence of more than one fluid phase, for example, classifies these soils as unsaturated. Unsaturated soils are therefore those soils whose voids are fill with liquids and gasses (Fredlund, 2006). Commonly, the liquid is water and the gas is air. The physical state of such soils, therefore, presents a three-phase component as schematized in Figure 2.8.

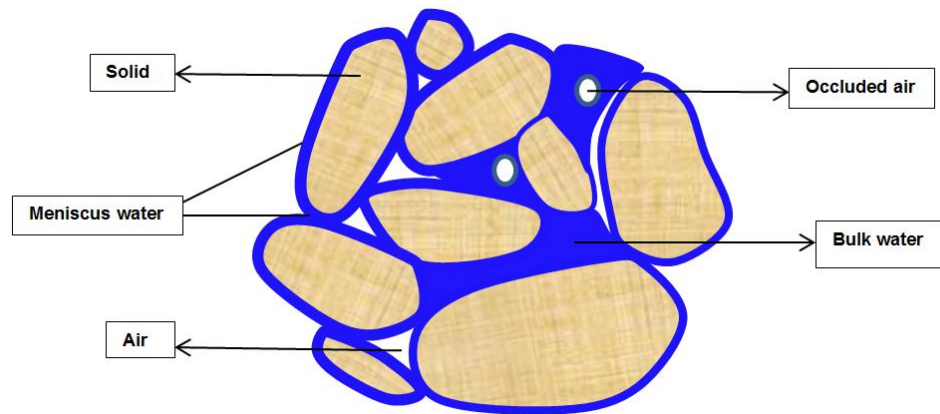


Figure 2.8: Interaction between the components of unsaturated soil

Because of the dynamic interaction between these components, pore water in unsaturated soils exists under two forms with different effects on the solid skeleton:

1. Meniscus water: water present as lenses at inter-particle contacts surrounded by dry (empty) pores
2. Bulk water: water filled pores as in saturated soils

The inter-particles water is commonly referred to as adsorb or residual water. The presence of water under these two forms is responsible for the difference in engineering behaviour of unsaturated soils and saturated soils. As the soil state changes between water-filled pores and strongly bonded inter-particle water the soil behaviour transits from saturated state to unsaturated state and vice versa. The constitutive relationship between stresses and strains in unsaturated soils was then defined in terms of two independent stress state variables, namely, the effective stresses ( $\sigma - u_w$ ) and the pore air pressure,  $u_a$  (Fredlund 2006). Because the pores are relatively open, the air pressure is assumed to be zero. Hence, the pore water pressure is characteristically lower than the atmospheric pressure. Under this condition, matrix suction,  $S$  becomes the pressure differential between air and water pressures in the soil expressed as:

$$S = u_a - u_w \quad 2.12$$

The pore-water pressure is therefore recognised as an important variable in unsaturated soils. The oldest relationship for unsaturated soils modified from the Terzaghi's effective stress concept is that proposed by Bishop

(1959). The equation is therefore referred to as Bishop's effective stress equation for unsaturated soils and has the following form:

$$\sigma'_{ij} = (\sigma_{ij} - u_a \delta_{ij}) + \chi(u_a - u_w) \delta_{ij} \quad 2.13$$

where  $\sigma'_{ij}$  is the effective stress tensor acting at a point,  $\sigma_{ij}$  is the total stress,  $\chi$  is a soil parameter related to the degree of saturation ranging from 0 to 1, and  $\delta_{ij}$  is the Kroenecker's delta. Bishop's equation therefore relates net normal stress to matric suction. If air pressure is zero (i.e. atmospheric), then suction is negative:

$$S = - u_w \quad 2.14$$

Soil shrinkage usually proceeds gradually as moisture evaporates resulting in particles aggregation by developing meniscus tension. This has enabled a categorization of volume change in clay soil during drying with corresponding interaggregate structure developed i.e. the shrinkage curve. Accordingly, four distinctive phases, progressing as the soil dries can be defined in a generalize shrinkage curve (Figure 2.9).

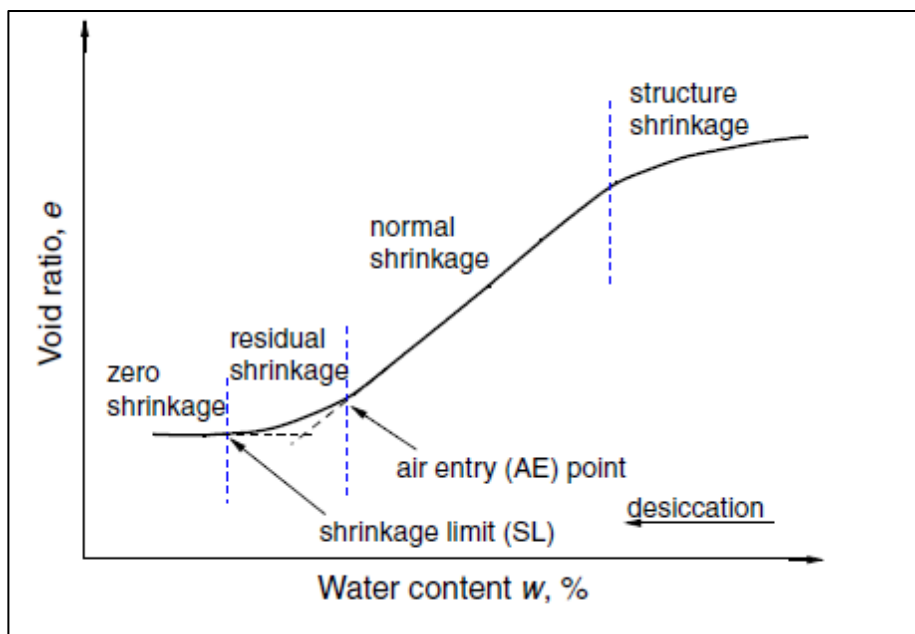


Figure 2.9: Typical shrinkage curve for clay soils (Tang *et al.*, 2011a)

At zero shrinkage, the soil does not shrink upon further drying. Normal shrinkage occurs when soil volume changes proportionally with water loss while residual shrinkage occurs at the phase of air entry into the soil and

the reduction in soil volume is less than the volume of water loss. The structural phase has similar characteristics to residual shrinkage but occurs at the wet end of the moisture range. It is associated with the removal of water from pores of coarser particles. The progressive shrinkage phases, therefore, define boundary conditions with respect to the level of saturation, which corresponds to a particular configuration of the soil hydro-structure (Figure 2.10).

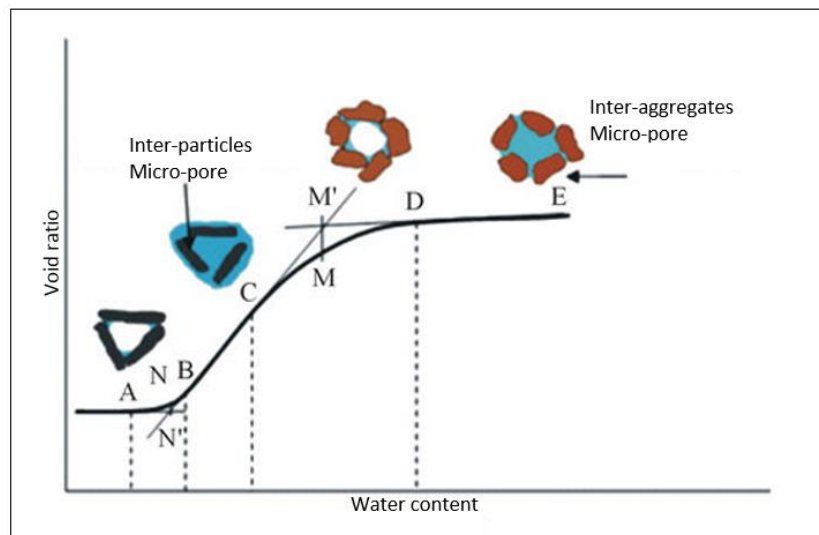


Figure 2.10: Soil hydro-structure during shrinkage (from Bensallam *et al.* (2012))

The normal and residual shrinkage presented by Tang *et al.* (2011b) are similar primary and residual drying in an initially saturated soil defined by Haines (1923). The primary drying stage involves exclusive removal of water without the ingress of air and as such, the soil remains completely saturated. The volume change, like in normal shrinkage is equal to the volume of water leaving the soil and this stage represents the period of greatest volumetric shrinkage. Further removal of water consolidates the soil until eventually, the soil particles come in contact and shrinkage slows as the clay loses its plasticity and particle aggregation stiffens. This stage is termed residual drying and essentially defines the period of air entry into the voids. Little change in the total volume of soil occurs during the residual drying due to the contact between solid particles. This suggests that total shrinkage is highly dependent on the volume of water present in the soil. A shrinkage curve is, therefore, useful in the evaluation of the active volume change during moisture loss with potential application in crack development, which this study would explore.

Lambe (1958), Gokhale and Anandakrishnan (1970), Stirk (1954) etc. showed that the actual amount of shrinkage due to drying depends on factors such as type and amount of clay minerals, soil fabric, initial water content and confining pressure. The extent of shrinkage increases with the plasticity of the soils. Therefore, for an equal amount of clay minerals in a soil, highly plastic clays e.g. montmorillonites, would undergo greater volume change upon drying and wetting than do low plastic clay such as kaolinites. Lambe (1958) reported that clays with dispersed structure shrink most while clay with oriented particles expectedly shrinks more in a direction perpendicular to the plates and least, parallel to the plates. Similarly, clays with randomly oriented particles shrink equally in all directions. Gokhale and Anandakrishnan (1970) also noted that addition of sand generally reduces shrinkage in clay soils because of increase solid contact potential. A similar result was also reported by Stirk (1954) and Kleppe and Olson (1985). Following the established hydro-structural dynamics in shrinkage of soil, the inclusion of coarse texture essentially increases the potentials of solid particles contact against shrinkage. Such experimental premise could be explored for improvement of expansive soils against excessive shrinkage deformation.

### 2.3.2 ***Shrinkage cracking***

It is widely believed that formation of cracks in the soil during desiccation is influenced by restraining shrinkage. This follows results of pioneer work, notably Lachenbruch (1961) and Corte and Higashi (1964). The early workers showed that a drying soil would shrink freely in the absence of restraints. On the contrary, when soil drying is restrained, tensile stress essentially developed in reaction to the compressive shrinkage. The potential of such stresses would vary across the soil media due to anisotropic properties. In addition, the magnitude of the induced tensile stress equals to the changes in the soil-water suction during drying.

Péron *et al.* (2009a) demonstrated the dependence of desiccation cracking on the restraining boundary in two different tests; one involving free, unrestrained shrinkage and the other, a restrained shrinkage. In the experiment, cracks only occurred in the restrained test. The explanation is that with no restraint whatsoever, the soil would shrink isotropically in full

scale without cracking. This is similar in principles to the test procedure for standard linear shrinkage limit (BS1377, 1990), where free shrinkage is enhanced by a greased soil mould, to reduce friction and prevent cracking. Using a remoulded clay bar fixed at both end (Figure 2.11:left), Towner (1987) also demonstrated that anisotropic shrinkage would occur in the width and depth orientations of the bar until tensile stresses induced in the longitudinal direction increased beyond the tensile strength, for the bar to crack.

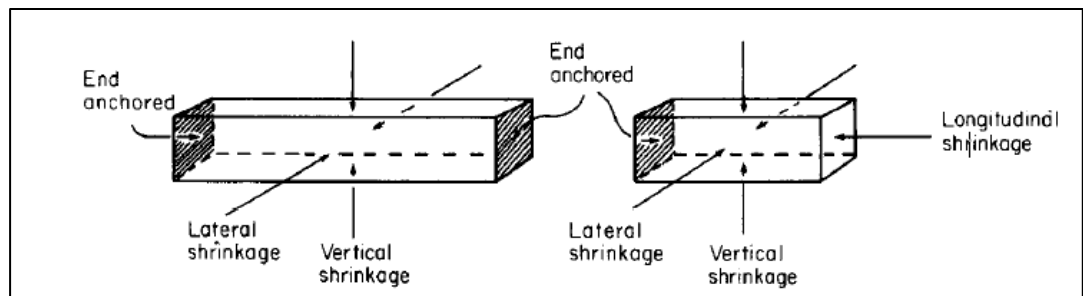


Figure 2.11: Shrinking clay bars (Left) Fixed at both ends, (Right) Fixed at one end. From Towner 1987

A second bar fixed at one end (Figure 2.11:rights) shrank in one direction similar in behaviour to the unrestrained test conducted by Péron *et al.* (2009a). This shows that the free end would only compressed towards the fixed end except opposed by equal stress induced in that plane for cracking to occur.

Restraints in soil shrinkage can be caused by different factors existing within and around the soil. External soil restraints commonly cited include physical boundary and frictional interfaces such as soil moulds used in laboratory investigations or invasive structures in the field (e.g. instrumentation, vegetation roots or buried infrastructure). Internal restraints, on the other hand, could be inherent soil properties such as soil texture and structure (e.g. inclusion of large particles), and moisture gradient brought about by inhomogeneous drying (Hueckel, 1992; Kodikara *et al.*, 2004; Hu *et al.*, 2006). In natural soil, internally generated restrain shrinkage is common.

The restraint shrinkage theory from early works lacked necessary constitutive elements. Kodikaral and Choi (2006) therefore presented a simplified physical model of the tensile cracking process of a clay layer. In this case, a clay layer represents an elastic material placed on a hard

base (Figure 2.12). The interface between the clay and the base is characterised by elastic-plastic condition, which enables prediction of maximum tensile stress that could develop in the clay for given moisture content. It also suggests that drying from the upper surface of a clay layer induces shrinkage strain within the clay, which in the presence of the base restraint, would generate tensile stresses.

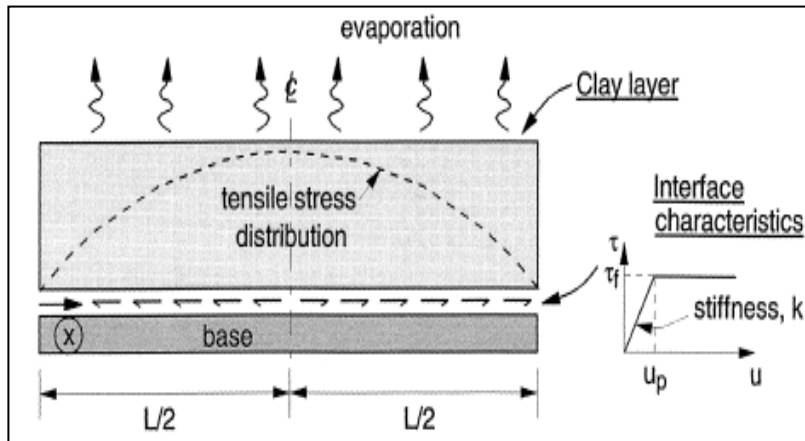


Figure 2.12: Idealised tensile failure in soil (from Kodikara and Choi 2006)

As shrinkage strain increases with desiccation, the interface is displaced in an elastic manner and the relative interface displacement ( $u$ ) can reach its peak value ( $u_p$ ) as indicated in Figure 2.12. When  $u > u_p$ , one part of the interface is assumed to be in a plastic state while the other part remains in the elastic state. A fully elastic interface condition would, therefore, develop when  $u \leq u_p$  while an elastic-plastic condition suffices when  $u > u_p$ . The model predicts that due to restraints provided at the basal interface, maximum tensile stresses would develop at midsections of the clay layer (i.e.  $x = L/2$ ). When the maximum stress exceeds the tensile strength of the clay, it is presumed that a crack would develop through the clay layer and precisely at the centre. While the model correctly represents the mechanism at the clay interface during drying, the prediction of the location of cracking appears to be more applicable to homogeneous elastic materials considered mainly in fracture mechanics. However, in soil materials, which are plastic and commonly heterogeneous, the textural characteristics could significantly influence the random appearance of cracks. This study would provide an opportunity to validate this position.

From above review and discussion, it is clear that soil desiccation is a set of processes that include drying, shrinkage and cracking. The cracking is a

consequence of soil tensile strength mobilization as suction increases in reaction to compressive forces of shrinkage. It means as a saturated expansive soil loses water to become unsaturated, the matrix suction inside the soil body increases at the same time. This cause the soil to shrink and deform, accompanied by a build-up of tensile stress, which gradually becomes strained the soil. That is to say, the deformation of the soil is because of the strain induced by tensile stress, which results from the increase of matrix suction after water loss of the soil. Therefore, in partially saturated soils, shrinkage strain can be visualised because of effective stress increase, which entrenches contributions of externally applied stress and internal pore fluid pressures. This implies a combination of mechanical and hydrological components. Essential, micro-fissures in the soil may begin to crack when the strain reaches limit deformation i.e. shrinkage strain > maximum tensile strength or matrix stiffness.

### 2.3.3 Air entry value and crack initiation: Soil water retention curve

In many crack related experiments conducted with fully saturated clay mass, crack initiation has been observed around the period of air entry in the soil. This has led to a common hypothesis that shrinkage can occur while the soil is still saturated (slurry), and defects and air-filled pores may act as crack initiators in soils. In line with this hypothesis, Péron *et al.* (2009b) carried out a desiccation experiment using three different soils. Their results showed that in all cases, the cracks initiated near air entry value when the soils were at about 95% saturation as presented in Figure 2.13.

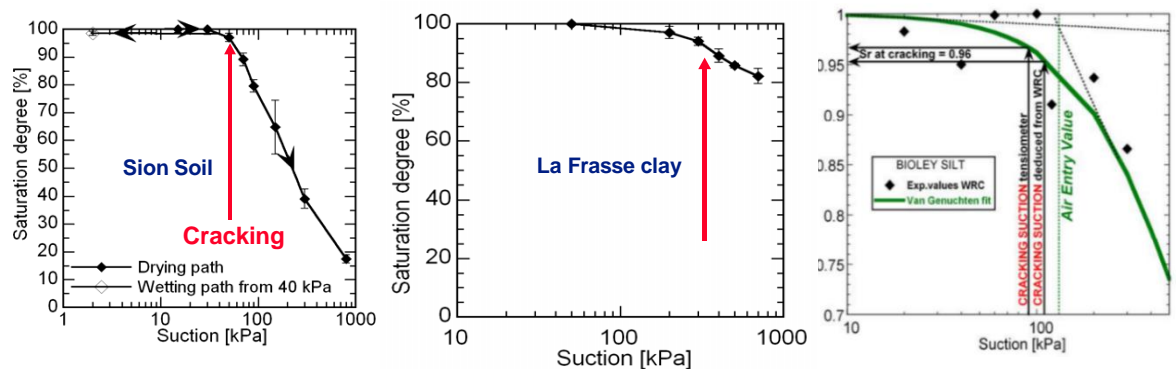


Figure 2.13: Crack initiation near Air entry value at saturation (from Peron *et al.*, 2009b)

A state of full saturation in soil essentially implies that water occupies all the voids (i.e. no occluded air or gas). However, as the solid particles draws closer, a significant magnitude of matrix suction would develop by a small reduction in the water content. The negative pressure developed in the soil would attract atmospheric air to the soil-water interface (Shin and Santamarina, 2011). Desaturation advances from the macropores because the smaller pores support menisci of smaller radii meaning higher water tension. According to Péron *et al.* (2009b), at this early stage virtually no air enters the soil until a critical capillary head or suction is reached. This point commonly defines the air entry value (AEV). When air begins to enter the de-saturated macropores, the drying front gradually increases as illustrated in Figure 2.14. This creates drain zone at the soil surface, which can be viewed as structural defects for crack initiation.

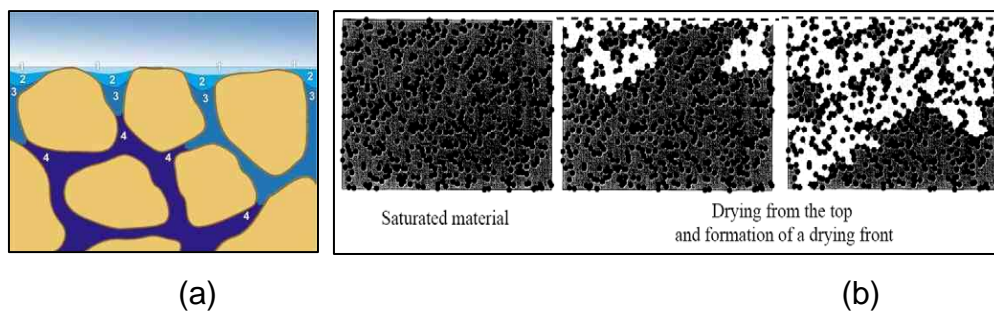


Figure 2.14: Air-water interface in porous media (a) drainage during drying processes and (b) advancing drying front. From (Fredlund and Rahardjo, 1993) and (Péron *et al.*, 2009a)

The progressive soil-water-suction dynamics in a saturated drying soil media leading to initiation of cracks during desiccation was also described by Tang *et al.* (2011b) as shown schematically in Figure 2.15.

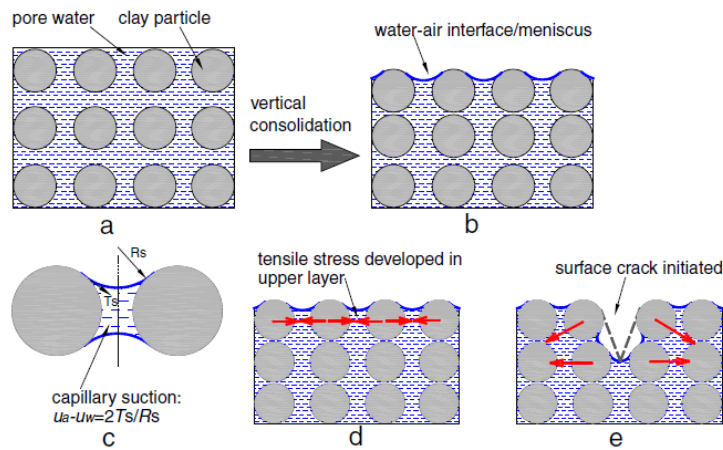


Figure 2.15: Schematic drawing of soil crack initiation process under saturation (a) Initial fully saturated soil; (b) water–air interface meniscus developed between soil particles; (c) capillary suction between soil particles; (d) tensile stress developed in the upper layer; and surface crack initiated (from Tang *et al.* 2013)

In addition, Tang *et al.*, 2013 showed that when suction exceeds AEV, water content rapidly decreases within a relatively narrow range of suction before reducing at a gradual rate. The latter condition happens when suction increase beyond the residual water content of the soil. Therefore, at high suctions the residual water remains in the form of immobile, pendula rings in the micropores. At this stage, a proportionately large amount of suction can only mobilize a relatively minor removal of water with no net effect on shrinkage. This corresponds to zero shrinkage. Suction as high as 1,000,000 kPa has been predicted beyond this stage for a variety of soils (Fredlund and Rahardjo, 1993). However, most natural and engineered soil presents non-uniform grain sizes and textures. These would lead to differentials in the capillary pressure acting between any two points in the soil. Therefore, the air entry and irregular drying front theories of desiccation can be combined to give a complete explanation of the mechanism of cracking in the soil.

Considering the different state of moisture attained in a drying soil from a fully saturated condition, soils in an unsaturated state would have very high AEV. This also implies a high potential for cracking would exist in the initial condition of such soil. However, cracks are widely observed to occur within a narrow range of moisture change when suction is relatively small. This is of interest since, from the foregoing hydro-mechanical standpoint, very large suction should lead to "intensified" cracking. This study is interested in further examining this condition. Near surface moisture and

suction changes in the embankment during soil cracking is marked for a comprehensive characterization.

#### 2.3.4 **Fracture theory and crack propagation in soil**

The mechanism of soil cracking has also been approached from the framework of linear elastic fracture mechanic (LEFM). Fracture mechanics is concerned with the study of the propagation of cracks in materials. It was developed both in the field of analytical solid mechanics to calculate the driving force in a crack and in experimental solid mechanics to characterize the fracture resilience in brittle materials. In this framework, the presence of microscopic flaws in a bulk material and the stress concentration at the tip of such flaws are considered as a source of energy for the intergranular displacement (propagation) in a linear elastic material. This approach follows pioneer work by Griffith (1921). A flaw in this sense can be micro fissures, air or bubbles, large particles, surface texture etc.

Analyses of stress state variables in desiccation studies carried out mainly in circular and rectangular moulds suggest that cracks are likely to initiate at/or near the centre of the drying soil mass. This is because tensile stress is considered to be highest at the centre of such geometrical moulds (Nahlawi and Kodikara, 2006; Amarasiri *et al.*, 2011; Varsei *et al.*, 2014). However, in some cases, cracks initiation have been showed to occur in other indiscriminate locations away from the centre of the soil mass as depicted by crack number three in Figure 2.16.

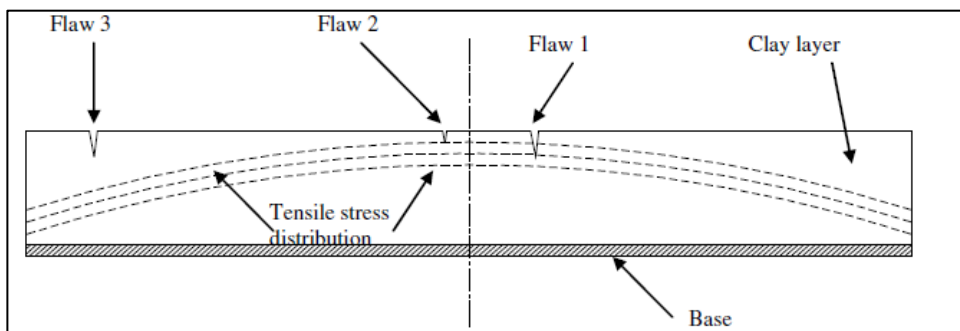


Figure 2.16: Combine influence of stress and flaws in crack initiation (from Costa *et al.*, 2013).

This is can be influenced by flaws at this location. Such features essentially constitute isolated points of tensile stress concentration. In LEFM, it is assumed that crack would first initiate at a location of micro flaws. The tensile stress required to activate a flaw is inversely

proportional to the square root of the flaw size. This hypothesis underscores the importance of textural flaws in the crack process.

In order to analyse crack propagation after initiation from a site of flaw, two approaches are commonly advanced in LEFM analysis; the “energy criterion” and the “stress intensity” approach (Anderson and Anderson, 2005; Pook, 2007). In the energy criterion, crack propagation is likely to occur when the energy available for crack growth is sufficient to overcome the resistance of the material. The material resistance may include the surface energy, plastic work, or other types of energy dissipation associated with a propagating crack. Thus, for a crack of length  $2a$  in an infinite plate subjected to a remote tensile stress (Figure 2.17), the energy release rate is given as:

$$G = (\pi\sigma^2 a)/E \quad 2.15$$

Where  $E$  is Young’s modulus,  $\sigma$  is the remotely applied stress, and  $a$ , the half-crack length.

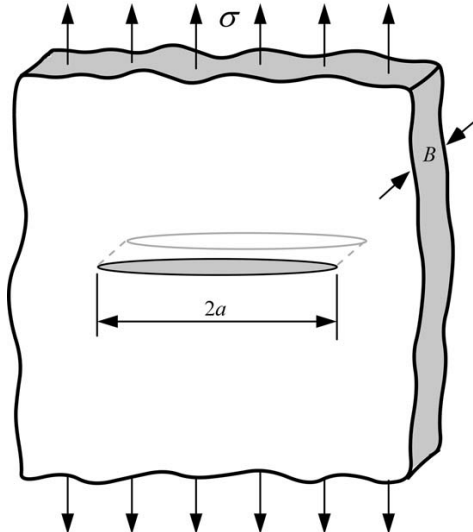


Figure 2.17: Crack in an infinite plate subject to a remote tensile stress. “infinite” practically means the width of the plate is  $\gg 2a$ . From (Anderson and Anderson, 2005)

At a point of fracture, the energy release rate equals the strength of the material, hence equation 2.13 can be rewritten to describe the critical combinations of stress and crack size at failure:

$$G_C = \frac{\pi\sigma_f^2 a_c}{E} \quad 2.16$$

Anderson and Anderson (2005) noted that for a constant value of  $Gc$ , failure stress  $\sigma_f$  varies with  $1/\sqrt{a}$ . The energy release rate,  $G$  is, therefore, the driving force for fracture, while  $Gc$  is the material's resistance to fracture.

In the stress intensity approach, stresses and displacements near the crack-tip are described by a single constant that relates to the energy release rate. Consider an elastic stress distribution and the in-plane stresses in the vicinity of the crack tip, the crack tip fields are express in terms of cylindrical-polar coordinates  $(r,\theta,z)$  with origin at the crack tip as shown in (Figure 2.18).

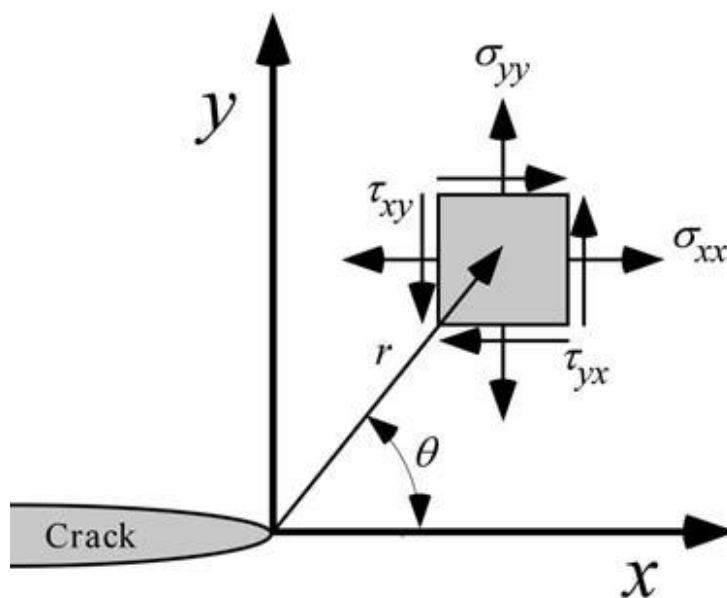


Figure 2.18: Stresses near the tip of a crack in an elastic material. (Anderson and Anderson, 2005)

Each stress component is proportional to a single constant  $K_I$ . This crack-tip characterizing parameter later became known as the “stress-intensity factor” (Irwin, 1997). It is presumed that if the material fails locally at some critical combination of stress and strain, then fracture must occur at critical stress intensity  $K_{IC}$  known as “stress intensity factor” i.e. failure occurs when  $K_I \geq K_{IC}$ . In this case,  $K_I$  is the driving force for fracture while  $K_{IC}$  is a measure of material resistance or fracture toughness. Thus, the energy and stress-intensity approach to fracture failure are essentially equivalent for linear elastic materials and reasonably compare with the critical strain condition of Kodikara and Choi (2006) presented in section 2.3.2 above.

Factors such as mode of cracking, orientation and size of cracks etc., affect the stress intensity factor. In practice, three possible modes failure is recognised as shown in Figure 2.19. Fracture mechanics presumes that a crack in a material propagates in a plane perpendicular to the axis of maximum stress (path of lowest strain energy). This implies that cracking in soil is a mode I failure since it is characterized by a tensile opening.

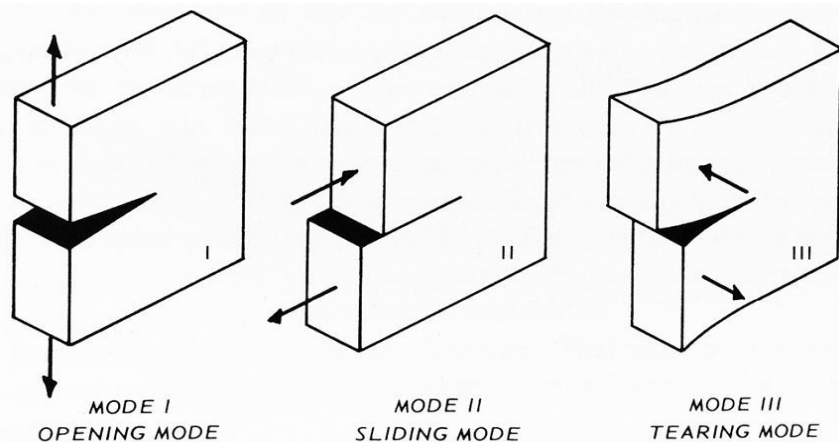


Figure 2.19: Fracture failure modes. From Pook (2007)

Early attempts to apply LEFM in soil cracking were not considered valid mainly because the soil is a nonlinear plastic material and cracks can occur in soil near full saturation. However, as a drying soil gradually attain a quasi-brittle tensile state, it seems justified to apply fracture mechanic principles in explaining crack propagation in particular. In addition, the later development of elastic-plastic theories has enabled a wider application of this failure concept to a wetter and more plastic material state (Prat *et al.*, 2008; Lakshmikantha *et al.*, 2012). Notwithstanding, application of LEFM principles in modelling crack properties in soil is increasing in recent research (Amarasiri *et al.*, 2011; Kodikara and Costa, 2013; Stirling *et al.*, 2013; Juárez-Luna and Ayala, 2014).

### 2.3.5 **Field and laboratory methods in the study of desiccation cracks**

Field and laboratory studies have been carried out in the past to investigate desiccation cracking in fine-grained soils. The laboratory methods investigate crack formation in different conditions of drying, sample sizes, thicknesses and engineering properties. Approaches range from tests in small compacted samples and slurries (Shorlin *et al.*, 2000; Kodikaral and Choi, 2006; Péron *et al.*, 2009a; Tang *et al.*, 2011a; Lakshmikantha *et al.*, 2012) to the thick, more engineered representatives

(Yesiller *et al.*, 2000; Zieliński, 2009), with some involving wetting and drying cycles to simulate environmental fluctuations. The variability in atmospheric conditions also informed the use of climate chambers in some studies (Nahlawi and Kodikara, 2006; Péron *et al.*, 2009a; Zieliński, 2009; Uday and Singh, 2013). To measure the environmental and soil parameters, selected instruments are employed e.g. Theta probe, tensiometer, hygrometer, infrared temperature sensor, dew point potentiometer. Instruments for measurement of soil moisture and suction are commonly inserted in the soil, some directly on the surface, which sometimes induced artificial cracking. In order to avoid such challenges and increase accuracy, non-invasive methods are used in some laboratory studies. The most common in this category is electrical resistivity (Samouëlian *et al.*, 2003; Samouëlian *et al.*, 2004; Zieliński, 2009; Hassan and Toll, 2013; Hassan and Nsaif, 2016). Electrical resistivity of a material describes its ability to resist the flow of electricity. The presence of cracks results in high resistivity contrast between the intact soil and the highly resistive air-filled cracks. Another emerging non-destructive method used in the laboratory studies is laser scanning. Sanchez *et al.* (2013) and Zielinski *et al.* (2014) demonstrated that 2D/3D scanners can effectively capture cracking in small samples. The set-up, which includes a computerized motion controller and electronic balance, provides information on volume change, crack depth, aperture and geometry.

The laboratory studies have proved useful in identifying the key factors influencing soil cracking and the development of theories of the mechanism (Kodikara *et al.*, 2000; Kodikara and Choi, 2006). However, a theory needs to be tested and verified in nature and desiccation cracking involves complex atmospheric conditions and presence of vegetation (Li and Zhang, 2011). Therefore, other studies of this type are conducted in the field. Notable field studies on desiccation cracking include Zielinski (2009), Dyer *et al.* (2009), Li and Zhang (2011). Dyer *et al.* (2009) and Zielinski (2009) investigated the development and effects of desiccation fissuring in flood embankments across the UK. On-site excavations of trial pits showed the upper embankment layer is transformed into a rubbilised zone by an interconnected network of cracks, with implications for

formation of breach failure in this type of earthen structure. Li and Zhang (2011) on the other hand investigated desiccation cracking in a backfill slope aimed to understand the mechanism from initiation to full development. The study suggests that a critical moisture condition exist during cracking and cracks are repeatable under drying-wetting cycles. Cordero et al. (2016) combined field and laboratory approaches where a large bespoke soil container filled with about 18000kg (~ 4.5m<sup>3</sup>) of silty clay was exposed to drying under natural atmosphere. The method was adopted to compare laboratory and field measurements. Due to the large volume of soil involved, the experiment took one year to run under the slow natural drying.

Other field procedures measured changes in soil water content and pore water pressure, which are important parameters in desiccation crack development and for the stability of slopes (Ridley *et al.*, 2004a; Li *et al.*, 2005; Smethurst *et al.*, 2006). However, manual field measurements are time consuming, costly and in some cases, destructive e.g. measurement of cracks. Therefore, like in the laboratory, innovative methods of investigations are emerging to solve these challenges. Utili *et al.* (2015) introduced a novel approach for monitoring the state of earthen slope in a cost effective and non-destructive way. The method employs a suite of standard geotechnical probes which measure soil water in limited locations in the embankment. These validated measurements are then used as reference to extrapolate the water content distribution at any other point and time in the embankment. Details of this extrapolation are found in Utili et al. (2015). However, in order to improve the accuracy and provide a spatially continuous monitoring, Utili *et al.* (2015) further integrated the geotechnical measurements with geophysical measurements from a portable electromagnetic probe. The latter involves a walk over, non-invasive electromagnetic probing, which relates ground electrical conductivity to the soil water content. Since the geophysical measurements are also recorded spatially, the water content records are therefore linked to the water content distribution of the geotechnical suite, with a susceptibility index which provides a qualitative indication about which zones of the embankment are likely to fissure. In the absence of

techniques that can directly detect cracks in vegetated slopes, this method seems promising in practice including cost effectiveness and capacity for long-term monitoring.

### **2.3.6 Influencing factors in desiccation cracking of soil**

Early studies on soil cracking were mostly conducted in agriculture, soil science and geology disciplines with the work of Kindle (1917) on mud cracks commonly referenced as pioneering. The existing studies showed the influencing factors in desiccation cracking of soil depend on the properties of soils and boundary conditions surrounding the desiccating layer. The soil properties experimentally proven as influencing soil cracking includes fines content, Atterberg limits, mineralogy, moisture content, tensile strength and density. On the other hand, boundary conditions affecting cracking include temperature, humidity wind velocity size of the sample of soil, the roughness of the base material, gradient, thickness of the soil layer, solar radiation and the cycles of wetting and drying etc., which are mostly external factors. A review of the influence of these factors is given as follows:

#### **Soil tensile strength:**

From the stress state principles generally advanced for crack initiation, it is reasonable to state that tensile strength of soil is a limiting condition in desiccation cracking process. However, tensile strength is commonly assumed as zero or negligible in engineering practice due to its relatively small values compared to shear and compressive strength. However, with its exceptional role in desiccation behaviour of soils, workers have attempted to evaluate this property experimentally.

Currently, there is no standard method for measuring tensile strength in the soil. Instead, workers have adapted different methods and formulation to determine this parameter. The procedures commonly involve uniaxial application of tensile loads to quasi-brittle soil samples with the load applied either vertically (e.g. 'gripping' or 'torn apart' tools) or horizontally. The triaxial device has also been used in the former case. More recent works, notably Trabelsi *et al.* (2012) and Stirling (2014), applied horizontal displacement using bespoke devices commonly adapted from direct shear

equipment. Accordingly, Stirling (2014) modified a direct shear box equipment to measure the tensile strength and stiffness of soil for a range of water contents. The bespoke device consists of a pair of specially designed sample carrier jaws mounted in the shear box (Figure 2.20). One jaw was restrained while the other was made a free carriage. A median brace was used to check effects of cantilever movement in the carriage jaw. The sample was also made into a unique bow-tie shaped to constrain it and induce failure at its centre due to the reduced cross-sectional area.

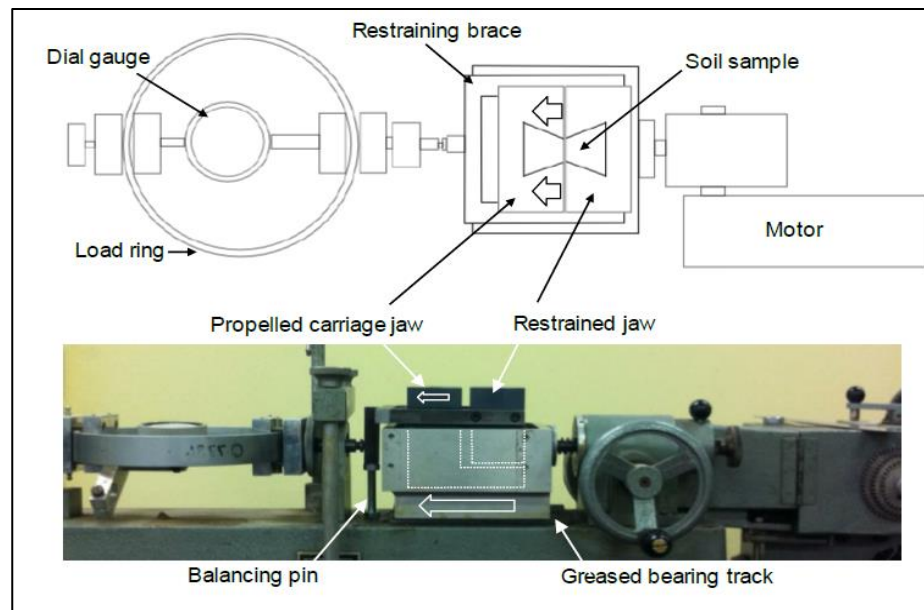


Figure 2.20: Bespoke soil tensile strength test apparatus (from Stirling 2014)

In this setup, the load is transferred evenly through the cross-section, and the peak load experienced by the sample over the area of fracture practically represents the soil tensile strength. Using tests results from the device, Stirling (2014) showed an equation for the ultimate bond strength of soil, ( $\sigma_t$ ) as a function of water content ( $w$ ) as follows:

$$\sigma_t = 228.85e^{-0.14w} \quad 2.17$$

The relation derives from the soil mechanics principles which indicate that tensile stress result as suction develops in a soil-water system. Bond strength is, therefore considered in terms of effective stress arising from particles aggregation during drying.

Another device which measures the tensile strength of soil based on the application of horizontal load was adapted by Varsei *et al.* (2014). The apparatus consists of a rectangular shaped soil box with two equal parts (Figure 2.21). One part was fix in position while the other was made to move freely on ball bearings, typical of a direct shear assemblage.

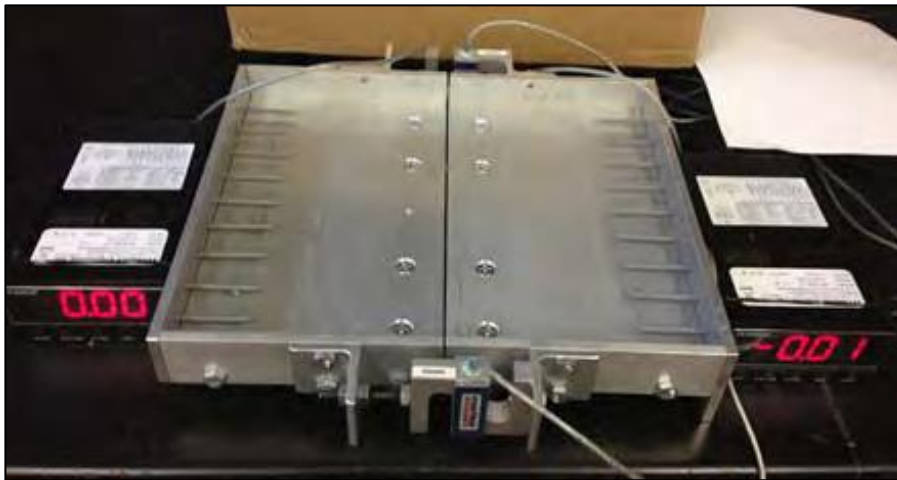


Figure 2.21: Desiccation Box/Tensile load device. From Varsei *et al.* (2014)

To measure tensile forces generated in the drying specimen, two load cells were attach to the box where the parts join. A Teflon sheet placed under the soil bed minimizes friction between the base of the box and the specimen, such that tensile loads developed in the desiccating soil are measure directly by the load cells. Since the mechanical property of soil represented by tensile strength is changing with changes in the water content, the development suggests a possible change in the profile condition. In the present study, estimation of the critical moisture and suction at cracking is considered.

#### **Effect of fines content and plasticity:**

Soil plasticity is a direct reflection of the type and amount of clay mineral present in a soil. It is an important property influencing the engineering behaviour of expansive soils, the shrink-swell behaviour principally.

Mitchell (1993) observed that fine-grained soils are more susceptible to the development of cracks than coarse-grained soils due to the development of higher suction in their smaller pores. From the concept of capillary tension, small pores mean large specific surface area for water bonding. Associated with this is the large shrinkage that can be obtained in very high plastic soils. Consequently, the presence of highly active clay

minerals in larger quantities can potentially lead to greater cracking than soils with less active clay minerals and a lower percentage of clay size particles. Similar findings were made by Tang *et al.* (2008), Albrecht and Benson (2001) and Yesiller *et al.* (2000).

The plastic behaviour in soil is also affected by water content and coarse inclusions. In a field study carried out in some plastic soils around the dry climate region of Australia and Canada, Morris *et al.* (1992) observed that at a selected strength level, high plasticity clays contained more water than low to moderate plasticity clays (otherwise called lean clays due to higher percentage of silt and sands). They also observed wider and deeper cracks in the plastic clays than in the lean clays. This is because plastic soils experience larger volumetric contractions on drying due to the wide range of moisture held in the clay surfaces when released. This would result in increase effective cohesion and tensile stress. The coarser soils on the hand exhibit relatively lower cohesion due to the larger voids, which as a rule, drain rapidly and prevent the reasonable development of tensile forces. Capillarity would be small in gravels and sands containing little fines hence suction is limited. Therefore, sand inclusions potentially inhibit shrinkage, even in very active clays as experimentally established by several workers including Stirk (1954), Gokhale and Anandakrishnan (1970), Kleppe and Olson (1985).

#### **Soil Density (Compaction):**

The properties of cracks formed in experiments conducted with slurry and compacted clay often showed characteristics difference. This has led to a hypothesis that cracking in soil is not only influence by fines content and plasticity but also by the density. Albrecht and Benson (2001) reported that both compaction effort and compaction water content play a significant role in this regards. Compaction is a process of soil densification by removing air voids by mechanical means. Essentially, the soil strength improves as unit weight increases by compaction. Compaction conditions would affect the desiccation behaviour of cohesive soils primarily due to the effect of compaction on intrinsic soil properties such as soil structure, hydraulic conductivity etc. Dry of optimum the soil fabrics flocculates, while wet of optimum they become more oriented or dispersed as pore water

pressure is increased. Practically, soil samples compacted wet of optimum would have highest shrinkage potential. Consequently, the resulting soil structures could influence cracking in a soil. Fang and Daniels (2006) showed that flocculating and dispersive structures create different cracking patterns, with a flocculated structure tending to produce larger crack areas than the dispersive structures (Figure 2.22).

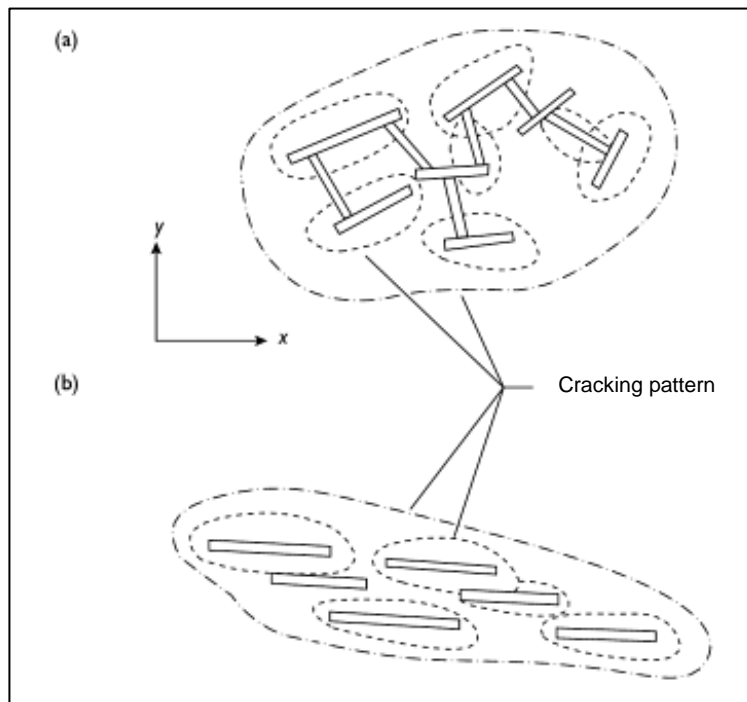


Figure 2.22: Schematic of the effect of soil structures on cracking patterns. (a) Flocculated structure, and (b) Dispersed structure (from Fang and Daniels, 2006)

On a macroscopic level, this behaviour can be linked to greater shrinkage anisotropy potential in flocculated structure. The orderly arrangement of the dispersed structure enables isotropic volume change. Although the volume can be large being one directional, the potential for cracking is low. This is significant when considering the compaction condition in earthwork construction whose aim is either to avoid excessive drying or excessive pore water pressure. Hence laying condition can be dry or wet of optimum moisture content depending on the prevailing environmental conditions. Compaction of clay fills wet of optimum results in a dispersed structure. This would prevent excessive swelling on further wetting but could exhibit a relatively large shrinkage on drying due to the large moisture loss. Inversely, clay fills compacted dry of optimum results in flocculated structure. This condition would tend to exhibit high swelling on further wetting but relatively small shrinkage on drying due to low moisture

condition in the soil. Most soil materials used in earthwork construction in the UK favours embankment placement in a moisture state that will prevent excessive swelling (i.e. slightly wet of optimum). However, evolving warmer climate has given serious concern on the performance of these structures, particularly with excessive shrinkage envisaged. Therefore, this study, which examines cracking potential in desiccating clay slope, would contribute to this contemporary issue.

Other experiments involving compacted clay have reported contradicting results with respect to potentials of cracking. Miller *et al.* (1998) conducted desiccation experiment on compacted clay soils with low plasticity and recorded large values of crack width and depth in the specimen compacted dry of optimum. This tends to contradict common views that desiccation cracking may not be significant for low plasticity soils and more likely for soils compacted wet of optimum water content than soil compacted dry of the optimum moisture content. A possible inference from this disparity is that soil cracking is not limited to any given sets of hydro-structural conditions. Therefore, every practical clay soil and environmental condition needs to be investigated for cracking potential as this study sought to establish.

#### **Temperature and rate of desiccation:**

Temperature is one of the most widely studied variables in soil cracking research. This is mainly because the temperature is a key factor in the thermodynamics of moisture exchange between the soil and its surroundings. Experimental evidence of temperature effects in desiccation crack process abounds in literature. Tang *et al.* (2008) conducted a desiccation experiment at three different temperatures (30°C, 40°C, and 50°C) and showed that the average length, width of cracks, and area of aggregates increased with increasing temperature. In a related study, Tang *et al.* (2010) further showed that cracking water content and rate of water loss also increases with temperature as shown in Figure 2.23.

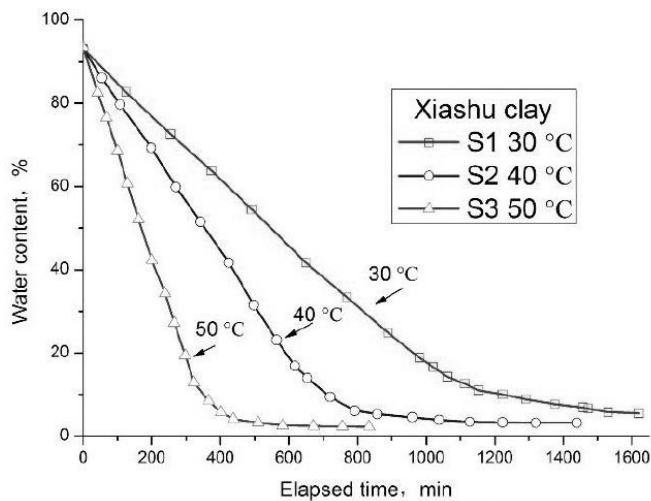


Figure 2.23: Changes in water content with time under different temperatures (from Tang *et al.*, 2010)

From various desiccation curves, Tang *et al.* (2011b) identified two distinct phases of evaporation in a fully saturated soil namely, constant evaporation stage and falling evaporation stage (Figure 2.24a). In the constant evaporation stage, water content decreases linearly with time and changes the gradient to a subsequent stage of falling evaporation during which water loss slow gradually towards the residual water content. The first and last stage corresponds with the stage of primary and residual drying and is characterized by the removal of free and bonded water respectively. Desiccation crack is presumed to form at the time of primary drying close to the air entry value (Haines, 1923). However, compacted soils mainly exhibit unsaturated condition, hence their desiccation curves do not clearly exhibit the normal evaporation boundaries observed in flooded soils. Instead, the falling head evaporation dominates the profile as shown in Figure 2.24b from Nalhawi and Kodikara, (2006). Due to increased dry voids in compacted soil, AEV would be very high and the available moisture increasingly tends towards tightly held residual moisture, or more specifically adsorbed water in clays. This caused the rate of evaporation to slow.

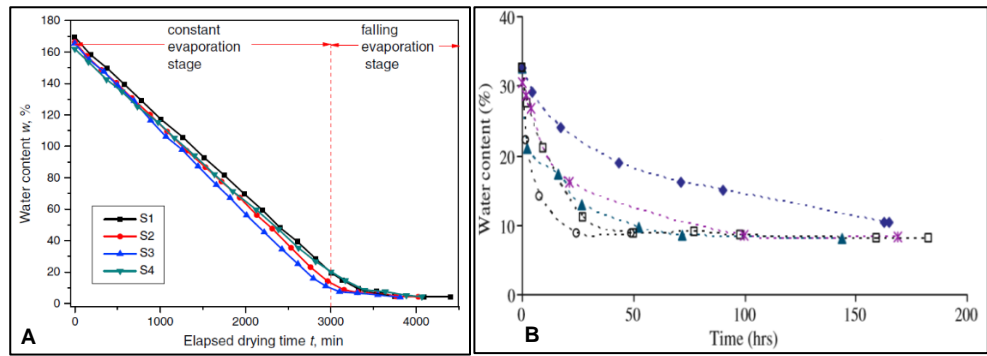


Figure 2.24: Stages of evaporation during soil desiccation (a) Slurry soil (b) Compacted soil (from Tang *et al.* 2011, Nahlawi and Kodikara, 2006)

In a related experiment, Kodikara *et al.* (2000) also showed that cracking water content decreases as temperature affected desiccation rate increases (Figure 2.25).

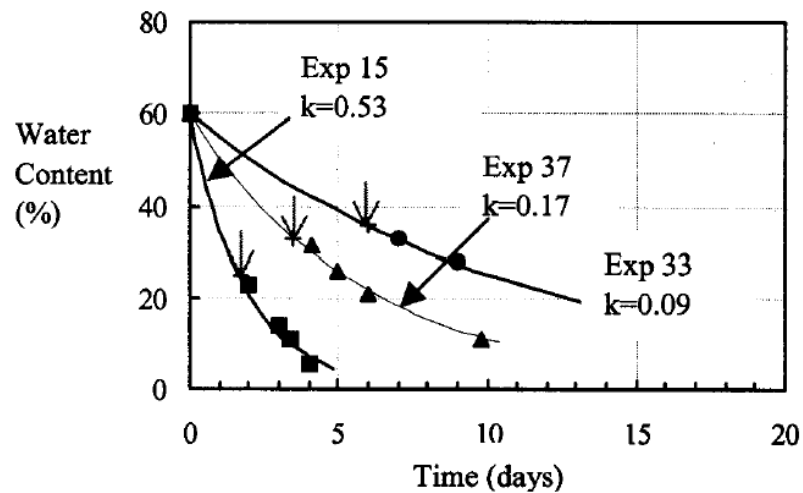


Figure 2.25: Profiles of desiccation in soils; cracking water content indicated by vertical arrows (from Kodikara *et al.* 2000)

Desiccation rate defines the decrease in water content of the soil with respect to time. From experimental results, Nahlawi and Kodikara (2006) define desiccation rate as a function of a dimensionless factor known as desiccation coefficient:

$$k(w - w_r) = (w_i - w_r)e^{-kt} \quad 2.18$$

Hence

$$\frac{dw}{dt} = -k(w - w_r) \quad 2.19$$

where  $w_i$  is the initial water content,  $W$  is the water content at desiccation time  $t$ , and  $w_r$  is the residual water content at the final stage. The desiccation rate is defined by  $|dw / dt|$  and  $k$  is termed desiccation coefficient ( $1/[T]$ ), a dimensionless parameter representing desiccation rate. The formation of the crack pattern and the intensity of cracking have been associated with the rate of desiccation. Kodikara *et al.* (2000) reported that when the rate of desiccation is high, cracks form simultaneously. This essentially arises from more uniformity in the drying of the soil surface. This premise also supports another common association of shallow, closely spaced cracks with rapid desiccation. Conversely, slow rate of desiccation potentially creates enough time for primary cracks to systematically developed and exert control on intersections of secondary cracks. This could also explain the association of deeper, widely space crack observed with a slow rate of desiccation. Furthermore, early authors notably Corte and Higashi (1960), Lachenbruch (1961) etc. considered soil cracking as a coalescence of micro cracks at a point in a soil mass proportional to the stress state at any given desiccation time. Therefore, when the desiccation rate is high, the time duration for crack coalescence at particular moisture content or tensile stress is low. This leads to the condition that lower cracking water content, hence higher tensile stress is a needed to initiate cracks when the desiccation rate is higher. The resultant crack distribution would be simultaneous once this critical condition is reach.

Another important understanding from analysis of desiccation rate is that cracks occur at different moisture content for a given soil as temperature conditions vary. This experimental observation suggests a rather interesting difference with the theoretical basis. The original theory of stress state variables for cracking imply that as far as suction is a function of water content in a soil mass, then crack would initiate at the same water content for any given soil irrespective of the test condition. Therefore, soil cracking remains a phenomenon that leaves much to understand, and this study seeks to contribute to existing knowledge.

**Soil layer thickness:**

Soil layer thickness is another factor investigated on soil cracking. Soil layer thickness and cracking is particularly significant in the performance of clay liners and covers where cracks can compromise the integrity of the impermeable cover constructed mostly with thin clay layers. Tang *et al.* (2008) prepared three soil thicknesses (5mm, 8mm, and 11mm) to test their effect in shrinkage crack development. In their results, the number of crack intersections, segments, the average width of crack, average area of aggregates and crack intensity all increased as the thickness of the soil layer increased. The same trend is reported by Kodikara *et al.* (2000) and Nalhawi and Kodikara (2006) showing increase in mean cell area with increased soil thickness. The increase crack intensity in thick soil computed to inverse trend in total length of cracks per cell area. Generally, thick soil layer slows desiccation rate due to the longer distance moisture have to travel for evaporation at the surface. This would lead to soil water content trending inversely with depth and concurrently, a suction gradient. Hence, a significant change in the mechanical profile exists in thick soil leading to a greater stress condition for cracking.

**Wetting and Drying Cycles:**

The recognition that natural soil experiences diurnal and seasonal changes in hot and wet weather justify investigation of the effect of wetting–drying cycles on their shrink-swell behaviour in general and cracking in particular. It is widely observed that near surface clay layers subjected to multiple cycles of wetting and drying undergo structural changes, which can significantly affect the soil properties e.g. soil strength, water retention characteristics, hydraulic conductivity etc.(Yong and Warkentin, 1975; Kodikara *et al.*, 1999; Tang *et al.*, 2011a; Tang *et al.*, 2016). The effects attributed to a possible re-arrangement of the soil particles as moisture condition fluctuates. A re-arrangement in soil particle essentially affects pore space distribution and the water retention capacity because of concurrent soil-water suction changes. An expansive soil experiences structural shrinkage as the particles draw closer into a stronger bond during drying. Subsequent wetting would increase the voids in the soil as the strong bonds are potentially broken and the wetted

particles separated under a relax menisci. This leads to the formation of aggregates. Figure 2.26 depicts dis-aggregation and cracking of an originally homogeneous soil after wetting and drying.



Figure 2.26: Homogenous to aggregated structure (Left to right) and volume change in a soil after 3 wet-dry cycles. From (Tang *et al.*, 2016).

Soil shrinkage and swelling, therefore, leads to increasing of weak zones, cracking and decrease in water retention capacity. The hydraulic conductivity increases while the overall soil strength decreases. The effect of wetting and drying on cyclic shrink-swell action and pore water pressure fluctuation is a significant factor encountered in instability of clay base slopes.

In some cases, however, it has been noted that a reduced potential in shrink-swell can occur with increase wetting and drying cycle. This means fabric re-arrangement can diminish or eventually reaches equilibrium with implication for a stable soil structure. A common hypothesis in soil research is that as wetting and drying continues in expansive soils, the particles are either re-orientate to attain a potential minimum energy state against external load or the bond is stiffened to resist total failure of the developed structure (Kodikara *et al.* 1999, Li *et al.* 2004 and Tang *et al.* 2016). Stiffening can be caused by increased particle-aggregate contacts following greater clusters of small size clay particles and sub-aggregates created in previous wetting. Therefore, the structure becomes increasingly stable against total collapse. Kodikara *et al.* (1999) and Kodikara *et al.* (2002) noted that this behaviour governs the structural transformation of normally consolidated or unconsolidated clay to stable over-consolidated clay.

An important debate this theme is the number of cycles it takes for a soil to reach an equilibrium structural state. Al-Homoud *et al.* (1995) noted that the tensile strength of soil initially decreased with the number of wet-dry cycles and can stabilize after about three cycles. Umana (2016) conducted a hand-shear vane test in the soil repeatedly wetted and dried up to 5 cycle and reported similar diminishing strength condition. Although the corresponding numbers of cycles to reach the equilibrium structural state is not well understood, some workers have noted that this would likely depend on nature of the material, particularly the clay fraction (Al-Homoud *et al.*, 1995; Alonso *et al.*, 2005; Rao and Revanasiddappa, 2006). A high plasticity soil would require more wetting and drying cycles to reach the equilibrium state than silty or sandy soils (Al Wahab and El-Kedrah, 1995; Omid *et al.*, 1996; Yesiller *et al.*, 2000). This is because of increased moisture retention as soil plasticity increases. Such soils would require more wetting before a significant state of aggregation can be reached.

From the foregoing, it is reasonable to state that strength degradation in soils undergoing cyclic wetting and drying is not necessarily permanent. However, more evidence is needed to validate the observation. So far, most cyclic experiments are limited to 2 or 3 cycles, which are not sufficient to observe substantial changes. In addition, microscopic study of the fabric of the cyclic soil is rare in literature. In order to contribute to this important theme, this study considers assessing crack intensity in at least six wetting and drying cycles to know their changes relative to mechanical state of the soil.

### **2.3.7 Quantification of cracking in soil**

In section 2.2.1, it was noted that desiccation cracks occur systematically in the soil, and can attain complex pattern. Account of the system of crack development can be useful in understanding the mechanism of their formation. In literature, this has been carried out in terms of the number cracks per unit area (or crack intensity), crack cells per unit area (i.e. the volume of soil separated by cracks), crack spacing, etc. Early works on crack quantification were mostly descriptive with authors adopting different approaches to describe the complex pattern and dimension of cracks. Kleppe and Olson (1985) used a scale of 0 to 4 to quantify the extent of

cracking in the field with 0 implying no cracking and 4 suggesting large surface cracks of width >20mm. Al Wahab and El-Kedrah (1995) also developed an index to quantify the extent of cracking. The cracking index is the ratio of the area of cracks to the total surface area of a soil. The product of length and width determined the area of a crack. A more conventional quantification developed with statistical evaluation of crack pattern from direct measurement. However, with advancement in image analysis technique, computer aided digital analysis became more common to measure and quantify cracks in the soil. The use of non-invasive techniques is also increasing (section 2.4.5) including 2D/3D laser scans (Sanchez *et al.*, 2013; Zielinski *et al.*, 2014) and electrical resistivity tomography (Samouëlian *et al.*, 2005; Hassan and Toll, 2013; Hassan and Nsaif, 2016).

Image processing often involved a computer-aided conversion of analogue camera images into a set of standard signal characteristics, commonly pixels and colours. In comparison with traditional manual methods, image processing has the advantage of simplicity and high efficiency. Tang *et al.* (2008) set out the general procedure for processing 2D digital image of a crack structure as follows:

1. First, the colour image of cracked soil surface is changed into a grey scale image.
2. Next, a good contrast is set between the cracks and soil clods in a process referred to as "binarisation". With this, the grey level image segments into black and white background representing the cracks and soil aggregates respectively. The contrast helps to determine the intensity of cracking.
3. Finally, in order to determine the crack intersections and lengths, a schematize structure of the crack network is created by "skeletonisation".

The procedure is further illustrated in Figure 2.27:

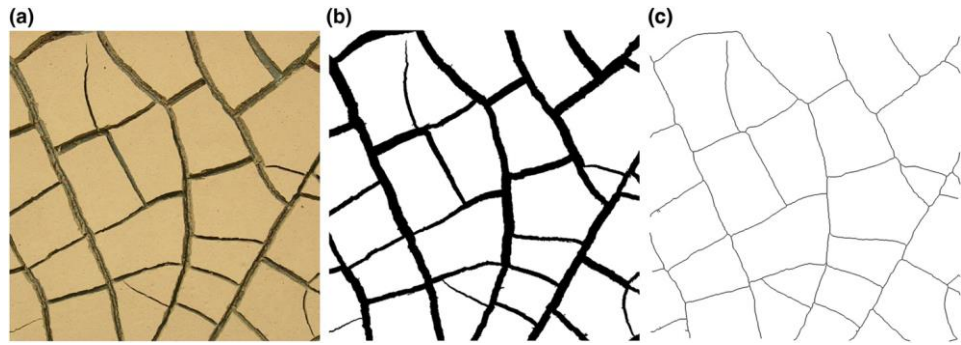


Figure 2.27: Digital image processing procedure. (a) Initial grey level image, (b) binary black and white image, and (c) skeleton of crack network (from Tang *et al.*, 2008)

To quantify the evolution and extent of cracking in field and laboratory, the two numerical parameters commonly employ by researchers are crack intensity factor (CIF) and length of the fissure (LF). Miller *et al.* (1998) introduced CIF, which is defined as a ratio of the total surface crack area to the total surface area of the clay soil. Likewise, Trabelsi *et al.* (2012) first used LF, which described the length of crack with respect to the total length of soil. Both parameters, often presented as time-variables, have been used to describe the progressive development of cracking in a soil. Typically, the curves present a linear region at the beginning of the desiccation process and then reached a steady state as shown in Figure 2.28. This behaviour is believed to characterise the progressive hydro-structural changes in drying soil, hence useful in quantifying the cracking process.

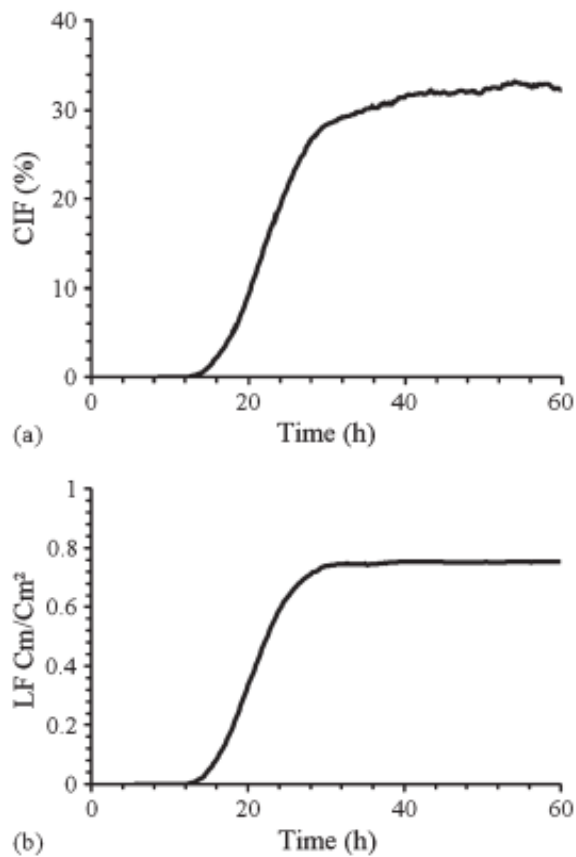


Figure 2.28: Experimental cracking results (a) CIF and (b) LF as functions of time  
From Miller *et al.* (1998) and Trabelsi *et al.* (2012)

Since its introduction, various authors have used CIF in particular to characterise crack properties. Miller *et al.* (1998) analysed changes in CIF during crack propagation and identified three distinct stages of crack formation; the initial stage, second stage and final stage. The initial stage represented the period when the first generation or primary cracks initiate and spread over the entire soil surface. The second stage, also called "enhanced cracking" represented the period when the first generation cracks became wider and deeper, with few secondary cracks later formed between the initial clods. The final stage is the stable stage with no significant change in crack geometry. Similar stages are reported by other workers who also employed image analyses technique i.e. Mizuguchi *et al.* (2005), Tang *et al.* (2008) and Li and Zhang (2011). The steady or stable stage, in particular, is described as the stage when aggregates size is stable, the soil approaches shrinkage limit and cracking generally ceases. Tang *et al.* (2008) and Tang *et al.* (2010) reported that the extent of cracking correlates directly to the fines content and plasticity. Hence, CIF can reflect the shrinkage properties of soil. The material with lower fines

content shrinks less, resulting in lower CIF while the fines-rich material exhibits a higher rate of volumetric shrinkage, hence higher CIF obtained. Wetting and drying leads to higher CIF. This attributes to greater aggregates instability induced by cyclic shrink-swell, even though this effect may not be perpetual as discussed in the preceding section. The potential of some clay soils to regain structural stability after multiple wet-dry cycle presume that potential for cracking in such soils would be reduced as the cycle increases. Considering the usefulness of image analysis technique, this study contemplates time-lapse photograph of the surface cracks in as part of the methodology to quantify and characterise the crack's morphological development.

## **2.4 Clay soils and performance of clay earth slopes**

Clays are soils that contain a high percentage of fine particles and colloidal substance. In geotechnical engineering, clay soils are characterised by the content of specific clay minerals, which are characteristically plastic when wet but hard, brittle and non-plastic upon drying. They are important engineering material commonly involved in civil works as either a foundation or a construction material. This is due to their broad range of mouldable states as well as their problematic characteristics under certain conditions, particular changing moisture content. Their engineering properties are therefore significantly influenced by the presence of water, which makes them prone to large volume changes. Commonly, the term expansive soil describes clay soil that is characterized by significant volumetric change with moisture fluctuations. This type of soil is a common cause of environmental related damages in civil structures.

### **2.4.1 Clay mineralogy**

Clay minerals are flaky crystalline particles with a diameter greater than  $2\mu\text{m}$ . They are also electrochemically very active. Figure 2.29 illustrates the size of clay particle relative to sand and silt.

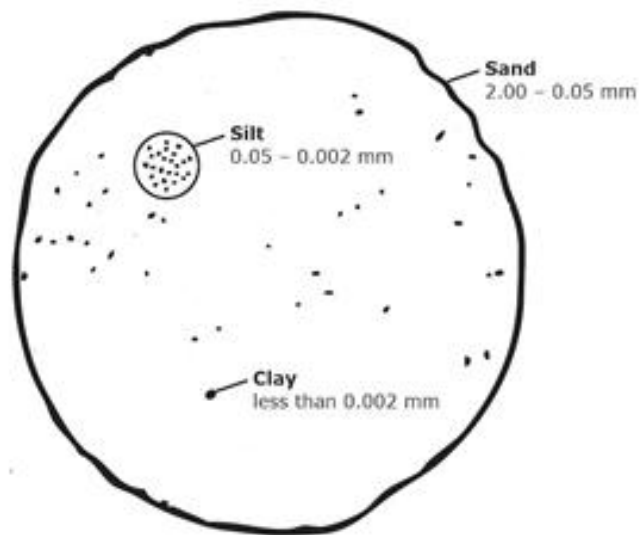


Figure 2.29: Particle size of sand, silt and clay

Overall, clays constitute around 16% by volume of material in the earth's surface and are very abundant in soils as a product of weathering. The volumetric change caused by shrinkage and swelling of soils are related to expansive clay minerals. Structurally, clay minerals comprise of arrangements of silicate (tetrahedral) and aluminium, magnesium and iron (octahedral) sheets contained in crystal units or layers, each being 0.1 to 1.0 $\mu$ m in size. The variations in the basic sheets structures make up the dozen of clay minerals with distinctive physiochemical properties. Despite their structural and compositional differences, the wide varieties, which have been identified can be classified into two main groups namely the 1:1 and 1:2 layer. The 1:1 layer-lattice silicate clays have a stack of one tetrahedral and one octahedral sheet. Successive layers of the basic units are held together by strong hydrogen bonds, which prevent hydration and allow stacking of the layers into a large crystal, typically 70–100 layers thick. The 2:1 layer-lattice silicate clays, on the other hand, have a stack of one tetrahedral layer sandwiched between two octahedral sheets and held by a weak van der Waals force with a net negative charge deficiency in the octahedral sheet. This enables water and exchangeable ions to enter and separate the layers. Thus, montmorillonite crystals in this group are very small but at the same time, they have a very strong attraction for water (Figure 2.30).

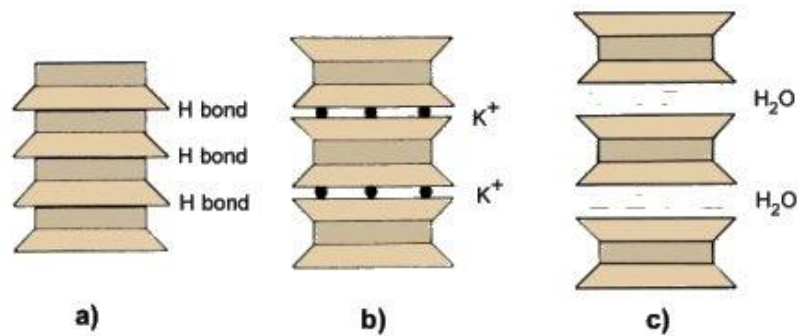


Figure 2.30: Structure of the main clay minerals: (a) kaolinite, (b) illites and (c) montmorillonite, based on combined sheets (Knappett and Craig, 2012)

The 1:1 silicate clays e.g. kaolinite is not prone to large shrink-swell as local moisture content changes. This is due to their small specific surface area. Specific surface is inversely proportional to the grain size of a soil i.e. the smaller the particles, the larger the specific surface. Some 2:1 silicate clays such as illites and chlorites do not expand and contract, changing little in the volume under wetting and drying. Other 2:1 silicate clays, e.g. montmorillonites also referred to as the smectites group are capable of significant expansion and contraction on wetting and drying because of their extremely large internal surface area estimated between 550-650m<sup>2</sup>/g (Brink *et al.*, 1982). This greatly enhances water bonding leading to a large expansion in the interlayer spaces. Conversely, as the 2:1 clay minerals dry out, water is lost from the layer-lattice structure and shrinkage occurs. Since the surface activity of clay relates to particle size, montmorillonites are therefore relatively more "active" than kaolinites. Characterisation of activity of common clay minerals and an indication of their shrinkage potential is as depicted in equation 2.20 and Table 2.1:

Table 2.1: Activity of clays

Clay minerals	Activity
Kaolinite	A=0.5 (low activity)
Illites	A=1.0 (medium activity)
Montmorillonite	A=7.2 (very high activity)

$$\text{Activity, } A = \frac{PI}{\% \text{clay finer than } 2\mu\text{m}} \quad 2.20$$

Due to their physicochemical characteristics, most clay minerals are usually hydrated i.e. layers of water called absorbed water, surrounds each crystal. The structure of clay soils and thus their engineering properties ultimately depends on the nature of this absorbed water layer. The phenomenon of absorbed water in clay arises from several reasons. First, even though water is electrically neutral in its dipolar nature, it has two separate centres of charge, one positive and one negative, which attracts the molecules to clay crystals. Secondly, water is bound to the clay crystal by hydrogen bonding such that hydrogen of the water attracts oxygen or hydroxyls on the surface of the clay. The third factor is that the negatively charged clay surface also attracts cations in the water. Since all cations are hydrous to some extent, they also contribute to the attraction of water to the clay surface. Holtz and Kovacs (1981) noted that of these three factors, hydrogen bonding is the most significant in the behaviour of the absorbed water.

#### 2.4.2 **Structure and Fabric of clay soil**

A given soil mass is made up of particles or mineral grains held together by inter-particle forces. The geometry and arrangement of the soil particles and the forces, which may act between them, are considered as the soil structure. Soil fabric refers only to the geometric arrangement of the particles or mineral grain. The structure of most naturally occurring clay deposits is complex ranging from microscopic aggregates to clusters and large pedes (Holtz and Kovacs, 1981). The behaviour of clay fills is strongly influenced by the macro- and micro- structures. Cracks, root holes, sand seams etc., are classified as the macrostructure. These act as defects and primarily affect soil strength and drainage. Consequently, they are crucial in geotechnical considerations involving drainage, settlement, and slope stability. The microstructure describes the geometry and relation of grains, and the pores between them. It is influenced by the history of the soil, including the stress history, from deposition to weathering.

### 2.4.3 **Clay fills and construction of infrastructure embankment**

The word “fill” is generic for soil or rock materials created by man for various purposes. This is different from natural soil deposits, which result from geologic processes. Likewise, engineered fills also differ from ordinary fills. Engineered fills are selected and prepared to exhibit specific engineering behaviour. Therefore, they possessed known engineering properties, and which could be characterised. On the other hand, ordinary or non-engineered fills generally arises as a bye product of human activities, commonly spoils, urban fills, building and demolition waste etc. Characterisation of their engineering properties and prediction of behaviour is difficult since their placements are usually not for any considered application (Charles, 1993).

Clay fills are frequently involved in earthwork construction e.g. creation of road and railway embankments, dams and flood levees, landfill liners/covers etc. In the constructions, large volume of clay lumps or clods of are compacted in layers of appropriate thickness. The nature and method of placement of clay fill can significantly affect performance and lifespan of engineering structures created from them. However, a major problem is volume change due to cyclic swelling and shrinkage, which characterised the behaviour of clay minerals upon wetting and drying. This condition can lead to several adverse behaviours in the soil including differential settlement, creep, susceptibility to erosion and overall strength reduction etc. Global damage cause by expansive clay to civil engineering structures are estimated in billions of dollars (Jones and Holtz, 1973; Bell, 2003). Pritchard *et al.* (2013) reported that shrink swell actions in clays pose the highest cost and risk to infrastructure systems in the UK where expansive soils of intermediate to high plasticity are widely involved in the construction of transport infrastructures, particularly embankments. This is mainly because of their abundance across the British Isles. However, the high plasticity materials are more prevalent in the South corresponding to the drier parts of the country (Figure 2.31). The distribution is attributed to factors like geology, climate, hydrology and geomorphology.

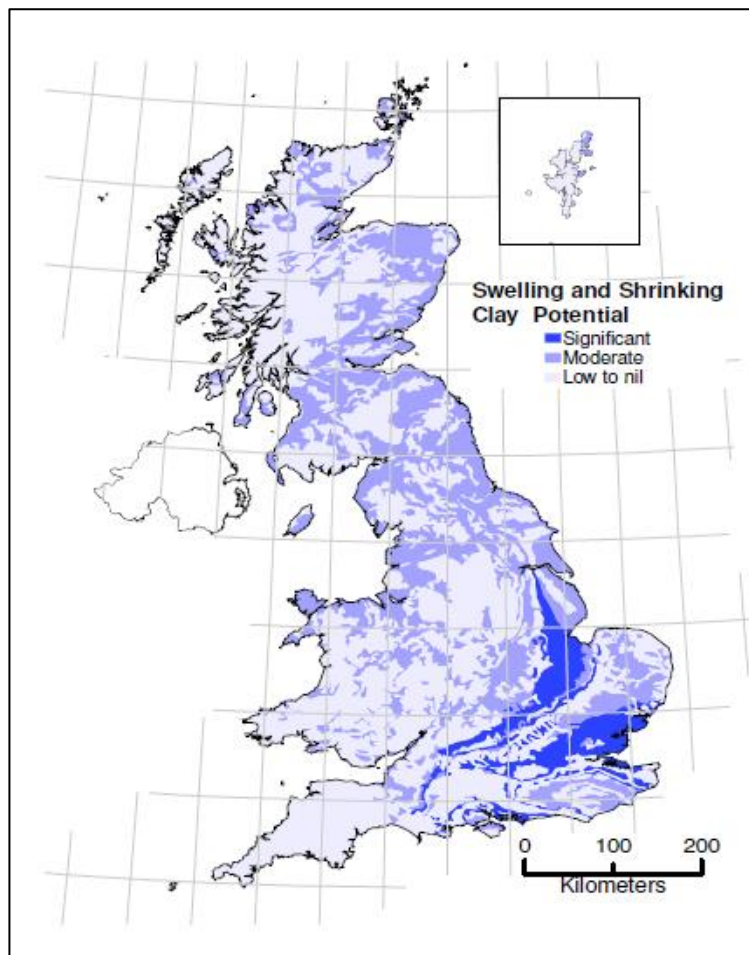


Figure 2.31: Shrink–swell potential map of UK (Jones and Jefferson, 2012)

In the southern part of the country, the London Clay Formation, Lias Group and Gault Clay Formation, are among the well-known sources of unstable slope materials (Dijkstra and Dixon, 2010). The high shrinkage and swelling behaviour of London Clay Formation, in particular, have a recognised history of foundations damages.

Two types of embankments are common in the UK with respect to era/method of construction namely; historic railway embankment and modern highway embankment. Their structural integrity and hence performance in short and long term have occupied geotechnical literature in recent times. This attributes to the need to improve knowledge on likely behaviour of the volume sensitive materials in the changing climate (Nelder *et al.*, 2006; Hughes *et al.*, 2009; Kilsby *et al.*, 2009; Loveridge *et al.*, 2010; Toll *et al.*, 2012; Wilks, 2015). The historic embankments also referred to as Victorian embankments were constructed in the late 19th century and early 20th century for the olden day railways. Their

construction is characterised by poor compaction using end tipping method, unselected vegetation type and poor drainage condition etc. These result predominantly in a soft foundation, a loose and permeable fill susceptible to a high rate of deformation. In contrast, the modern highway embankments were constructed from the early 50's, with the development of modern compaction methods and equipment. The fills are therefore compacted in successive layers and placed on a suitable foundation, with adequate drainage and standard vegetation regulation. Figure 2.32 illustrates the basic engineering differences in the construction of the two types of embankments, which characterised an ideal embankment condition with potential stability and relatively unstable embankment encountered in reality.

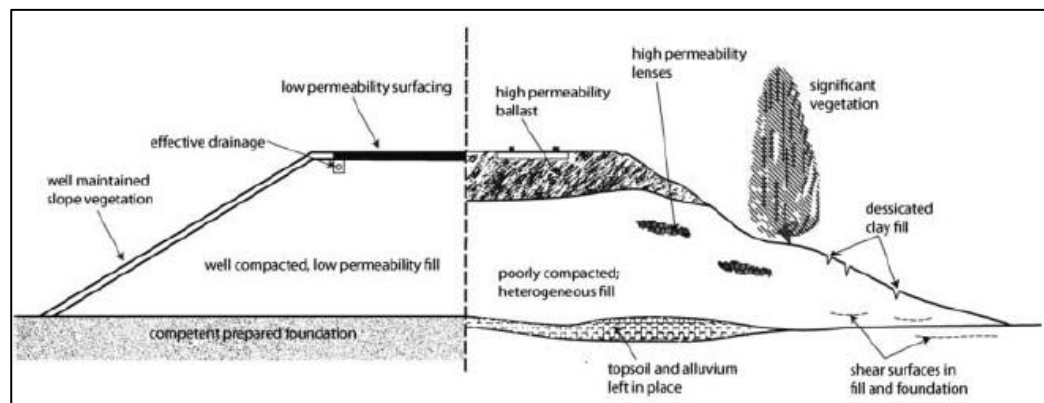


Figure 2.32: Modern highway embankment (Left) compared with historic rail embankment (Right). From Loveridge *et al.* (2010).

#### 2.4.4 Performance of clay embankments in the UK

In the UK, embankments estimates about 10,000km of the total length of transport infrastructure, and together with cuttings, constitutes a third of the total transport asset value. Increasing failure incidences in these earthwork slopes are being experienced across the country in recent times. The significance of these failures is enormous. Speed restrictions, route closure, a high cost of maintenance are discussed in the literature as issues arising from minor and ultimate failures (Perry *et al.*, 2003; Ridley *et al.*, 2004a; Kilsby *et al.*, 2009; Dijkstra and Dixon, 2010; Loveridge *et al.*, 2010). The potential risks facing the transport infrastructures sector are complicated by other interdependent sectors e.g. energy, telecommunication etc. The performance of transport earthwork slopes

(road and rail networks) in the country is therefore central to the national economy.

Infrastructure slopes in the UK have been experiencing different levels of failures. The failures ranged from minor soil deformation in the form of surficial slips and settlements with implication for speed restriction, to major failures leading to routes closures (Kilsby *et al.*, 2009; Rouainia *et al.*, 2009; Dijkstra and Dixon, 2010; Loveridge *et al.*, 2010). There is sufficient evidence that most failures in clay embankments in the country are caused by environmental factors, especially an extended period of rainfall. Seasonal and diurnal changes in climate give rise to repeated cycles of shrink-swell with a net increase in cyclic pore water pressure. These factors are regarded as the common trigger of slope failures in the UK. Importantly, during cyclic shrink-swell process plastic strain can accumulate over time leading to the reduction in soil shear strength, a mechanism referred to as progressive strain softening (Davies, 2008; Take and Bolton 2011). The initial placement conditions (e.g. optimum moisture content, good compaction, low permeability) of the over-consolidated clay fills usually result in high negative pore water pressure, which favours stability of the slopes immediately after construction. The stable condition can last up to 20 years (Rogers and Glendinning, 1993; Fredlund, 2006). However, with time there is gradual deterioration of this favourable negative pore pressure to positive values, commonly due to the high ingress of water into the slope during high rainfall. This anomalous behaviour can be facilitated by the presence of cracks on the slopes etc. (Anderson *et al.*, 1982; Zhang *et al.*, 2005; Bradley *et al.*, 2007; Glendinning *et al.*, 2009; Wilks, 2010). Cracks can also form part of slip surface that has zero shear strength and water in crack will generally tend to soften the soil and reduce its strength properties (Baker, 1981). Since pore water pressure tend to reduce the effective stress in soil, loss of shear resistant can occur in the soil especially under cyclic shrink-swell. Researchers envisaged that progressive strain softening could dominate future slope deformation considering the trend of future climate scenarios in the country. In the future, hotter summers and wetter winters are forecasted for the UK (UKCP09). Annual and seasonal temperatures, and therefore evaporation, are expected to increase in all parts. It is widely

acknowledged that the increase climate seasonality will likely affect the behaviour of both natural and engineered slopes. Essentially, cyclic shrink-swell and pore water pressure are likely to increase due to increase in annual temperature and rainfall variability especially in the very high plasticity soils in the southern part of the country. However, there are evidences that the UK's climate is already changing. The Department of Business, Energy & Industrial Strategy reported that average temperature in Britain is now 1°C higher than it was 100 years ago and 0.5°C higher than it was in the 1970s ([www.gov.uk/guidance/climate-change-explained](http://www.gov.uk/guidance/climate-change-explained) 23, Oct 2014). Increasing incidents of heat waves, flooding, landslides etc. reported across the country in recent times, with 2012 adjudged as the wettest year since 1910. A Recent report of National environment research council of the British geological survey (BGS, 2017) showed a significant increase in the number of landslides and slope failures, particularly railway embankments.

Since degradation of shear strength under cyclic wetting and drying is time dependent, the current trend of major failures in historic embankments would tend to support the argument that older embankments would experience a higher frequency of failures (Wilks, 2010; Wilks, 2015). However, since the shrink-swell response can be affected by several factors including the nature of fills, past stress history and environment (Mokhtari and Dehghani, 2012), it implies older slopes may not necessarily fail the most. Under the latter consideration, Rogers and Glendinning (1993) had noted that there exists some geology experiencing most failures in younger slopes. Overall, the arguments suggest that both railway and highway embankments are susceptible to a different degree of failures. Speculations of the likely behaviour of slopes under the changing climates have prompted various researches. Geotechnical studies involving combined used of projected climate variability and material properties to predict the future hydromechanical stability of slopes in the UK have yielded contradictory reports. Some suggest a balance between high evapotranspiration and precipitation with no net effect on the current level of slope failures while others suggest a potential for increase shrink-swell leading to greater slope deformation. However, both divides acknowledged the potential of desiccation cracking in changing hill slopes

hydrology thereby playing a decisive role in the future scenario. Therefore, the study of cracking embarked upon here is very crucial in the understanding of the behaviour of infrastructure slopes in the country in the future.

#### **2.4.5 Volume change analysis and effects of cracking in drying soil**

Volume change in an expansive soil mass is closely associated with moisture changes. This is attributed to shrink-swell properties of the expansive minerals in such soil. When the hydrophilic minerals are flooded with water, porewater induces swelling pressure leading to soil heave. In contrast, when the absorbed water dehydrates, the particles are drawn closer by capillary action developed between the dehydrated pores and the soil particles. The soil would shrink horizontally and settle vertically. At the interparticle level, the tensile stress developed in drying soil can lead to cracking thereby increasing the macro-porosity. Subsidence and cracking therefore characterise volume change in expansive clay soil.

The difference in the magnitude of volume change with planes in the soil mass is commonly referred to as shrinkage anisotropy and relate to non-uniform drying in the heterogeneous soil system. This factor contributes to a non-linear stress state in unsaturated soil (Fredlund and Morgenstern, 1976; Fredlund and Rahardjo, 1993). Anisotropic phenomena in soil can lead to subsidence in the vertical plane and cracking in the horizontal plane (Bronswijk, 1990; Gomboš, 2012; Chertkov, 2013). During wetting, initially cracked soil will swell both in the vertical plane causing heaving and in the horizontal plane causing cracks to close. The shrink-swell action therefore results in three-dimensional volume change in soil as illustrated in Figure 2.33.

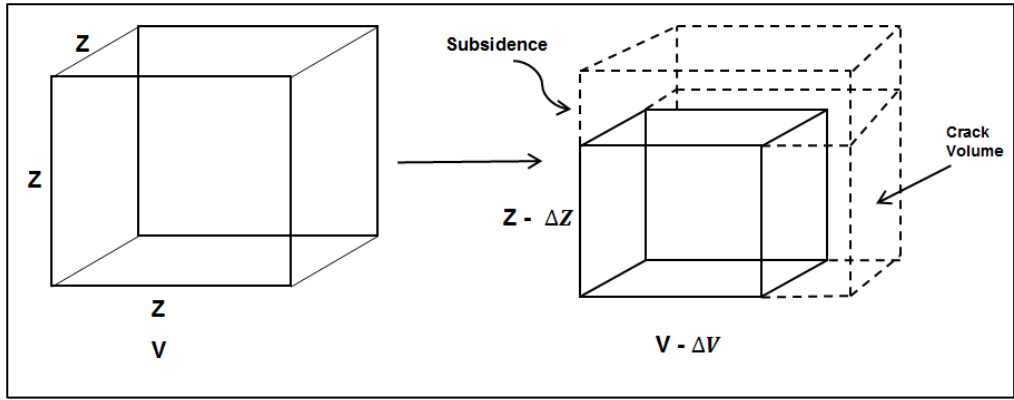


Figure 2.33: Schematic diagram of 3-D shrink-swell in soil (the dashed line express the sample in saturated state, while the continuous line express the sample after shrinkage – adapted from Bronswijk, 1990)

Despite the presence of crack being an indicator of soil movement in the horizontal plane, shrinkage analysis commonly involves only vertical movement. This is because the latter is easier to measure and quantify in the field for any reference height. The changes in volume of the soil block during wetting and drying can be visualize in a 3-dimensional cube shown in Figure 2.33. In this case, a soil with initial layer thickness  $Z$ (m) and volume  $V$ ( $m^3$ ), shrinks isotropically into a cube with volume  $V - \Delta V$  and sides  $Z - \Delta Z$ . Mathematically,  $V = Z^3$ ,  $V - \Delta V = (Z - \Delta Z)^3$  and  $\Delta V = Z^3 - (Z - \Delta Z)^3$ .  $\Delta V$  is the volume change upon shrinkage ( $m^3$ ) and  $\Delta Z$  is the surface subsidence upon shrinkage (m). Bronswijk (1989) showed that;

$$1 - \frac{\Delta V}{V} = \left(1 - \frac{\Delta Z}{Z}\right)^3 \quad 2.21$$

In the case of one-dimensional subsidence i.e. no cracking has occurred:

$$1 - \frac{\Delta V}{V} = \left(1 - \frac{\Delta Z}{Z}\right)^1 \quad 2.22$$

The exponent in this expression changes in value depending on the dominant geometric condition. Consequently, a dimensionless geometric factor,  $r$  is introduced in the analysis to account for shrinkage anisotropy as well as resolved the influence of cracking and subsidence (Bronswijk, 1989; Bronswijk, 1990; Gomboš, 2012; Chertkov, 2013; Stewart *et al.*, 2016). A general form of geometric shrinkage equation then becomes:

$$1 - \frac{\Delta V}{V} = \left(1 - \frac{\Delta Z}{Z}\right)^r \quad 2.23$$

In the literature,  $r$  is defined by arbitrary values ranging from 1 to 3 such that when:

$r = 1$ , it means one dimensional subsidence i.e. no cracking process, all soil volumetric changes are vertical

$1 < r < 3$  means vertical movement predominates over crack formation

$r = 3$ : three dimensional isotropic shrinkage

$r > 3$ : crack formation predominated over vertical movement

$r \rightarrow \infty$  all soil volumetric changes are horizontal i.e. only cracks are formed.

When  $r$  is known, then by direct substitution, equation 2.22 is applied to convert measured vertical changes in layer thickness into a three-dimensional volume decrease,  $\Delta V$  as follows:

$$\Delta V = \left[1 - \left(1 - \frac{\Delta Z}{Z}\right)^r\right] Z^3 \quad 2.25$$

Although these formulations have paved the way for expression of dimensional volume change in soil in terms of change in inter-aggregate pores with moisture loss e.g. moisture ratio and void ratio, the application of the term  $r$  remains practically undefined. This is because it does not provide a numerical account of the cracks occurring in the soil which essentially affect the volume change. Considering that horizontal shrinkage during desiccation is largely represented by cracking, it is thought here that the volume of crack per unit soil area or crack intensity factor can be used to give a real value to the geometric factor.

#### 2.4.6 Role of desiccation cracks in pore water pressure response in soil

The theories of soil cracking discussed earlier in section 2.3 directly relates the development of cracks in a drying soil with changes in porewater pressure. On the other hand, when cracks exist, they can significantly influence the behaviour of porewater pressure in slopes. This is primarily because porewater pressure equilibration on slopes is mainly controlled by the facility for rainwater penetration. Cracks generally act as preferential pathways for rainwater infiltration, distribution and accumulation across a soil block as illustrated in Figure 2.34.

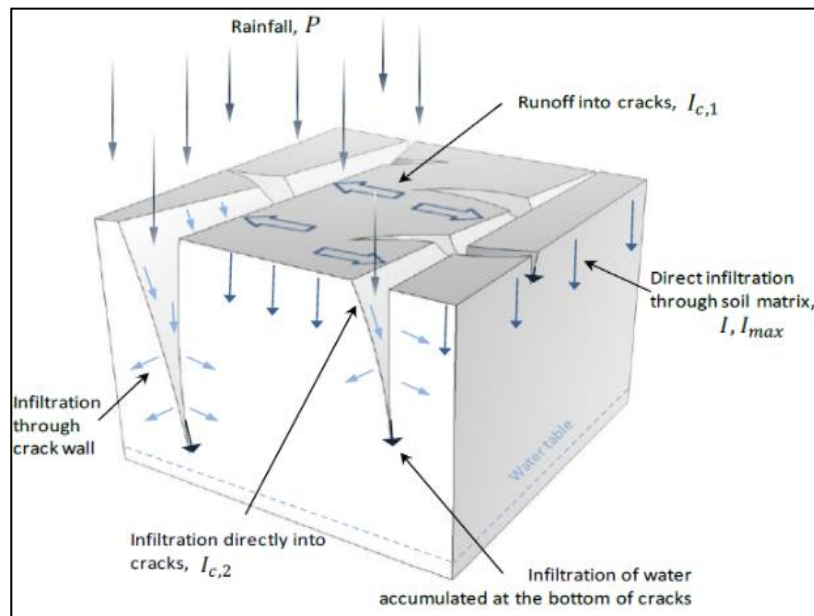


Figure 2.34: Model of rainwater infiltration in a crack soil (from Stirling, 2014)

Overall, a cracked soil exhibits permeability orders of magnitude higher than un-cracked soil (Novak *et al.*, 2000; Albrecht and Benson, 2001; Fan *et al.*, 2005).

A crack formed during summer drying can persevere and sustain water infiltration in slope thus facilitating the development of excess pore water pressure over hydrostatic pressure in the following winter. Particular during large rainfall event at the end of the dry season, such cracks causes by-pass of water which increases soil moisture at a deeper level and differentially dissipates the pore water pressure. Investigating the impact of permeability and surface cracks on soil slope, Sasekaran (2011) showed by results of numerical modelling that greater pore water pressure occurs at the bottom of the crack in a slope. This can be caused by the

development of perched water table, especially when condition favours the development of horizontal cracking in the deeper soil layer. Such a development was reported by Anderson *et al.* (1982), who observed an accelerated porewater pressure degradation in a clay embankment along a motorway in the UK. The condition linked to the existence of deep cracks observed at this site in the previous year, with permeability measurements around the crack sites after closure being higher than the intact clay material. The workers also reported the existence of a wedge of positive porewater pressures that developed mainly in the middle section of the slope where cracking was intense. Therefore, a preponderance of desiccation cracks could define a new hydromechanical dynamics that may dominate the mode and mechanisms of future slope performance under the impact of changing climate.

#### **2.4.7 *Methods of analysis of slopes with cracks***

Several procedures of analysis of slopes with cracks exist in practice. The methods aimed to model the mechanism (initiation and propagation) of cracking in soil influenced by transient environmental conditions or to assess their contribution in slope stability problems. The various methods can be classified into analytical and numerical ones. The analytical studies mainly focused on the stress-strain involved in the mechanism of desiccation cracking. Commonly, the constitutive soil parameters e.g. tensile stress, water content, shrinkage strain, soil stiffness etc., which influenced this behaviour are experimentally studied and theoretically modelled and validated (Konrad and Ayad, 1997; Morris *et al.*, 1992; Kodikara and Choi, 2006; Wu *et al.*, 2012; Kodikara and Costa, 2013). The efforts have provided basic understanding of the mechanism of cracking including shrinkage strain and tensile stress development as moisture changes in expansive soils.

The numerical methods are mainly the finite element method (FEM) and limit equilibrium method (LEM). Finite element analysis conceptualise a system or geometric structure as a continuum which is generally divided into finite number of elements. The characteristics of the system are therefore made up of interpolated properties of the discrete elements

(Knappett and Craig, 2012; Cheng and Lau, 2014) typically interconnected in a mesh (Figure 2.35)

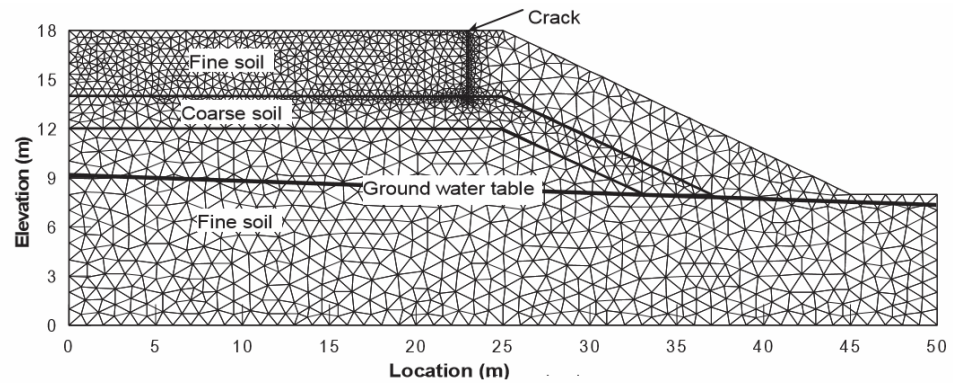


Figure 2.35: Finite element mesh of a slope with crack at the crest (from Wang *et al.* 2011)

In geotechnical applications, the finite element method allows the modelling of progressive deformation in slopes with no pre-chosen slip surfaces. It is therefore useful in modelling effects of changes in environment and the soil response hence the mechanisms of desiccation cracking. Recent works on soil cracking involving the finite element method include Wang *et al.* (2011), Sima *et al.* (2013), Sánchez *et al.* (2014). A related numerical method useful in the analysis of shear strength reduction in soil is the finite difference method (Stirling *et al.*, 2017). The finite difference approach also involved a discretisation of complex a complex domain into smaller parts. The value of the parameter within each part is related to the parts it is connected to, so that by applying suitable boundary conditions, a complete solution may be obtained (Knappett and Craig, 2012).

Unlike finite element method, the traditional limit equilibrium method requires the soil mass to be subdivided into vertical slices or soil wedges (Anderson and Richards, 1987; Smith and Smith, 1989; Knappett and Craig, 2012; Cheng and Lau, 2014). The method is widely used in the analysis slope stability where each slice is treated as a potential mass sliding on a critical slip surface (Figure 3.26) and the equilibrium of forces acting on each slice is imposed.

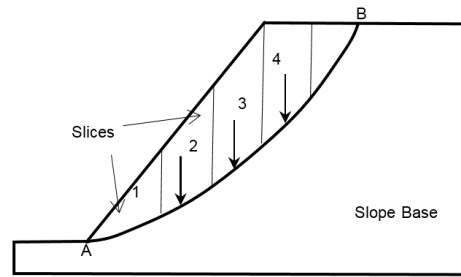


Figure 2.36 : 2D illustration of method of slices in traditional limit equilibrium analysis of slope stability (slip surface = AB)

It is assumed that the shear strength of the materials along the potential failure surface is governed by the relationship between shear stress and the normal stress on the failure surface. This relationship can be linear (Mohr-Coulomb criterion) or non-linear (e.g. for fine-grained soils where pore water pressure changes affect effective stress path). Failure occurs on slopes when the sliding moment of the soil weight about the centre of rotation of the slip surface,  $O$  and radius,  $r$  (Figure 2.37), is greater than the soil shear strength. With the limit equilibrium approach, a crack is represented as part of the composite slip surfaces (figure 2.37) and usually, its hydromechanical effects on the shear parameters are added to the analysis (Smith and Smith, 1989, Broomhead, 1999).

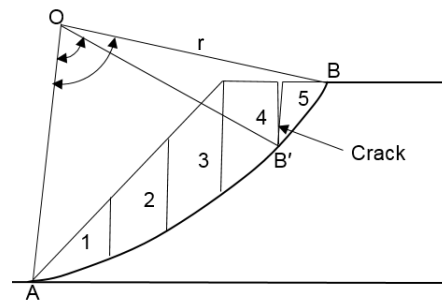


Figure 2.37: Composite slices with crack at the top of the slope. The crack reduced the slip surface from AB to AB' (adapted from Smith and Smith, 1989)

The limit equilibrium method commonly involves analysis of slopes in static equilibrium (Anderson and Richards, 1987; Knappett and Craig, 2012; Cheng and Lau, 2014), and the slip surfaces are pre-chosen (Michalowski, 2013; Utili, 2013). Desiccation cracks characteristically exhibit a non-linear behaviour i.e. open and close with changes in environment and occur randomly in slopes. These dynamic characteristics tend to limit the application of the traditional limit equilibrium method in a comprehensive analysis of cracking, particularly the formation mechanisms (Broomhead,

1999; Anderson and Richards, 1987). However, other numerical methods notably limit analysis, have been employed in a more rigorous analysis of cracking in slope stability. In the limit analysis approach, the soil is conceptualised as a rigid perfectly plastic material. The general procedure of limit analysis is to assume a kinematically admissible failure mechanism for upper bound solutions or a statically admissible stress field for lower bound solution (Yu *et al.*, 1998; Leshchinsky, 2013; Cheng and Lau, 2014). Following this approach, Utili (2013) and Michalowski (2013) used the kinematic method of limit analysis to address cracking and some of its dynamic behaviour on slopes taking into consideration boundary conditions at the soil surface and the limiting stress conditions at depth. With this robust approach, Utili (2013) determined critical failure mechanisms for a wide range of problems involving specified and unspecified crack depths and locations. The results are presented in the form of dimensionless, ready-to-use charts, which can be used for any value of engineering interest e.g. angle of shearing resistance and slope inclination, dry and water-filled cracks etc. including regions where the presence of cracks is most likely to affect the stability of the slope (Figure 2.37).

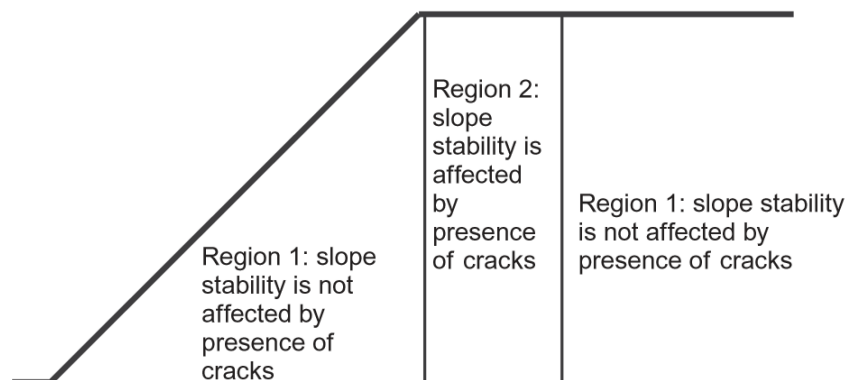


Figure 2.38: Sketch of regions where cracks do and do not affect slope stability (from Utili, 2013)

Compared to experimental work on cracking, the analytical and numerical methods are relatively new and still developing. More input from field measurement is therefore invaluable to improve on them. As parts of present study, in situ cracks are investigated, including evolution, distribution, and sub-surface morphology in an embankment. The field measurements and relationships (sections 4.3, 4.4, 5.4) can validate or

improve the analytical solutions. For example, the time series morphology development of desiccation cracking analysed in this study, can improve the approach of representing the changing cross-section volume of cracks and the effects in the dynamic stability of the slope, considering the potential influence on the behaviour of the pore water pressure and shear strength.

#### **2.4.8 Influence of vegetation on clay slope deformation**

Vegetation is a common feature of a planned roadside corridor, usually planted for aesthetics and more importantly, for positive effects on slope stability. Plants improve slope stability through beneficial changes in mechanical and hydrological properties of the soil. These arise mainly by roots anchorage of soil particles against shear failure, interception of precipitation and initiation of evapotranspiration leading to increase in prevention of erosion and suction respectively. High soil suction benefit derived from vegetation for slope stability would be more prominent in summer while in wet winter, the mechanical reinforcement provided by the root structure, would be far more relevant (Chirico *et al.* (2013)).

Roots anchorage in soil essentially contributes to increasing the tensile strength of a soil mass. Tensile strength in the range of 5-85MPa is reported from field studies (Chok, 2008; Stokes *et al.*, 2008), depending on the root diameter. In addition, a general decrease in tensile strength as root diameter increases is common. Although this relationship is currently not well understood, it is however presumed to arise from the difference in the root structures. Genet *et al.* (2005) reported that thinner roots possess more cellulose than thicker roots, cellulose being more resistant than lignin in tension. Roots exudates are also known to impart hydrophobicity (or water repellence) in the soil. This has implication for lowering soil wettability and increasing aggregates. A widely acknowledged model which explains the effect of mechanical root reinforcement in soil was given by Wu *et al.* (1979). According to the model, coalesced roots system improves the binding force of a soil mass by an additional apparent cohesion factor,  $C_R$  as given in equation 2.26:

$$S = C' + C_R + (\sigma - \mu) \tan \phi^I \quad 2.26$$

Where  $S$  is the shear strength of the soil-root composite,  $C'$  is effective cohesion,  $\sigma$  is normal stress,  $u$  is pore-water pressure and  $\phi'$  is the effective angle of internal friction. The model showed that the magnitude of  $C_R$  varies with the distribution of the roots within the soil and the tensile strength of individual roots. Other studies have shown that mechanical stability of vegetation root is more significant at shallow depth hence would have a greater effect in planar surface failure than in deep-seated failure (Chok *et al.*, 2004; Stokes *et al.*, 2008).

Notable studies on soil wettability and aggregate stability by rhizosphere include Chenu *et al.* (2000), Hallett *et al.* (2003), Hassan *et al.* (2014), Sepehrnia *et al.* (2017). The studies suggest that soil organic matter associated with the root zone increases aggregate stability by lowering the wettability and promote apparent cohesion of the soil mass. Generally, water repellence of the root zone arises from root exudates and secondary microbial metabolites. These organic plant materials essentially coat hydrophilic soil particles and clog the pores thereby increasing their contact angle, CA. The lower the contact angle the more the wettability. Therefore, a contact angle of  $0^\circ$  signifies hydrophilic (wetable) condition,  $CA > 0^\circ$  is water repellent, and  $CA > 90^\circ$  signifies a hydrophobic soil.

The concept of soil wettability mainly develops in the field of agriculture and soil science. However, the hydromechanical significance can be apply in stabilization of expansive soil in geotechnical practice. For instance, following this principle, Lourenço *et al.* (2015) used dimethyldichlorosilane (DMDCS), a Silanes group as capping materials in a slope and reported that the additive proved significantly reduced infiltration by increasing the repellence potential of the soil particles.

In some cases, vegetation can have detrimental effects on the performance of expansive clay slopes and foundation. Vegetation water demand is seasonal and frequently lead to cyclical volume change in the soil. This process is influential in transient changes in porewater pressure, with implication for a progressive reduction in shear strength. Common problems observed on clay slopes such as settlement and heaving are linked to the vegetation-influenced pore water changes (Davies *et al.*,

2008; Hamza and Bellis, 2008; Glendinning *et al.*, 2009). In partially saturated soils, the water available for plants, defined as water holding capacity can fall below a limiting value. This occurs between suction of 0-100kPa (Loveridge *et al.*, 2010). Such deficit hydrologic condition can cause plants water uptake to reduce up to the wilting point where the plants lose turgidity and are no longer able to draw water. Limiting moisture condition occurs as the drying perseveres with estimated suction reaching approximately 1,500kPa. The continuous water uptake by root also contributes to changes in the soil suction regime. In a study on water use by trees, Nisbet (2005) reported that some high water demanding trees (e.g. conifers) can uptake and transpire equivalent of 800mm moisture from the soil after a rainfall of about 1000mm. This suggests a large potential soil moisture deficit, which can lead to high suction in the affected profile soil. Such extreme drying can induce high strain in the soil with potential for cracking. Lim *et al.* (1996) measured suctions beneath the surfaces of two adjacent vegetated slopes and reported average values of 48, 43 and 27 kPa at depths of 0.5, 1.0 and 1.5m respectively. While under the bare soil surface, the suctions averaged 40, 25 and 10 kPa at same depths. Although these suctions are small, they essentially demonstrate the isolated effects of evaporation from the soil and the additional effect of transpiration by vegetation. Similarly, Blight (2005) showed that grass and bushes can cause desiccation of soils comparable with that caused by large trees. This is considering the fact that most research on soil-vegetation interaction concentrates more on the effects of large trees on desiccation shrinkage. This is worthy of note in the present study which is earmarked for a grass covered slope.

By-pass drying between soil layers by invasive tree roots can lead localize increase in suction in the subsurface. This can result in subsurface cracking and horizontal crack propagation at deeper soil profile around the root. In a field study, El Abedine and Robinson (1971) observed deep cracking within the depth of invasive tree roots. The by-pass drying mechanism may be responsible for the formation of sub-aerial cracks revealed in excavations e.g. Dyer *et al.* (2009). This mechanism suggests that while surface evaporation leading to surface cracking is common,

sub-aerial cracking can also initiate by enhancing suction due to moisture uptake around the root zone. Sub-surface crack can trap percolating rain water and contribute to form a perched water table (Anderson *et al.*, 1982). Invasive tree root in the soil also constitutes an internal restraint and mechanical stressor, which is an established premise for crack initiation. Hamza and Bellis (2008) suggests that the pressure exerted by penetrating plant roots can facilitate cracking in the drier upper layer of a desiccating soil. This arises as wedges of soils are displaced along the route of a penetrating root. However, this will be more significant for roots with reasonable thickness and strength, which suggests a limiting condition can be reach between the soil-root cohesion modelled by Wu *et al.* (1979) and the soil-root tension assume here. From the foregoing, vegetation on slopes have potential which can affect desiccation crack development.

#### **2.4.9 Estimation of soil evapotranspiration**

Moisture loss can be directly from the soil surface, indirectly from plant or both. Evaporation described the conversion of liquid water to vapour in a surface and its transfer as vapour into the atmosphere, whereas transpiration is the process by which water absorbed from the soil by tree roots evaporates through the pores or stomata on the surface of leaves. Evapotranspiration is a general term used to describe the two processes of water transfer to the atmosphere as far as plants are involved. Energy is required to change the state of the molecules of water from liquid to vapour (i.e. vaporisation). Direct solar radiation and, to some extent, the ambient temperature of the air provide the energy. The driving force to remove the water vapour from the soil is the difference between the water vapour pressure at the soil surface and that of the surrounding atmosphere (i.e. relative humidity). The replacement of the saturated air with drier air depends on wind speed and turbulence. Hence, solar radiation, air temperature, air humidity and wind speed are key climatic factors that drive evapotranspiration process (Allen *et al.*, 1998; Song, 2014).

The combined effect of climate factors on evapotranspiration is showed in Figure 2.39 for two different climatic conditions.

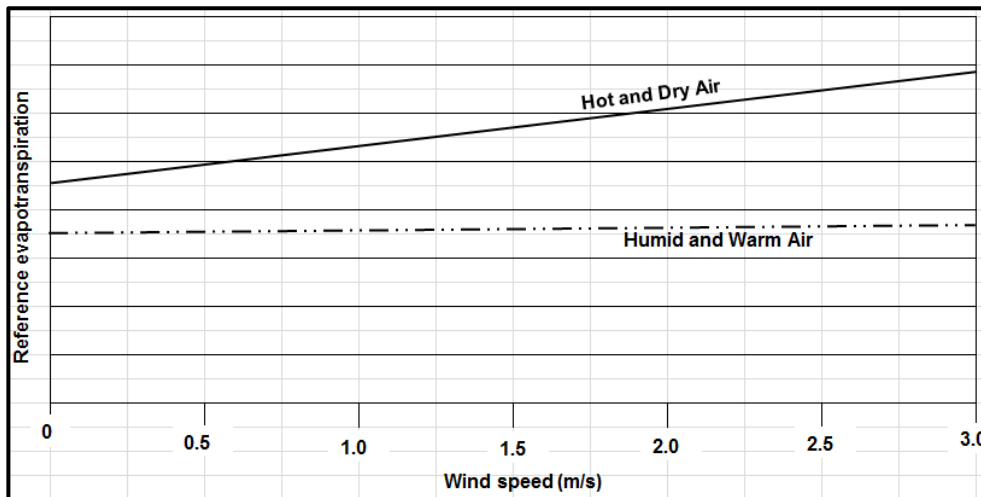


Figure 2.39: Illustration of the effect of wind speed, temperature and humidity on evapotranspiration (from Allen *et al.*, 1998)

The figure indicates that evapotranspiration is high in hot dry weather due to the dryness of the air and the amount of energy available as direct solar radiation and latent heat. Under these circumstances, much water vapour can be stored in the air while the wind promote the transport of water allowing more water vapour to be taken up into the surrounding atmosphere. On the other hand, under humid weather conditions, the high humidity of the air and the presence of clouds cause the evapotranspiration rate to be lower. The influence of these climate parameters on evapotranspiration has also been experimentally proven in a study by Cutts (2014). The study who showed that a small change in most of the climatic variables significantly affected the computed potential evapotranspiration.

Climatic parameters are commonly used for the estimation of evapotranspiration. Among several empirical relations employing climate parameters for estimation of evapotranspiration, the combined Penman-Monteith equation adopted by the United Nations food and agricultural organisation (FAO) is use in geotechnical engineering (Fredlund *et al.*, 2012; Glendenning *et al.*, 2014). The equation is used with weather parameters measured at a height of 2m above the ground surface. The method is convenient, as it requires only routine climate data such as average temperature, wind speed and relative humidity from which other important variables can be derived including missing data. The Penman-

Monteith equation for calculation of evapotranspiration from any reference surface is express as:

$$ET = \frac{0.408\Delta(R_n - G) + \gamma \frac{900}{T+273} U_2(e_s - e_a)}{\Delta + \gamma(1 + 0.34U_2)} \quad 2.27$$

Where;

ET = reference evapotranspiration potential (mm day<sup>-1</sup>)

$R_n$  = net radiation at the crop surface (MJ m<sup>-2</sup> day<sup>-1</sup>) – difference between the incoming net shortwave radiation and reflected longwave radiation, and represents the balance between energy absorbed and reflected  
 $G$  = soil heat flux density (MJ m<sup>-2</sup> day<sup>-1</sup>) – a minor factor that is often ignored, this is the energy utilized in heating the soil, a positive during warming and a negative during cooling.

T = mean daily air temperature at 2 m height (°C) – a factor that is used both by itself and a major factor in determining saturation pressure.

$U_2$  = wind speed at 2 m height (m s<sup>-1</sup>) - a substantial factor in determining the rate at which vapour is removed from the site.

$e_s$  = saturation vapour pressure (kPa)

$e_a$  = actual vapour pressure (kPa)

$(e_s - e_a)$  = saturation vapour pressure deficit - the difference between the actual vapour pressure and saturation for a given period, an important value determining the amount of evapotranspiration. This value is sensitive to temperature and represents the deficit between the total and maximum amount of water the air.

$\Delta$  = slope vapour pressure curve (kPa °C<sup>-1</sup>) – the relationship between saturation vapour pressure and temperature.

$\gamma$  = psychometric constant (kPa °C<sup>-1</sup>) – this value is a function of altitude, as the atmospheric pressure within the calculation is an average.

The amount of water in the soil and the tensile condition affect the magnitude of evapotranspiration. When soil water is reduced below field capacity, water uptake from the soil is determined mainly by the deep rooted trees, which draw virtually water from the lower layers at relatively low suctions. Such situation is capable of increasing the depth of unsaturated layer (or active zone) on a desiccating slope.

#### 2.4.10 ***Estimation of suction developed in unsaturated soil***

Soil suction is an important factor, which affects the behaviour of unsaturated soils. It represents the moisture stress condition in the soil and is made up of two major components, matrix suction and osmotic suction. Matrix suction describes the pressure potentials of pore water in terms of capillary forces acting in the soil while osmotic suction describes the pressure of dissolved ions in the soil. In geotechnical practice, matrix suction is commonly measured as it directly relates to the soil water content.

Several techniques have been developed for measurement of matrix suction in the soil. These are group into direct and indirect methods, with each group having their peculiar limitations. In the direct methods, matrix suction is measured as negative water pressure (i.e. less than atmospheric) using pressure gauge or transducer e.g. tensiometer, suction probes, pressure plate extractor (axial translation technique) etc. In principles, a high air entry, semi-permeable material, usually a ceramic disk or a ceramic cup is used in the instrument to create a capillary interface between air and water in the soil. With time, the pressure of water in the ceramic material come to equilibrium with the soil water pressure making it possible to measure negative soil water pressures. The range of matrix suction that can be obtained from any of the direct measurements generally depends on the air entry value of the ceramic material. Commonly, the problem of occluded and diffuse air in the material leads to an erroneous estimation of the suction particularly at the higher range suction ( $>100\text{kPa}$ ). However, in recent times, significant advances have been made in the measurement of higher ranges of suction accurately. For example, high capacity tensiometers have been developed with features that can prevent rapid cavitation and sustain suction development for extended period. The innovations include a reduced water reservoir, used of integral strain gauge diaphragm rather than ceramic plates. The indirect methods of measuring suction are mainly those depending on the calibration of soil matrix suction with other physical quantities measured in the soil through sensor devices. Hence, they can be used to estimate a wider range of suctions as far as these

quantities are determined. The physical quantities commonly measured include soil dielectric constant, thermal conductivity, electrical conductivity and water absorption. These quantities theoretically depend on the bulk water in the soil hence relates to the soil matrix suction. The accuracy in this group depends on the sensitivity of the sensor materials, which differ depending on the physical quantity measured. In recent practice, time domain reflectometry technique (TDR), which measures the apparent dielectric property of the soil is popular in this group, especially those dealing with clay soil. In the TDR technique, the apparent dielectric constant of the bulk soil water is the physical quantity measured and related to the volumetric water content of the soil. For a wide range of water content and suction in clay soils, water occurs in the clay clusters as adsorbed water. This is the bulk porewater, which gives rise to the capillary phenomenon (i.e. matric suction) in the absence of a true semi permeable membrane. Therefore, time domain reflectometry practically measures matric suction. However, this technique requires soil-water retention curve of the soil tested to relate the volumetric water content to matric suction.

#### 2.4.11 ***Soil water retention curve***

The amount of water present in the soil at an equilibrium state is a function of the soil suction or pressure potential of the soil moisture. The relationship defines the water retention of soil and is known as soil water retention curve (SWRC). A typical SWRC is depicted in Figure 2.40, with the volumetric moisture content plotted against the logarithm of soil suction. This because a small change in moisture induces a very large amount of suction. Distinctive boundary conditions exist along the curve which is crucial in the characterization of a wide range of soil behaviour e.g. suction, grain size, and permeability as moisture changes. The curve is therefore distinctive for different types of soil due to different structural compositions and water distribution.

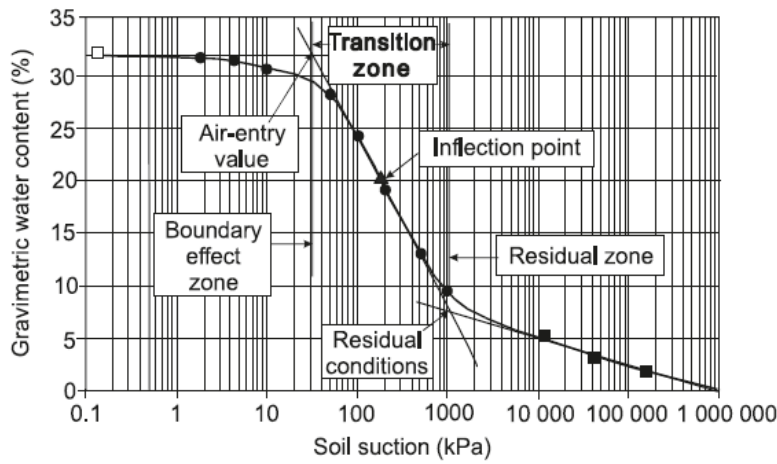


Figure 2.40: Drying curve with a definition of variables for a SWRC (from Fredlund, 2011).

However, because environmental control makes suction hence the unsaturated soil behaviour to be transient, the data of SWRC are usually adjusted to reflect this characteristic. Therefore, several empirical equations of soil water suction using best-fit curve have been developed. The fitted equations take into consideration relevant soil parameters. These include the *a*-type parameter, which relates to air-entry in the soil, an *n*-type parameter, which relates to the rate of desaturation of the soil as suction exceeds the air-entry (i.e. residual region), and in some case, an *m*-type parameter used to enhance the flexibility of the curve. These are in addition to the measured soil water content. Most of the SWRC equations can, therefore, be rearrange to estimate the soil suction if the soil water content is known. One of the most commonly used SWRC equations in geotechnical and environmental practice is the Van Genuchten (1980) equation. It is a three parameter equation which expresses water content as a function of soil suction using the three soil parameters *a*, *n* and *m* as follows:

$$w(\varphi) = \frac{w_s}{[1 + (a\varphi)^n]^m} \quad 2.28$$

Where  $w(\varphi)$  is the water content at a given suction,  $\varphi$ . The equation can be re-arranged to solve for soil suction as follows:

$$\varphi = \frac{1}{a} \left[ \left( \frac{w_s}{w} \right)^{1/m} - 1 \right]^{1/n} \quad 2.29$$

The Van Genuchten (1980) equation is mainly applicable in the SWRC region between the air-entry value and residual soil suction of the soil. Initially, estimation of suction from SWRC was not ideal due to the hysteresis that characteristically exists between the drying and wetting curves. This hypothetically leads to a large range of suction computed from the drying curve. The wetting curve, on the other hand, results in underestimated suction. However, later work by Fredlund *et al.* (2011) showed that the SWRC could be used to obtain a conservative estimate of soil suction. The framework for this estimation is the computation of a soil dependent lateral shift to obtain a median SWRC, halfway between the drying and wetting curves as shown in Figure 2.41.

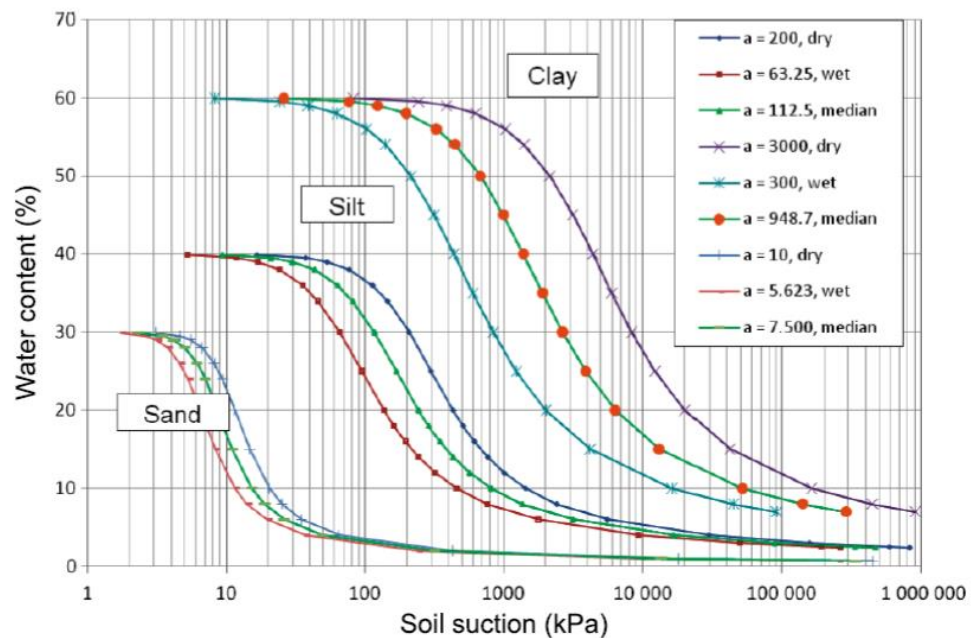


Figure 2.41: Comparison of suctions obtained from drying moisture paths in soil (from Fredlund *et al.*, 2011)

In the procedure, the point of inflection on the SWRC is used as a reference for the lateral shift. In order to derive the required control values for congruent average and wetting curves, the following empirical equation is derived from several analytical data:

$$\xi = 100[\log(\varphi_{ad}) - \log(\varphi_{aw})] \quad 2.30$$

where  $\xi$  is the “percentage lateral shift”,  $\varphi_{ad}$  is the suction at the point of inflection,  $a_d$ , on the drying curve, and  $\varphi_{aw}$  is the suction at the point of inflection,  $a_w$ , on the wetting curve. Based on analyses of different soils, an

average shift (% of a log cycle) of 25, 50 and 100% is suggested for sand, silt and clay soils respectively. The concurrent curve is then used to estimate average suction values. The average estimate is shown to significantly reduce the large percentage of error that can occur in soil suction derived directly from the drying and wetting curves as illustrated in Figure 2.41. The approach is useful in estimating a wide range of suction in desiccation studies where the very dry condition exists and cavitation is likely to occur. It is therefore considered as part of the methodology to be incorporated in this study.

## 2.5 Research gaps

Despite advances in knowledge achieved on soil cracking in the last few decades, this review shows that existing understanding of the phenomenon is insufficient. The tensile strength failure hypothesis leaves much to be desired especially with the occurrence of cracks at a wide range of soil conditions. The disparity between experimental and theoretical results implies that under a set of condition, soils possess limiting stress states that cannot be generalize. The foregoing therefore calls for improved understanding of desiccation cracking mechanism and the characteristics of cracks in a wide range of field conditions for a comprehensive solution of the instability problems in engineered slopes associated with cracking.

Desiccation cracking is more common in hot climates. However, the change in global climate has made it increasingly important in other non-arid regions. A substantial progress has been made in physical and numerical modelling to understand the impact of present climate and predict climate change impact on infrastructure slopes. However, the literature review reveals that numerical and analytical works on stability of slopes affected by cracking are few and some of the approaches do not adequately represent the changing behaviour of desiccation cracks. Inadequate representation of crack parameters in numerical models can lead to an unrealistic account of the hill slope water regime. Ideal model should include information on soil cracking such as the orientation, depth, size and density, as well as consider their changes with time since cracks

are relatively unstable features. Detail field analysis is therefore indispensable.

The environmental condition of modelling desiccation cracking in an experiment is important to produce practical results as desiccation cracking is an environmental-related phenomenon. To represent and control the environmental variables acting on the soil during cracking, a climate chamber is ideal. The literature revealed that many desiccation crack experiments do not involve these devices (Lozada, 2013). The use of thin slurry soil models does not only compromise the unsaturated condition, which characterized most engineered soils but also the textural composition and geometric properties of earth slopes. The literature shows that the stress-strain response of compacted clay fills and clay slurries are different.

Associated with climate impact is the cyclic condition under which embankment materials can undergo transient changes unimaginably. The question of structural stability of soil under such condition requires convincing evidence. Existing understanding on this theme is mainly based on examination of soil structure under multiple wetting and drying. However, because of time constraint, the number of cycles achieved in most desiccation experiment is inadequate to observe the slow changes in the soil for a convincing conclusion on this theme. Thus, the effects of multiple cycles require understanding.

Furthermore, many research findings on soil cracking experiment emanate from non-engineering disciplines e.g. agriculture and soil science. The geotechnical application is therefore limited mainly because principles of soil mechanics are mostly emphasized in the latter, especially stress state, which is important in quantifying engineered soil behaviour. The transient behaviour of unsaturated soil conditions, particularly the role of suction, lends support to this consideration.

## **2.6 Summary and Conclusion**

The review of the literature has outlined the interdisciplinary advances in soil crack research. Desiccation cracking in soil is a natural phenomenon brought about by changes in soil moisture and is commonly associated

with shrink-swell properties of fine-grained soil e.g. clay. It is widely acknowledged that cracks in a drying soil occur when shrinkage is restrained and the built-up tensile stress exceeds the soil tensile strength. Both soil properties and environmental variables including soil plasticity, density, amount of fines, water content, temperature, humidity, the rate of desiccation etc., affect desiccation crack development in the soil. Repeated shrink-swell cycles also enhance conditions for increase cracking through rearrangement in the soil structure. The significance of soil cracking cuts across a wide range of discipline and mainly arises from the role of cracks in degrading soil strength. Their role in porewater pressure response through accelerated permeability is emphasized in geotechnical problems related to an unstable slope. Consequently, it is presumed that cracks may play a key role in future clay slope deformation in view of extreme future climate which is likely to result in conditions for increased desiccation cracking. However, despite the recognition of the role of cracking in the dynamics affecting the performance of both natural and engineered slopes, current understanding leaves a lot to be desired on characteristics of cracks, particularly under a temporal environmental influence. Most literature on desiccation cracking present the general properties in a natural soil. A comprehensive quantification and characterization of cracks in an engineered soil are few.

In conclusion, the review of existing work on soil cracking has provided a general background to set the context of the present undertaking. It has helped in identifying essential themes and influencing factors so far generally understood in this subject. Therefore, selected aspects of these findings, which are important in present undertaking, are incorporated. However, necessary adaptations are considered in the study approach to address some of the important gaps while meeting its specific objectives. These include a combined field and laboratory investigation, use of climate control system, selected control variables adequate to represent real and ideal engineered fill etc. In the end, the present study would broaden existing knowledge as it addresses a wide range of practical conditions involved in crack development in engineered clay fills.

## **Chapter 3 Methodology**

### **3.1 Introduction**

This study focuses on a natural phenomenon involving soil-atmosphere interaction. Soil conditions resulting from this interaction can be complex, hence a wide range of experimental approaches exist across various practice dealing with soil. In order to derive a rational basis to achieve the aim and objectives of present study, extensive background of desiccation cracking in soil are explore (section 2.3.5). Since an embankment is a geotechnical structure, core methodological principles of this study are centre on theories of soil mechanics, particularly for partially saturated soil. The variables selected for testing were considered based on the fact that environment affects soil behaviour. Coupled with the need to address pertinent gaps existing in soil crack research, a complementary methodological framework, essentially field and laboratory procedures was developed. The field study provides realistic conditions, which formed the baseline for simulating varied laboratory testing. Parametric selection involved widespread embankment materials and construction conditions in the UK. The laboratory programs are expected to increase understanding of the processes involved in the field phenomenon. Details of the study approach and the targeted applications are given in this chapter.

### **3.2 Field procedures**

Since desiccation cracking is a natural phenomenon, the study of in situ cracks allows direct observation of their mechanism and geometric behaviour. Environmental impact on embankment soil presents a condition of unsaturation in the near surface layer primarily because of seasonal and diurnal moisture fluctuation. Therefore, monitoring and recording of changes in field moisture and associated pore water pressures are essential to understanding embankment behaviour. In order to carry out such a practical investigation in this work, a suitable site was required, specifically an existing clay based infrastructure embankment. This requirement was realised at a research embankment built for the EPSRC project named Biological and Engineering Impact of Climate Change on Slopes (BIONICS).

### 3.2.1 *The BIONICS experimental embankment*

The BIONICS project was set up in recognition of the potential of climate impact on the performance of transport infrastructures slopes in the UK. This considers the fact that a large number of earthwork slopes in the country involves volume sensitive soil materials prone to environmental changes, and there has been a significant increase in the number of infrastructure slope failures in recent times (BGS report, February 2017). The project therefore involved construction of a heavily instrumented experimental embankment for monitoring ground-atmosphere interaction and provide relevant experimental data that can help improve essential understanding of climate effects on slopes (Hughes *et al.*, 2009). The BIONICS embankment is henceforth referred to as “the embankment” in this work.

The embankment is located at Nafferton ecological farm near Newcastle city, and managed by the Newcastle University. The embankment geometry was design to offer important features of modern embankments including steep but low slopes. Accordingly, the structure is 6m high, 90m long and 5m wide with side slopes of 1 in 2 (V: H) wide. However, the length of the embankment is divided into six different test panels for multidisciplinary researches, mainly hydrological, biological and geotechnical interest. Figure 3.1 shows the embankment layout and physical structure. The two outermost tests plots, each 4 m long are for biological studies while the four inner plots (panels A, B, C and D), each 18 m long are for engineering tests.



Figure 3.1: Layout and part of physical structure of the embankment. adapted from (Hughes *et al.*, 2009; Toll *et al.*, 2012)

The east-west oriented embankment resulted in a South and North facing slopes intended to examine aspects response to climate intensities. The end slopes, each inclined at an angle of  $45^{\circ}$ , were constructed with reinforced earth.

The fill material used in the construction of the embankment is documented as Durham boulder clay, a glacial till dominant in northeast England. However, to reflect the location of this important facility, the material is commonly referred to as Nafferton clay in several related documents. This specific name is also adopted in this study. To prevent the formation of unrealistic boundary conditions and desiccation cracking, a 0.5m free draining gravel capping was spread on the crest, while to facilitate vegetation seeding, a top soil layer (200mm) was spread on the side slopes. The main fill material has been classified in several researches conducted on the embankment as summarised in Table 3.1.

Table 3.1: Properties of the Nafferton Clay of the BIONICS (adapted from Hughes *et al.* 2009; Toll *et al.* 2012, and Glendenning *et al.* 2014)

<b>Engineering properties</b>	<b>Average values</b>
Liquid limit	41.7%
Plastic limit	22.3%
Plasticity index	21.6%
Natural moisture content	19.4
Dry density (Proctor)	1.82Mg/m <sup>3</sup>
Dry density (Modified)	2.0Mg/m <sup>3</sup>
Moisture content (Proctor)	15.5%
Moisture content (Modified)	12.9%
Laboratory permeability:	
<i>Well compacted panel</i>	1.6 x 10 <sup>-10</sup> m/s
<i>Poorly compacted panel</i>	8.8 x 10 <sup>-11</sup> m/s

Based on these properties, particularly the plasticity index, the soil material of the embankment classifies as clay of intermediate plasticity (CI). According to Hughes *et al.* (2009) boulder clays are found in over 60% of the British Isles and are involved in the construction of transportation embankments in the UK. Particle size distribution reported for the embankment soil shows the material composed 12% gravel, 16% sand, 35% silt and 37% clay which further classify it as sandy clay. Clay minerals assemblages in the material include illites/smectites (42 to 54 %), chlorites/smectites (3–7%), illites (16–26%) and kaolinites (23–31%).

The engineering tests panels of the embankment in particularly were created with features, which represent two types of transport embankment common in the UK (see section 2.4.3). Accordingly, the essential difference in the engineering characteristics of the panels arises from their methods of construction particularly, the level of compaction. Panel A and D (Figure 3.1) were constructed with control compaction and no drainage resulting in positive pore water pressure at the centre. In this case, the fill was place in 1m lifts and compacted using a moving tracked hydraulic excavator to keep the limit of compaction minimal. These panels therefore represent the heterogeneous, poorly compacted railway embankments constructed by end tipping methods in the 19th century. Panel B and C on the other hand were constructed using modern compaction equipment and highway specifications. The clay fills were place in thin layers (300mm) and subjected to 18 passes using a 7,300kg self-propelled, smooth drum

vibrating roller to attained uniform layers. Combined with good drainage, these panels had better engineering characteristics, which represent the well-compacted modern highway embankment. Post constructional tests conducted on the embankment showed that the two engineered panels achieved a marked difference in density and permeability, with the well-compacted panels exhibiting highest density and lowest permeability (Table 3.1). The well-compacted panels also exhibited diametrically opposing negative pore water pressure typical of post-construction stable slope. A mixture of grasses and wildflowers sown after construction covers the embankment surface. Engineered condition and slope orientation were the main factors affecting vegetation diversification on the embankment. Influence of the slope factors on crack behaviour is one of the principal objectives of this present study.

To provide record of events related to embankment soil, common monitoring instruments and specialized devices were installed across the structure and regularly upgraded. These include piezometers, tensiometers, theta probes, rainfall sprinklers, climate cover etc. Two mini-weather stations were also mounted on the South and North Slope to record artificial rainfall simulation. A third and major weather station, which belong to the Nafferton ecological farming group of Newcastle University is further located about 300m east of the embankment. This gives benchmark measurement of micro-climate parameters that benefit the nearby embankment. Figure 3.2 shows a part of the South facing embankment structure with some of the instruments installed.



Figure 3.2: Some of the monitoring instrument on a section of the embankment

With the detail instrumentation, continuous records of experimental data relevant for evaluation of the behaviour of a typical infrastructure embankment can be obtained from the facility including vertical and horizontal ground displacement, soil moisture distribution, pore water pressure changes, soil temperature and climate parameters. A comprehensive description of the monitoring instrument installed on the embankment and their application is given by Hughes *et al.* (2009). In this study however, attention focuses on measurement of changes in soil moisture and suction on the embankment as well as the climatic controls, which essentially affects shrink-swell behaviour of clay materials. Consequently, only records from a selected instrument types providing these relevant experimental data were considered for the assessment of the desiccation cracking behaviour namely, the MPS-1 Theta probes and the weather stations (Figure 3.3).

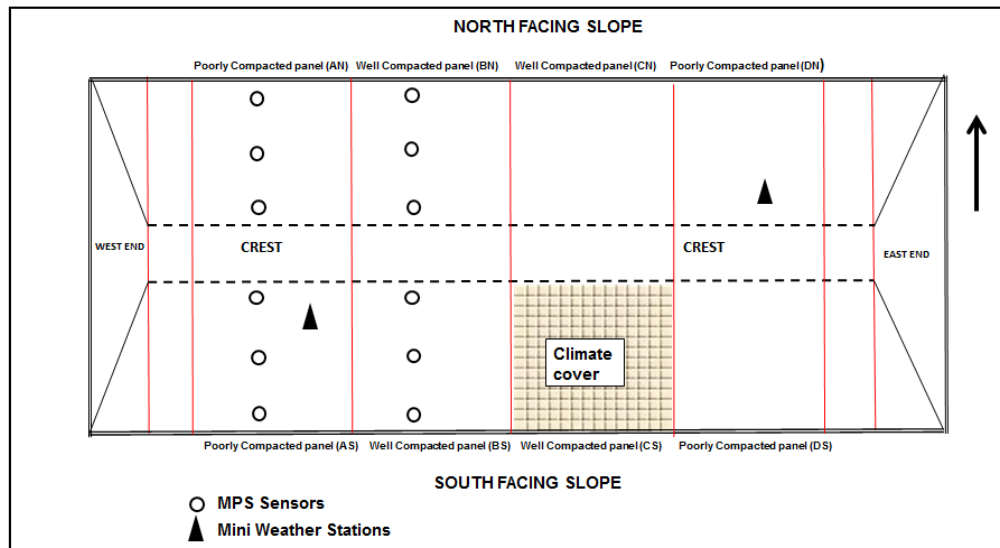


Figure 3.3: Illustration of instrument plan in the embankment (not to scale) arranged on the lower, middle and upper sections of the slopes

The MPS-1 device is a special soil probe manufactured by Decagon Corporation. Theoretically, the device generates an electromagnetic field to measure the dielectric properties in the surrounding soil where it is embedded. The sensors are design to convert the dielectric properties into soil parameters including soil water volume, temperature and pore water pressure. The Decagon MPS-1 Theta probes installed on the embankment (Figure 3.3) measures volumetric water content (VWC %), while the porewater pressure is measured in terms of dielectric water potential in kilopascal (kPa). However, this instrument measures porewater pressure in the range of 0 to -600kPa, hence negative porewater pressure or suction are customarily recorded. The sensors were installed across the slope face at depths between 0.5 and 1.5m and monitor near surface moisture changes within the unsaturated condition inherent in the near surface embankment soil layer. Compatible multichannel EM50 loggers are also mounted and linked to log the soil information at hourly intervals. Each channel on the logger therefore records specific soil information from the MPS-1 sensor at a given depth and location on the slope. The logged information was regularly downloaded using a field computer. Figure 3.4 illustrates a cross section of the embankment with the arrangement of the MPS-1 sensors and EM logger.

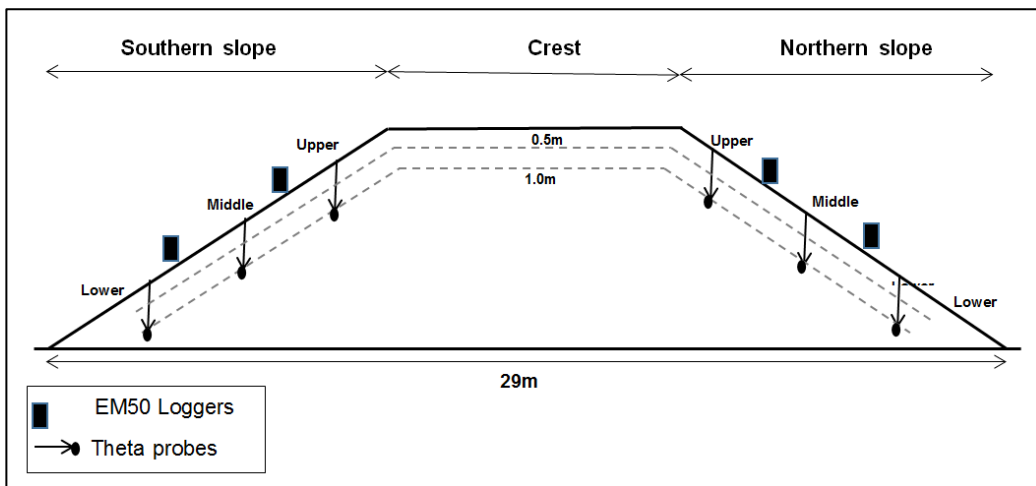


Figure 3.4: Cross section of embankment showing slope faces and soil probes.

Since inception of the project, novel research has been conducted in the facility including Masters (MSc) and Doctoral (PhD) projects. These works have essentially given leading insight into the likely behaviour of clay based infrastructure slope under climate change impact. However, a comprehensive work on cracks has not been carried on the embankment. This study will therefore fill this important gap.

### 3.2.2 Crack Survey

Walk-over surveys were repeatedly conducted to locate and measure desiccation cracking occurring in the embankment. Zielinski (2009) employed similar methods to locate surface cracks in flood embankments. Crack surveys commenced in May, 2014 and lasted until February, 2016. This was to cover different seasons and multiple cycles of shrink-swell. Investigations on cracking are sometimes carried out under a simulated climate and within a few days or weeks. These lengths of time do not adequately represent field conditions, which proceeds slowly and could be affected by the presence of top soil in typical embankments. In this study therefore, such systematic changes in the development of established cracks were closely monitored across the embankment throughout the survey period, particularly the formation of secondary cracks, crack propagation, opening and closing etc.

The method involved a visual search for surface cracks on the embankment and direct measurement of the morphological changes. The search was conducted by walking over the embankment surface panel by

panel with each panel sampled in 2m wide grids starting from the toe up to the crest and down to the toe. This survey system implies that each panel of 18m width is traverse nine times to ensure that cracks are not missed out. The located cracks are number sequentially. Once a crack is discovered, the location is peg with a red flag marker for easy identification during subsequent surveys. The slim steel base of the marker is push into the ground, a reasonable distance away from the crack front to avoid interference with the crack development. Furthermore, geographic coordinates of the crack locations were established using a Trimble global positioning instrument (GPS) for future reference. Figure 3.5 shows the crack survey on the embankment.



Figure 3.5: Crack survey on Bionics embankment. Crack location marked with red flags

Each crack found on the embankment was given a unique reference number, which indicates the slope face (North or South) and the engineered panel in which they occur. For example, the label BE/AS/01 represents a crack on the embankment (BE) found on panel A of the South facing slope (AS) and allocated serial number 01. Accordingly, all measurements were recorded and tabulated into a detail, easy-to-read field record. During the survey, both the re-opening of old existing cracks and initiation of new cracks were observed. The old cracks were identified by their very obvious furrowed outlines. Missed cracks and new cracks were constantly look out for at each repeated survey outing. A few newly initiated cracks were later discovered as the grasses withered in autumn

and gave a clearer view of the slope surface. To further preserve and illustrate prominent in the cracking, digital pictures of the cracks were taken at each survey using a 15 megapixel digital SLR Canon camera. The images were usually taken between the heights of 300 and 500mm depending on amount of detail needed.

### 3.2.3 Method *to measure* cracks

Once a crack was located, changes in its geometric features including pattern, surface length, width and depth, were monitored and measured weekly throughout the entire survey period. The weekly interval between surveys was to allow sufficient time for a measurable development of the slowly evolving crack features while adjusting to any surface disturbance during previous measurement. However, the measurements were carefully carried out to keep impact on the cracks minimal. Crack geometric features were measured using mechanical and electrical line gauges while crack pattern were visually inspected and captured in photographs. The traditional method of measuring crack directly is generally thought to give results that are more accurate. In this study crack width was measured using a 300mm rule and a Venire calliper. The two instruments were combined to increase the precision. To take a measurement, the tools were normally placed across the crack aperture perpendicular to the crack walls. Crack depth on the other hand was measured using a flat (1-2mm thick) flexible plastic probe, which varied in length between 300 to 1,000mm depending if a crack is shallow or deep. The probes were gently inserted into any visible crack, its flexibility allowing vertical penetration of subsurface curvature. When no more penetration occurs, the probe is slightly wiggled to establish the lowest point. By so doing, care is taken not to underestimate depth by not reaching the bottom and conversely, not to overestimate depth by pushing too hard especially when the soil is wet. Practically, only those cracks wide enough (~2mm) for the probes to be inserted were measured and further monitoring depended on whether the crack features reasonably develop in the next two or three survey outings. The surface length of the cracks were also measured using a fibre rope to enable manoeuvring along any surface curvature or change in orientation. The total length covered by the rope for each crack is then validated with a

metered tape. Depending on the length of a particular crack, the width and depth were measured at two or more intervals, the points of measurement also referred to as “nodes”, being determined by factors such as curvature, change in width, secondary cracking, burrows etc. All measurements were maintained within accuracy of  $\pm 1\text{mm}$ . Figure 3.6 shows measurement techniques of crack geometric properties in this study.



Figure 3.6: Line gauges and probes for crack geometric measurement

In order to compare any lateral movement in the soil related to crack opening and closing, data from the spring gauge installed at one of the established crack location was examined. For safety policy, risk assessment and safety procedures associated with field work of this nature was evaluated and implemented (Appendix I).

#### 3.2.4 **Method of estimation of volume of a crack section**

Crack intensity analyses in a soil mass often involved crack width, depth and length. Understandably, crack depth is commonly emphasised in slope stability analysis because of its potential role in the architecture of the slip surfaces as well as depth of wetting. However, none of these parameters in their singular form can adequately characterise cracking intensity since geometry may change in direction. Also, when considering water holding capacity and infiltration potential in a slope, crack volume, which defines the amount of space the cracks occupy in the soil, is a quantitative parameter that cannot be overlooked. Since a standard unit volume comprises 3-dimensional geometry, crack volume can also serve as a good indicator of the shrink-swell or horizontal volume changes in expansive soil. Therefore, estimation of the volumes of cracks is introduced in this study to characterise cracking intensities and their time morphological changes in the field.

Several techniques have been used to estimate the cross-sectional volume of crack in soil. Transect, soil layer subsidence and COLE methods are discussed in the literature review (section 2.2.2). In this study, the approach employed empirical relation which utilises the geometric properties of the cracks measured in the field. The derivation followed personal communication with Dr Andrea Kishné of Texas A&M University who provided the background illustrations and mathematical basis from Math Forum (<http://mathforum.org/kb/message.jspa?messageID=4683199&tstart=0>) and theorems of plane and solid geometry (Holgate, 1901). The derivation is presented below.

Consider a triangular pyramid presented as a truncated fulcrum with parallel triangular cross-sections perpendicular to the length in Figure 3.7.

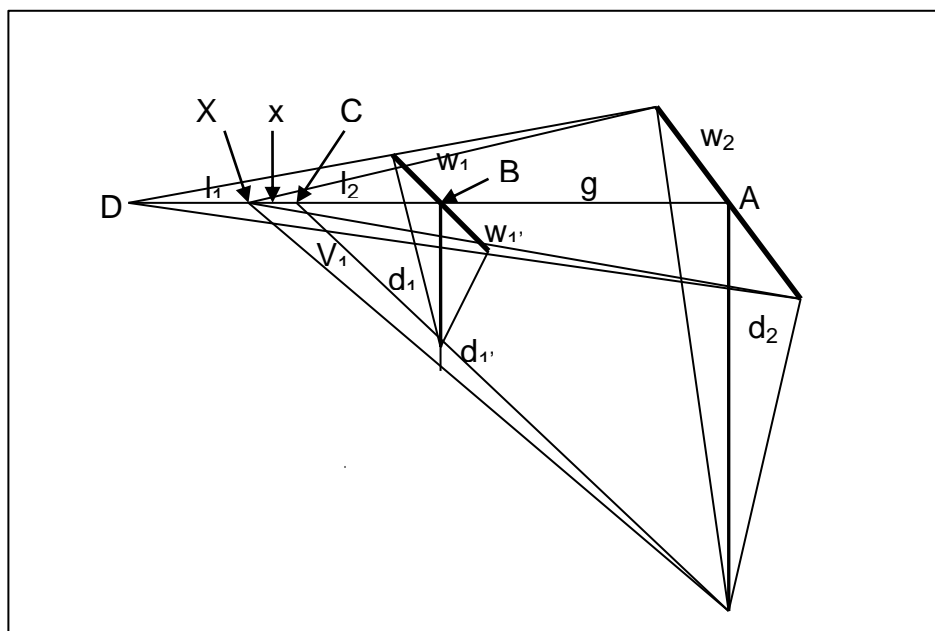


Figure 3.7: Cross section of a truncated fulcrum (adapted from Holgate, 1901)

Theorem 522 for prismatic structures state that “the volume of a triangular pyramid is equal to one-third the product of its altitude and the area of its base” while theorem 524 states that “the volumes of any two pyramids are in the same ratio as the products of their altitudes and the areas of their bases” (Holgate, 1901). Following these background theorems, The Math Forum shows that the area  $A$  ( $\text{mm}^2$ ) and volume  $V$  ( $\text{mm}^3$ ) of the composite sections in Figure 3.7 can be derived as follows:

$$l_1=BD, \quad 3.1$$

$$l_2=BC, \quad 3.2$$

$$x=BX, \quad 3.3$$

$$A_1=1/2 \times w_1' \times d_1' \quad 3.4$$

Based on similar triangles:

$$w_1/w_2 = l_1/(l_1 + g), \text{ and} \quad 3.5$$

$$l_1 = g \times [w_1/(w_2 - w_1)] \quad 3.6$$

Also,

$$d_1/d_2 = l_2/(l_2 + g), \quad 3.7$$

$$l_2 = g \times [d_1/(d_2 - d_1)] \quad 3.8$$

Based on similar pyramids with apex X:

$$\frac{w_1'}{w_2} = \left[ \frac{(l_2+x)}{(l_2+x+g)} \right] = \frac{d_1'}{d_2} \quad 3.9$$

$$\frac{A_1'}{A_2} = \left[ \frac{(w_1' \times d_1')}{(w_2 \times d_2)} \right] = \left[ \frac{(l_2+x)^2}{(l_2+x+g)^2} \right] = \frac{A_1}{A_2} \quad 3.10$$

This implies  $A_1' = A_1$

So, for any two pyramids,

$$\frac{V_1}{V_2} = \frac{A_1 \times L}{A_2 \times (L+g)} \quad 3.12$$

The condition in equation 3.12 therefore satisfies theorem number 524 stated above. This principle can be applied to any given point in an irregular crack section when treated as a triangular prism or truncated fulcrum (Figure 3.8).

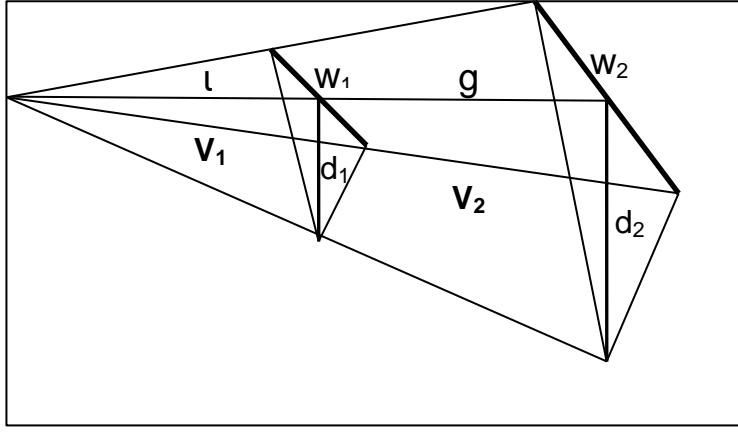


Figure 3.8: Geometry of crack section:  $w_1$ ,  $w_2$  are crack width,  $d_1$ ,  $d_2$  are vertical crack depth,  $g$  is the gap between the sections (length of crack section),  $l$  is a hypothetical length of the first pyramid.  $V_1$  and  $V_2$  are volumes of the first and second pyramid.

The volume between the two triangular cracks geometries can then be derived from theorem 522 as follows:

**Volume of the triangular pyramids:**

$$V_1 = \frac{1}{3} A_1 \times l \quad 3.13$$

$$V_2 = \frac{1}{3} [A_2 \times (l + g)]$$

Where  $A_1 = 1/2 \times w_1 d_1$  and  $A_2 = 1/2 \times w_2 d_2$ , areas of the two triangular cross sections.

**Volume of the truncated triangular pyramid is:**

$$V = V_2 - V_1 \quad 3.14$$

$$= \frac{1}{3} [A_2 \times (l + g)] - \frac{1}{3} A_1 \times l \quad 3.15$$

From similar triangle also:  $l/(l + g) = w_1/w_2 = d_1/d_2 \quad 3.16$

This implies that  $l^2/(l + g)^2 = A_1/A_2 \quad 3.17$

Solving for  $l$ :  $l = [\sqrt{A_1} \times g]/[(\sqrt{A_2}) - (\sqrt{A_1})] \quad 3.18$

Substituting  $l$  in equation 3.15,

$$V = \left[ (1/3 \times A_2 \times g) + \frac{(1/3 \times A_2 \times \sqrt{A_1} \times g)}{[(\sqrt{A_2}) - (\sqrt{A_1})]} \right] - \left[ \frac{(1/3 \times A_1 \times \sqrt{A_1} \times g)}{(\sqrt{A_2}) - (\sqrt{A_1})} \right]$$

$$= 1/3 [A_2 \times g + (A_2 - A_1) \times \sqrt{A_1} \times g]/[(\sqrt{A_2}) - (\sqrt{A_1})] \quad 3.19$$

Since,  $(A_2 - A_1) = [(\sqrt{A_2}) + (\sqrt{A_1})] \times (\sqrt{A_2}) - (\sqrt{A_1})]$

$$\begin{aligned}
\text{Then, } V &= 1/3 [A_2 \times g + (\sqrt{A_1} \times \sqrt{A_2}) - \sqrt{A_1} \times g] \\
&= 1/3 \times g [A_2 + (\sqrt{A_2} \times \sqrt{A_1}) + A_1] \\
&= 1/3 \times g [A_2 + \sqrt{A_2 \times A_1} + A_1] \tag{3.20}
\end{aligned}$$

Where  $A_1 = 0.5(w_1 \times d_1)$  and  $A_2 = 0.5(w_2 \times d_2)$ , represent the area of the triangular cross sections for first and second nodes. Substituting the area functions in equation 3.20, a crack volume equation, and the correct version of the encompassing the three regularly measured crack geometric parameters; length, width and depth is obtained as follows:

$$V = \left(\frac{1}{3}\right) \times L \times \left[ \left(\frac{1}{2} w_1 \times d_1\right) + \left(\frac{1}{2} w_2 \times d_2\right) + \sqrt{\left(\frac{1}{2} w_1 \times d_1\right) \times \left(\frac{1}{2} w_2 \times d_2\right)} \right] \tag{3.21}$$

### 3.2.5 *Measurement of soil moisture and suction changes in the field*

Fluctuation in soil moisture is a key factor influencing shrink-swell action in expansive soils. It is also recognised that there is a coupling between moisture changes and suction developed in soil with significance implication in desiccation cracking phenomenon. Assuming there are no external load and material loss on the experimental embankment, the changes in the soil condition can be regarded as effect of changes in the soil-water suction. Therefore, time series record of near surface soil moisture and suction condition as the cracks develop are obtained in this study. The MPS-1 devices installed on the experimental embankment carry out a continuous recording of volumetric water content and matrix suction at different depths up to 1.5m in the embankment. This range of depth reasonably covers the active zone where unsaturated soil conditions are known to be very unstable leading to different kind of geohazard reported in literatures. The robust data set of soil moisture and suction recorded in the embankment were, with due authorization, accessed from Newcastle University P-drive for used in this study. The data are processed and analysed with time for the different depth across the embankment using excel spread sheet. Attention is particularly paid to recordings around crack locations in order to streamline the analytical information stored since commencement of construction of the

embankment in 2005. The magnitude of data is also limited to the period of study except for comparison with selected years of relevant events.

### **3.2.6 *Evaluation of climatic parameters***

The effect of microclimate on soil condition is recognised in geotechnical research. In section 2.4.4, it was noted that patterns of pore water pressures on a slope reflect direct response to microclimate conditions. Rainfall is the principal source of atmospheric water flux into the soil while evapotranspiration is responsible for upward flux of soil water back into the atmosphere. The difference between these two fluxes at any point in time largely controls the pore water pressure conditions in the soil. In this study, the patterns of micro-climate around the embankment were analysed and used to assess changes in near surface moisture and crack morphological evolution. A full climate data were derived from the weather stations within and around the embankment. The climate data used included wind speed, net radiation, relative humidity, atmospheric pressure, ambient air temperature, amount of rainfall etc. Important climate parameters e.g. rainfall, sunshine etc., are plotted in time series to reflect their changes and identify periods of extreme events. The wind-rose was also plotted to evaluate the prevailing wind directions across the embankment surfaces. The climate parameters were further combined in the FAO Penman-Monteith equation for estimation of evapotranspiration. Necessary unit conversions were carefully carried out as well as estimation of missing climatic data with standard equations where applicable. Evapotranspiration was estimated for both North and South facing slope for the period covered by the survey.

During the field study, cracks were observed to show seasonal and diurnal response to wetting and drying events, with extremes between summers and winter period characterised by highest drying and wetting respectively. The cracks also occurred in different proportion across the engineered panels of the embankment. These observations were noted as part of the baseline field conditions necessary to build the framework for complimentary laboratory studies.

### 3.2.7 *Influence of vegetation on soil cracking*

The mechanical role of vegetation root anchorage in soil is widely reported as well as the role of vegetation in transient pore water fluctuation (section 2.4.6). The influence of vegetation on cracking is relatively less investigated. As one of the objectives, this study seeks to understand the influence of vegetation, particularly root systems in the formation of crack patterns as well as any measurable hydrological effect. Interestingly, the embankment is colonised by rich species of grasses and herbs, which have been noted to show preferential diversification influenced by aspects and engineered conditions (Glendinning *et al.*, 2009). It is reasonable to expect that crack distribution could be affected by the pattern of vegetation diversification in addition to the slope properties. Consequently, the root mass and network of vegetation within and around the location of in situ cracks were closely examined with a hand lens while the hydrologic effect was evaluated using evapotranspiration results from the weather stations. Figure 3.9 show the grass covered slope and common vegetation assemblages on the embankment. A rooted soil block was also collected from an experimental lysimeter in the field to further investigate the effect of vegetation in the laboratory.



Figure 3.9: Vegetation cover on the embankment (March-September 2014)

### 3.2.8 *Summary of field study*

The study of cracks in a natural setting is essential in understanding the factors and characteristics associated with their formation in situ. The embankment provided this study a direct opportunity to monitor and measure natural cracks development in the field. A systematic crack survey was therefore conducted during which geometric parameters useful

in characterising the crack development were directly measured. The engineered properties in the embankment enabled recognition of potential response of embankment structure to environmental driven changes. Specifically, high quality soil and climate data were synthesised for their influence on crack formation on the embankment. Overall, the field program was successful in partial fulfilment of study objectives.

### **3.3 Methodological development for laboratory testing**

Like most natural phenomenon, holistic understanding of field processes involved in natural cracking is challenging. The central process of soil shrinkage and swelling is not easy to observe in a natural setting because of its slow and transient behaviour. In addition, soils characteristically present heterogeneous properties. Therefore, physical models are commonly employed for better understanding of the field behaviour. Some field and laboratory methods investigating desiccation cracking was outlined in section 2.3.5. Following the background of existing experimental approach in this genre, laboratory experimentation was set out to simulate desiccation cracking. However, experimental framework of present study is concern with cracking in fine-grained soil under the properties and conditions involved in creation and performance of transport infrastructure embankment, essentially a slope-vegetation-atmosphere interaction. As mentioned earlier in section 3.1, the laboratory test programs were essentially designed using baseline conditions from the field study. Therefore, the test procedure was developed with principles and parameters adapted to represent important conditions in the embankment. Accordingly, selected control variables included soil density, moisture, suction, layer thickness, plasticity, vegetation presence, cyclic wetting and drying, etc.

The field study generally indicates that cracks showed reasonable response in warmer and drier conditions as well as period of intense rainfall. Fluctuation in these conditions is also crucial in earth slopes deformation process. In order to simulate these environmental variables, an innovative soil-climate interaction system was designed and assembled using bespoke apparatus. Climate controlled has been used in other desiccation cracking experiments (section 2.3.5) to practically represent

environmental factors, which drives desiccation process. In this study, the climate control system essentially creates a constant low humidity climate inundated by rainfall in a cyclic manner, replicating the conditions operational in the field for cracking. The system was comprised of a soil box (soil mould), climate control unit and an atmospheric cover mounted with various research standard monitoring instrument. A full design of the experimental system is as shown in Figure 3.10 below.

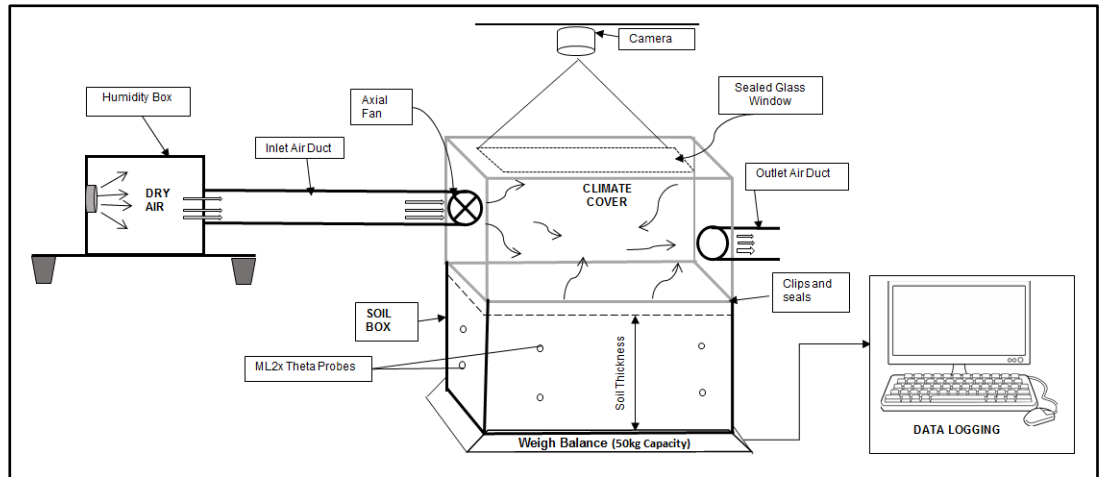


Figure 3.10: Schematic of the experimental system for laboratory desiccation crack experiment

The test principle follows the established restrained shrinkage condition for crack development (Kodikara *et al.*, 2000; Peron *et al.*, 2009b). Focus was on pore water changes, shrinkage and cracking characteristics in the soil under specific climate and embankment construction conditions. Digital image analysis, Microsoft Excel etc. was used for data handling and characterization.

### 3.3.1 **Design and construction of soil mould**

Different types and shapes of materials have been used as soil mould in desiccation crack experiment including wood and glass. They are usually considering on their potentials to provide the base restraint necessary to achieve shrinkage cracking. In this regard, glassy surface has been noted to offer greater restraint than wood (Kodikara *et al.*, 2000; Yesiller *et al.*, 2000). This is likely due to greater adhesion of wet clay to glass-like surface and therefore produces a high shear restraint. Roldane (2010) conducted soil cracking experiment using a wooden soil box measuring 500 x 500 x 500mm. No significant crack occurred in this experiment,

which could have arisen from the mould factor mentioned above. In addition, the volume of soil compacted in full volume of this mould appears have required a longer time to produce significant drying and shrinkage under the slow natural drying adopted in this MSc.. Consequently in this study, a soil box material and size was conceived which would enable good development of desiccation cracks within a laboratory scale. A trial test was carried out in a special grade of factory made high impact thermal plastic box with a glossy surface (Figure 3.11).



Figure 3.11: Trial test in the plastic mould

The trial test was primarily to validate the suitability of the perspex-like box in the friction/adhesion-dependent restrain shrinkage experiment. A 20kg of soil was compacted in the box. When desiccated under a gentle fan speed simulating wind impact, the specimen developed clear polygonal cracks as shown in Figure 3.11. The reinforced base and corners of the rectangular box gave good rigidity and tensile strength for soil compaction without breakage and excessive expansion. Apart from being transparent, the box is also calibrated at different levels, which provide a good measure of the soil volume, layer thickness, visual observation and installation of monitoring instruments. With this success, a 35 litre capacity plastic box measuring 310mm deep, 380mm wide and 330mm long was adopted as the soil mould for the laboratory desiccation experiments. Pre-calculations showed that this capacity was sufficient for a soil volume that would achieve a reasonable laboratory scale experiment with regard to workability, layer thickness, desiccation etc. The volume was also considered based on the maximum capacity of an electronic weigh balance intended

for monitoring moisture loss in the experiments, which was 50kg. Other innovations on the soil box include boring of a 3mm diameter holes for installation of moisture probes and other monitoring devices.

50kg of soil preliminarily compacted with different effort in the box resulted in soil layer thicknesses ranging between 180mm and 230mm. This was considered reasonable for layered soil experiment. It also compared to the scale used by notable workers (Miller *et al.*, 1998; Yesiller *et al.*, 2000). This range of soil thickness was then used as a reference to position instrumentation holes on the sides of the soil box. The nearest instrument to the top and bottom of the proposed soil thicknesses was 40mm each. This was to minimise their influence in the development of surface cracks.

### **3.3.2 Design of climate control unit**

Different climate chambers are employed in desiccation cracking experiment. They are commonly user specific bespoke systems to simulate and/or control climate variables, mainly humidity, temperature and rainfall to be. Environmental drying on embankment involves warm, low humidity atmospheric conditions. Rainfall is also a characteristic factor acting as opposite condition i.e. wet, high humidity. In order to simulate these fundamental atmospheric conditions affecting a natural embankment, a climate system was designed in this study to perform a cyclic wet and dry experiment. In the first instance, a system that would generate and maintain a warm atmospheric condition driven by gentle air to interact with the engineered clay soil was required. This was achieved by constructing an air conditioning unit linked to a climate cover according to the master plan shown in Figure 3.10. To generate dry, low humidity air, a Compco air compressor system in the geotechnical laboratory was used. For this experiment, the compressor was set to create air temperature at 25°C, an average value to simulate a typical warm day temperature in the UK. To step down and normalise the high air pressure from the compressor to a laboratory scale wind speed, a dedicated compressed air line was connected through control valves into the air condition box as showed in Figure 3.12.

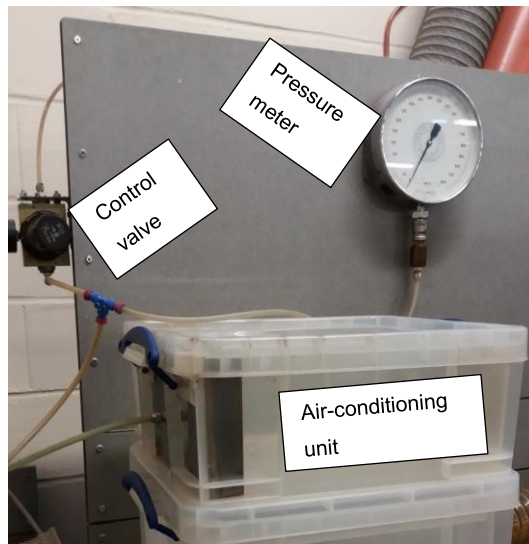


Figure 3.12: Air conditioning unit

At the opposite side of the unit, a 105mm hole was created in order to fit a flexi-hose that would conduct the conditioned air to a climate-soil cover representing the atmospheric envelop. The decompressed dry air resulted in average relative humidity of 30% as against the surrounding laboratory humidity of 45 – 50%, and average of 80% for Newcastle area. There were also 5 to 8°C difference between the air in the climate system (24°C) and the fluctuations of the warmer laboratory air temperature (29-32°C). With these values, the unit was considered effective in simulating a practical atmospheric conditions for a laboratory scale desiccation of engineered soil.

The climate cover was created by using a second transparent box upturned and firmly clipped with a foam seal over the soil box. Additional innovations on the cover include provision of a glass window for photography and boring of two opposing holes, each 105mm in diameter for inlet of dry air and outlet of wet air from the soil surface respectively. A two speed axial fan was also attached at the in-let hole on the cover to simulate turbulent air flow over the soil surface. The speed control switch was to enable further variation of wind circulation when required. Figure 3.13 shows the finished climate cover with provisions for fittings (Left) and the axial fan in place (Right).



Figure 3.13: The climate cover fitted with axial fan

All cut edges and fittings including the contact with the soil box, were sealed with draught excluder to maintain the conditioned climate against external influence. In this set up, wetting (i.e. rainfall simulation) was done manually by using spray bottle to spray water on the soil at the end of each drying stage. The quantity of water used in each wetting was proportional to the amount of water loss during the drying. This was to maintain consistent test conditions.

### 3.3.3 *Instrumentation and measurements*

In geotechnical practise, monitoring and measurement of events and analytical parameters are very crucial to arrive at good engineering judgement. Various kinds of soil monitoring instrument exist in the industry depending on the parameter required. The choice of instrument is usually guided by sensitivity and reliability. In this study, relevant soil and environmental parameters were required including soil moisture, soil temperature, humidity, wind speed, crack images etc. Moisture changes in the soil box were measured both volumetrically and gravimetrically. The volumetric moisture was measured using ML2X Theta probe, a widely used soil moisture instrument in desiccation cracking practice. The device is a type of time domain reflectometer (TDR) designed to measure soil moisture by the well-established principles of material respond to changes in apparent dielectric constant. Essentially, the ML2X probe (Figure 3.14) consists of a cylindrical waterproof housing (112mm in length, 40mm in diameter), which contained the electronics and an input/output cable. Attached at one end are four sharpened stainless steel rods for insertion in the soil to serve as an internal transmission line in the probed body. The rods are 60mm in length and 3mm in diameter, and arranged in a radial

spacing of 15mm. The outer three forms an electric shield around the central rod, which is the signal rod.

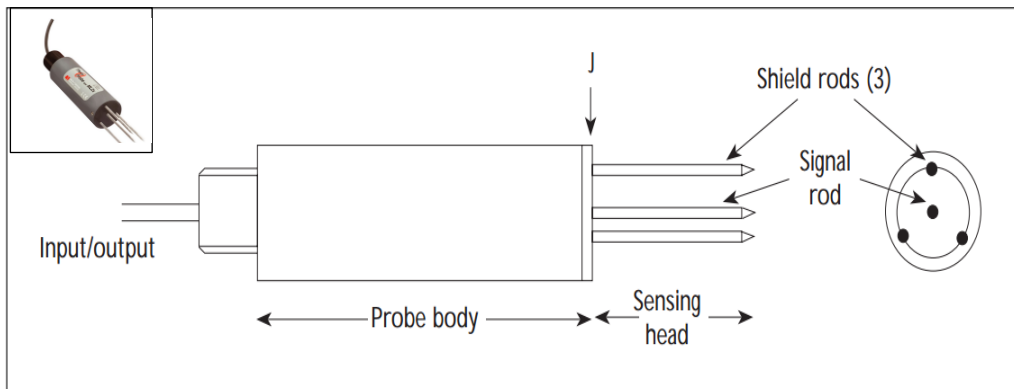


Figure 3.14: Schematic of ML2x Theta probe, actual probe inserts (Miller and Gaskin, 1999)

When powered, the device creates a sinusoidal waveform which is transmitted into the soil by its array of stainless steel rods. The permittivity (a measure of material response to polarization in an electromagnetic field) of the water content surrounding the rods strongly influences the applied field. This influence essentially creates impedance to the arrays, which is measured by the probe as it responds to changes in the dielectric constant of the soil. The frequency of the changes are converted into a DC voltage output, virtually proportional to the soil moisture content. The lower the voltage, the greater will be the impedance (or resistivity) and the lower the soil moisture content. The probe therefore requires a compatible logger to power it as well as record moisture information. The logger type used in this study was a Delta-T's DL6 with multiple channels to connect different moisture sensors. A total of six moisture sensors were used with the DL6 Logger in this experiment. The sensors are lined on the sides of the soil box from top to bottom to enable assessment of the gradient of moisture and suction with depth in the desiccating soil. The top probes were at least 40mm from the soil surface to reduce interference with the cracking. The array of sensor covers about 80% of the soil volume. To install the probes, the signal rods are set in the bored holes and gently pushed into the soil specimen through the 3mm thick wall of the soil box after compaction. This means about 95% of the signal rod is embedded in the soil to achieve the prescribed level of contact. The logger data are downloaded through a compatible software (i.e. data links) installed on a

dedicated laboratory computer. Before filling and compacting soil in the box, all instrument holes are sealed with duct tape to prevent the soil and moisture seepage from the holes. Similarly, the outside contacts of the sensitive probe with the soil box are also sealed round with duct tape to prevent interaction with surrounding atmosphere.

The gravimetric water content on the other hand was determined by mass loss as the soil dries. To achieve this, a 50kg capacity bench top electronic weigh balance (Defender 3000XtremeW) was employed. The box with the compacted soil specimen prepared at predetermined moisture content was placed on the balance which was connected to a dedicated computer to continuously log the mass loss in the soil box at one hour intervals. Every other weight being constant, including mass of the dry soil, the mass loss recorded from the weigh balance is considered as the mass of moisture evaporated from the drying soil. The known mass of dry soil and moulding water content are then combined with the successive mass of remnant water at any given time during the process to back-calculate the corresponding gravimetric moisture content following the procedure of BS 1377:1990 Part 2. The moisture data acquired in the laboratory test were used to characterise the soil hydrology during the cracking process. The data were also used in used in the Van Genuchten (1980) empirical soil water retention equation for estimation of soil suction developed as the soils desiccate.

Relative humidity and air temperature levels within and outside the climate controlled system were monitored using Thermo-Hygrometer fitted with a remote sensor for non-invasive measurement. The instrument measures relative humidity between 0 to 100 % to an accuracy of +/- 2% and air temperature between -20 to 50°C to an accuracy of +/- 1°C. To monitor the speed of wind delivered into the experimental system, a hand held digital anemometer was used. Wind is a key driver of evaporation from soil surface and is strongly coupled with other climatic factors like temperature and relative humidity.

Since crack evolution is systematic as soil moisture changes, time series images of the morphological features are useful to analyse and quantify

their development. In this study, time lapse photography was incorporated into the experimental system to record images of surface cracks developed. The photography was carried out using a 15.1 mega-pixel SLR Canon camera mounted on a tripod stand to take pictures through the glass window added on the roof of the climate cover and perpendicular to the crack plane. Timing of the photography was achieved with the aid of a hand-built micro-control circuit which was assembled with the assistance of University technical staff. The micro-circuit operates using C++ program language where input electrical voltage are regulated by a metal-oxide-semiconductor field-effect transistor (MOSFET) switch and converted into distinctive mechanical signals. The mechanical signals manifest in the camera trigger according to programmed time. In this study the circuit was programmed to trigger at hourly interval to record close stages of the cracking, particularly crack initiations. A white fluorescence light incidence from the top of the climate chamber was added for uniform brightness and to enhance good contrast between the soil clod and cracks.

### 3.3.4 *Validation of laboratory experimental system*

Components of the bespoke apparatus were finally coupled into a unique, fully automated climate-soil interaction system as shown in Figure 3.15. This actualised the original design shown earlier in Figure 3.10.

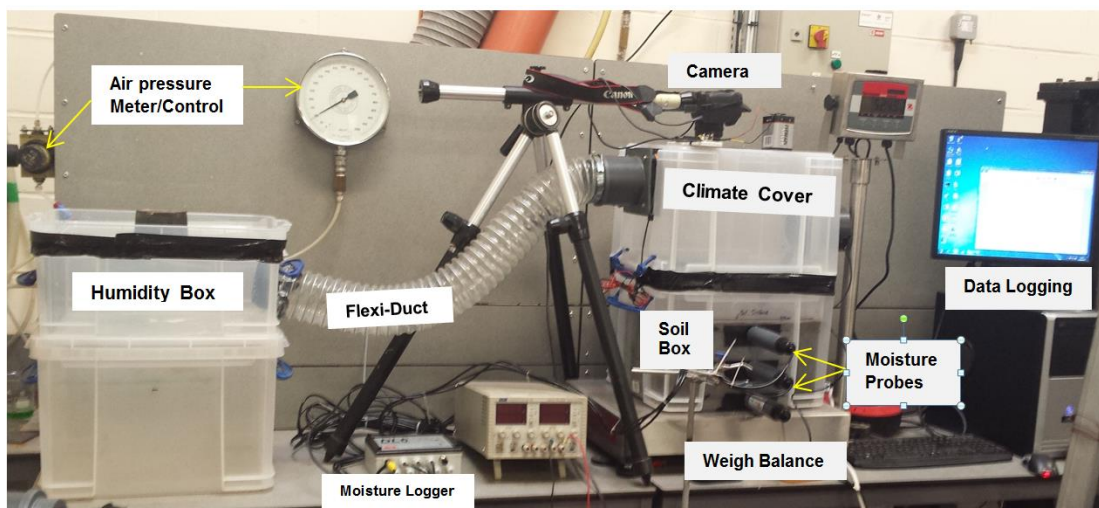


Figure 3.15: Laboratory scale soil-atmosphere interaction system

The air conditioning unit was linked with the climate cover through a 500mm flexi hose. Both ends of the hose was firmly clipped to the flange

extension provided on the boxes. A dry run test shows the system could maintain the conditioned humidity and temperature to about  $\pm 1$  unit each. However, humidity was slightly higher above the soil surface, in order of 5% while the outlet air temperature dropped by average of 8%. Cracks occurred in a preliminary specimen desiccated in the system and the features were clearly captured in the automated camera images. The soil hydrology was also successfully logged by both the moisture probes and weigh balance. With these results, the system was validated as effective for the laboratory experiment.

### 3.4 Soil Materials

In line with the focus of this study, soil materials were selected for testing of the influence of plasticity, compaction characteristics, layer thickness etc. on desiccation cracking. However, the models were adapted after characteristics of the Nafferton Clay used in creation of the embankment. To represent other common embankment materials in UK, a Gault Clay material and very high plasticity fill created by soil mix were used to represent a high to very high plasticity extreme reported in the Southern part of the country, particularly the London Clay. Nafferton Clay (Durham boulder Clay) is the dominant construction materials in the North while Gault and London Clays are dominant in the South with well-known geotechnical significance associated with their plasticity.

Samples of the Nafferton Clay were dug out from a stockpile near the main embankment where some of the material was reserved for research purposes and to prevent direct sampling from the instrumented structure. Sampling was carried out in February 2014, taking into consideration the presence of natural moisture content. In total, 100kg of soil samples were collected. These were transported in water proof bags to the soil laboratory store at Newcastle University. Samples of Gault Clay were donated to this study by Electrokinetic Ltd who worked on embankment stability along the A14 carriageway around Cambridgeshire. The samples were collected from boreholes at depths between 600 – 1,000mm. Natural samples of very high plasticity material could not be readily sourced for this study. Therefore the desired plasticity range was created in the laboratory as presented later in this chapter.

### **3.4.1 *Material preparation and testing***

The method of preparation of soil specimen for laboratory testing is important in obtaining reliable data for practical interpretation. Standard specifications emphasizes on sample size, grains size distribution, handling procedures, environmental conditions etc. In this study, the considerations for specimen preparation were based on the type of test and control variables. Cardinal in the investigation is assessment of the cracking characteristics of two main type of embankment construction in the UK, a well compacted modern highway embankment, and a poorly compacted historic railway embankment. Consequently, the soil samples were prepared for standard test to characterise the soils. As properties of soil types used in this study are widely published, only a few essential tests were carried out to validate existing characteristics e.g. plasticity and density.

Sample preparation for plasticity and density tests followed the procedures stipulated in BS 1377:1990 part 2 and 4, which relate to Atterberg limit and compaction. Accordingly, for Atterberg limit tests, a reasonable quantity of collected soil samples were washed through a 425 micron sieves after picking out the coarser materials (BS 1377:1990 part 2, section 3 and 4). After 24 hours, the predominantly clay particles were recovered from the settled solution after decanting the clear supernatant water. The specimens were then air-dried to appropriate moisture state for the plastic limit, liquid limit and linear shrinkage tests. For the standard proctor test, both the Nafferton and Gault clay soil materials were shredded through a 5mm sieve and compacted in a 1,000cm<sup>3</sup> steel mould. The results of material properties are presented later in section 3.4.3.

### **3.4.2 *Simulation of a very high plasticity clay material***

Since a natural sample representing very high plastic soils could not be sourced during the period of study, the property was simulated in the laboratory by mixing Bentonite with the Nafferton clay to upgrade its plasticity. Bentonite is very high plasticity clay containing mainly montmorillonite mineral. It is expected that the additive will increase particularly the liquid limit of Nafferton material, hence the plasticity index. The targeted PI was 52% to represent upper range median reported for

very high plastic soils (CH – CV) in the southern part of England. In order to estimate the right material quantity for the simulation, a preliminary mix of Bentonite in a progressive proportion (5%, 10%, 15%, 20% etc.) by mass of a representative sample of Nafferton soil (350g of fine content) was conducted. However, since Bentonite is highly hydrophilic and active, two soil mixing methods were tested in order to achieve optimal results. The first method was a dry mix of Bentonite and Nafferton Clay powders while the second was a pre-hydrated Bentonite mix with a slurry of Nafferton clay. In the first design, air-dried and pulverized sample of Nafferton soil was mixed with the required percentage of Bentonite powder, initially by hand before finally adding de-ionized water in a quantity of about five times its liquid limit to make a smooth paste. The paste was then re-mixed in a plastic container with a spatula and later left for 72 hours for the clay particles to saturate and interact. In the second method, the Bentonite powder was first pre-hydrated separately for 24 hours for the clay to saturate into a smooth gel before mixing with the appropriate quantity of Nafferton soil slurry. The slurry mix was also left to interact for 72 hours. Using the two design, four specimens each were made out with increasing percentages of Bentonite inclusion by mass of 350g of Nafferton clay and subjected to Atterberg limit test. A plot of the PI of specimens for each methods against their respective percentage of Bentonite indicates a significant increase in the plasticity with the increasing Bentonite content (Figure 3.16) resulting in a linear relation for estimation of material required to arrive at the targeted PI.

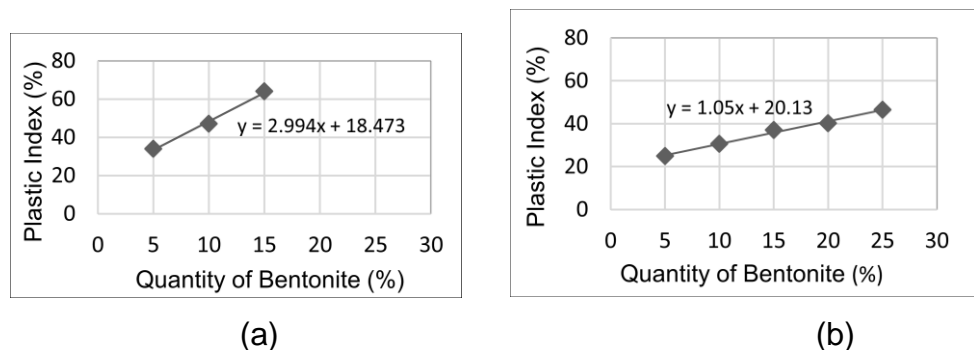


Figure 3.16: Results of the mix design for material estimate (a) Pre-hydrated, (b) Dry mix

The resulting relations means to achieve a PI of 52% will require 11.2% and 33% by mass of Bentonite mix with the appropriate quantity of

Nafferton Clay for the pre-hydrated and dry mix methods respectively. These values were validated with a 350g of Nafferton Clay, implying addition of 39.2g and 99.4g of Bentonite from the pre-hydrated and dry mix design respectively. Atterberg limit results for slurry mixture with 11.2% Bentonite correctly resulted in targeted PI while that of 33% mix resulted in a rather too high PI (over 100%). The difference in these values certainly arises from the plastic indexes resulting from the material quantities estimated in the methods of mixing. The mixing carried out in the dry, powdery form is thought to inhibit the volume potential of the highly hydrophilic (or absorbent) Bentonite material and maximal interaction with the Nafferton Clay at inter-particle level. This resulted in much lower consistency for any given proportion of Bentonite mixed. The implication is the higher amount of Bentonite extrapolated for the targeted plasticity. The pre-hydrated slurry mix on the other hand allows the Bentonite to fully disperse and expand to its full physio-chemical characteristics thereby enabling a more effective mixing with the Nafferton Clay to result in optimum plasticity for any corresponding proportion of Bentonite in the mix. This therefore resulted in a reduced proportion of Bentonite required to attain the desired plasticity as obtained from the plot. The foregoing underscores the importance of appropriate sample preparation and mix design, particularly for reactive materials, in obtaining reliable results. Hence, the need to adopt a methodology founded on a good understanding of mechanics of soil materials.

The pre-hydrated mix model was therefore adopted to create the third soil sample for the desiccation experiment. To achieve the very high plastic soil specimen of at least 50kg required in the experiment, 40kg of dry Nafferton clay from a semi wet soil bank of known moisture content was used. Accordingly, this required 4.8kg of powdered Bentonite (11.2% by mass) with moulding water expected to make up the remaining mass. However, for convenience, 6kg of Bentonite powder was pre-hydrated to about 5 times its liquid limit and mixed into smooth gel after 3 days. The equivalent quantity of dry Bentonite was then derived from this bank by calculation with the known moisture content of the gel. With this, material shortage was avoided. The predetermined quantity of Nafferton soil was

also soaked and mixed into a uniform slurry in a large plastic drum large enough to contain the two specimens. On attaining the right state of uniformity, the appropriate portion of Bentonite gel was then scooped in bits into the container of the Nafferton slurry and mixed gradually until full hydration. The two mixtures were then remixed for 30 minutes each day for 3 consecutive days to form homogenous slurry. The mixing of this quantity of soil slurry was accomplished with an 800watt hand-held electric mixer. The uniformly mixed Nafferton- Bentonite slurry was then spread out in two large aluminium pans (Figure 3.17) and air dried under a laboratory fan, churning daily to avoid particle segregation. On reaching a workable moisture state, the samples were stored in a sealed container for use as the third soil material in the desiccation experiment.



Figure 3.17: Bentonite-Nafferton clay mixture undergoing drying processes

### 3.4.3 *Materials Property*

As noted earlier, engineering properties of the three types of soils materials modelled in this study have been extensively studied. The results of index property tests carried out in this study for the Nafferton Clay and Gault Clay materials reasonably compare to the ranges of median values published in the literature as depicted in Table 3.2.

Table 3.2: Summary of material property

Plasticity Soil type	Literature*			This work		
	Liquid limit (%)	Plastic limit (%)	Plasticity index (%)	Liquid limit (%)	Plastic limit (%)	Plasticity index (%)
Nafferton Clay	40- 45	22 - 24	18 - 21	42.6	22.5	20.1
Gault Clay	55 - 80	25 - 30	30 - 55	64	25	39
London Clay	60-105	25 - 37	35 - 68	**72.6	**21.3	**51.3

\* Foster *et al.*, 1994; Gasperre, 2005; Hughes *et al.*, 2009; Bell, 2013, Glendenning *et al.*, 2014

\*\* Simulated very high plastic soil from Bentonite – Nafferton clay mix

The synthesized very high plastic soil was targeted to represent the median values of the upper ranges reported for London Clay, particularly in the London Basin. The values derived for Gault Clay particularly agree with typical values around Cambridgeshire area where the embankment fill was sourced. Mineralogically, Gault and London Clays contain a significant suite of highly expansive clay minerals, particularly montmorillonites which have been reported to vary with location across the respective geology. The Gault Clay material collected for this study was described as sandy, slightly gravelly clay indicating a significant amount of coarser particle sizes. This was reflected in wet sieve tests with nearly 15% by mass retained in the 5mm sieve size. The Bentonite additive significantly increased the liquid limits of the natural Nafferton material resulting in very high plasticity.

The optimum proctor density (ODD) and moisture content (OMC) determined in this study were  $1.9\text{Mg/m}^3$  and 16.5% respectively for the Nafferton Clay, and  $1.71\text{Mg/m}^3$  and 17% respectively for Gault Clay. Average clay content is 37% in the Nafferton Clay with a predominantly low swelling Kaolinites/Illites suite while Gault Clay is documented as having clay content higher than 40% with significant content of high swelling montmorillonites. Having created the required very high plastic soil, the Bentonite-Nafferton clay mix is now referred to as VH plastic clay.

#### 3.4.4 **Sample preparation for desiccation experiment**

In addition to the samples prepared for the index tests, the three soil materials were also prepared for the desiccation experiment. This involves compaction design as indication of specific engineered conditions to

rationality compare with field results especially in the case of the embankment fill material (i.e. Nafferton Clay). It therefore required the soil preparation to represent each embankment fill condition, particularly the density, texture and moulding moisture. Accordingly, about 50kg of each soil sample was first spread out in a large laboratory pan and large stones and organic debris were picked out by hand. The soils were then chopped through a 20mm sieve to further screen out larger particles, while maintaining reasonable grain sizes and texture with field sample. The percentage of coarse inclusion in the processed samples was determined by washing a representative quantity of the pre-sieved material through a 425micron sieve. The average coarse contents (retained in a 425 microns) was 10 - 15%, implying fines content of over 80%. Coarse inclusion is a factor that can affect compaction and cracking behaviour of fine grained soils.

#### **3.4.5 *Compaction of soil for desiccation experiment***

The semi-dry specimens prepared from the three soils were wetted to moulding moisture content above the optimum and close to their respective plastic limits/natural water contents for compaction into the soil box. Accordingly, moulding moisture contents of 22.7% (+/- 0.2%) and 25% were attained for the Nafferton and Gault Clays materials respectively. Embankments constructed with expansive clay soil are commonly designed with consideration to density and moisture content. They are compacted wet of optimum moisture and sometimes close to the plastic limit in order to minimize the problem of excessive expansion in the volume sensitive materials upon wetting. For example, the embankment was constructed wet of optimum. Also high intensity rainfall events characteristic of emerging climate change can increase natural moisture in the soil developing a new state condition that is essential to understand. The wetted soils were gradually churned with a spade to distribute the moisture and further break up larger clods before storage in air tight containers for proper moisture equilibration. The volume of soil used in the compaction ranged between 45kg and 47kg, depending on moisture content and nature of material.

The method of compaction of the specimens followed the standard proctor principles where the soils are compacted by application of mechanical effort. However, considering the large volume of soil involved in this experiment, the compaction was carried out by tamping the soil specimens with a flat end laboratory rammer. The rammer weighed 6kg and the dimension of the flat end was 100x100mm. The height of lift was approximately 500mm with reference to the soil surface in the box. The edges and corners of the compacted soils were given further short tamping to equilibrate the density. After compaction, the soil surfaces were carefully scrapped and smoothen up to remove any mechanical marks that could become a preferred surface for cracking. The smoothed surface was also to enable visibility of cracks in camera images. Before coupling with the climate system, the height of the compacted soil layer was measured and the compacted soil weighed for estimation of degree of compaction i.e. density. The volume occupy by water in the box filled to the height of each compacted soil was used in their density determination.

In order to achieve baseline compaction levels to relate with known engineered characteristics of Nafferton embankment, trial compactions were carried out with different numbers of tamping blows ranging from 15 to 40. The compaction was carried out in three thin layers measuring 15-16mm. As expected, there was increased density with increasing number of tamping. The densities resulting from 15, 30 and 40 tamping showed a good spread with  $1.34\text{Mg/m}^3$ ,  $1.51\text{Mg/m}^3$  and  $1.62\text{Mg/m}^3$  respectively. These values were adopted to represent a low to high density soil related to compaction conditions of the embankment, which are poorly compacted to a low density and well compacted to a high density (Table 3.1).

#### **3.4.6 Method for estimation of soil suction in desiccated soil**

Direct measurement of soil suction in laboratory experiment is not straight forward, and most instrumentation cavitate at suction greater than 100kPa. Cavitation can be further complicated in desiccated soil by cracking. Therefore soil suction in this experiment could not be measured directly with instrument as extreme drying was expected. As an alternative, the suction developed in the desiccating soil was estimated indirectly following the method described by Fredlund *et al.* (2011). The method requires at

least the water content data and a model drying curve of the soil. The model desorption curve is then used to estimate the wetting (adsorption) and median curves through empirically determined congruent curve shift procedure. The median curve was shown to reasonably normalise large percentage errors due the hysteresis between the drying and wetting curve. In this study, gravimetric and volumetric water contents of the samples were obtained from the moisture loss and theta probe records respectively. The drying curve of the specimens were then determined from the measurement of suction in small representative samples using WP4C dew point potentiometer shown in Figure 3.18.



Figure 3.18: Dew point potentiometer with soil specimen for measurement of suction

The WP4C is a research standard device, which can measure pore water potential in small representative soil samples quickly and accurately. The device uses the chilled-mirror dew point technique where the water potential is obtain from the vapour pressure of air in equilibrium with a sample placed in a sealed measurement chamber. The chamber contains a mirror, which serves as a surface for detecting condensation from the soil sample. For this measurement, a reasonable amount of soil materials to be tested was initially wet-sieved through a 2mm mesh and subsequently consolidated in a bespoke consolidation apparatus to attain uniform saturation and draining to moderate moulding moisture content.

The consolidated sample was first extruded from the cylindrical casing as a bulk sample. Thereafter, it was cored using a 50mm cylindrical metal corer. Many rounded specimen, 3 to 4mm thick were then cut from the cored samples for use in the customise cups provided for testing in the potentiometer.

To take measurement, specimens were place in the instrument cup holder and gently pushed into the sealed chambers. Under appropriate mode e.g. for clay material, the device took approximately 15 minutes to read and display the result once the sample was inserted. For the drying curve, a set of consolidated specimens with the same starting moisture content were allow to air-dry for different lengths of time to provide a range of initial moisture state. After testing, each specimen were taken out and immediately weighed for calculation of moisture content, and thereafter successively dried to the next state of reduced moisture content.

Accordingly, suction results were obtained for a reasonable moisture range (3 and 40%). For the wetting curve, the same batch of samples was allowed to dry out completely, until they showed a constant weight. The samples were then put in a humidity box to gradually re-wet with the aid of mist fog generator. However, the wetting series tests were not successful because the instrument readings appeared anomalous. This was thought to be likely due to non-uniform saturations in the samples, especially at lower moisture content. Hence, only the drying curve was used in the estimation which is normal with this procedure.

The successive suction values obtained from the drying samples were plotted against corresponding moisture contents. Following the Van Genuchten (1980) curve fitting procedure, best fit SWRC was obtained as shown in Figure 3.19 and Figure 3.20 for the Nafferton and Gault Clays respectively. These unique SWRC were used for assessing suction changes in the desiccated soils, and to determine the suction and moisture content at crack initiation.

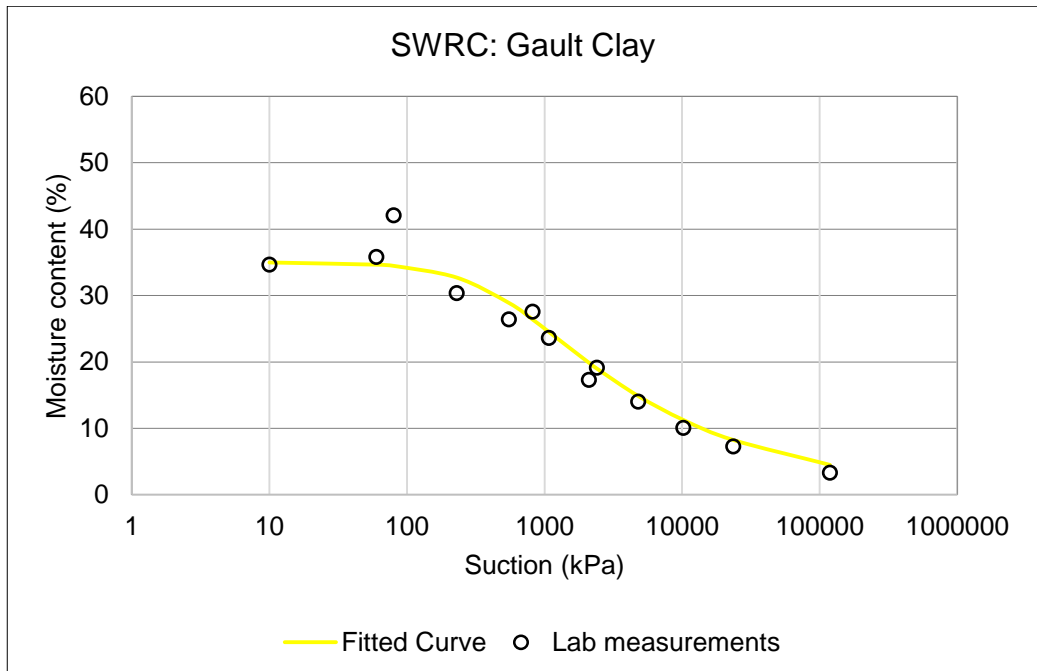


Figure 3.19: Soil water retention curve for Nafferton Clay

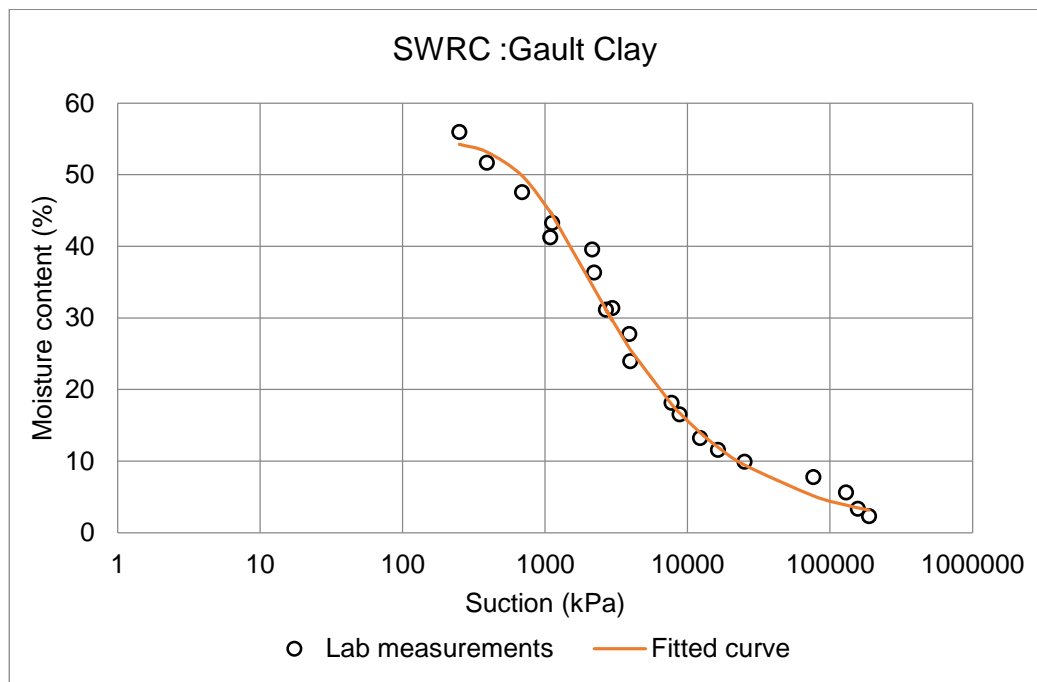


Figure 3.20: Soil water retention curve for Gault Clay

Unfortunately, the curve could not be determined for the VH plastic Clay representative. This was because the potentiometer became faulty when this soil mix sample was to be tested. Due to time constraint, it was decided to carry out the suction analysis with successful test results of the Nafferton and Gault Clays, which nonetheless were natural samples that could practically be related to field behaviour.

### 3.4.7 Method for crack image analysis

Crack geometry and pattern changes with time. In order to describe and quantify the complex network of cracking, computer aided image processing was carried out on the time lapse crack photographs taken in the experimentations. The computer software used in the crack image quantification is known as PCAS (particles and cracks analysis system). Liu et al. (2013) introduced PCAS as a professional software for analysis of photographic images of pores, particles, cracks and veins network in soils and rocks. The software was provided free for this work by Dr Chu Liu of the School of Earth Sciences and Engineering, Nanjing University through personal contact. For analysis of soil cracking, a sub-algorithm called “crack image analysis system” (CIAS) which resolves the geometric parameters of the crack images in terms of crack intensity factor (CIF) was developed in PCAS. The procedures of CIAS involve conversion of original crack images to grey-level histogram where the cracks and clods are distinguished by contrast, similar to the procedures described by Tang et al. (2011). With this conversion, binary images in white and black, representing soil clods and cracks respectively are generated. Any bridge between spots and real clods are eliminated using the “Closing” command. The procedures are fully automated. Figure 3.21 shows schematic of the CIAS program.

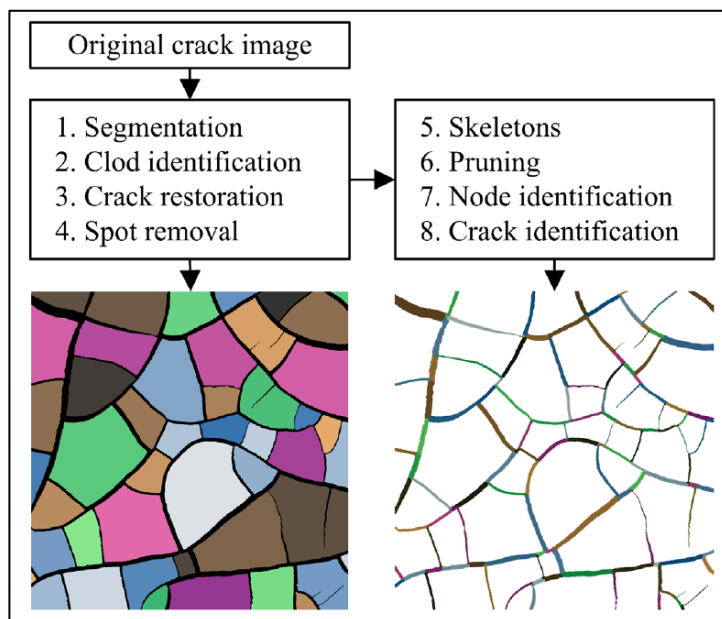


Figure 3.21: Automated procedures in the CIAS (from Liu et al., 2013)

However, binary images of the time series crack photographs in this study were commonly affected by background noises. This occurred because of limitations in camera focusing on the closed bespoke climate control system. In addition, loose particles appearing on the drying soil surface increased the pixel noise. These made it difficult for the software to execute aspects of the operations. Following advice of the provider, the original photographs were edited to reduce the background noises and the cracks also painted in some cases to increase their grey scale level and hence, the binary contrast with the clods (Figure 3.22).

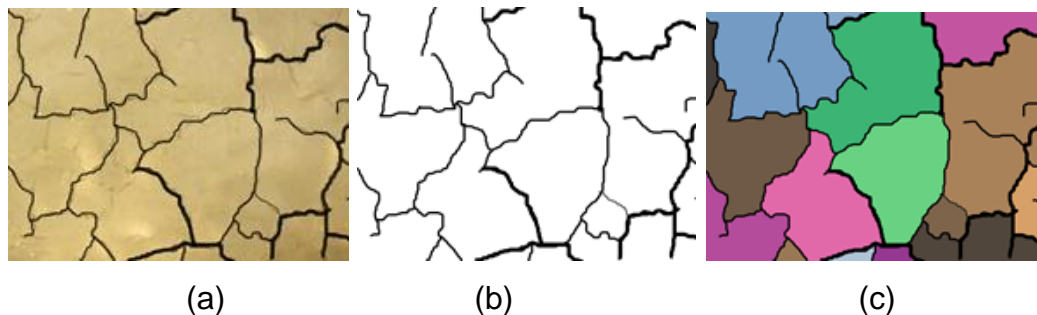


Figure 3.22: Crack photo editing (a) painting (b) enhanced grey scale contrast and (c) colour pixels of cracks and clods

Apart from the computer aided quantification, the cracks geometry were also directly measured using suitable metal probes (for the depth) and meter rule (for the width). The measurement was carried out at the end of each test when the atmospheric cover was opened to access the cracked soil surface.

#### 3.4.8 *Three-dimensional crack model*

Subsurface cracks are hidden from direct observation. Therefore, most conclusions made about crack subsurface morphology are speculative or at most drawn from observations made from soil excavations. However, to adequately account for the effect of cracks, it is important to understand crack subsurface characteristics, especially the cross section and occurrence of horizontal cracks etc. In order to contribute to this theme, this study conceived a method of determining the true crack morphology. After several considerations, making of mold cast of the crack soil was adopted. Consequently, two different types of fast curing, nonreactive mold cast materials were used namely; epoxy (polyurethane) casting resin and T28 silicone rubber. Both are low viscosity materials, which could flow

into the crack soil to make a cast impression of the cracks. The silicon rubber as the name implies would become an elastic material after drying. However, the material did not cure very well inside the soil due perhaps to insufficient aeration to dry it within the crack soil. Therefore, the full crack cast could not be recovered. The epoxy resin, on the other hand, cured into a hard plastic material with a reasonable imprint of the subsurface cracks. COSHH risk assessment was carried out on both substances by the University Geochemical laboratory staff. They were certified of low risk and the recommended personal protective equipment were used during handling including gloves, laboratory coat, safety spectacle and dust mask.

### 3.4.9 ***Control variables and laboratory testing programs***

Important in this study are common conditions associated with embankment construction and performance. These formed the basis of parametric selection for the different test programs. From soil materials to environmental factors, six fundamental variables were selected for the study in different testing including soil density, plasticity, soil moisture, soil layer thickness, cyclic wetting and drying and vegetated slope. Coupled in these test variables are rate of desiccation, soil suction, crack intensity, volume changes etc. These factors are expected to present detailed information for in-depth analyses and interpretations to arrive at rational conclusions and valuable contributions in this study. The different tests were conducted under a consistent initial conditions such that any resulting cracking characteristics are considered to arise from the effect of the variable being tested. The initial conditions involved in the Nafferton clay test which serve as the control model are as follows:

Moulding Water content	-	22.7 +/- 0.1%
No. of Blows (Compaction)	-	15 (loose), 30 (dense), and 40 (very dense)
Material Quantity	-	47-50Kg
Temperature	-	20 +/- 0.5°C
Relative Humidity	-	30 +/- 0.5%
Wind Speed	-	3(m/s)

Other soil materials used in this study were only prepared in the well compacted (very dense) state to deal more specifically with contemporary issues in modern embankment performance. Each test was subject to two desiccation cycles, i.e. compacted-dried, rewetted-dried. The duration of each cycle varied between twelve and fourteen days depending on the desiccation condition. For time management, the tests were stop when moisture loss began to show equilibration i.e. no change after 3 to 5 hours. Therefore, each test program took approximately 6 weeks including preparation, set up and measurement. In all, nine sets of compacted, cyclic desiccation tests were carried out as follows:

1. Well-compacted soil test (Nafferton Clay)
2. Moderately compacted soil test (Nafferton Clay)
3. Poorly compacted soil test (Nafferton Clay)
4. Gault Clay test (in well compacted state only)
5. Very high plastic clay test (in well-compacted state)
6. Soil layer thickness test (2 Lifts in well-compacted state)
7. Soil layer thickness test (1 Lift in well-compacted state)
8. Vegetation test
9. Multiple cycle test (in well compacted state)

Once set up, the measuring instruments were automated. Nevertheless, routine monitoring was maintained to check for troubleshooting and to also directly observe important changes e.g. crack initiation, volume changes etc.

Relevant laboratory safety induction was attended at the geotechnical laboratory unit of the University.

### **3.5 Summary on laboratory methodology and testing**

Desiccation cracking mechanism involves response of volume sensitive soil materials to climatic soil moisture changes. Soil mechanics theories common in geotechnical engineering were combined with rational soil desiccation principles to develop a robust framework for the laboratory experimentation. This led to construction of a bespoke soil-atmosphere interaction system for cyclic wetting and drying experiments. The laboratory study is particularly carried out in common embankment

materials and construction methods in the UK. Accordingly, the soil materials, method of preparation and test procedures were selected with the engineered characteristics leading to a wide range of experimentation to compliment the field results. The soil processing and testing mostly followed standard soil test procedures and the test programs developed took into consideration some of the existing gaps in this subject, including use of environmental chamber and conditions suitable to describe engineered fills etc. Accordingly, high quality data were generated which adequately supply this undertaking with comprehensive variables with which to derive a more in-depth understanding of the mechanism of cracking in clay slopes. Syntheses of laboratory results comprising of material, hydrology and crack characteristics are summarised in Appendix III.

### **3.6 Conclusion on study approach and methodology**

In order to derive coherent and practical results to satisfy the aims and objectives of this study, field and laboratory procedures were implemented. The methodological framework was developed following background knowledge of the behaviour of unsaturated expansive soil and in consideration of a wide range of conditions associated with the performance of engineered clay fills.

After rigorous investigation, a robust, high quality data set was generated. A comprehensive computer aided processing and syntheses of the data revealed interesting trends in the test results. The trends relate mainly to the soil material and the moisture movement during desiccation from which two broad themes have been identified namely:

1. Material characteristics
2. Hydrological characteristics

These themes are therefore constituted into two different chapters succeeding this section for extensive discussion and presentation of the tests results.

## **Chapter 4 Hydrology characteristics of desiccation cracking in soil**

### **4.1 Introduction**

The field and laboratory programs have revealed distinctive trends of soil hydrology as the cracks developed. From conditions of loose to dense soil, low to very high plasticity, thin to thick soil layer etc., the soil materials tested displayed characteristic moisture profiles thought to be influential in their cracking responses. Moisture profiles of the Nafferton Clay specimens are mainly presented in this chapter since there is an existing embankment created from it, with field and laboratory components that can be related. The time series hydrologic changes are characterised with the trends of crack morphology development.

### **4.2 Moisture characteristics and suction development on clay embankment**

Soil desiccation primarily involves moisture loss by evaporation drying. However, in nature, evaporation moisture loss in soil is not perpetual because precipitation introduced water back to the soil. The dynamic moisture exchanges between embankment and its environment can result in measurable effects as the soil continuously adjusts to a new state of equilibrium between its skeleton and the changing void. In view of this, it was necessary in this study to characterise the climate-driven hydrologic changes and the effect in desiccation cracking in the embankment.

Aspect defines the compass direction or orientation of a slope. The embankment has a North and South slope. Aspect among other factors can influence the hill slope processes. This is because of the disparate solar radiation which can result in non-uniform soil temperature regime on slopes of different exposures. Comparing representative trends of soil temperature of the embankment, Figure 4.1 shows that the South aspect record higher values than the North.

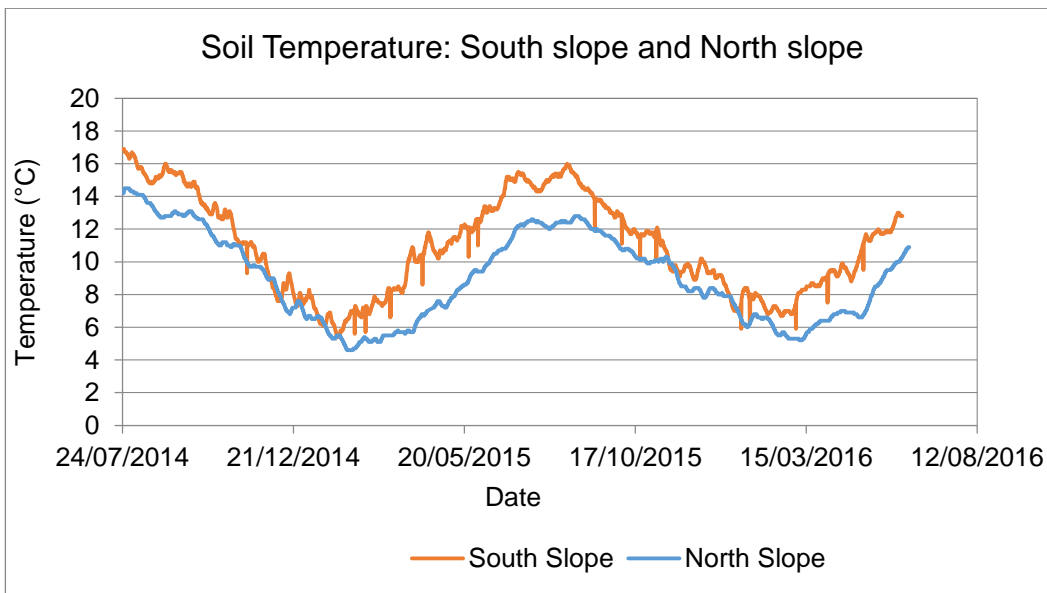
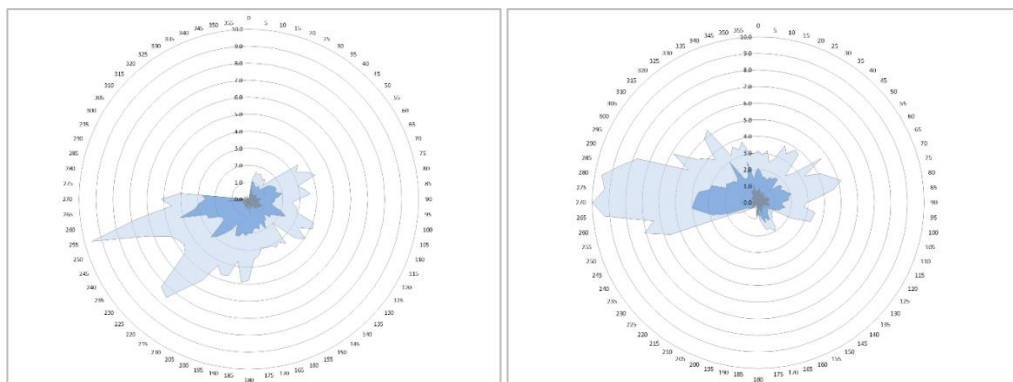


Figure 4.1: Soil temperature with aspect of the BIONICS embankment

The wind-rose of the embankment location was also analysed, and indicates a prevailing south easterly wind in the area (Figure 4.2). The pattern agrees with climate features of northeast England given by the Met office.



(a)

(b)

Figure 4.2: Wind-rose of the embankment (a) South slope (b) North Slope

This trend of wind means the South facing slope of the embankment, particularly the west end, experiences a higher impact of insolation. Therefore, in a typical dry spell, this part of the embankment would have a warmer and drier condition than the potentially shaded North face. Since atmospheric conditions essentially drives evaporation, the disparate insolation would therefore affect moisture distribution across the embankment. To relate this weather trend, evapotranspiration around the

embankment was estimated based on the Penman-Monteith equation and the result indicates higher peaks occurring in the South slope for a given measurement time (Figure 4.3).

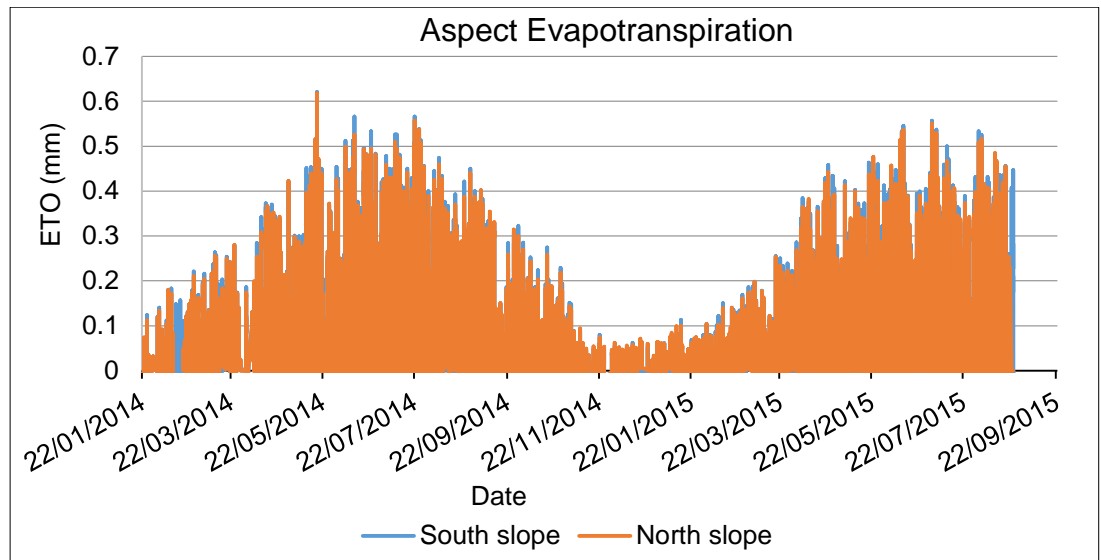
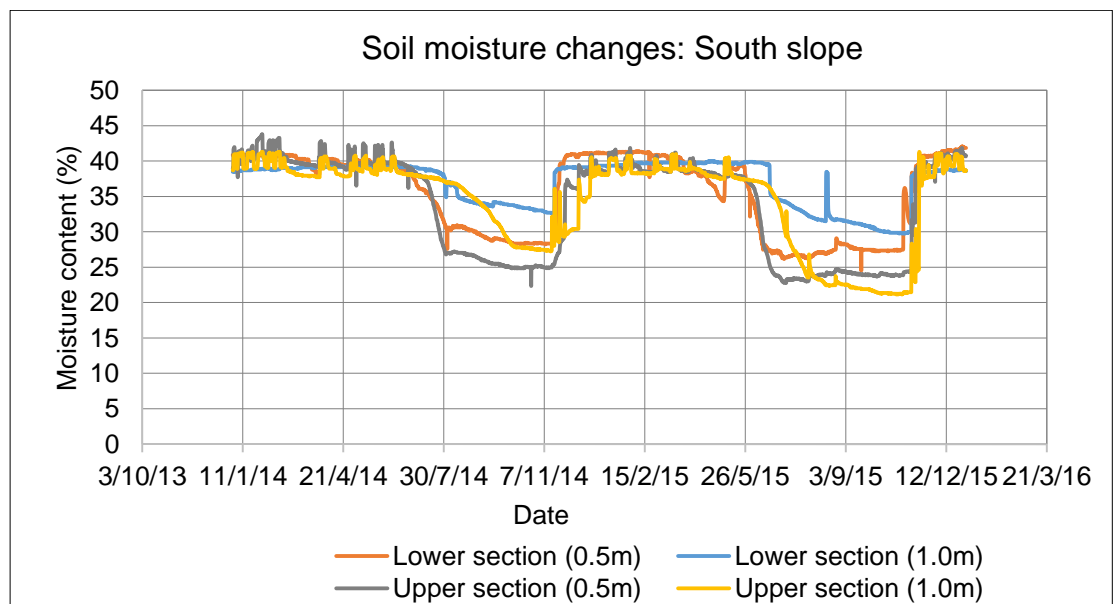


Figure 4.3: Evapotranspiration with aspect of the embankment

The pattern of weather can explain the trend of soil moisture recorded across the embankment. Figure 4.4 shows moisture profiles of the middle sections of the South and North facing Slopes between 2014 and 2015 when the crack survey was carried out (instruments layout on the slope is shown in Figures 3.3 and 3.4).



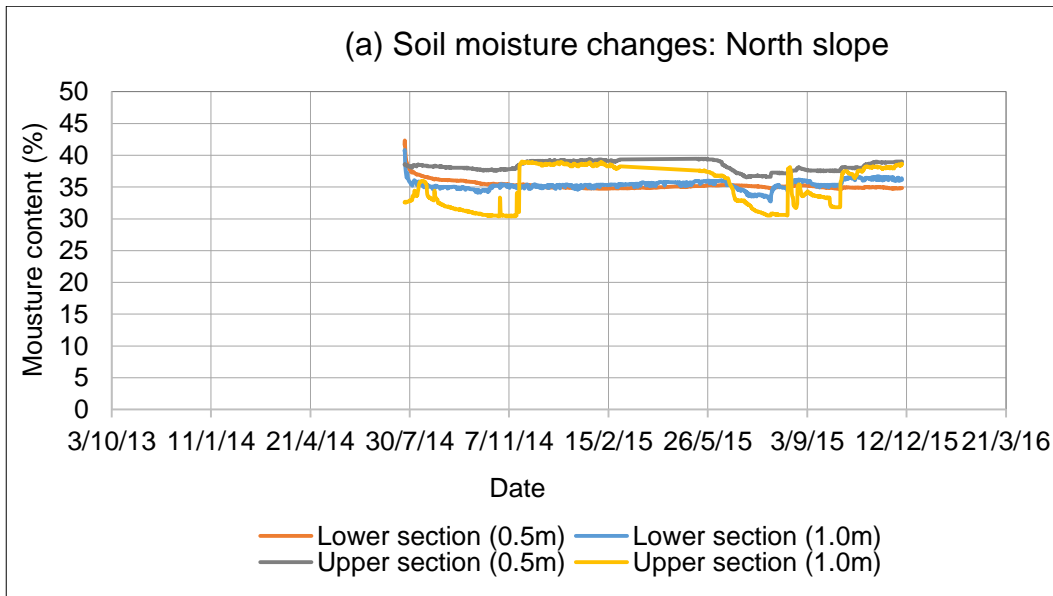


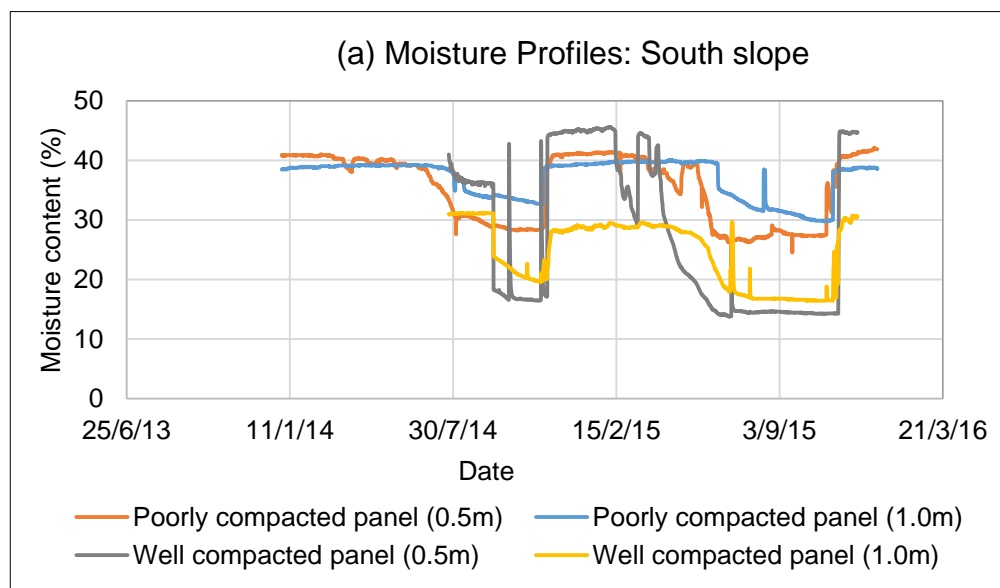
Figure 4.4: Profiles of moisture change with aspect across corresponding sections of the embankment (a) South slope and (b) North Slope

The moisture profiles show significant fluctuation in response to changes in the weather. The fluctuation is greater in the south slope, averaging 15% to 35% compared to the North slope, 30% to 40%. A difference of 3-10% in the volumetric moisture generally exists in the record between the 0.5m and 1.0m depth, which on the average, is also more significant in the South slope. The offset between the profile at 0.5m and 1.0m can be regarded as time elapsed in moisture saturation with depth. During the field study, the embankment soil in the North Slope appeared relatively moist at any given survey visit compared to the South slope. The top soil condition of the 90m long embankment was also relatively drier at the west end than east end of the south slope. Water ponding was observed at the toe at east end of North facing slope for most part of winter in the year 2014 but at the opposite end in the South slope, no such condition was observed. This also implies that soil moisture can vary across the height of the embankment slope. In slopes, gravity can influence water movement leading to accumulation of more moisture at the lower section of the slope. However, considering the fact that wind and solar intensity generally increases with elevation due primarily to less frictional drag with height above the ground, it is considered here that this can also result in more evaporation moisture loss at the upper slope section. As depicted in Figure 4.4, the upper section of the South slope shows lower volumetric moisture ranges in the near surface (0.5m) than the lower section close to

the toe. The trend of volumetric moisture between the upper and lower section in the North facing slope does not change significantly. This further suggests increased climate drying with elevation. The disparities in the soil water regime caused by climate effect across the slope can lead to measurable difference in process responses including the rate of desiccation as reported by Churchill (1982). Since desiccation cracking relates to moisture loss, it is reasonable to expect that the changing hill slope hydrology would play a role in the mechanism of cracking.

#### 4.2.1 *Moisture profiles in engineered clay fills*

Moisture profiles recorded across the engineered panels of the embankment also displayed remarkable differences. For illustration, field records of near surface volumetric moisture profiles of the engineered panels taken from the middle slope section of the embankment (Figure 3.4) are presented in Figure 4.5.



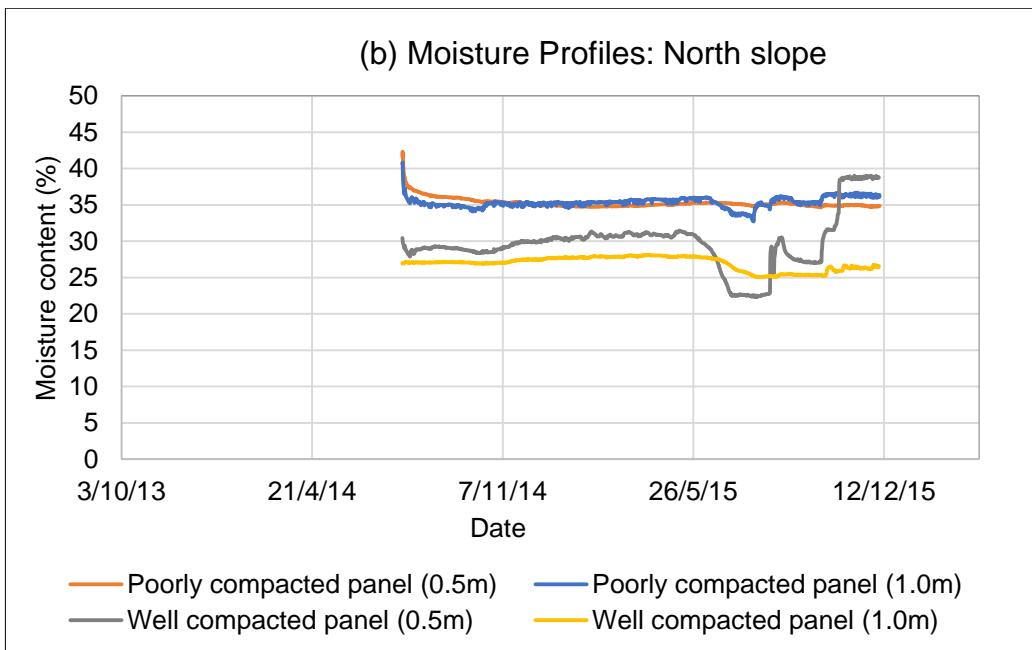


Figure 4.5: Moisture profiles in well and poorly engineered panels of the BIONICS embankment (a) South slope and (b) North Slope

The engineered panels of the South facing slope displayed greater moisture fluctuations with time and depth than the North slope as can be seen from the increase spikes and greater separations of the profiles in Figure 4.5 (a and b). Generally, hydrology profiles of the well compacted panels showed greater difference between 0.5m and 1.m layer than the poorly compacted panel for each face of the slope. Since both panels are made of the same soil material, this difference in volumetric moisture trend can be attributed to the overall soil structure resulting from the level of compaction characterising the construction of the two engineered panels. The poorly compacted panel would result in a loosely packed soil structure through which soil moisture can move freely. Under such structure, hydraulic conductivity hence infiltration increases, and with continuous wetting, the difference between soil moisture at the 0.5m and 1.0m depth would be less. On other hand, the densely packed soil particles of the well compacted panel would present soil structure that results in increased runoff and less infiltration. However, runoff can be highly reduce in a vegetated slope. In this case, there will be greater volume of moisture within the upper soil layer of the well compacted panel for response to environmental changes. As depicted here the well compacted panel display a rapid moisture response at the 0.5m and a more pronounce difference with depth.

The dynamics of moisture movement was also assessed in the laboratory specimens. In this case, the soil was compacted to a low density ( $1.34\text{Mg/m}^3$ ) and high density soil ( $1.62\text{Mg/m}^3$ ) specimens. A third specimen was also compacted to a density intermediate of these two ( $1.51\text{Mg/m}^3$ ). The moisture losses with time of these specimens under alternate wetting and drying conditions are shown in Figure 4.6. Moisture loss profile of the loosely compacted specimen trend below that of the denser specimens, especially in the first cycle (Figure 4.6a).

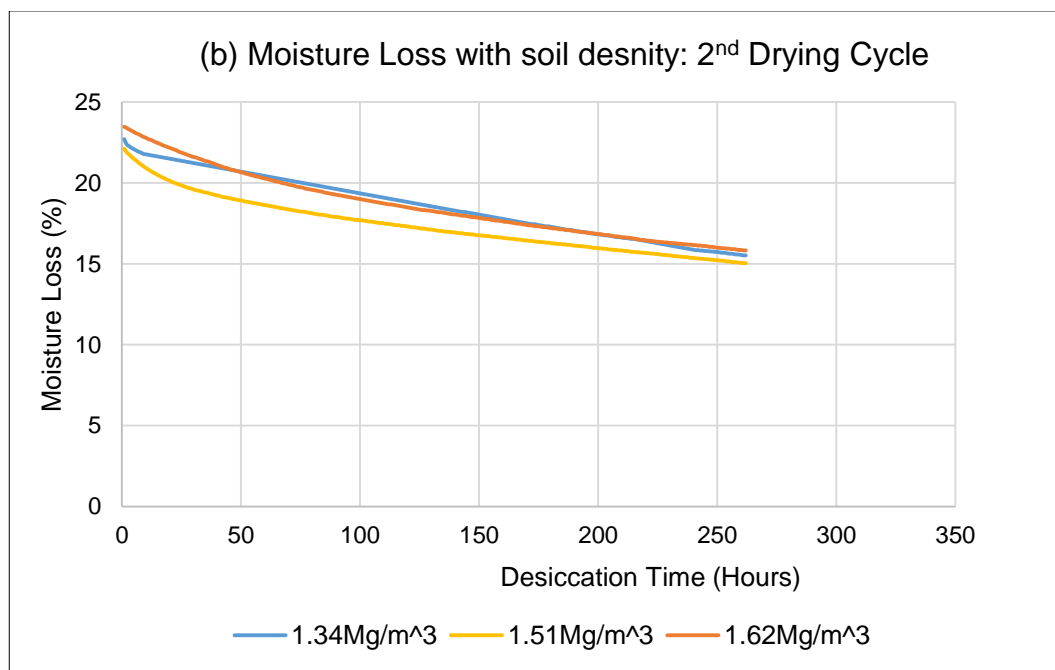
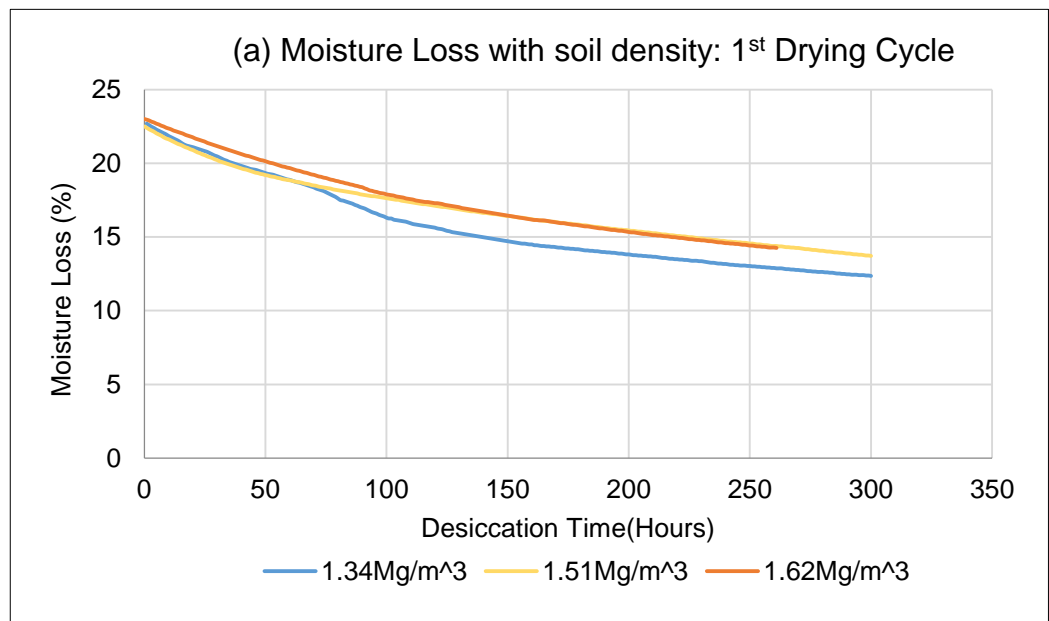


Figure 4.6: Moisture loss in a clay soil with different densities

From the first drying cycle, the curves generally indicate that rate of moisture loss tend to decrease as the soil density increases. Despite the slight difference in the starting moisture, which possibly aroused from time taken to complete each preparation, the lowest density soil exhibits a faster rate of moisture loss under the same desiccation condition described in the methodology. This again points to effect of loose soil structure attained by the low level of compaction. In the second cycle, the sequence was inconsistent possibly arising from the following factors. First, there were slight leakages from instrument positions during the rewetting particularly in the intermediate density specimen. This was checked by reinforcing the seals, and in subsequent tests, the gaps around the moisture sensor instrument caused by soil shrinkage in the drying phase were re-sealed with fresh duct tape before rewetting. The second factor is difference in infiltration in the specimen during rewetting which would potentially arise from the different crack intensity in the drying phase. In addition, repeated wetting and drying can cause structural changes in soil (Kodikara *et al.*, 1999; Tang *et al.*, 2011a). The last two factors are considered here as important in the moisture loss behaviour of the 2<sup>nd</sup> cycle as they can change the initial uniform state and evaporation behaviour of the soil mass. Overall, there is potential for greater changes in the cracked low density specimen resulting in disparate moisture distribution in the soil mass, which will in turn significantly slow rate of moisture evaporation during subsequent drying as depicted in the figure. The curve of moisture loss in the intermediate density soil trends at lower moisture ranges apparently because of the leakage, which reduced the moisture content. However, the moisture decay trend appears relatively slower compare to the high density specimen. This is evident as the former gradually slows after about 50 hours of drying and closes the gap with the later towards the end of the drying. This is consistent with the behaviour of moisture movement in the transformed low density soil mass during the second wetting and drying cycle but to a lesser extent due to the increase density. Therefore, it is reasonable to consider that repeated wetting and drying affect moisture movement in compacted soils, particularly with occurrence of cracks.

Moisture records of the theta probes inserted in the desiccating soil specimens also displayed differences in rate of desiccation at successive depths (Figure 4.7).

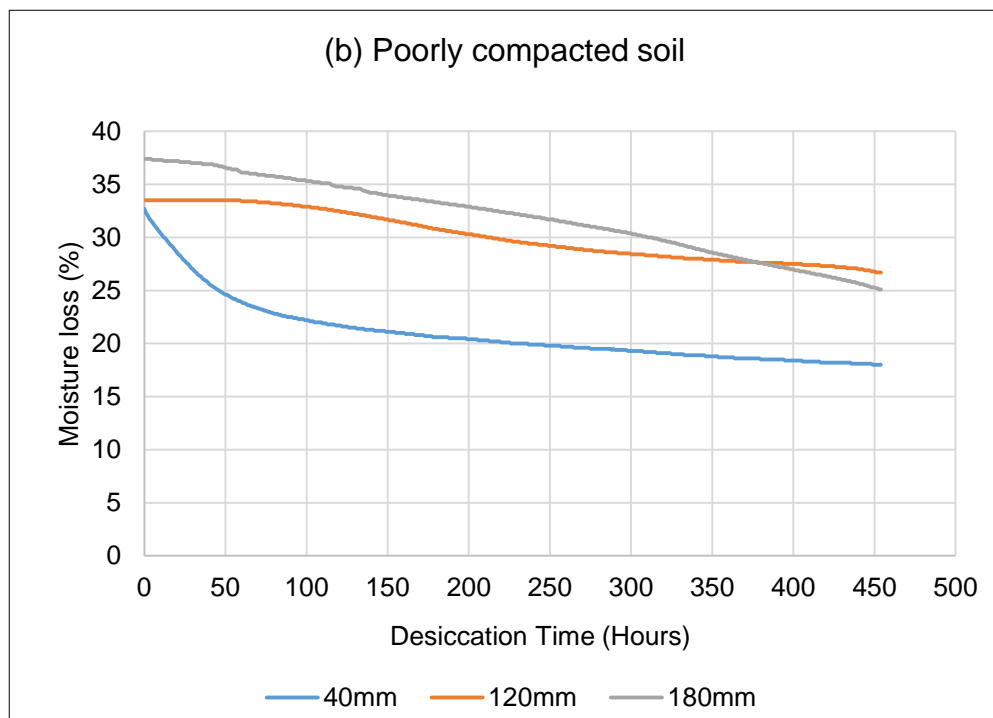
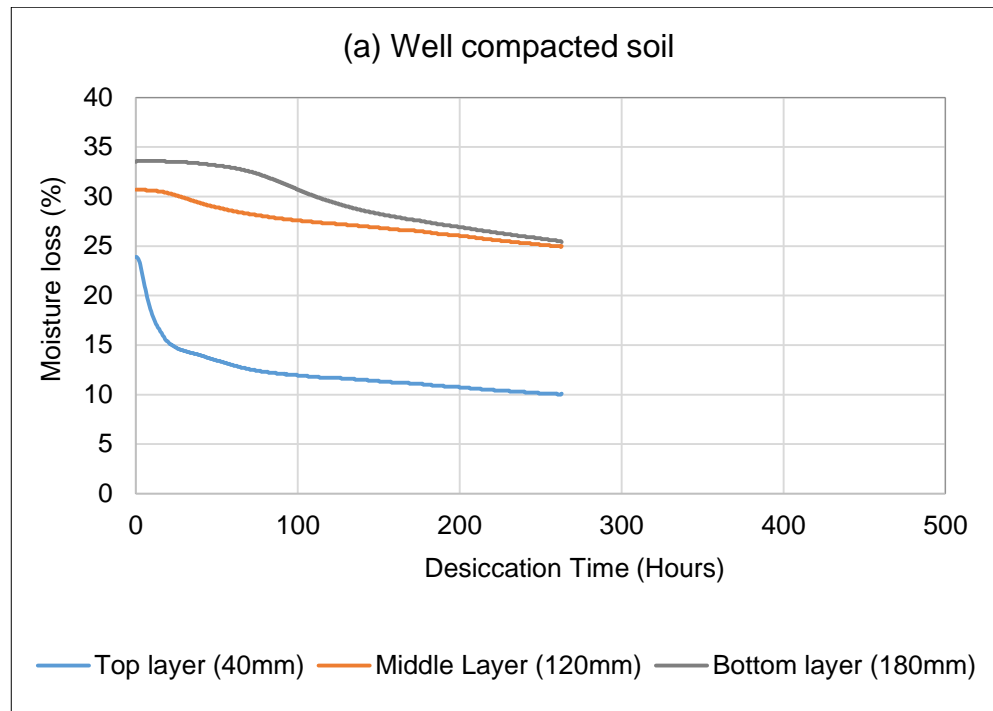


Figure 4.7: Moisture loss with depth (a) well compacted soil (b) poorly compacted soil

Greater desiccation occurred in the near surface soil. Since desiccation is brought about by evaporation, this agrees that evaporation is greater at

the surface. As displayed in Figure 4.7, moisture loss from the top layer (40mm) as soon as drying begins while the middle (120mm) and bottom (180mm) layers only experienced notable changes after about 14 and 30 hours respectively after start of desiccation. The layer moisture profiles are consistent with field behaviour of moisture between 0.5m and 1.0m (Figure 4.5) and indicate that hydraulic properties change with depth. As evaporation moisture loss proceeds gradually, the surface layer dries and set up a suction gradient with which moisture could be drawn from deeper layers of the soil. The gradation in moisture with depth is capable of creating a decreasing mechanical profiles in the soil with implication for greater tensile strength at the upper soil layer during drying shrinkage(Tang *et al.*, 2016).

The thickness of the compacted soil block as well as the number of compacted layers was also observed to display characteristic differences in the soil hydrology. In this study, a counterpart of the 195mm thick well compacted soil model was created with approximately half thickness (100mm) in order to compare their crack features. The thin soil model was also compacted in one and two layer variants to further compare the effects of the number of lifts. The methods resulted in specimens with densities of  $1.63\text{Mg/m}^3$  and  $1.65\text{Mg/m}^3$  for the 1-layer and 2-layers compaction respectively. While these values are close to the density for original 195mm thick model ( $1.62\text{Mg/m}^3$ ), the reduced soil thickness model expectedly presented slightly increased densities with the highest resulting from the compaction in 2-layers. This is likely due to enhanced transmission of the compaction effort per unit area on the reduced bulk soil. The resulting desiccation profiles for the different soil layer thicknesses are presented in Figure 4.8.

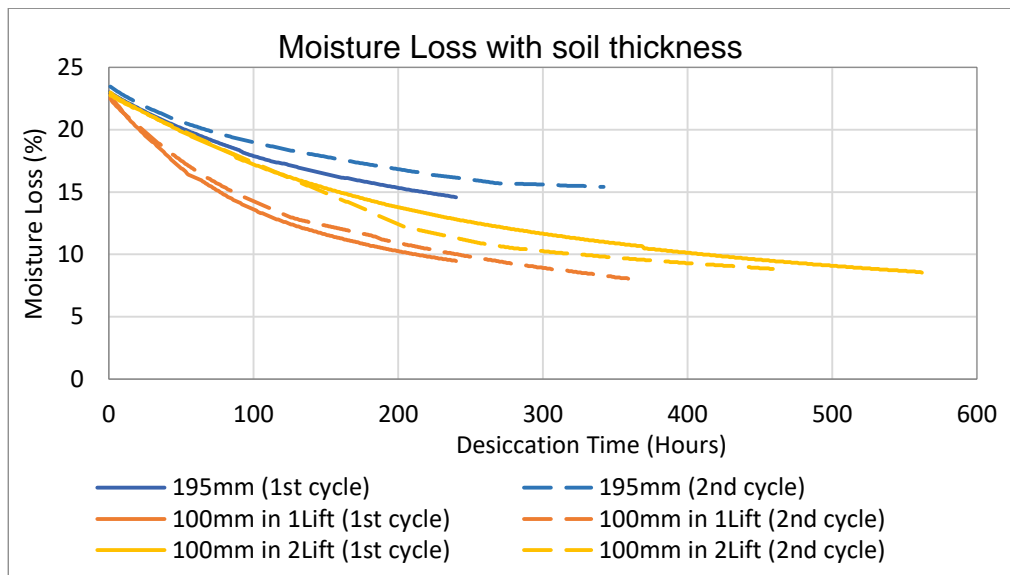


Figure 4.8: Moisture loss in compacted soils of different thicknesses

Clearly, in both the 1<sup>st</sup> and 2<sup>nd</sup> cycle of desiccation, the profiles of thin soils indicate faster moisture decay than that of the thick soil. Neglecting the slight density difference, the trend between the thick and thin soil layers can be attributed to the distance of moisture movement within the soil blocks before evaporation at the surface. Vertically, the thin soil block presents a shorter distance for moisture movement for evaporation hence the faster moisture loss. In addition, the thick soil was compacted in three layers, which are likely to impose hydrologic boundary that can affect moisture movement. For this reason also, the thin soil variant created with 1lift of compaction presents a relatively faster moisture loss than the 2-lifts counterpart. However, the slight densities differences could also cause significant response in the specimen. Despite the close densities attained in the well and poorly compacted panels of the embankment ( $1.8\text{Mg/m}^3$  and  $1.7\text{Mg/m}^3$  respectively), laboratory test shows their saturated permeability was significantly different and much higher in the soil of poorly compacted panel (Toll *et al.*, 2012). This can also support the slower rate of moisture loss recorded in the higher density thin soil variant compacted in 2-lifts which implies lower permeability compare to the 1-lift counterpart which would result in higher permeability hence the faster rate of moisture loss. However, when comparing the thin and thick soil here, it seems effect of thickness is more significant than density as the thick soil with the lowest density display the highest rate moisture loss in the figure among the three models. Embankment construction typically involves

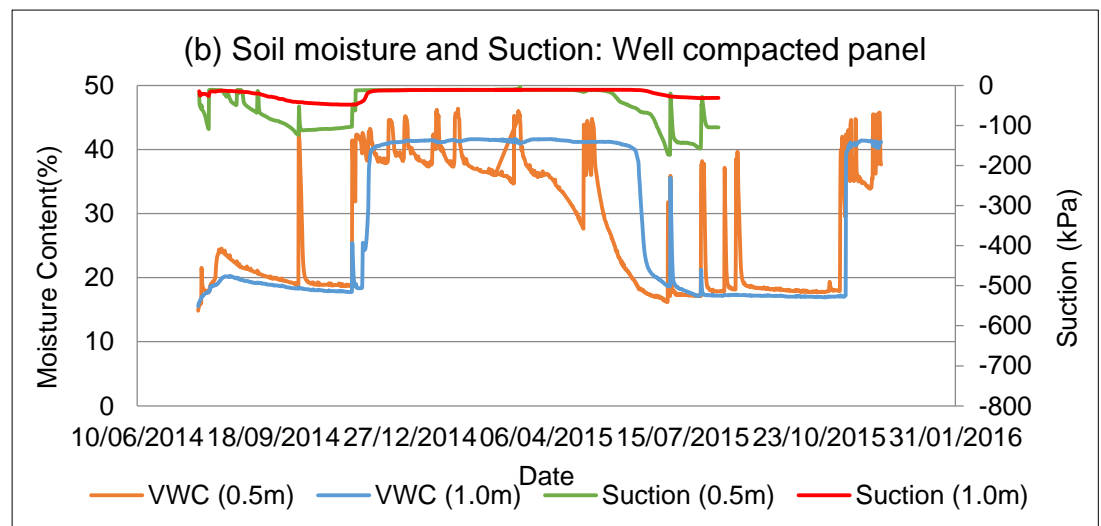
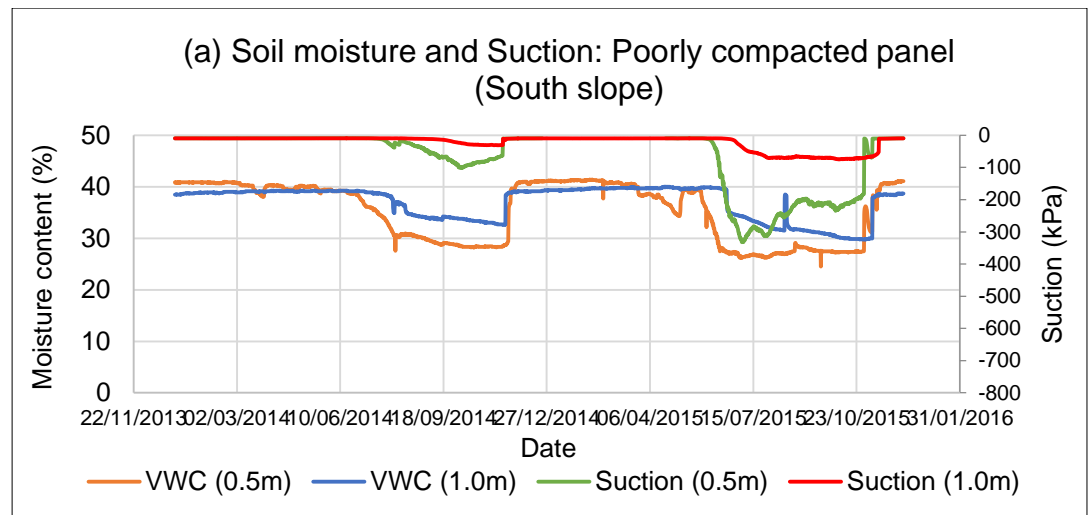
compaction of fills in different layers in order to achieve optimum strength. Depending on the engineering purpose, the layers can be thin e.g. just enough to prevent leachate movement in soil liners for landfill and waste covers, or relatively thick e.g. to support mechanical loads in transport embankments. In any case, an increase in desiccation of the compacted fill can have adverse effects and greater implications in thin soil layers. This is more significant in the performance of clay liners and covers where the occurrence of cracks could compromise performance of the impermeable soil layer. The moisture records in the embankment show fluctuations in the near surface soil layer as depicted earlier in Figure 4.5. Such condition means the near surface soil is never saturated (Fredlund *et al.*, 1996; Fredlund, 2006) and in expansive fills, increase shrinks-swell in response to alternate wetting and drying can lead to instability in slope arising mainly from irregular pattern of pore water pressure and net reduction in the shear characteristics that stabilize the slope. The potential of cracking in the different soil layer thicknesses is discuss in the next chapter.

#### **4.2.2 *Development of soil suction in drying dense soil***

Since soil is a three-phase system, it was considered as important to assess the complex interaction of air, solid and liquid (water) in the voids under wetting and drying condition. In drying clay, the most important forces acting on soil water are identified as a capillary force, which arise from concave menisci in the dehydrated spaces between the solid particles, and adsorptive forces, which are due to adhered films of water to the solid surfaces (Holtz and Kovacs, 1981; Hillel, 2003). Changes in the soil water essentially imply changes in the pore water pressure and a rearrangement in the solid particles leading to changes in the soil's bulk volume. Under unsaturated condition, these changes can result in a negative pore water pressure potential or matrix suction, and the volume change in this case is by shrinkage. In the laboratory study, the clay materials were observed to show significant volume changes. In the drying phase, the soil specimens settled by 10-12mm of the original soil layer thickness and shrank by about 6-8mm laterally as measured from soil marks on the sides of the box. Soil cracking has been attributed to the

shrinkage process and suction developed in a drying soil (Kodikara *et al.*, 2000; Péron *et al.*, 2009b).

The above soil mechanics principle largely employed in unsaturated soils was explored in this study. Therefore, matrix suction changes in the field are recorded along with changes in the near surface soil moisture to characterise the surface crack development. A representative suction and soil moisture profiles at corresponding location in the embankment are shown in Figure 4.9. As may be expected, the two soil parameters clearly exhibit close correlation with peaks and troughs, although suction (or negative porewater pressure) increases as soil moisture decreases.



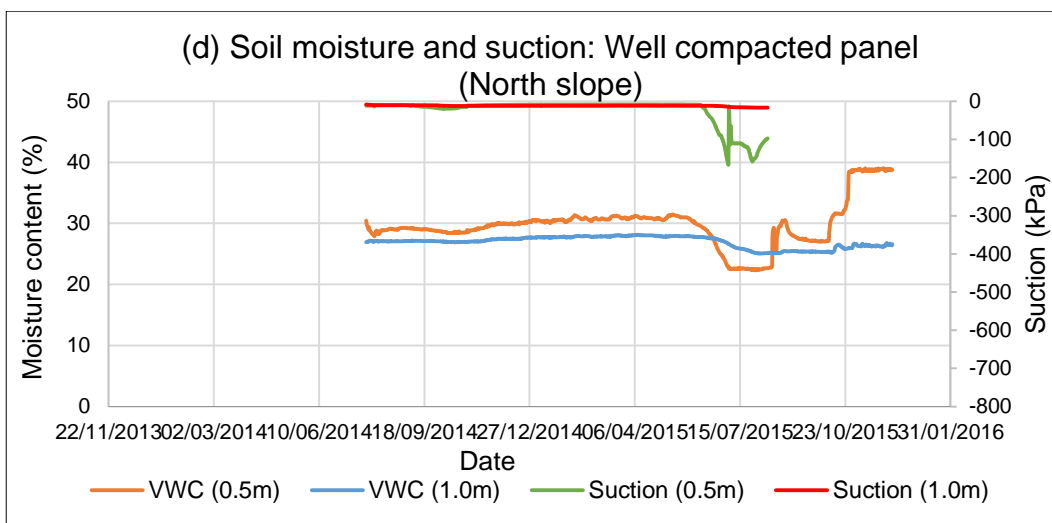
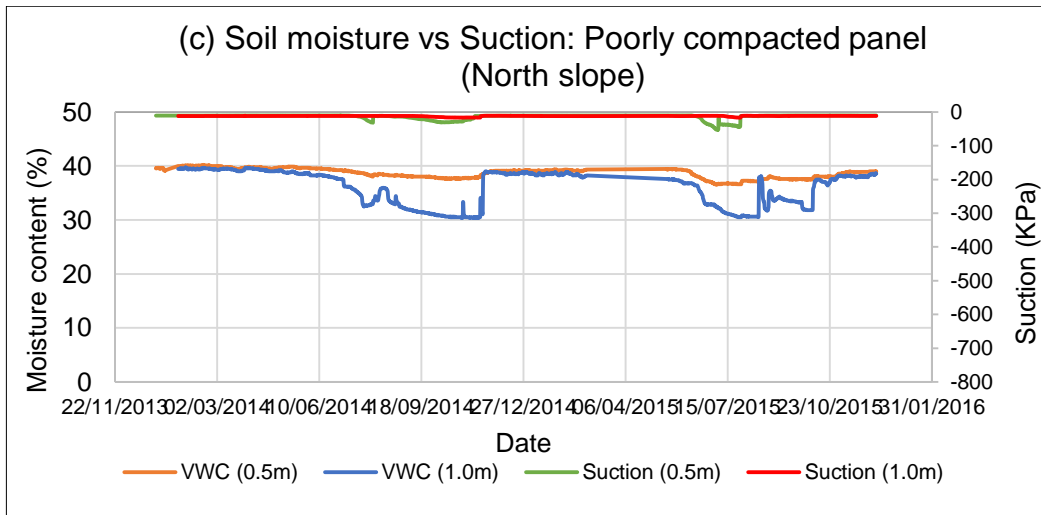


Figure 4.9: Profiles of moisture and suction in engineered slope (a) and (b) South slope, (b) and (c) North Slope

Suction differentials developed in partially saturated soil media influences upward moisture movement towards a deficit evaporation surface until a state of equilibrium is reached with the atmosphere (Fredlund and Rahardjo, 1993; Péron *et al.*, 2009b). The coupling of soil suction with changes in the state of soil moisture clearly manifested in differences in profiles of these parameters across the engineered variables. The highest suction ranges and greater fluctuations were exhibited in the South slope. On this face of the slope, suction reaches about 100kPa and 150kPa in the well compacted panel in 2014 and 2015 respectively (Figure 4.9b). While in the neighbouring poorly compacted panel suction reached 100kPa and 320kPa in 2014 and 2015 respectively. Suction in the North facing slope is small, with just a little above 100kPa is developed in the well compacted panel in 2015.

Suction profiles slightly higher in the poorly compacted panels. This is considered in terms of a more pronounced effect of the moisture movement in the loose pack structure which the level of compaction in this panel conveys. The loose structure means increased permeability, which eases moisture movement and allows a more dynamic particle interaction within the emptied pore spaces. In contrast, a dense particle packing in the well-compacted soil would generally tend to restrict moisture movement and shrinkage, hence less capillary tension changes. This mechanistic behaviour of soil moisture relative to the level of compaction can also explain rapid porewater pressure changes commonly recorded in the historic embankments in the UK. This has implications for shear strength reduction hence increase potential for failure.

Suction development in relation to the engineered soil condition was also studied in the laboratory using the compacted specimens of Nafferton Clay. The suctions were estimated from the experimental SWRC using the curve shift procedure described earlier in section 3.4.6, where the maximum, average and minimum range of suctions in the soil were obtained as shown in Figure 4.10.

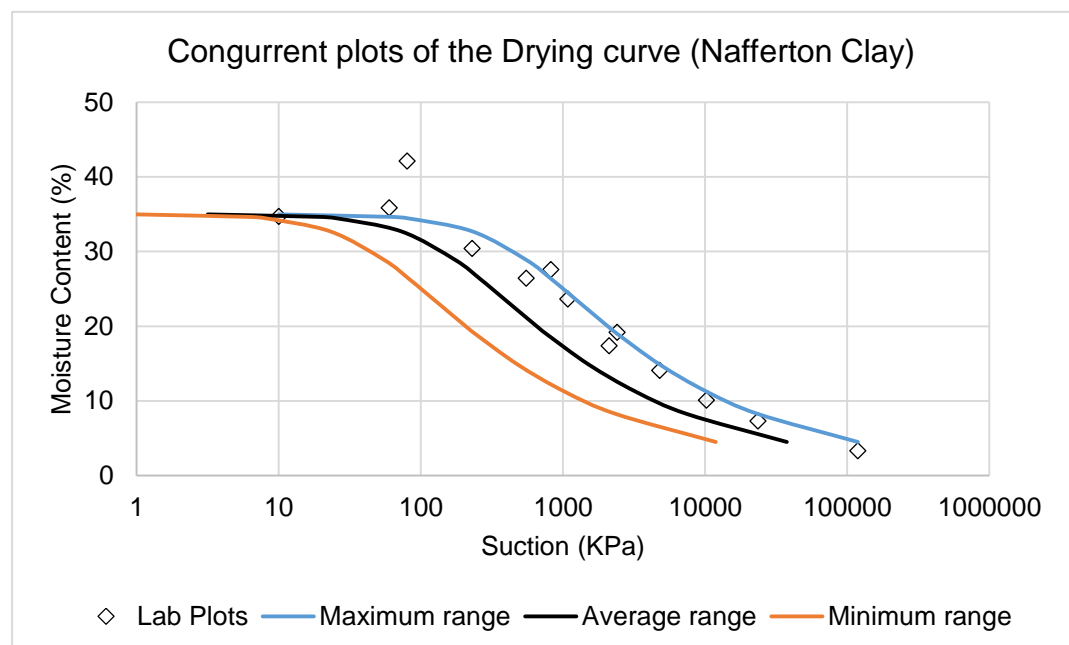


Figure 4.10: SWRC for estimation of soil suctions in drying

Using moisture records of the theta probe in the top 40mm layer (Figure 4.7) for example, suction results from the three curves were estimated as shown in figure 4.11.

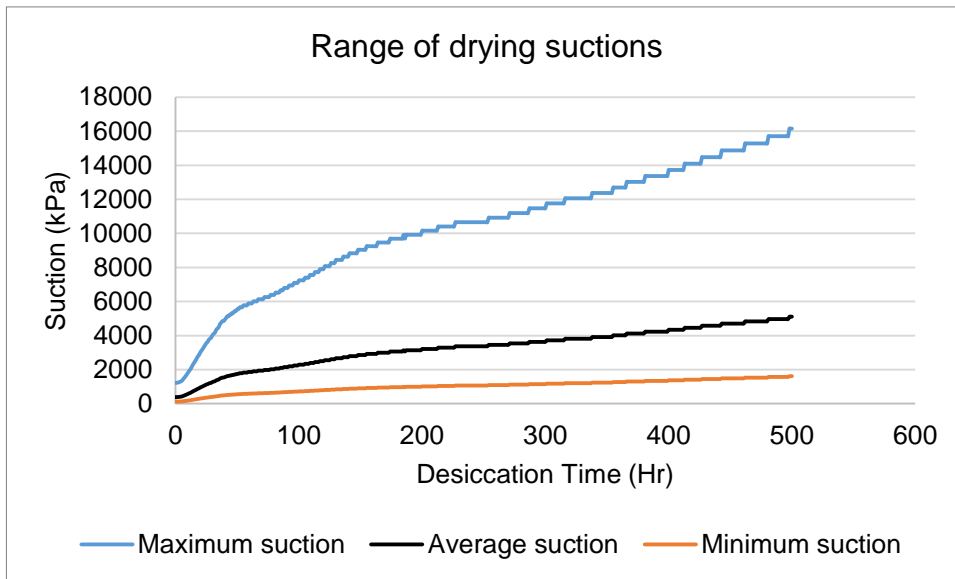


Figure 4.11: Changes in estimated range of suctions in a drying soil

Clearly, the suction profiles obtained from the three congruent drying curves vary significantly. The profile of the average range of suction is closer to the minimum range. Soils typically exhibit hysteresis between the wetting and drying curves, and this leads to a significant difference in the suctions estimated from the two conditions. Although the Fredlund *et. al* (2011) congruent shift procedure locates the average curve mid-way between the maximum and minimum suctions, the actual value is not exactly an average of the two extreme measurements. This is possibly due to nature of the soil materials. The lateral shift parameters used by Fredlund *et. al* (2011) (section 2.4.11) were deduced from tests in different soils. However, for a conservative estimate, the average curve is used in this study to represent suction developed with time of desiccation in the soil. Notwithstanding, the estimated average suction from the laboratory test is significantly higher than average field measurements (section 4.2.2). This is because of a higher degree of drying in the laboratory samples leading to a relatively lower moisture content. The average moisture content of the laboratory samples at the end of desiccation was 12% while natural moisture content in the field was 23% on average.

For illustration of the estimated suction during desiccation, moisture loss profiles earlier shown in Figure 4.7b is re-presented with the corresponding estimated suction at the different depth in the compacted soil specimens (Figure 4.12).

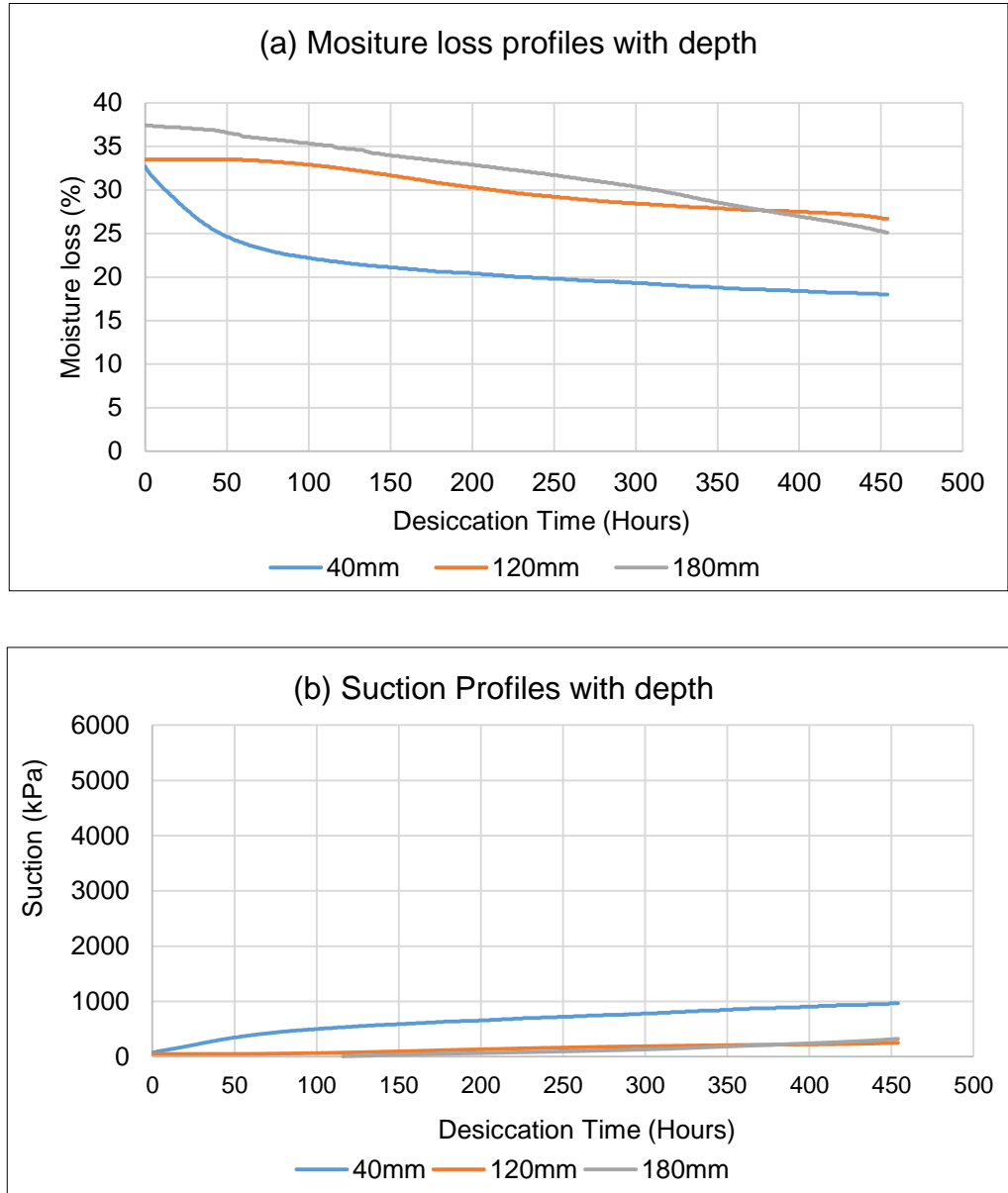


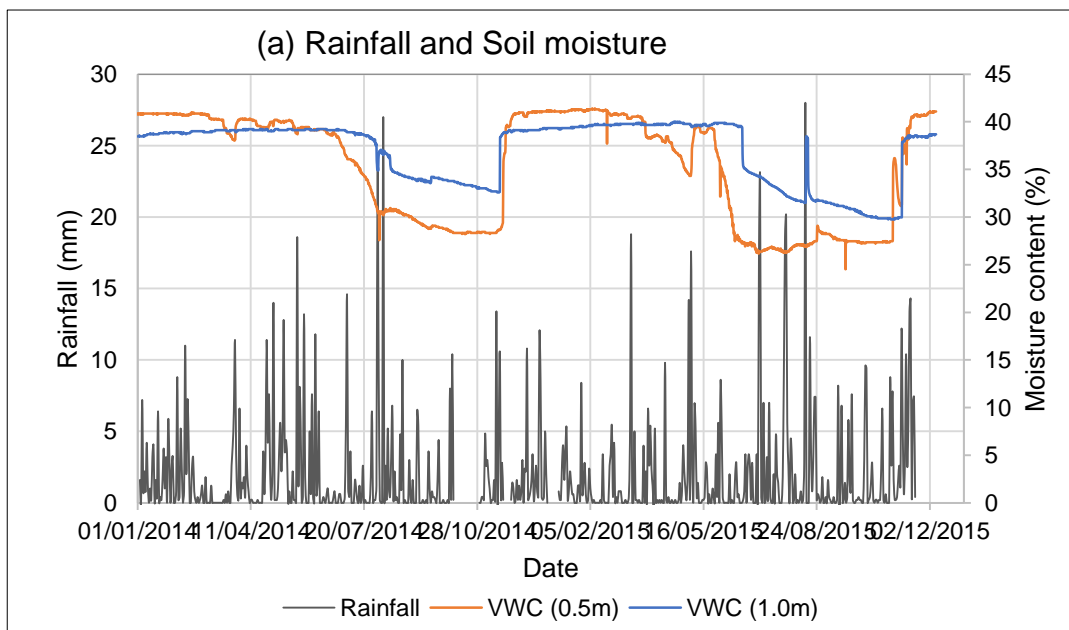
Figure 4.12: Profiles of moisture and suction with depth in a compacted soil specimen

Similar to the trend of field results, the laboratory-estimated suctions indicate the top layer of the soil exhibit significantly higher suction values than the middle and bottom layers. The suction developed at the bottom also gradually equilibrate the trend of middle layer, with a crossover after nearly 350 hours of desiccation (Figure 4.12a). This behaviour can be attributed to an enhanced desiccation brought about by gaps between the

shrunken soil block and the box, which provides a by-pass for air to desiccate the bottom layer. This is supported by the corresponding moisture profiles given in Figure 4.12b. This process is analogous to accelerated evaporation at deeper soil layers through cracks leading to complicated transport phenomena in soil media. The trend of moisture and suction from field and laboratory results reasonably suggests engineering control on the slope hydrodynamics. It is likely that this would also have effect on the soil mechanical response with implication in the cracking behaviour of the engineered conditions.

#### 4.2.3 *Cyclical characteristics of soil moisture and suction*

The results discussed in the preceding sections shows that the soil structure and the climate conditions are influential in the magnitude of hydrologic response recorded. The field moisture profiles shown in Figure 4.4 above are records of series of repeated wetting and drying due to series of rainfall and sunshine events affecting the embankment. In order to assess the effects of cycles of microclimate on crack characteristics, the field moisture and suction profiles are compared with natural rainfall events during the period of crack development. The results are presented in Figure 4.13.



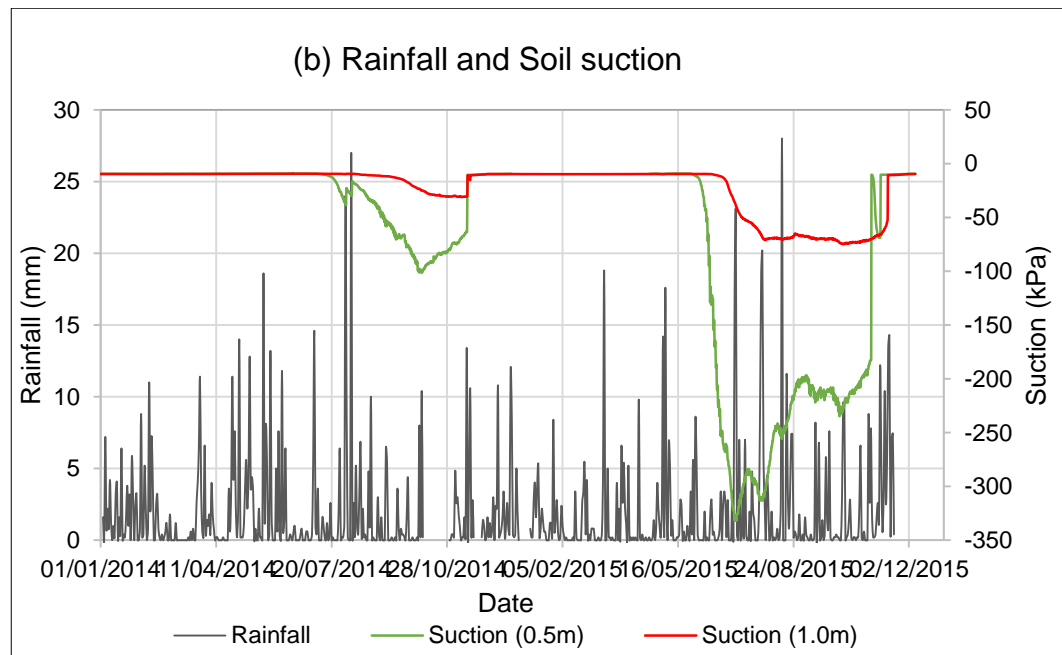


Figure 4.13: Relationship between rainfall and hydrology in the embankment

From the graphs shown, it is clear that periods of low and high hydrologic changes in the soil correlate with ranges of low and high rainfall events. A similar correlation was reported in other studies conducted on the embankment (Hughes *et al.*, 2009; Glendinning *et al.*, 2014). The soil moisture and suction response here shows offset as a function of depth. However, comparing the trends at 0.5 and 1.0m (Figure 4.13 a and b), the soil response is more significant in terms of suction than moisture, indicating the sensitivity in the response of the unsaturated soil to changes in suction (Fredlund and Rahardjo, 1993). As captured by the SWRC, typically a small change in moisture content can potentially lead to large suction response in fine grain soil and vice versa. This can be attributed to factors including texture, permeability and moisture path (drying vs. wetting). The change in these conditions essentially effect menisci forces in soil water. The state of soil water and the rate of moisture movement are therefore critical to the hydrologic response.

#### 4.3 Hydrodynamic controls in desiccation cracking of soil

The dynamics of soil-atmosphere interaction leading to the general trends observed in both field and laboratory hydrology clearly indicate a reducing desiccation rate hence, decreasing volumetric moisture from top to bottom layer of the soil mass. The vertical hydrologic variation can impose a mechanical gradient in the soil and is likely to generate differential stress

condition, which is considered as a key factor in shrinkage and crack. In section 4.3.1, the influence of soil moisture behaviour on crack formation and distribution on the embankment soil are examined.

#### 4.3.1 Occurrence and distribution of cracks in the embankment

As part of the methodology, a walk over survey for natural cracks was carried out on the embankment found. A total of 19 cracks were found during the survey period which lasted for 2 years. Figure 4.14 shows typical cracks occurring on the embankment. The cracks were mostly linear although a few had short secondary branches tending towards a polygonal pattern. LVDT sensors are installed in one of the cracks (Figure 4.14d) to monitor opening and closing.



Figure 4.14: Surface cracks in the embankment and displacement monitor installed in one of the cracks location (d).

The distribution of the cracks in their approximate locations on the embankment throughout the period of survey is shown in Figure 4.15.

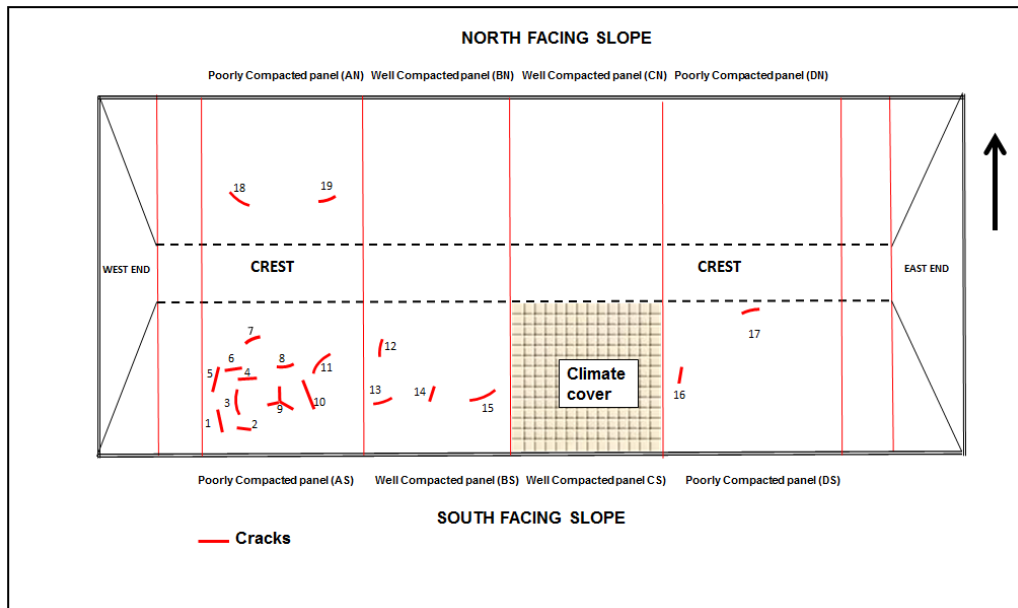


Figure 4.15: Illustration of crack distribution in the embankment (May 2014 – February 2016)

As depicted in the layout, the cracks are widely distributed over the slope faces. This widespread distribution can suggest an environmental control rather than slope movement. Tension cracks resulting from slope movement commonly formed on the crest of the slope and in area of net maximum load (Take and Bolton, 2002). In this survey, more cracks were found on the South facing slope. The first sets of cracks found at the beginning of the survey in May 2014 were all within the westerly located poorly compacted panel i.e. panel AS(P/C) and at the end of the entire field survey, the cracks on this panel totalled eleven in numbers. This represent about 58% of the total cracks found on the entire embankment and 68.8% of the total cracks found on the South facing slope alone. First crack initiation on the neighbouring well compacted panel i.e. panel BS (W/C) was observed in June, 2014 nearly one month after first set of cracks were found on the poorly compacted panel. The size of new crack initiated appeared relatively small (~1mm). Two other cracks were found at the easterly located poorly compacted panel (panel DS) making a total of 17 cracks on the South slope. On the North Slope, two cracks were found throughout the entire period of the survey and these were initiated in July, 2014 when the soil was significantly dry. Both cracks occurred on the poorly compacted panel (panel NS). Therefore, cracks on the North Slope

constituted only about 11% of the total cracks found on the embankment. The increase cracking in the poorly compacted panel is associated with the susceptibility of this apparently weak soil structure to mechanical breakdown by a given magnitude of hydrologic stress recorded.

The frequency in occurrence and distribution of cracks was also analysed in terms of intensity of cracking in the modelled laboratory tests. However, unlike the linear outlines commonly exhibited by cracks studied in the field, the laboratory simulated cracks developed complex network pattern, a difference which shall be explain later in this study. The intensity of surface cracking developed in the laboratory specimens were quantified by the digital image analysis technique described in section 3.4.7. Example of cracked soil surfaces and the crack intensity for the well-compacted and poorly compacted soil specimens are presented in Figure 4.16.

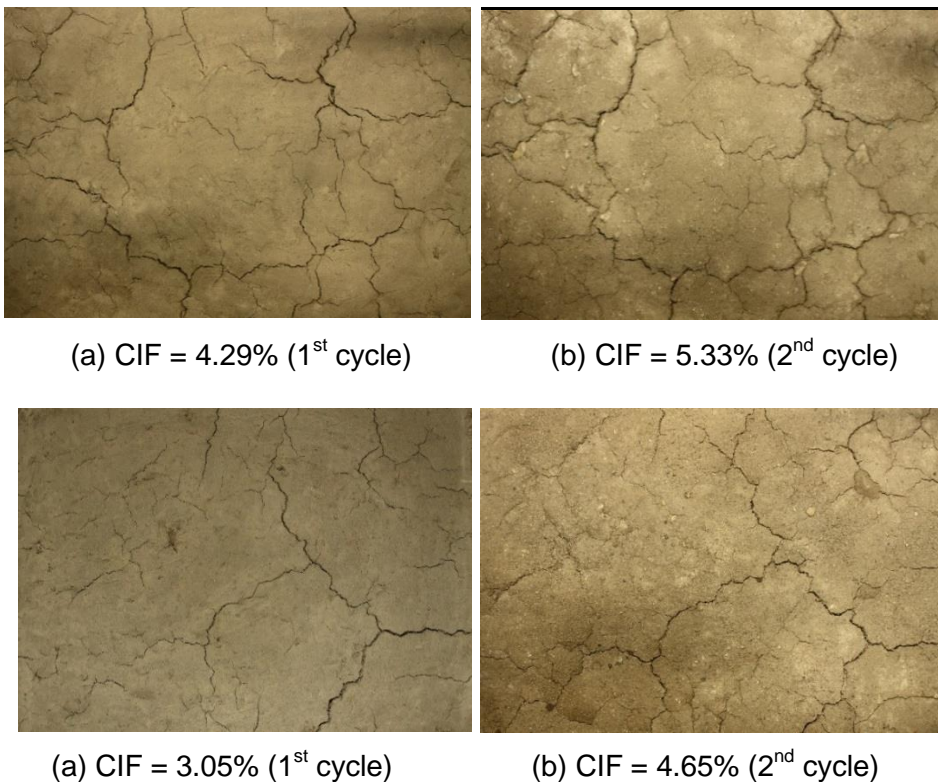


Figure 4.16: Crack Intensity in (a) Low density soil (b) High density soil

The CIF values, which were determined from final images in each case, indicate that there were more cracks per unit area of the low density, poorly compacted soil specimen compared to the high density, well compacted counterpart under same environmental condition and duration

of test. This compared well to the field scale cracking where greater number of cracks occurred in the poorly compacted panels. Comparing the crack intensity of the thick and thin soils compacted to high density, the thin soil exhibits significantly less cracking at the same conditions of wetting and drying (average of 0.8% and 2.1% in the 1<sup>st</sup> and 2<sup>nd</sup> cycle respectively). It is considered here that the resulting crack intensity could arise from their slight density difference. The thick soil is less dense in this case (1.62Mg/m<sup>3</sup>) resulting in more cracking compared to the thin soils (1.63 and 1.65Mg/m<sup>3</sup>). Also, a thick soil block implies a wider vertical space, which would enable greater moisture and suction gradients. Pronounced cracking is likely to result under such increased hydrologic conditions and the thick soil provides a larger area for cracks to propagate including the potentials for development of deeper cracks. Increased cracking with increase in sample size have also been reported in other works notably, Miller *et al.* (1998), Tang *et al.* (2008) and Dyer *et al.*, (2007). Overall, these results confirmed a greater susceptibility of low-density soils to mechanical breakdown caused by hydrologic stress during the drying.

#### **4.3.2 Crack morphological development**

In addition to the pattern development and distribution of the cracks across the slope aspects and engineered panels discussed above, seasonal and diurnal changes in the crack morphology were also observed. The crack geometric properties changed as the hydro-mechanical condition in the soil changed. This is evidence in support of the association of this phenomenon with the periodic changes in soil moisture discussed in section 4.2.1. The crack survey started in April 2014. Although there were a few closed old cracks found during this period, judging by their linear imprint relative to the surrounding surface, they later re-opened towards the end of May, 2014. During this period, new cracks also initiated as the weather conditions became drier in late spring. In the summer months (June to August), crack morphology significantly developed, characterised by widening, lengthening and deepening. Most of the cracks developed in the drying months of 2014 were completely closed by end of March 2015 after the winter. None of the closed cracks re-opened after this period. In

addition, new cracks were not observed even up to summer 2015. This prompted interest in examining the underlying cause of such distinction in crack formations in the embankment between the two years. Possible reasons were found in two important events associated with the embankment within these periods. First was the amount of rainfall on the embankment (Figure 4.17). The graph shows net higher rainfall intensity in 2015 compared to 2014, particularly around the summer months (July – August).

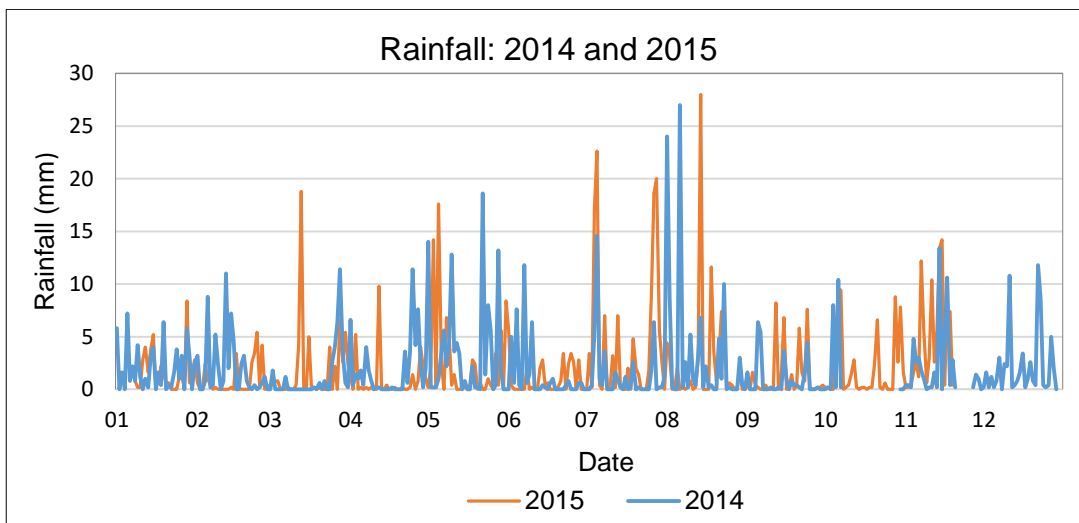


Figure 4.17: Rainfall intensity of the embankment in 2014 and 2015

This agrees with the Meteorological office record (Met, 2015), which classified the year 2015 as having the wettest summer in recent times in England. The wet condition influenced the soil moisture regime with a net higher range occurring in 2015 (Figure 4.4).

The second explanation was found in the fact that around the middle of May, 2014, vegetation on the embankment was mowed as part of the management of the facility while in 2015, the vegetation was not touched, with intention for carrying out agricultural research by other workers. A possible implication of clearing vegetation on the embankment would be a direct climate intensity impact on the exposed soil surface. This is expected to increase evaporation particularly around the summer months. Therefore, the evapotranspiration, ET around the embankment was compare for the two years as shown in Figure 4.18.

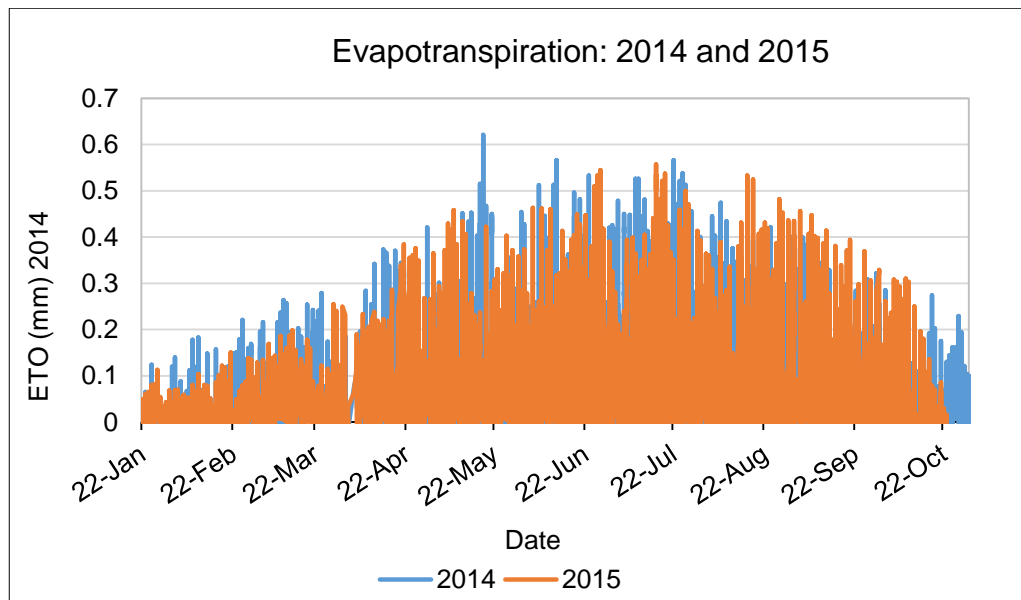


Figure 4.18: Evapotranspiration on the embankment in 2014 and 2015

The ET trends are close but on average, there are greater intensities in 2014 between the months of April and August which usually have a progressively less rains. Transpiration by plants contributes significantly to overall moisture loss in soil. However, in the present case, the direct exposure of the soil to the elements is thought to contribute more in the evapotranspiration result since vegetation was cleared. The soil moisture profiles shown in Figure 4.4 also reflect less volumetric moisture in 2014. From this results, it is reasonable to say that any surface changes observed in the soil condition is associated with climatic interaction since the inherent engineered characteristics and structure of the embankment remain unchanged during the period of study. Moreover, the most important soil property that commonly characterise this interaction is soil moisture. Crack initiation, re-opening and morphological changes accelerated in the drying seasons while most cracks were closed in the wet seasons. Between the two seasonal extremes, cracks showed transient behaviour, especially reduction in depth during intermittent rainfalls. The above fact can therefore lend emphasis to the role of the amount of moisture present in the soil in crack development, with control of material and climate properties.

Both in the field and in the laboratory, the cracks were observe to develop systematically. That is, the cracks first initiated on the soil surface as micro flaws of ~1mm and gradually developed geometrically. In order to quantify

this development, the volume of each crack measured in the field was estimated as they changed in time. This was computed using an empirical equation (equation 3.21) involving the crack width, depth and length measured in the field. The result is shown in Figure 4.19.

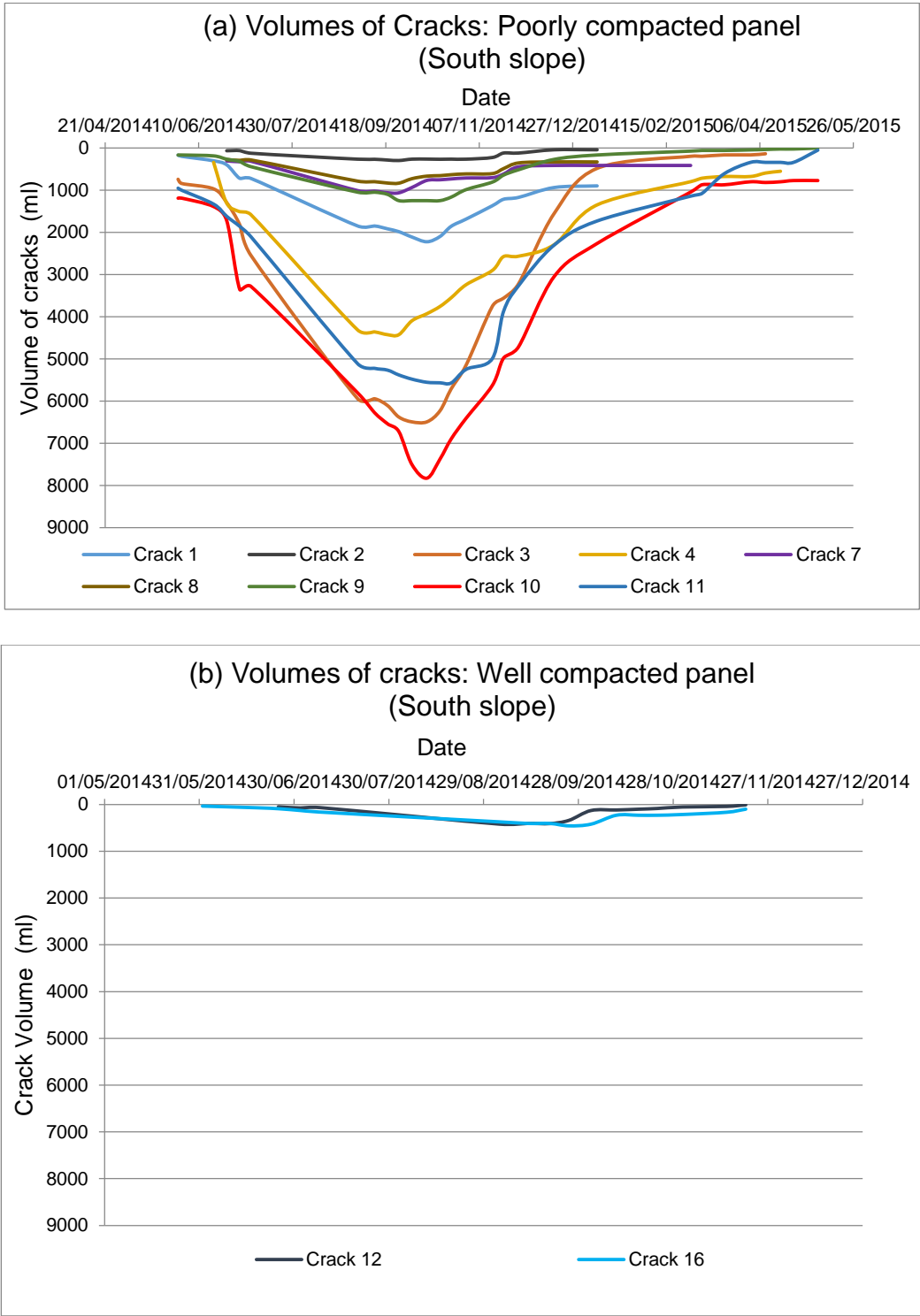


Figure 4.19: Profiles of crack morphological evolution (a) Well compacted soil (b) Poorly compacted soil

From the figure above, the volumes of cracks increased considerably from July and reached their maximum between August and September. From the record of hydrology and climate shown in section 4.2.1 and 2.2.2, this period is marked by low rainfall, high evapotranspiration leading to low soil moisture increase soil suction, both in 2014 and 2015. Base on the potential of these conditions in causing significant desiccation in the soil, it is here assumed that this led to the significant development of the cracks. The field summary of the cracks geometry property presented here in Table 4.1.

Table 4.1: Summary of crack geometry property in the embankment

Engineered Conditions Crack Property	SOUTH SLOPE		NORTH SLOPE	
	Poorly compacted panel	Well compacted panel	Poorly compacted panel	Well Compacted panel
Maximum/Average depth (mm)	400/300	330/180	60/45	No cracks
Maximum/Average width (mm)	70/32	40/12	5/3	No Cracks
Maximum/Average Length (mm)	2000/800	800/400	400/nil	No Cracks

The summary shows that the cracks development was more in the south slope, and the cracks geometry properties of the poorly compacted panel were significantly higher than those of the well compacted counterpart. Cracks 1, 4, 11, 3, and 10, occurred in the westward part of the poorly compacted panel in the south slope (Figure 4.15) ranged highest in volumes with 2,000ml, 4,000ml, 4,000ml, 7,000ml and 8,000ml respectively. This is likely due to a higher effect of the prevailing wind and solar exposure. Only two of the cracks found in the well compacted counterpart developed a considerable volume change, averagely 400ml while the only crack found in the North facing slope was less than 100ml throughout the survey period.

A similar trend in the crack morphology was also observed in the laboratory experimentations, although the crack geometries were much lower apparently due to the laboratory scale (Appendix II). However, the cracks geometry generally increased in the second cycle as presented earlier in Figure 4.16. Due to the irregular pattern of rainfall and sunshine events, and the periodic nature of the survey, this mechanism could not be

studied in details in the field. Hence, the laboratory models complement the understanding of the complex natural process. However, after reaching their maximum value, it was generally observed that the volume of the cracks began to reduce from October, a period characterised by the onset of wet condition i.e. autumn rains. The cracks began to close from this period as marked by a decreasing volume of their cross sections. The laboratory study revealed more details of this behaviour. During re-wetting of the soil for the 2<sup>nd</sup> drying cycle, the water were observed to first infiltrate the soil through the cracks. As the cracks became filled with water, the excess water floods the soil surface before subsequent infiltration on the entire soil surface. Simultaneously, loosed soil particles, mostly fines are washed off the soil surface and some settled round the crack aperture driven by the water current. As the water completely permeates the soil leaving a wet surface, the soil block swells and the cracks gradually closes. This suggests that the observed crack closure in the field relates to rainfall wetting. Therefore, cracks open as the soil dries and vice versa. However, the field measurement around this period shows the crack closure was more significant in depth, usually decreasing between 20 to 50mm before a small decrease in the width, commonly between 3 to 4mm. The relationship between crack width and depth in particular points to the cracks being triangular in cross-section. In both the field and laboratory, the magnitude of crack depth was several orders greater than the width (see Appendix I and III). It also suggests that the dynamics of soil cracking presents a directional difference in magnitude, likely to be concomitant with the pattern of stress distribution around the crack body. Fracture mechanics principles suggest that greater energy is dispense in crack propagation in the direction perpendicular to maximum stress. This implies greater development in direction of less strain energy.

To further evaluate the mechanism surrounding the crack behaviour, an analysis of the preliminary data recorded by the LVDT sensor installed at one of the established crack was carried out. The result shows that the embankment soil experiences temporal horizontal movement as shown in Figure 4.20. The ground movement strongly correlates with the rainfall record on the embankment, and further validate the fact that hydrology

property of the soil is influenced by the prevailing climate condition, essentially wetting and drying by rainfall and solar temperature.

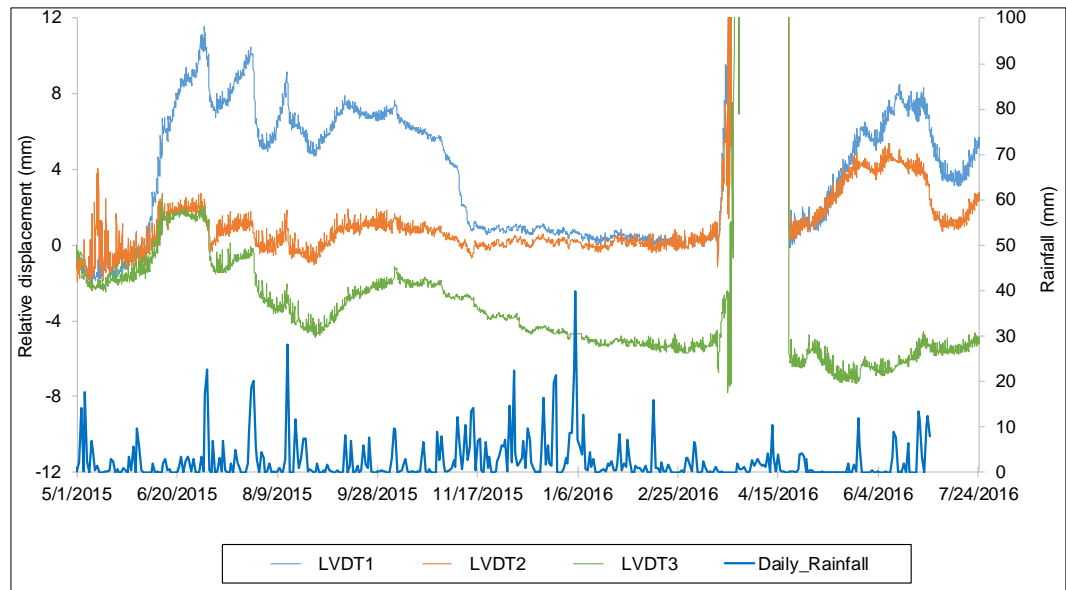


Figure 4.20: Horizontal ground movement at a crack location in the embankment. Negative and positive recordings here are indication of expansion and contraction recorded at each end of the 200mm long sensors installed perpendicular to the crack outline. The recordings can therefore potentially describe the behaviour of crack opening and closing. However, from the walk over crack survey record, this particular crack (see Crack BN/AS/09 in Appendix I) was closed for a greater period represented by the LVDT record. The closure of this crack like other counterparts in the embankment began in early November 2014 with onset of wet season. Then, it became accelerated with loose soils, which fell into the crack from the LVDT installation work in December 2014 and the crack was eventually recorded as closed on May 7<sup>th</sup>, 2015 when the surface no more presented any measurable geometry. The LVDT recordings display low amplitude cycles (1-2mm) at the beginning of the record, which corresponds to the month of May 2015. This period is also characterized by increased in soil moisture (averagely 40%) and low suction (less than 10kPa) in direct response to the increase rainfall as captured in both Figure 4.13 and Figure 4.20. The amplitude of ground displacement later increased in June 2015 (4mm) while the condition of the crack did not change. The later event is also marked by a period of gradual increase in suction record as soil moisture begins to reduce with low rainfall (Figure

4.13b). However, the increased movement recorded by the LVDT did not result in the crack opening, as this particular crack remains closed when the data was collected in January 2016. In the interim, the LVDT records reflect the soil behaviour as changes in weather-driven hydrology condition likely influence soil shrinkage and expansion. The monitoring of the LVDT recordings continues as part of the BIONICS project and is hope that the crack would develop in later times in order to relate with the displacements.

#### **4.3.3 *Characterisation of cracking with changes in near surface soil moisture***

Following the seasonal hydro-mechanical trend observed during crack evolution, it is reasonable to attempt their characterisation with soil moisture changes in the embankment. In order to quantify with the field hydrology, the changes in crack geometric volume is used while for the laboratory characterisation, CIF is used. Figure 4.21 compares suction profiles and crack volume changes at close measurement points in the field.

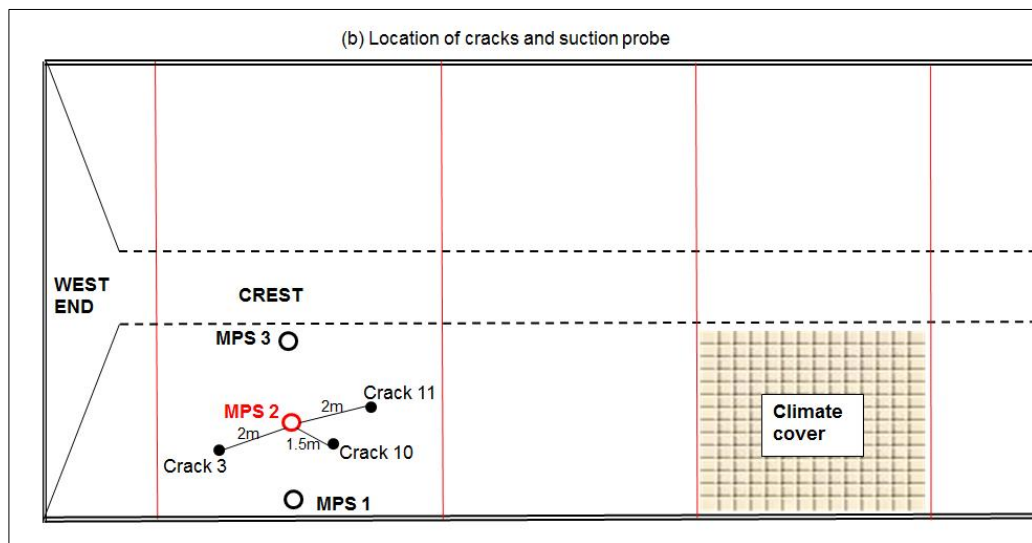
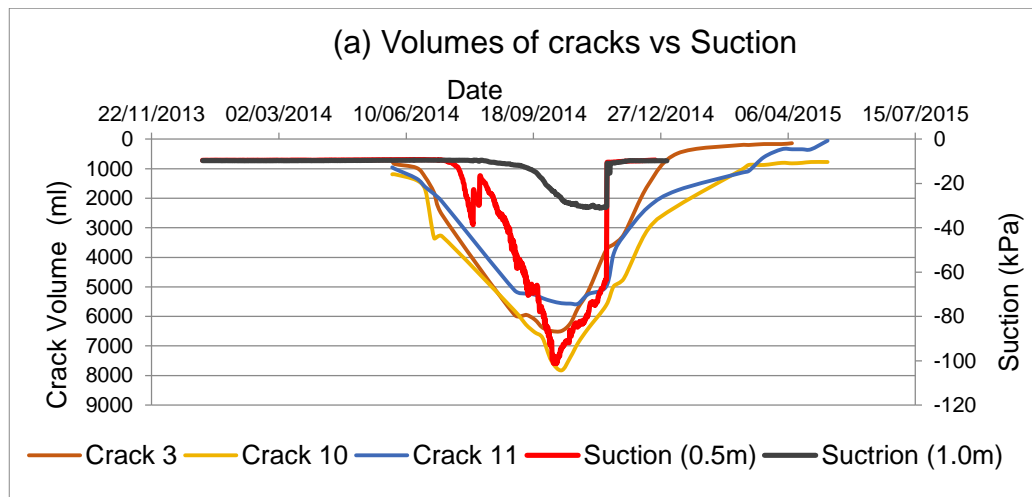


Figure 4.21: (a) Comparison of changes in the volumes of cracks and soil hydrology (b) Distances of cracks 3, 10 and 11 from the soil probe (MPS 2), which recorded the hydrological data in Figure 4.21a.

The plots show that the crack volumes changes as the hydrologic parameter changes in the climate-impacted embankment fill. Maximum crack volumes occurred between the month of August and September, and this corresponds with period of maximum suctions. The maximum suction record corresponds with the period marking or immediately succeeding the end of summer and agrees with other field observation (Ridley *et al.*, 2004b). The trend of crack volumes however correlated more with the suction profiles at the depth of 0.5m. This suggests surficial suction is likely to have greater influence in the cracking. Since soil generally dries from the surface, suction change would present a decreasing gradient with depth. Considering the large disparity in suction profiles recorded between 0.5m and 1.0m depth, it is likely that another suction regime may exist at less than 0.5m depth and would therefore be

more influential in the measured cracks. The nearest surface suction recording on the embankment was limited to 0.5m. In order not to disturb the crack development, the use of hand probes to test continuous moisture and suction changes at lesser depth was avoided.

The correlation between changes in crack volumes and suction developed on the embankment arises from net variation in the soil moisture. This suggests that analysis of soil moisture deficit and the rate of suction degradation can provide, in the first instance, a qualitative assessment of the propensity of cracking in desiccating clay slope. Suction development in a drying soil and relief of associated tensile stress against the soil tensile strength is the widely recognised premise for crack formation (Nahlawi and Kodikara, 2006; Péron *et al.*, 2009a; Péron *et al.*, 2009b). Cracking intensified in the embankment in the near surface zones where suction ranged between 10kPa and 300kPa. This corresponds to average soil moistures between 35% and 20% during the summer period (Figure 4.9). From Figure 4.21a, the crack volumes tend to change proportionally with suction and significantly increased within the stated range of hydrology changes in the summer. The extent of cracking in the soil therefore tends to relate to the rate of suction change and invariably the moisture state in the soil. Understanding the rate of these changes can provide a quantitative relationship between crack volume and moisture state in soils. Smethurst *et al.* (2006) reported a significant correlations between soil moisture deficit, volumetric soil water content and suction development in the upper layer of a vegetated embankment. Lees *et al.* (2013) also observed similar relationships and occurrence of cracks during periods of high soil moisture deficit (i.e. low volume of water relative to field capacity). With the possibility of linking soil moisture content to suction through the soil water retention curve, it seems reasonable to think that the hydraulic stress that occurs during cracking can be estimated by the state of soil saturation. Consequently, soil water deficit and desiccation cracking may be directly related and this further highlights the importance of climate conditions e.g. the balance between rainfall infiltration and evapotranspiration in desiccation cracking of fine-grained soils.

From the foregoing crack morphology-near surface soil water-suction changes, it is reasonable to consider desiccation cracking as a phenomenon arising from coupled hydro-mechanical process in expansive soil. The coupling arises from the close association between soil microstructure and the moisture content. Moisture loss would enable the solid particles to interact more closely in the empty voids. Under this condition, the menisci surface between neighbouring particles would reduce. A net mechanical effect is therefore envisaged at the interparticle contacts (including friction, capillary forces etc.) leading to increases in apparent cohesion, hence the soil strength (Colmenares Montanez, 2002; Wang *et al.*, 2007; Zeh and Witt, 2007). During drying therefore, soils undergo shrinkage volume change accompanied by generation of tensile stress, a factor which signifies a mechanical response to the hydrology-related change in the soil fabric. This relationship underscores the hypothesis that cracking occur when drying induced tension in the soil exceeds the soil tensile strength. Therefore, a limiting hydrologic condition is likely to exist for cracking in soil materials.

#### 4.3.4 ***Significance of volume of crack in slopes water regime***

Soil essentially derives water from rainfall and loses water back to the atmosphere by evapotranspiration. The balance between the two processes practically determines the field capacity i.e. the maximum amount of water the soil can hold) and soil moisture deficit i.e. the amount of rain needed to bring the soil moisture to field capacity (Kirkham, 2014). The amount of moisture present in soil at any given time (soil moisture storage) largely depends on soil properties such as soil texture and macrostructures (Fredlund and Rahardjo, 1993). While the former is relevant in the water retention property of soil (fines retain more water than coarse texture), the latter is more applicable in soil water storage and movement. Cracks are key macrostructural features in soil, hence can host and transmit soil water. They are therefore an important factor to consider in geotechnical practice involving rainwater storage and drainage in slopes, of course depending on their cross sectional volumes.

The moisture storage potential of the cracks measured in this study was evaluated from the computed volume of the cracks. Synthesis of maximum

and minimum crack volumes discussed in section 4.3.2 indicate that the measured cracks can hold between 2,000ml (2.0litres) and 7,800ml (7.8litres) of water at any given time. In terms of rainwater capture (or harvest) in the field, potential of the crack can also be estimated. Rainwater capture is commonly calculated from the product of average precipitation and catchment area (in this study, area of the crack). Prominent crack apertures measured have an average surface area of  $5,000\text{mm}^2$  ( $0.05\text{m}^2$ ). Using typical annual precipitation of 73mm estimated for UK (Met report), it means such cracks can capture on average,  $3.65\text{m}^3$  of water annually. This can amount to a substantial quantity of rain water for infiltration into the soil. The impact of this magnitude of water harvest and infiltration into the soil through cracks can significantly increase soil water storage against actual potential evapotranspiration resulting in increased field capacity. The impact on hill slope water regime can further be exacerbated by proliferation of cracks during intense summer drought and the unfolding extreme climate conditions. This in effect agrees with a double capacity of infiltration estimated in crack soils (Novak *et al.*, 2000) and further suggests here that high evapotranspiration is unlikely to balance intense rainfall in summer as envisaged by some soil-climate impact study summarised in section 1.1.2. This analysis underscores the potential role of cracking in future slope response as climate seasonality increases.

#### **4.4 Quantifying crack intensity in drying soil**

Time-lapse photograph images of surface cracks recorded during the laboratory desiccation study provided a tool for analysis of the crack evolution. In response to hydrologic changes during the drying, the specimens produced distinctive images of cracking as exemplified in Figure 4.22.

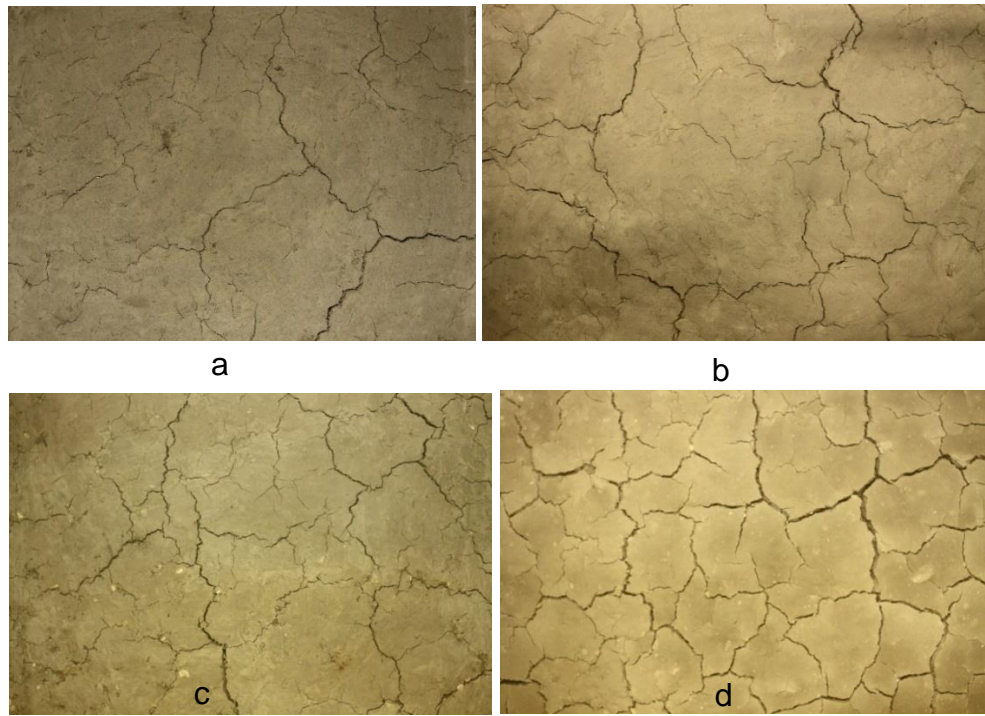


Figure 4.22: Photographs of desiccation cracks (a) Well compacted soil Nafferton clay soil (b) Poorly compacted Nafferton clay soil (c) Gault clay soil (d) Bentonite-Nafferton clay soil

The representative images have enabled a comprehensive characterisation of the factors involved in the cracking process which could not be directly observed from field result. As shown in the images, the laboratory generated cracks display complex patterns of polygons. Looking at their intersections, the cracks meet predominantly at  $90^\circ$  which classify them as orthogonal cracks (Kodikara *et al.*, 2000). Orthogonal cracks are considered to result from a slow rate of desiccation. In the absence of any catastrophic event, most natural processes are slow and gradual. Some desiccation experiments are carried out under conditions that result in very high desiccation rate e.g. oven drying. While these sets of studies are useful in explaining what can be expected under astronomic conditions, the common scenario of soil-atmosphere interaction in civil construction is a slow and gradual process with long-term effect. Consequently, a moderate atmospheric condition represented by a dry and gentle wind was simulated in this study in a bespoke climate control system. Although field climatic conditions are more complex, as shown by various meteorological parameters recorded at the BIONICS weather stations, the laboratory system represents the basic parameters that could

be readily simulated in this study e.g. wind velocity, relative humidity and temperature.

The crack intensity factor quantifies the propensity of soil cracking. Hence, it is used in this study to compare and characterise cracking in the different engineered conditions as moisture changes with time. The computer aided image analysis essentially quantifies the crack development in terms of crack intensity factor for every stage of drying. An hourly interval of digital photograph was programmed to see detailed trends of the changes in the crack geometry relative to area of the soil clod. In the average, 200-300 images were recorded for each depending on the duration. Therefore, in order to rationalise the large volume of data, the cracks images were analysed every four hours. When plotted as time series, the CIFs displayed exponential growth trends with distinctive gradients as presented in Figure 4.23 for a 2-cycle test. The change in gradients (defined by dashed lines) on the profile can be regarded as representing important phases in the crack evolution.

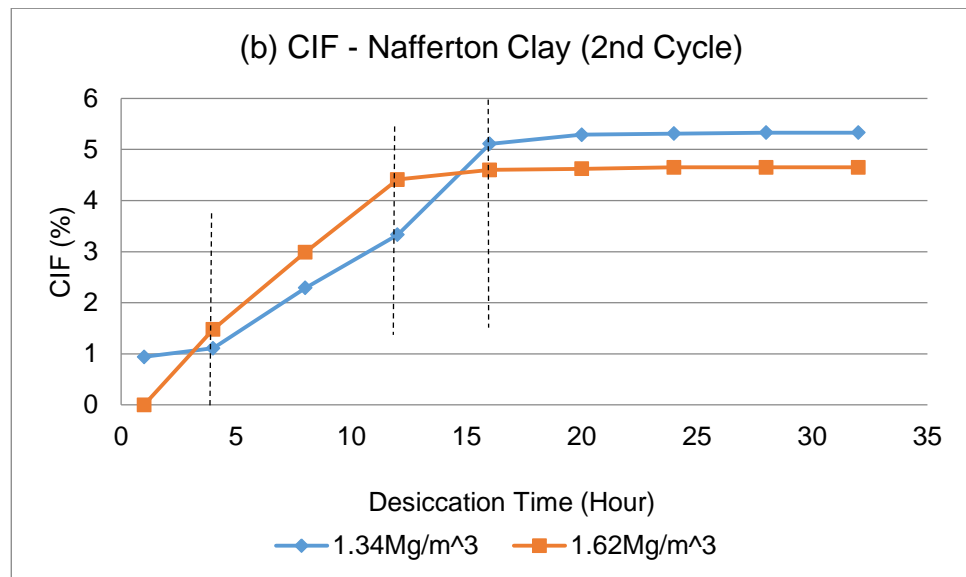
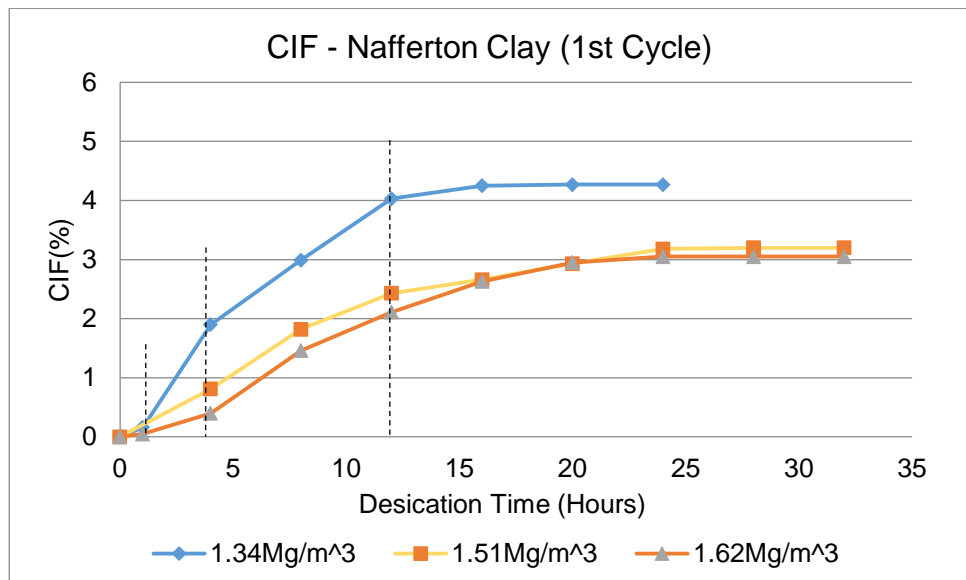


Figure 4.23: Desiccation crack intensity of a clay soil with different compaction quality

Initially, the profiles present a slow development before increasing linearly with time to a peak rate. This is followed by a gradual reduction in rate towards equilibrium values. The periods of desiccation were typically between 10 and 14 days (i.e. 200 to 300 hours), however the analysis covers the period when the values begin to be constant i.e. repeated. The trend of CIFs can be explained by the rate with which crack formation in the soil progresses. It was observed that at the beginning of the desiccation, few microcracks initiated on the soil surface within 1-4hours. This is regarded as the initial stage of crack generation. As desiccation progresses, more parallel to sub-parallel cracks continued to initiate and propagate in width, depth and length towards each other. This period of

crack proliferation is referred in this study as the “active stage” of cracking and was found to occur between within 24 hours of desiccation depending on the test condition. Following this active period of cracking, initiation of new cracks generally ceases and further development was characterised by geometric increase in existing crack morphology, mainly crack width that also gradually slows towards constant values. This later stage is here referred to as the “stable stage” and was commonly observed after 2-5 days of desiccation. This series of crack development are exemplified in Figure 4.24.

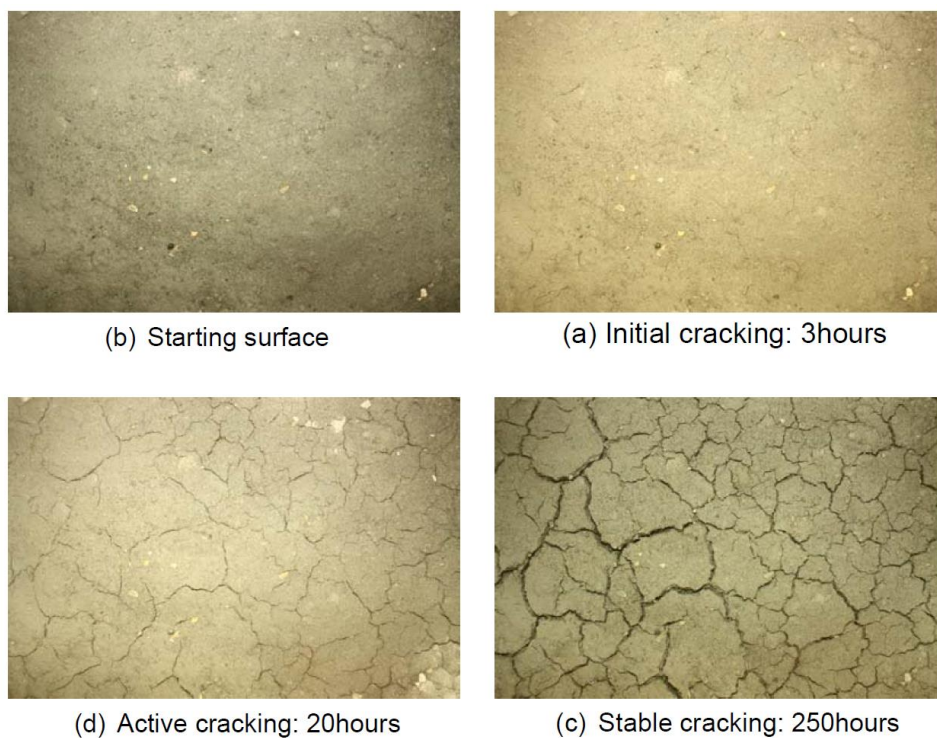


Figure 4.24: Stages of cracking in a drying compacted soil

Similar stages of cracking were also observed by Miller *et al.* (1998) and Li and Zhang (2011). These workers referred to the three stages as initial, secondary (or primary) and stable (or steady) stages. The active stage described here is equivalent to secondary or primary stage but the adjective “active” is preferred here to more directly convey the important event at this stage. Note that the boundary of each stage differs according to the engineered condition with cracks commonly reaching the stable stage much earlier in the relatively less dense soil with more cracking. The active stage is relatively longer in the well compacted specimen, ranging between 10 and 24 hours. This can be caused by prolonged moisture

movement in the dense soil with lower permeability. Overall, the trend shows that crack intensity is not really indefinite but seems to occur within a limited range of amount of moisture in the soil in any given engineered state. In addition, the active stage is generally more prolonged in the second cycle for any engineered state.

Since the phases are developed as moisture is lost in the soil, the CIF can therefore be used to characterise the desiccation process. For illustration, desiccation curves presented in Figure 4.5 is repeated below as Figure 4.25. The profiles present an exponential gradient, which is relatively greater in the initial 30-50 hours and gradually reduces as desiccation progresses. Within the test periods, the soil moisture starts to equilibrate towards 300 hours depending on the engineered characteristics.

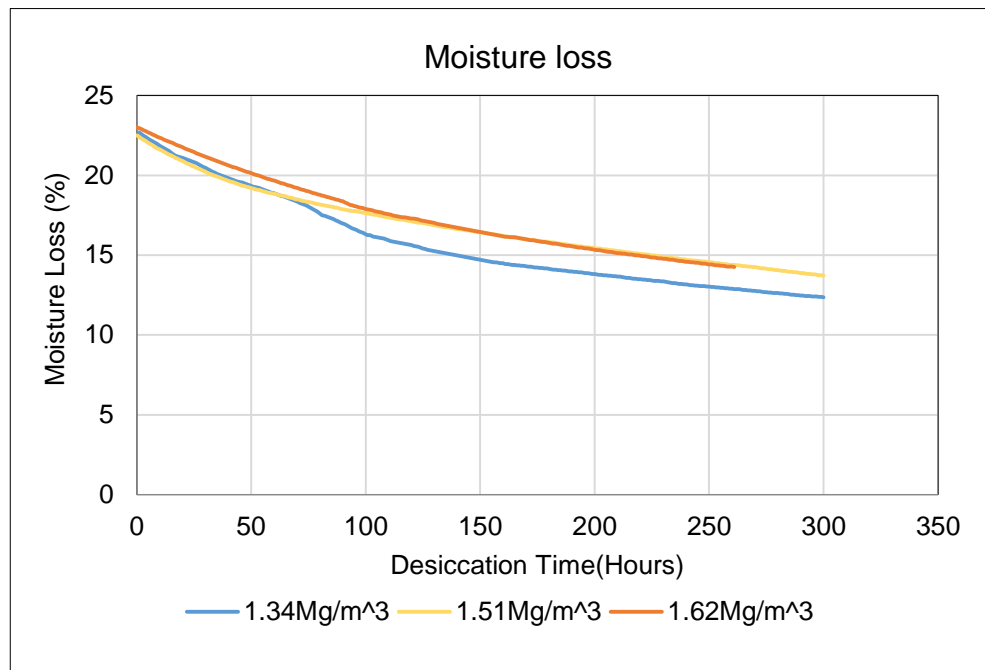


Figure 4.25: Profiles of moisture loss in a soil compacted to different densities

The changes in crack intensity with moisture loss in the soil is shown in Figure 4.26.

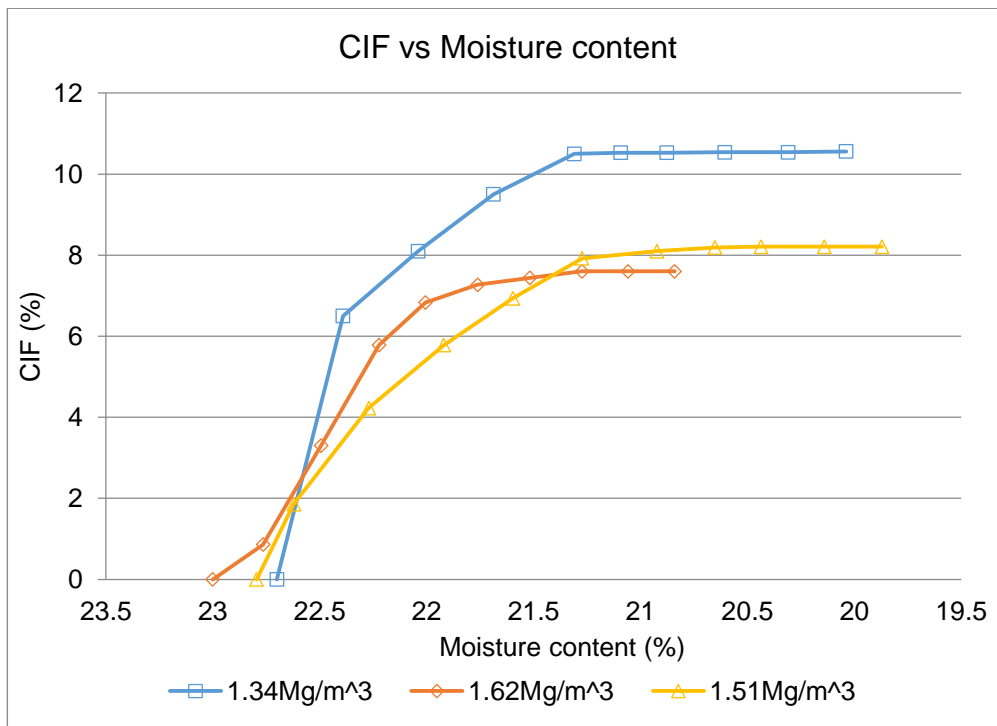


Figure 4.26: Crack intensity with moisture loss in the soil compacted to different densities in the laboratory

The relatively rapid change in the initial period of desiccation is thought to contribute significantly to the progress of crack formation and propagation which as shown here occur within a narrow range of soil moisture. Within this context, the stages of crack intensification are further explained in the three subsections below.

#### 4.4.1 *Moisture changes in initial stage of crack development*

Desiccation of the soil specimens commenced from the moulding moisture content similar to a state of natural moisture in the field after rainfall. Although not very apparent in the profiles presented in Figure 4.24, this stage is commonly characterised by an initial near horizontal line in slurry clay i.e. at full saturation. Therefore, the profiles presented in this study can be regarded as unique for compacted condition. Nahlawi and Kodikara (2006) showed that hydrologic profiles of compacted soils do not present all the phases defined in slurry specimens. The reason of course lies in the moisture condition of the two states of soils, with the initial stage of evaporation corresponding to structural shrinkage incommensurate with moisture loss not likely in the profile of unsaturated specimens. At the start of desiccation with the low humidity air imposed on the soil surface, moisture loss proceeds slowly giving rise to gradual air entry in the near

homogenous soil at this stage. As the soil pores becomes increasingly empty, initial low air entry enabled the development of capillary forces, which would be large under the initial unsaturated condition. The magnitude of this action can be viewed by looking again at the suction profile presented earlier in section 4.2.2. For both the field and laboratory measurements, the engineered soils present a significant suction at the start of drying. This is expected since the soil condition is already in unsaturated condition and the suction is essentially greater in the denser soil. Therefore, the inherent suction potentially supports an almost instantaneous initiation of cracks as drying commenced. These early cracks were initiated randomly with their distribution commonly observed around locations of textural defects in the soil, especially coarse stones and local curvatures as shown in red in Figure 4.27.



Figure 4.27: Cracking around location of flaws in the soil (top photo) Laboratory (bottom photo) Field

Some cracks were also observed to initiate in drier parts of the desiccating soil due to the greater impact of wind turbulence on the opposite side of the box relative to the position of the axial fan. In the field, non-uniform moisture distribution is recognised as a common source of internal restraint during cracking of soil. Such disparate hydrology condition potentially leads to anisotropic volume change in the soil during shrinkage (Bronswijk, 1990; Chertkov, 2013). The moisture distribution in slopes can be affected by aspect exposure to climate elements earlier discussed in section 4.2.

#### 4.4.2 *Moisture changes in active stage of crack development*

During the active stage of cracking defined in the preceding section, the desiccation curves show an accelerated rate of moisture depletion. It is worthy to note that the only difference in the soil state of the initial and active stage of cracking is the occurrence of cracks in the soil, which now defines a new initial condition. Being a secondary surface in the soil, moisture will also evaporate through the open crack walls, thereby increasing the rate of desiccation at this stage. A similar observation was reported by Song (2014) who carried out an experimental study of evaporation involving cracked soils while Li and Zhang (2011) illustrated the underlying mechanism as shown in Figure 4.28. These workers showed that after cracking, moisture loss by evaporation becomes two dimensional, proceeding both vertically from the soil surface and horizontally from the open crack walls.

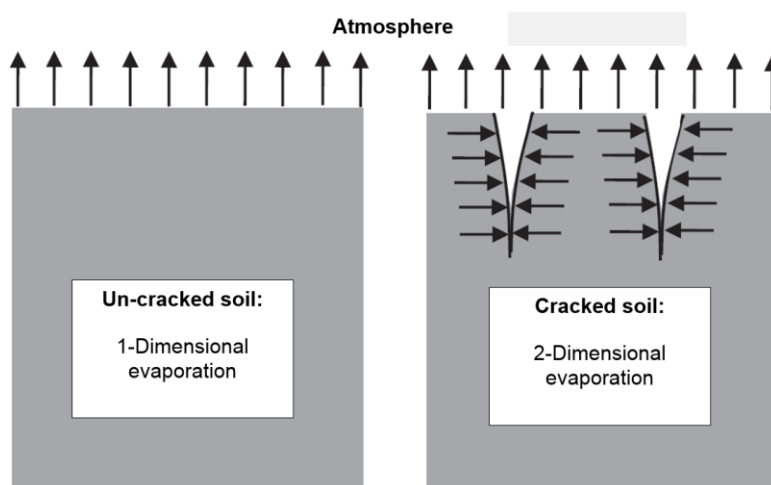


Figure 4.28: Evaporation characteristics in crack soil (adapted from Li and Zhang, 2011)

The increased rate of moisture loss is likely to exacerbate conditions for cracking, including high air entry, increased shrinkage and tensile stress. This is reflected in the proportionate increase in the range of suction in the embankment within this period (Figure 4.12). As moisture reduces rapidly, air entry into the soil increases and the soil particles would be drawn much closer by greater capillary forces developed in the emptied pores leading to an increase effective stress in the soil. The resultant tensile stress from shrinkage would also increase correspondingly. Stirling (2014) showed that the tensile stress occurring in an expansive soil at any given time is a function of the remnant moisture content. Therefore, a study of antecedent moisture in a slope is essential in understanding the stress state condition expected especially in geo-environmental hazard monitoring.

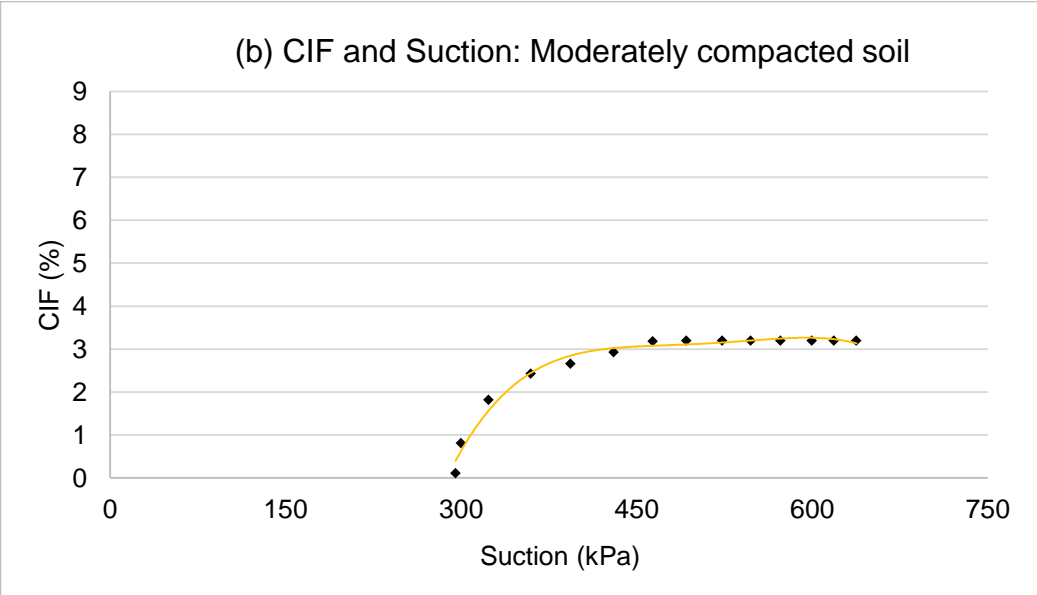
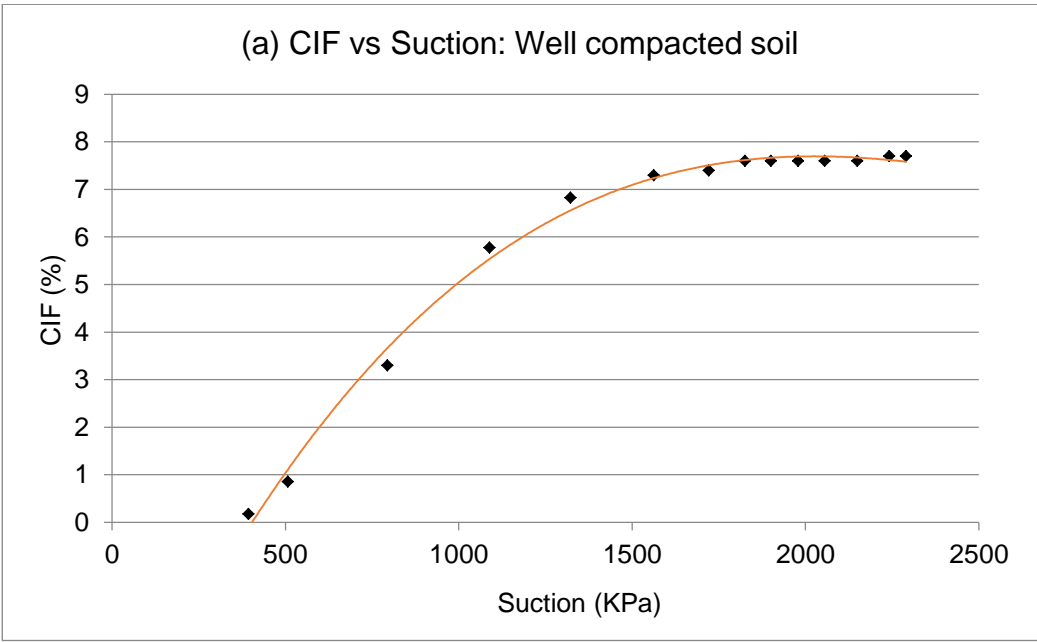
As shown in Figure 4.23, the active stage is more prolonged in the relatively denser soil yet presents a shorter range of moisture loss in Figure 4.25. This infers that the dense soil structure inhibits moisture loss likely through decreased permeability. Despite this behaviour, the CIF is much lower in the high density soil, which suggests that fabric geometry hence the mechanical property, is a limiting factor in the cracking. This is quite instructive regarding the placement condition of embankment fills to inhibit potential for cracking.

#### **4.4.3 *Moisture changes in steady stage of crack development***

It is expected that as moisture is lost from the soil, the air above it gradually become saturated and this will slow further evaporation. Many workers have consider these dynamics as typically representing the later stage of crack development where the soil profile becomes mechanically stable relative to limit of moisture loss, and cracking does not show any reasonable changes. However, the design of the present climate control system is not expected to present a steady increase in humidity above the soil during the desiccation. This is because the evaporated water would be evacuated from the atmospheric cover through the outlet hole (Figure 3.10), which is more representative of a natural environment affected by dynamic wind turbulence. This is notwithstanding the humidity gradient recorded in the atmospheric chamber, which essentially drives the

evaporation. In the present experimental set up, the air above the soil is not completely saturated. The equilibrium condition in moisture loss here is therefore considered as an effect of absorbed moisture, which the dry soil at this stage would essentially approach. The moisture at this stage will become increasingly difficult to mobilise as large suction develops in the relatively drier state. The soil water is now occurring as the tightly held residual water at the smaller pores. From this observation, it is reasonable to assume that the magnitude of suction do not necessary translate to magnitude of cracking.

Although full moisture equilibration was not attained during the desiccation experiment due to time constraint, it has been established that the stage where moisture began to equilibrate reasonably approximates the shrinkage limits of the soil (Miller *et al.*, 1998; Tang *et al.*, 2011a; Khan and Azam, 2017). Suction at this stage can only mobilize very little water now restricted to the effective small pores, hence the volume change is slowed as suction reduces. This can explain the corresponding approach to a steady state in the crack development since with no further shrinkage, stress in the soil is normalised with net zero strain. Coupled with common observations of crack initiation at full saturation, workers have hypothesized that active cracking in soil occurs at relatively low suction (Miller *et al.*, 1998; Péron *et al.*, 2009b). The results of this study can further validate this hypothesis. In the well compacted soil for instance, estimated suction was nearly 5,000kPa at the end of desiccation, but the corresponding CIF does not change significantly after 1,500kPa, 450kPa and 250kPa as shown in Figure 4.29 for the poorly compacted, intermediate compacted and well compacted soils respectively.



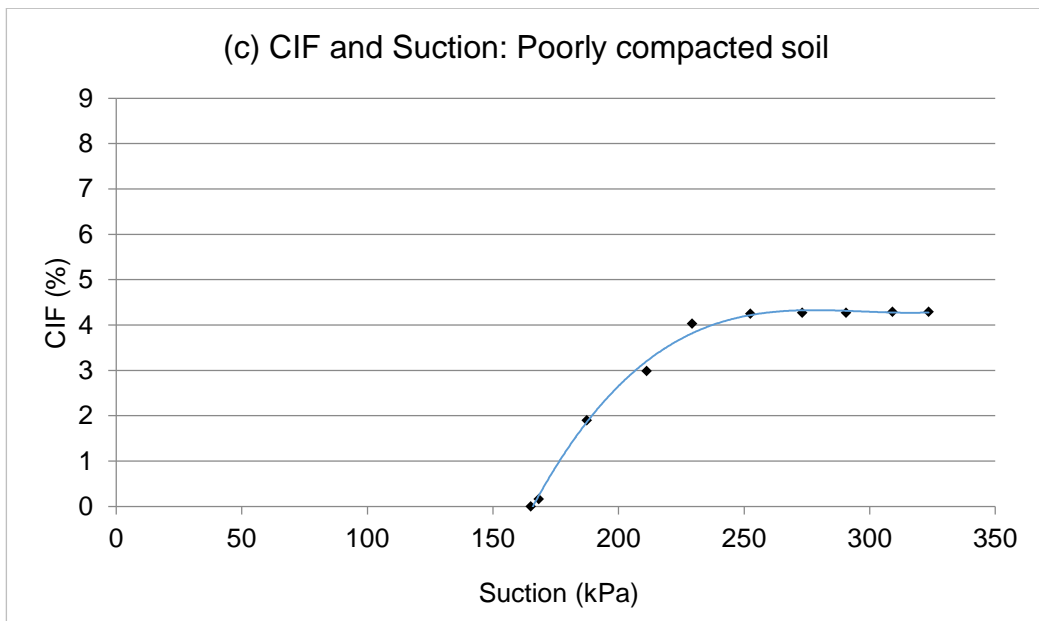


Figure 4.29: Laboratory measured suction in compacted soils during crack formation

The trends were derived by extrapolating suction records at corresponding times with respective CIF. While cracking occurred intensively within a narrow range of moisture change, suction occasioned by this change is significantly larger. This is typical of the SWRC of clay soils, a function which arises from the large surface area of the clay particles with which greater capillary tension can develop for any small change in moisture.

Generally, crack development at the stable stage is characterised by an increase in geometry of the existing cracks. This can be seen in the graphical relationship between total number of crack initiated and CIF shown in Figure 4.30.

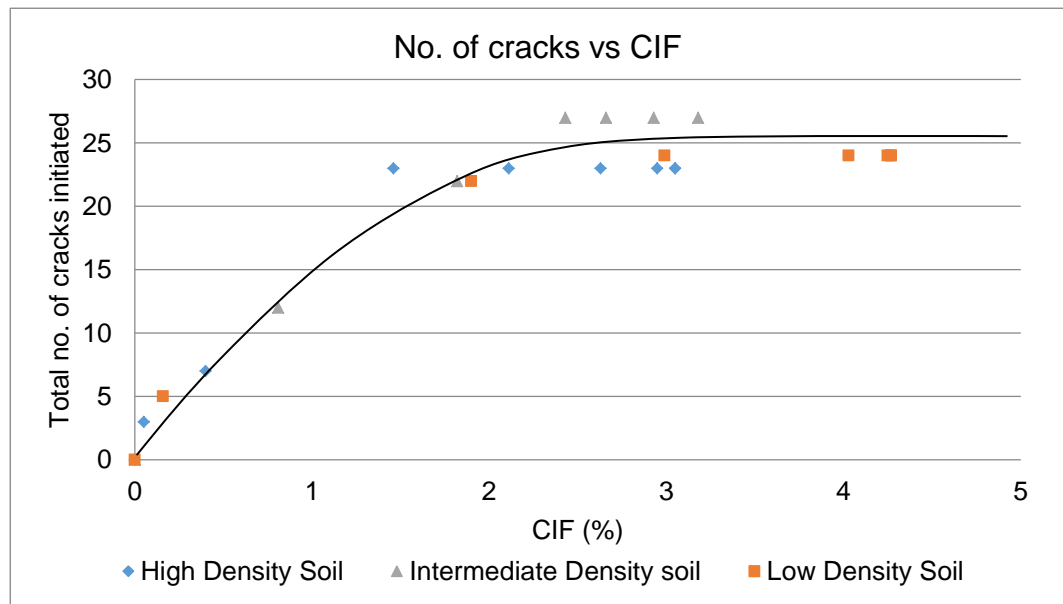


Figure 4.30: Effect of total number of cracks on CIF

Initiation of new cracks contributed to the CIF mainly in the first half of the profile. The second half shows the total number of cracks remains constant as CIF increases further, which implies the influence of the number of cracks becomes insignificant in the CIF at the later stage. Comparatively, average crack length and crack width recorded continue to increase when the initiation of new cracks had ceased. This implies that the CIF in the later stage of crack development mainly resulted from increases in length and width of the existing cracks. In the field, the crack geometry was also observed to increase in width and depth towards the end of summer and new cracks were not observed during this period. Overall, the stages of crack development implies a limiting moisture condition exist for crack initiation and propagation in soil.

#### 4.4.4 **Critical cracking moisture and suction in soil**

Syntheses of crack intensity in the drying soils reveals two hydrologic boundaries in the crack formation, which can be related to critical moisture conditions in the soil specimens. These are the moisture content in the soil when the cracks first initiated and the equilibrium moisture content when the crack development transits to the stable state. In this study, these critical boundaries are referred to as the crack initiation moisture (CIM) and the residual cracking moisture (RCM) respectively. The CIM was determined by back-calculating the moisture content corresponding to the

time of crack initiation using moisture loss records. In the engineered soil tests involving Nafferton clay, moulding moistures were controlled at 22.7+/- 0.2% and crack initiations were observed under one hour after desiccation with less than 1% loss in moisture. This therefore gave rise to approximately the same crack initiation moisture almost corresponding to the moulding moisture. The near instantaneous cracking, which occurred as desiccation commenced can be attributed to significant soil suction expected in unsaturated soil conditions which the specimens depict. However, cracks initiation was relatively faster from the high to low density soil specimens.

The RCM on the other hand was determined at a later stage of desiccation when the CIF values began to equilibrate. This was estimated graphically at the meeting point of tangent lines defining the change in slope between the active and stable phase of cracking as shown in Figure 4.31.

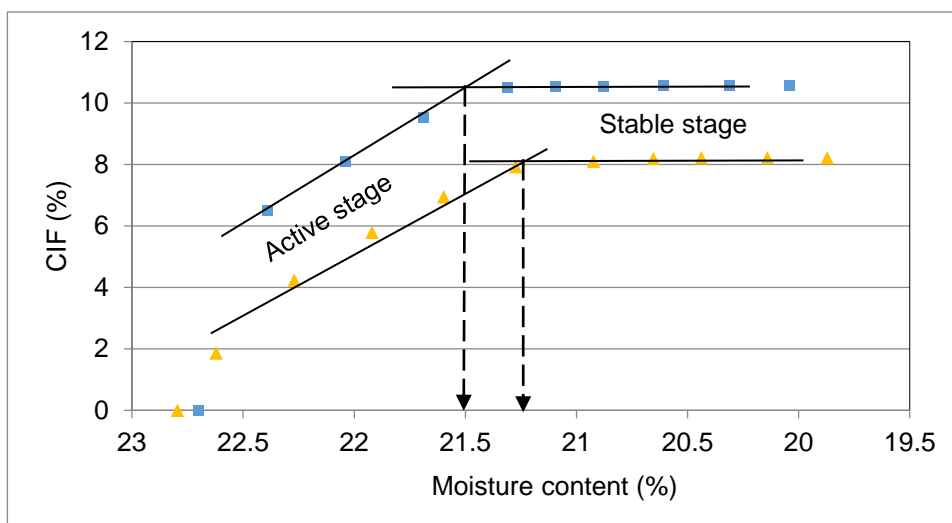


Figure 4.31: Estimation of the residual moisture for cracking (RCM)

Soil suctions corresponding to the two critical moisture conditions were also determined using the SWRC of the soil material. Accordingly, these are referred to as the crack initiation suction (CIS) and residual cracking suction (RCS) respectively, and were estimated from the individual suction profile using the same procedure as CIM and RCM. Crack initiation suction for the low density soil ( $1.34\text{Mg/m}^3$ ) is about 165kPa while for the high density soil ( $1.62\text{Mg/m}^3$ ) is nearly 400kPa. The values were estimated from the laboratory derived SWRC using soil moisture data of first drying

cycle test whose state is considered more approximating to natural slope. Despite the significant difference in the suctions estimated at crack initiation in the respective engineered conditions, the corresponding moisture contents were nearly the same. This may suggest that the volume of moisture in the soil is an important condition for cracking. A summary of the critical hydrologic conditions identified in cracks development in the engineered soil is shown in Table 4.2.

Table 4.2: Summary of hydrologic conditions for cracking

	Hydrologic Conditions			
<b>Engineered condition</b>	<b>CIM (%)</b>	<b>RCM (%)</b>	<b>CIS (kPa)</b>	<b>RCS (kPa)</b>
1.34Mg/m <sup>3</sup>	22.7	21.5	165	222
1.51Mg/m <sup>3</sup>	22.40	21.3	304	400
1.62Mg/m <sup>3</sup>	22.80	21.8	393	540

The values reasonably compare with field and laboratory moisture and suction reported by Dyer *et al.* (2007) during cracking in related plastic materials. Following same principles explained in section 4.2, a lower pore water pressure (negative) or higher suction is generated in the reduced pore sizes of the well compacted soil at any given moisture change condition. As earlier presented, cracks developed in the soils within a narrow range of moisture and suction, within 10% of the total duration of desiccation. In practical terms, this suggests that significant cracking can occur in the field when drying is intense and soil moisture reduces to the critical state. For example, after initiation, accelerated development in the crack geometry was recorded in the embankment within a brief period of sustained drying i.e. no significant rainfall between July and September 2014 (Figure 4.18 and Figure 4.19). Subsequently, the maximum geometry attained remains constant until a significant closure began with regular autumn rains. The effect of the later condition also reflected in the hydrology response i.e. a decrease in suction with increase soil moisture.

The recognition of these critical hydrologic boundaries involved in crack development can be useful in assessing the limiting conditions for cracking in slopes. Under this consideration, the crack initiation moisture

approximates moisture conditions between wet of optimum and the plastic limit, which formed the initial state of the soils. Similarly, (Miller *et al.*, 1998) also suggested that a possible relationship may exist between the stable state of cracking and the shrinkage limit.

Climate projections for the UK suggest warmer and more prolonged summers in the future. This may lead to significant moisture loss by evapotranspiration. Under such intensive drying condition, a significant soil moisture deficit can occur. Embankments constructed wet of optimum would dry considerably with potential for sustained critical condition for cracking defined in this study. For slopes constructed at or below optimum i.e. drier condition, cracking can occur instantaneously. However, the cracks, in this case, may not develop considerably as the critical cracking moisture boundary observed for active cracking would be potentially restricted being small in range. Dyer *et al.*, (2007), also reported the tendency of reduced cracking under low soil moisture following the observation of increases in the critical cracking ratio when samples are laid in drier conditions. The critical cracking ratio is a geometric factor defined as the ratio of the diameter to the depth of the sample at which only one crack extends from edge to edge when fully dried under laboratory conditions. Higher ratios therefore indicate less cracking and vice versa.

Cracking in the soils slowed down as moisture content approached the shrinkage limit. However, it is not clear how much of the measured suction translate into actual soil cracking (tensile strength was not in the scope of this study and its measurement is not straightforward). Since soil moisture can be more easily measured in the field than suction, knowledge of the crack initiation moisture for a slope material can be used to monitor the hydrology condition prior to cracking. However, the relationship between the cracking moistures and soil consistency limits or optimum moisture content requires a validation in other soil materials, which is an area of further investigation in this genre.

#### **4.4.5 *Properties of cracks under cyclic moisture behaviour in soil***

Crack development in the laboratory specimens were also monitored under repeated wetting and drying cycles to specifically understand the effect of this process that could not be quantify in the field. The different conditions of embankment construction simulated with the Nafferton clay specimen where first tested under 2-cycles of wetting and drying. Then in a separate test, the well compacted model was subjected to six cycles of wetting and drying in order to appraise contemporary issues surrounding improved embankment construction methods under multiple wetting and drying conditions. In both the 2- and 6-cycle tests, the desiccation curves gradually vary for each successive phase of wetting and drying. As noted earlier in section 4.2.1, the changes in corresponding phases between the engineered characteristics manifest in the rate of moisture loss, which understandably is greater in the loosely packed soil condition. Desiccation curves obtained from the 2-cycle record of moisture loss in each of the compaction conditions are presented in Figure 4.32.

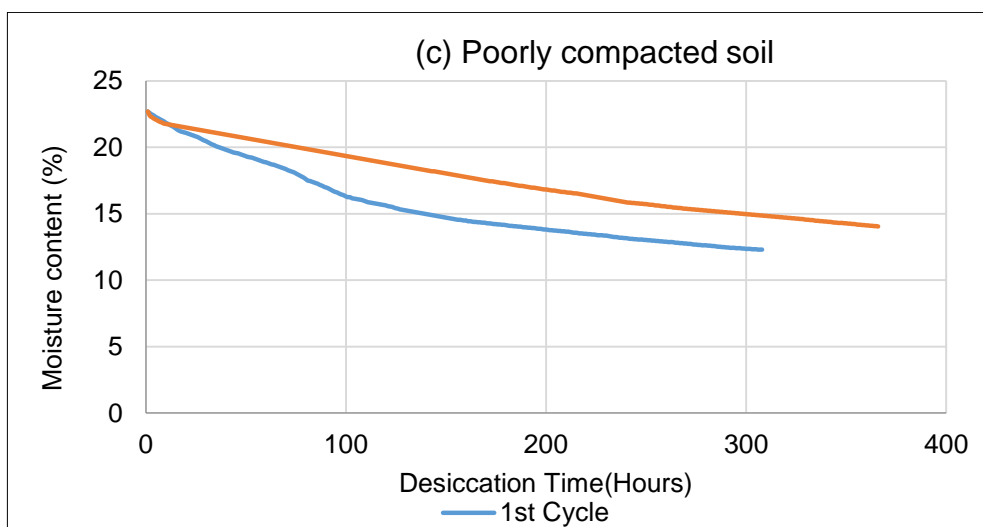
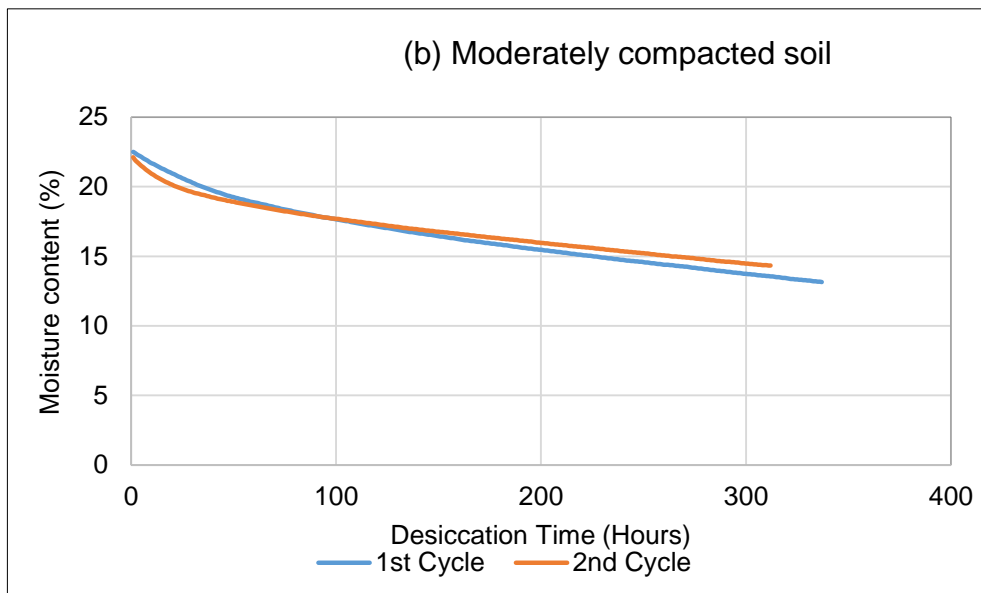
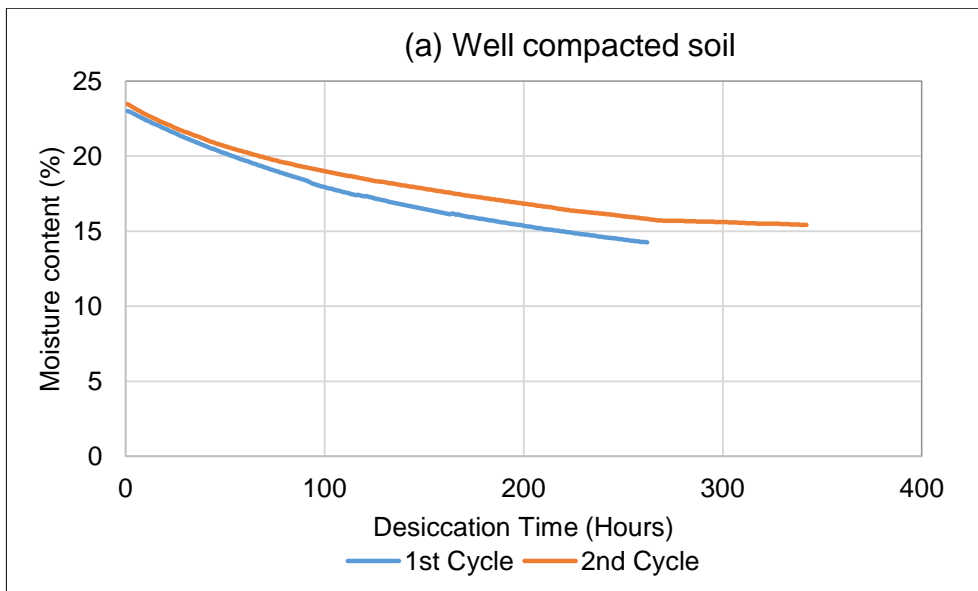


Figure 4.32: Profiles of moisture loss in 2-wetting and drying cycle (a) well compacted soil (b) moderately compacted soil (c) poorly compacted soil

Comparing profiles of individual engineered condition, the rate of desiccation is relatively slower in the 2<sup>nd</sup> cycle as its profile plots above the profile of the 1<sup>st</sup> cycle. Since other test conditions remained constant e.g. environmental condition, soil type, these differences would arise from the state of moisture distribution between the cycles in each engineered condition. The first wet condition before commencement of drying (1<sup>st</sup> cycle) results from a relatively uniform moisture mix prior to compaction whereas the 2<sup>nd</sup> wet condition results from infiltration of water poured directly on the dried soil to simulate rainfall inundation on the embankment. During rewetting, the flooded water gradually infiltrates the upper layer preferentially through the cracks and shrunken sides between the box and the soil. It was expected that this would result in a new state of moisture distribution in the second cycle, which was less homogeneous due to differential wetting of soil layers and infiltration in cracks formed after the first drying cycle. A dissection of a rewetted soil block in one of the tests showed that even after the 12 hours allowed for moisture equilibrate in the soil, the soil block still displayed significant wetting variation with the top and bottom layer appearing wetter than the mid-section. By-pass wetting of subsurface soil is primarily caused by cracks (Stirling, 2014).

Considering the different moisture state likely between the cycles, it was therefore expected that in the 1<sup>st</sup> cycle, moisture essentially mobilise relatively freely from the bottom of the soil block to recharge the lower potential caused by greater evaporation at the surface. In the 2<sup>nd</sup> cycle on the other hand, the drier layers and/or particles occurring at the mid-section would cause a delay in the upward moisture diffusion, hence the slower rate of desiccation. In this case, the desiccation proceeded freely in the early stage from the relatively wet top of the soil resulting in a comparative rate with the 1<sup>st</sup> cycle profile at this stage. Then, as this surface moisture depletes, it would take a longer time to by-pass moisture from the bottom across the dry area sandwiched in the middle of the soil profile. The result is a slower rate of desiccation immediately following the initial stage, hence the profile of the 2<sup>nd</sup> cycle of drying trends above the 1<sup>st</sup> cycle in all the compacted conditions (Figure 4.32).

A broader understanding of the cyclic moisture response in soil was derived from the 6-cycle test, which was simulated to represent more closely the multiple cycles of wetting and drying obtained in the field. Each cycle was desiccated within three to four days before re-wetted for the next drying. This represents alternate dry and wet weather conditions i.e. sunshine and rainfall. As shown in Figure 4.33, desiccation profiles of each cycle also vary, with successive cycles presenting increasingly complex profiles.

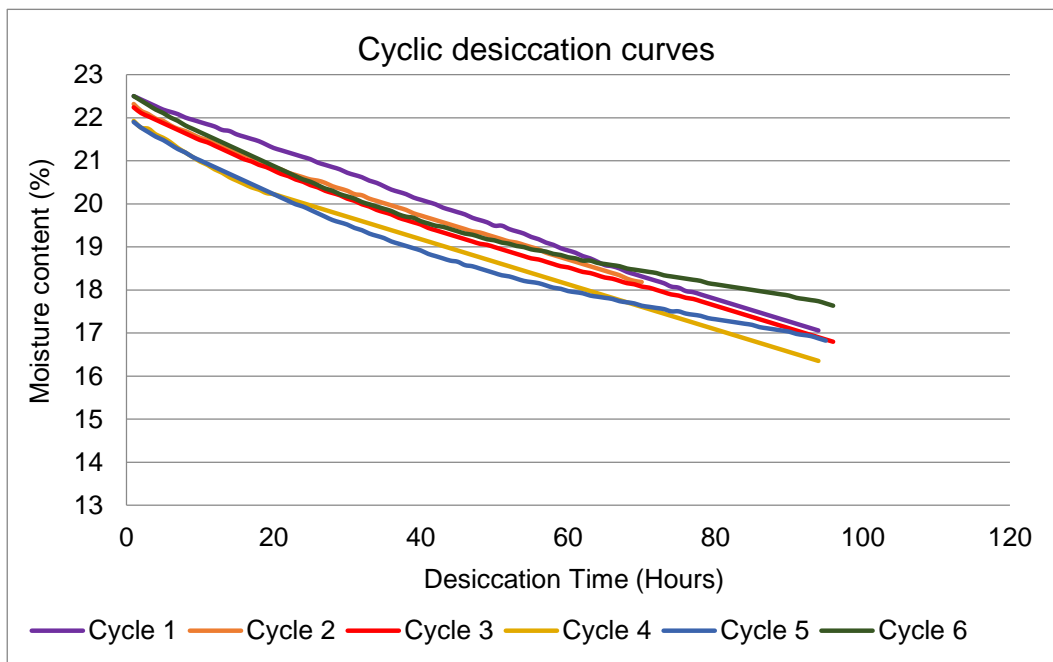


Figure 4.33: Moisture profiles in the 6-cycle of wetting and drying test

Generally, the trend of desiccation of each cycle follow the common pattern of exponential decrease with the rate of decay becoming increasingly pronounced as the cycle number increases. The 1<sup>st</sup> cycle desiccated throughout at a near constant rate while subsequent cycles display enhanced desiccation at the initial hours of desiccation. This gradually decreased as depicted by a gentle change in slope commonly between 15-20 hours. However, the soil specimen seems to present an overall increase in rate of desiccation with successive cycle up to the third and fourth cycle. Thereafter, the trend began to display a comparatively slower rate. This is indicated by the sharp upward turn in the desiccation curve of the last two cycles (5 and 6). Although the short wetting and drying intervals applied in this test does not present moisture loss profiles long enough to compare with profiles of the 2-cycle tests, the dynamics of

soil-water-suction still applies. The short duration of desiccations in this case result in a small amount of moisture loss per cycle. A re-introduction of the equivalent amount of water loss does not wet the entire soil layer. Consequently, wetting in the initial cycles is restricted to a thin layer at the soil surface. This layer therefore becomes available moisture pool, which enhanced evaporation as depicted by a faster desiccation trend exhibited from cycle 1 to 4 approximately. As rewetting episodes continues, moisture increasingly penetrates deeper in the soil whose structure would have changed, including cracking in previous wetting and drying. A change in the moisture behaviour therefore occurs after the 4<sup>th</sup> cycle with profiles of the later cycles trending relatively slower. Moisture profile of the 5<sup>th</sup> cycle in particular initially approximates that of the preceding 4<sup>th</sup> cycle but subsequently slowed above the later. Following this reversed trend, the desiccation curve of the 6<sup>th</sup> cycle jumped back significantly into a much slower trend. It is therefore reasonable to presume that further cycles would tend towards the initial desiccation trend of this test, which agrees with the desiccation trend of the 2-cycle test presented earlier in Figure 4.32 where rewetting lead to reduction in the rate of moisture decay. However, the different moisture loss behaviour displayed by the short interval of wetting and drying in the 6 cycle test can suggest that different intensity of environmental impact could show varying response in the same soil conditions with implication for different behaviour of cracking. This suggests the need for regular field monitoring to update weather-related slope process in geotechnical practice.

The trend of moisture loss exhibited in successive cycles of drying and wetting also presents a corresponding sequence of cracking. Generally, cracks were more in numbers and increased geometrically in the second cycle leading to higher CIF than in the first cycle. Figure 4.34 shows a range of crack width and length compared in the 2-cycle test conducted in this study.

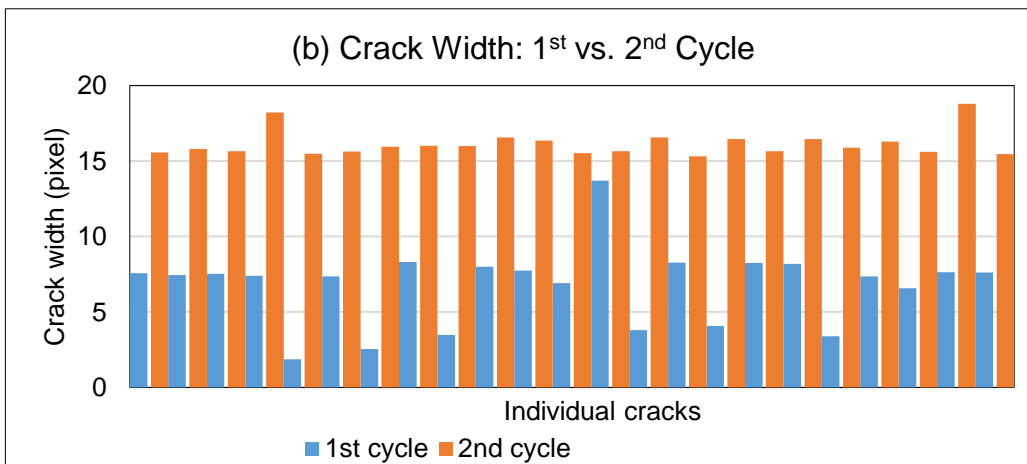
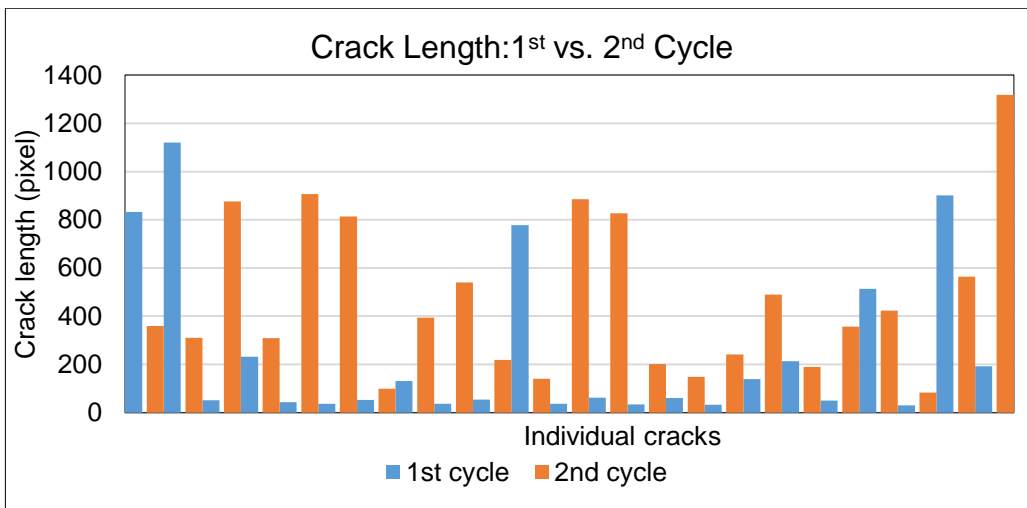


Figure 4.34: Comparison of cracks parameter in a 2-desiccation test (a) Length (b) width

Although the image analysis results were not tabulated for a corresponding set of cracks since the crack pattern often changes, overall the ranges of maximum length and width are higher in the second cycle. The difference is more pronounced with the crack width which is nearly double in the second cycle, and therefore significantly contribute to the estimated CIF.

The CIF analysis showed a general trend of increasing potential of cracking with repeated wetting and drying. This is because soil expectedly disaggregate and would exhibit a low bond energy when wetted (Tang *et al.*, 2011a). This is in addition to the presence of previous cracks formed during the first drying. The latter constitutes a structural discontinuities which degrade the soil mass. Consequently, after the wetting and drying induced shrink-swell process, the soil would possess low cohesion with a general reduction in overall soil strength, a process significant in climate-

induced deterioration of infrastructure slopes (Stirling *et al.*, 2017). The weak inter-aggregate bonds created between the disintegrated clay particles can enable suction related strain energy in the soil to be released with greater ease leading to a higher potential for cracking. Figure 4.35 shows results of crack intensity in the multiple wetting and drying test.

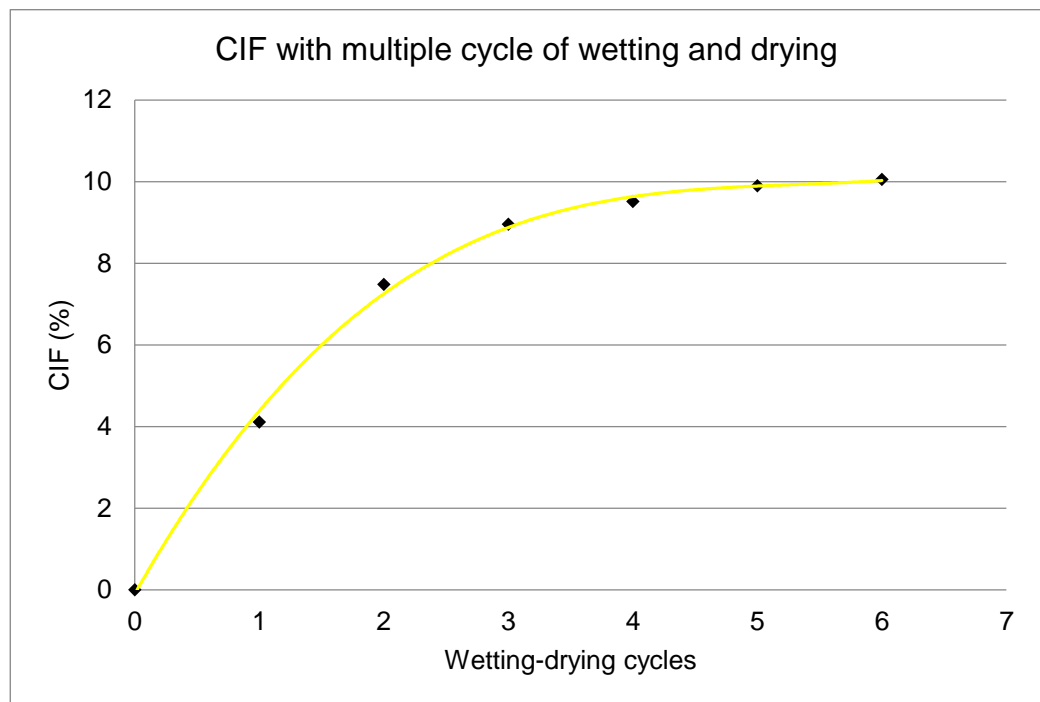


Figure 4.35: Change in crack intensity with increasing cycles of wetting and drying

Clearly, cracking in the soil specimen increases gradually from the first cycle. The increase is sharp in the 1<sup>st</sup> three cycles covering a greater percentage of the crack intensity developed. However, the intensity of cracking tends to decrease and gradually equilibrate after the 3<sup>rd</sup> cycle as shown here. This is of interest as it is likely that a reduction in cracking potential or material resistance to tensile stress is developed in the soil in later cycles of wetting and drying. Contemporary debate among scholars seeks to determine whether a soil can retain aggregate stability under cyclic conditions. The cracking characteristics showed here, which directly result from multiple shrink-swell action in the clay soil can contribute to this understanding.

The existing hypothesis of wetting induced inter-aggregate disintegration can support a fully saturated soil system. In this case, the breakdown may be total and irreversible. However, under unsaturated condition as

presented in most embankments, different structural behaviour controlled by suction is likely to dominate. The wet soil loses its strength initially and at the same time, gradual structural changes take place through aggregate coalescence without a complete disintegration often associated with flooded surfaces. Essentially, the clay soil under unsaturated conditions results in enhanced aggregate cohesion by capillary forces. In this analysis, it is considered that the coalescence gradually rebuilds stronger interparticle bonds in successive drying until the effect of wetting collapse is no more visible. In Figure 4.35, cracking significantly reduces after the 3<sup>rd</sup> drying cycle. In the moisture profile, a significant reversal of desiccation was observed around cycle 4. Since the soil mass under test remained constant, the change can be considered to arise from a significant structural rearrangement. Visual observation of the crack images from the 4<sup>th</sup> cycle indicate that cracks increasingly display different patterns and fewer although they are relatively wider, which largely accounts for the CIF obtained (Figure 4.36).

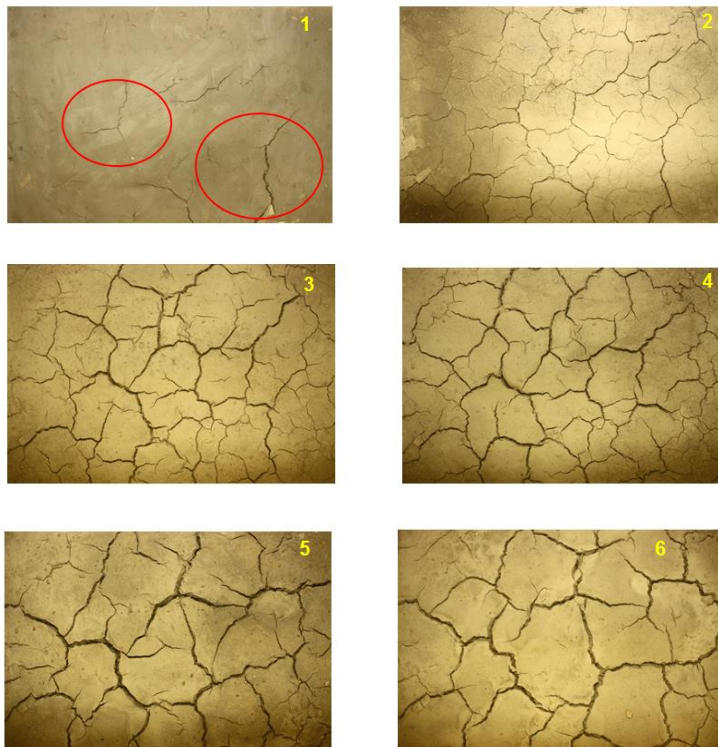


Figure 4.36: Final crack patterns in 6 progressive cycles of wetting and drying in the soil (number of cycle shown at top right corners)

Considering the trend of moisture loss profile and the CIF presented for the multiple cycle test (Figure 4.33 and Figure 4.35), the 3<sup>rd</sup> cycle can be

consider as the transition that marks the beginning of a stable soil structure as wetting and drying progresses in the soil. It is believed here that in the later cycles (5 and 6), the wetting would have caused a significant disaggregation of the clay particles and upon this would coalesce into a strong bond during the drying phase. In addition, the soil is likely to have a profile of particle gradation with the fine particles dispersing during the previous wetting settling at the top to form a dry crust surface. The stiff structure attained by the soil at the later drying cycle can strongly resist strain deformation, leading to the reduced cracking observed. The few cracks that initiate upon further wetting would tend to exploit the relatively weaker layer of fines to propagate rather laterally hence wider cracks in 5<sup>th</sup> and 6<sup>th</sup> cycle. This is also supported the relatively constant crack depth measured at the end of the 6<sup>th</sup> cycle despite the increased width (Table 4.3). The crack widths also tend to correlate with crack depth in the active cracking cycles. Overall, the change in crack intensity is largest in the 2<sup>nd</sup> cycle as particles bonding intensify by increased disaggregation.

Table 4.3: Crack geometric properties in multiple cycles of wetting and drying

Cycle	CIF (%)	Change in CIF (%)	Average width (mm)	Average depth (mm)
1	4.11	-	1	20
2	7.48	82	2	30
3	8.95	20	3	50
4	9.51	11	3	50
5	9.89	2	4	50
6	10.05	-	5	50

#### 4.4.6 *Rate of desiccation and residual moisture*

From the results presented in this study, it is clear that cracking occurred in the soils as they lost moisture. The action directly correlates with the soil water suction, which essentially generates the strain energy within the soil skeleton for crack initiation and propagation. The difference in the moisture response as well as associated suction manifests in the rate at which moisture is lost in each of the engineered characteristics tested.

Generally, moisture loss presented in this study shows exponential decay function, which means moisture in the soil layer decreased with time of drying until an equilibrium state is reached. The trend commonly changes from a rapid decay at the beginning to moderate and then gradually slowing towards the equilibrium state. The developed cracks on the other hand present an exponential growth, which occurs within critical moisture boundaries. This is because cracking in soil is a function of the soil strength, a parameter that generally increases as moisture reduces in clay soil. Therefore, a consideration of the rate of desiccation can help to summarise the mechanism of cracking in embankment soil for any prevailing environmental conditions.

Consider a hypothetical exponential graph given in Figure 4.37. Mathematically, an exponential curve can be represented by the equation inserted where  $a$  is any initial value when  $x = 0$ , and  $b$  is any real number which can be greater than or equal to 1.

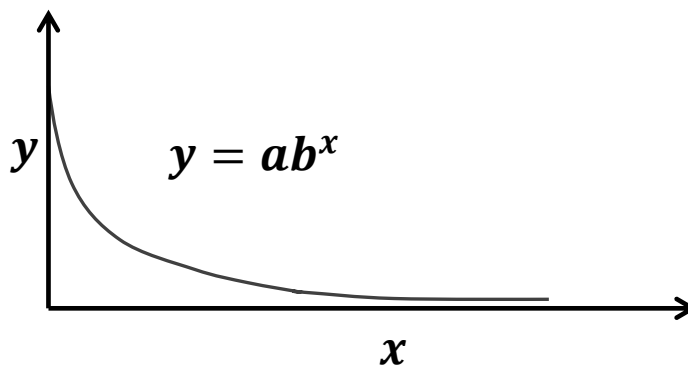


Figure 4.37 An exponential graph

For exponential decay function,  $b < 1$  while for exponential growth which is a reflected decay function,  $b > 1$  implying a negative and positive power of exponent respectively. However, since exponential graphs decay or grow at various rates along the profile, a constant of proportionality,  $r$  is normally introduced to define this rate of change. Hence, the above expression can be written as:

$$y = ab^{-rx} \quad \text{For the exponential decay} \quad 4.1$$

$$y = ab^{rx} \quad \text{For the exponential growth} \quad 4.2$$

Following the method of Nahlawi and Kodikara (2006), the above equation can be apply to analyse the desiccation rate of the profiles obtained from moisture loss records in this study. In this case, the curves can be represented by the general form

$$w = w_i^{-rt} \quad 4.3$$

Where  $w_i$  is the initial moisture condition,  $w$  is the moisture state at any time,  $t$ . The term  $r$  therefore defines the desiccation rate or speed, a dimensionless function whose value can then be express in terms of moisture loss with time as follows:

$$\frac{dw}{dt} = -r(w) \quad 4.4$$

Therefore, the exponent of the equation defining the desiccation curves gives the desiccation rate. A summary of average rate of moisture loss of the soil block for the period of desiccation is presented in Table 4.4.

Table 4.4: Summary of rate of moisture loss in three compacted clay soil

Density	Desiccation rate		Moisture loss (%)	
	1 <sup>st</sup> Cycle	2 <sup>nd</sup> Cycle	1 <sup>st</sup> cycle	2 <sup>nd</sup> cycle
1.34Mg/m <sup>3</sup>	0.0022	0.0019	40.6	31.6
1.51Mg/m <sup>3</sup>	0.0020	0.0019	36	32
1.62Mg/m <sup>3</sup>	0.0019	0.0017	38	32.6

In the 1<sup>st</sup> cycle, the rate of moisture decay is clearly highest in the least dense specimen and decrease toward the densest specimen. This reflects in the percentage of moisture loss calculated from net moisture at the end of 261 hours of desiccation (equivalent drying period of the densest soil). Within this length of desiccation, the loose soil lost an average of 40.6% moisture as against 38% for the densest soil. In the 2<sup>nd</sup> cycle, the rate of desiccation not consistent with the pattern of density as in the 1<sup>st</sup> cycle. The densest soil specimens rather show an increase in average rate of moisture loss. This is attributed to leakages experienced at some stage during rewetting of the specimens. However, the crack occurrence and the

depth of moisture infiltration could also affect the rate of moisture loss in the second cycle with a slow rate likely to occur in the low density soil where deep infiltration would lengthen the distant of evaporation moisture movement. This can be seen in the initial trend in the desiccation profiles in (Figure 4.38). The curves start from different moisture content.

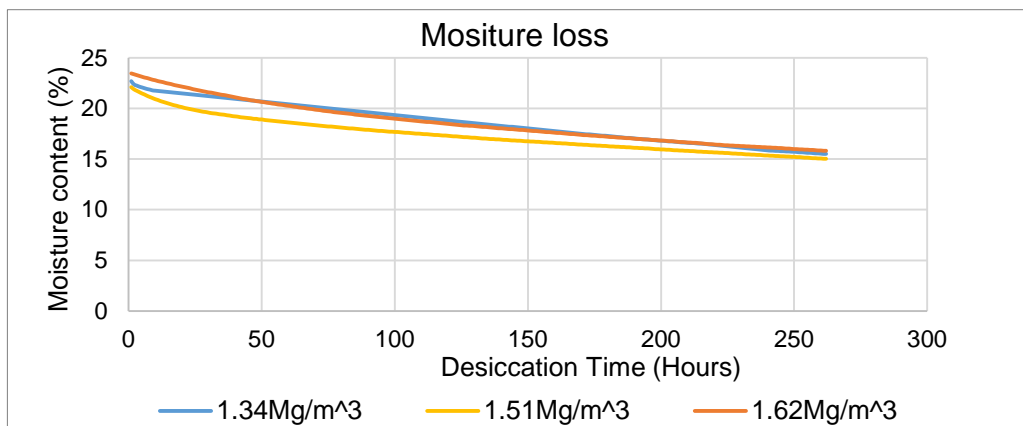


Figure 4.38: Profile of moisture loss in the 2<sup>nd</sup> drying cycle

As moisture saturates the disaggregated soil layers, profiles subsequently begin to reflect the effect of density with the denser representatives tending to slow after 100hrs of desiccation. At the end of desiccation, the densest soil representative is seen slowing over the loose soil counterpart. The profile of the intermediate density is also moving upward. Therefore, the average rate of moisture decay increases with decreasing soil density, which also suggests the role of low permeability. Since cracking occurred within a limited range of moisture change, the initial (antecedent) moisture and desiccation rate can therefore be reasonably considered as more significant factors in the crack development analysis than the residual moisture used by Yesiller *et al.* (2000).

#### 4.5 Summary and conclusion

In this chapter, characteristics of the cracks as hydrologic conditions in the soil changes during desiccation was presented and discussed. The themes of discussion emerged from the finding that both in the field and laboratory cracking significantly occurred in the soil under drying and wetting conditions. The cracks changes in geometry and orientation with time and the changes were holistically quantified using volume of the crack section. Since test variables remained constant, it was reasonable to consider this trend in terms of moisture state in the soil largely affected by

weather-related changes, principally rainfall and temperature. This was further supported by experimental simulation of series of wetting and drying tests. The results presented in this chapter show a close relationship between the profiles of soil moisture and suction with the trend of crack geometric development. On a larger scale, the trend was evident in the relatively drier condition in summer months of 2014 when cracks significantly occurred in the embankment and later close in the winter months. The closed cracks did not re-open throughout 2015.

The different engineered conditions presented distinctive hydrology. The profiles of moisture loss in the poorly compacted and well compacted embankment vary. It was found that this correlated with the trend of crack development quantified in each condition with volumes of cracks reaching about 8,000ml in the poorly compacted panel compared to about 2,000ml, which was the maximum recorded in the well compacted panel. The estimated crack volumes could potentially capture and store significant amount of water, which could affect field capacity. Analysis of the moisture loss record in the laboratory specimens identified the rate of moisture decay in each of the modelled engineered conditions as a key factor resulting in the differences displayed in the respective hydrology profiles. The rate of desiccation was discussed from the context of inter-aggregate structure achievable in the different compaction soil and further identified the role of strength related property in the cracking intensity. Applying the theoretical background of soil water-suction development in a drying unsaturated soil, the pore geometry of the loose soil specimen exhibits hydromechanical conditions with greater potential for shrink-swell deformation. This is because of the higher permeability, hence a greater propensity for moisture fluctuation leading to weak bonds between the particles. This clearly manifested in higher crack intensity in the poorly compacted soil compared to the dense structure of the well compacted soil. Correspondingly, a greater number of cracks occurred in the poorly compacted panel in the field study. In addition, slope geometry including aspect and thickness were shown to affect the moisture regime with the South facing slope and thin soil block both displaying greater rates of moisture loss and concomitantly higher cracking intensities. The critical

factor influencing differences in the hydro-mechanical response of the slope aspect was found to be disparate climate intensity impacted across the slope faces with the dominant south westerly wind of Northeast England. This led to a drier embankment soil layer particularly in the west end of the South facing slope where most of the cracks occurred. In the case of layer thickness test modelled in the laboratory, the rate of moisture loss was greater in the thin soil specimen. This is because the thin layer provides a low gradient for evaporation compared to a thick layer in the same condition of drying. Vegetation cover also contributed to the hydrologic changes with enhanced desiccation and intensified cracking occurring in soil surface without vegetation cover.

However, in all cases of embankment construction method and features considered, cracking in the soil specimens occurred within limited moisture and suction boundaries. These crack initiation moistures were close compare to suction, and led to believe that volume of moisture in the soil is more critical in cracking than the magnitude of suction developed. Monitoring of moisture changes is therefore a potential factor that can be useful in effective management of desiccating clay slope.

In conclusion, the results presented and discussed in this chapter suggest a coupling between hydrologic changes in the near surface soil of the embankment and crack development. This is related to the inter-aggregate response of soil to environmental driven moisture fluctuation. The drying shrinkage in the soil with moisture loss induces soil water suction which is thought to result in a non-uniform tensile stress respond with greater effects likely to occur in the soil with a loose structure. Consequently, more cracks developed in the poorly compacted soil and are intensified by cyclic wetting and drying. The rates of moisture loss significantly affected intensity of cracking thereby presenting a limited boundary of hydrologic conditions for crack development in each engineered condition. In all the tests, the rates of moisture loss were found to be significantly different and were influenced by both external and internal factors related to the embankment. These include soil density, slope aspect, soil thickness, humidity and repeated wetting and drying. The random occurrence and morphology changes (i.e. opening and closing) of desiccation cracks

observed in the embankment suggest a complex behaviour with environmental changes. Such characteristics can affect the behaviour of pore water pressure and shear strength in slopes. The morphological development of cracks therefore needs to be recognised in slope analysis to adequately capture the effects of this dynamic behaviour.

## Chapter 5 Role of material properties in desiccation crack behavior

### 5.1 Introduction

Infrastructure embankments have been constructed using different kinds of soils, mainly depending on local geology. The performance of these structures is highly affected by the response of the fill materials to changes in the environment, especially embankments constructed with clay soil. This is because clay materials changes volume in response to changes to their moisture content. A key property of clay soils, which influences this behaviour, is plasticity. The shrink-swell action involved in desiccation crack development is significantly controlled by plasticity. In this study, three plastic soils representative of common embankment construction fills in the UK were tested for the influence of plasticity in crack development. The soil materials tested are the intermediate plasticity Nafferton clay (from Durham boulder clay), high plasticity Gault clay and VH plasticity clay synthesized with the Bentonite-Nafferton clay mixture. The first material is a common construction material in Northern England while the latter two are dominant construction materials in the southern part of the country (Hughes et al 2009). Results of Atterberg limit tests conducted on the experimental materials are presented in Table 5.1. During the tests, the materials were compacted to approximately the same density, taking into consideration the same procedure used for the well-compacted Nafferton clay.

Table 5.1: Atterberg limits of tested soil materials

<b>Plasticity</b> <b>Soil type</b>	Liquid limit (%)	Plastic limit (%)	Plasticity index (%)
Nafferton clay	42.6	22.5	20.1
Gault clay	64	25	39
VH Plastic clay	72.6	21.3	51.3

The widespread incidence of failures on transport infrastructure across the country suggests the increasing effects of climate in the slope deterioration process. Therefore, serious concerns are raised on long-term

performance of clay-based slopes. This problem is examined in this chapter by assessing the cracking potential of the representative embankment materials. Although results of the laboratory tests are mainly presented here, the discussion nevertheless covers the field response in the case of Nafferton clay due to having access to the embankment.

## **5.2 Influence of plasticity on desiccation behavior of compacted soils**

In Chapter 4, change in hydrologic conditions showed significant influence in the development of cracks. This relationship is further examined in three soil materials whose major property difference is plasticity. In a 2-cycle wetting and drying experiment, the soil specimens exhibited distinctive decreasing trends of moisture content during desiccation and moisture loss trend was slowest in the VH plasticity Clay soil for both 1<sup>st</sup> and 2<sup>nd</sup> cycle of wetting and drying (Figure 5.1).

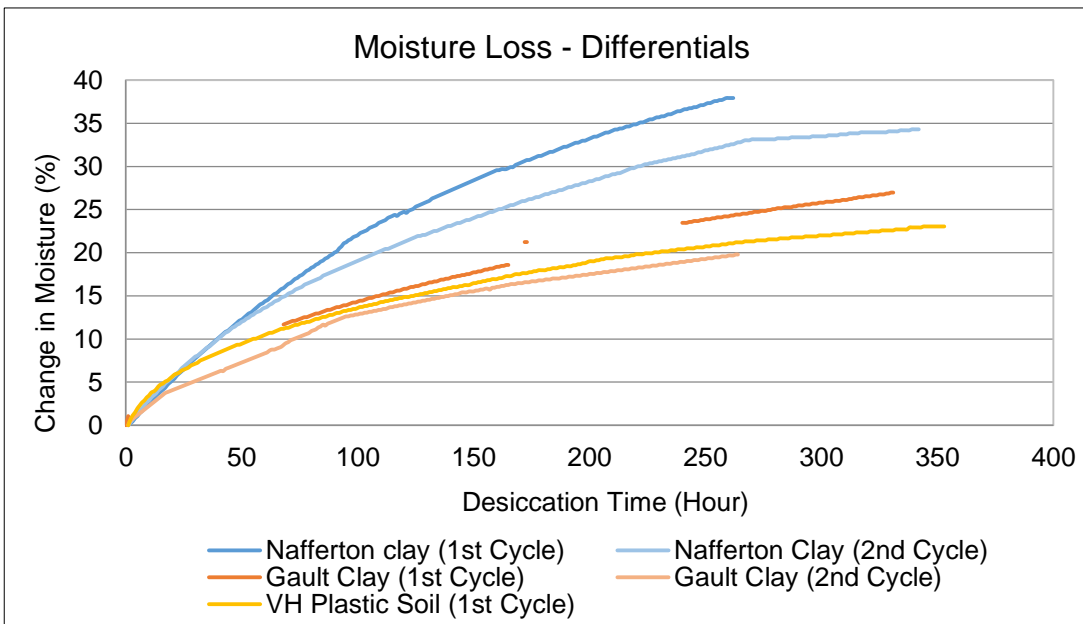
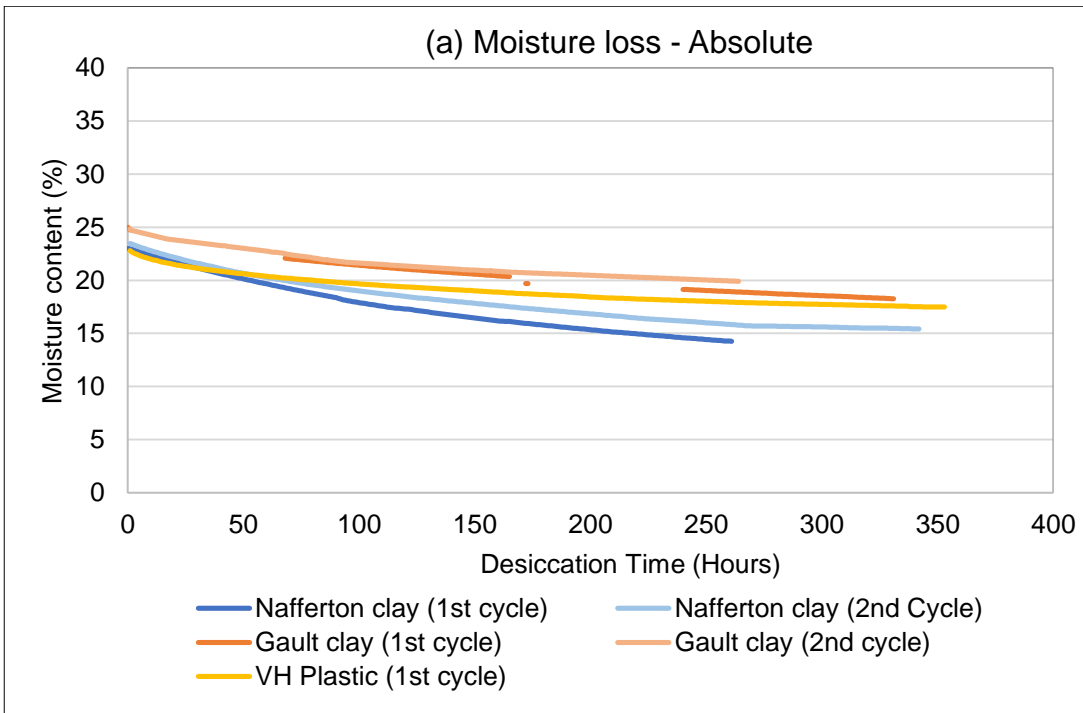


Figure 5.1: Desiccation profiles of three common clay embankment soils in the UK (a) Absolute moisture content (b) Change in moisture

There was an unforeseen problem in data logging during the 2<sup>nd</sup> cycle test with Gault clay and VH plastic soil. The problem was later discovered to be associated with internet connectivity to the PC logger and was subsequently rectified by the University IT staff. Since the soil materials were compacted to approximately the same density, the difference in hydrologic profiles is assumed to arise from their plasticity characteristics. More fundamentally, the difference in water removal rate is likely down to the difference in charge bonding at the different clay mineral surface with

additional influence of pore size/structure change upon differing shrinkage behaviour. To understand the decreasing moisture behaviour during desiccation, absolute moisture content profile (Figure 5.1a) was preferred in this study. Despite starting initially with a rate of moisture loss nearly parallel to the profile of the Gault Clay, profile of the VH plasticity clay material gradually slow as desiccation advances, and is therefore slowest amongst the three. However, same trend is displayed in figure 5.1b plotted in terms of change in moisture. This behaviour was also compare by quantifying the desiccation coefficient i.e. the exponential function of the trend line covering the period of desiccations (Table 5.2). The results suggest a decreasing desiccation rate with increasing plasticity resulting in a strong correlation of  $R^2 \sim 0.91$  (Figure 5.2).

Table 5.2: Summary of desiccation parameters in three plastic soils

Soil Material		Desiccation coefficient		Residual Moisture (%)	
Soil Type	PI (%)	1 <sup>st</sup> cycle	2 <sup>nd</sup> cycle	1 <sup>st</sup> cycle	2 <sup>nd</sup> cycle
Nafferton clay	20.1	0.0019	0.0017	38	32.6
Gault clay	39	0.0018	0.0016	24.31	19.68
VH plastic clay	51.3	0.0016	Not available	21.28	Not available

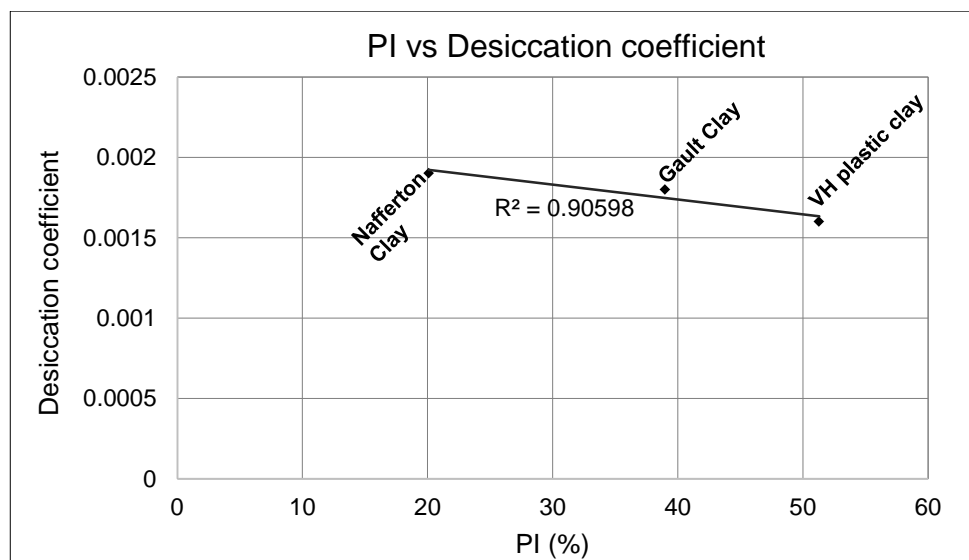
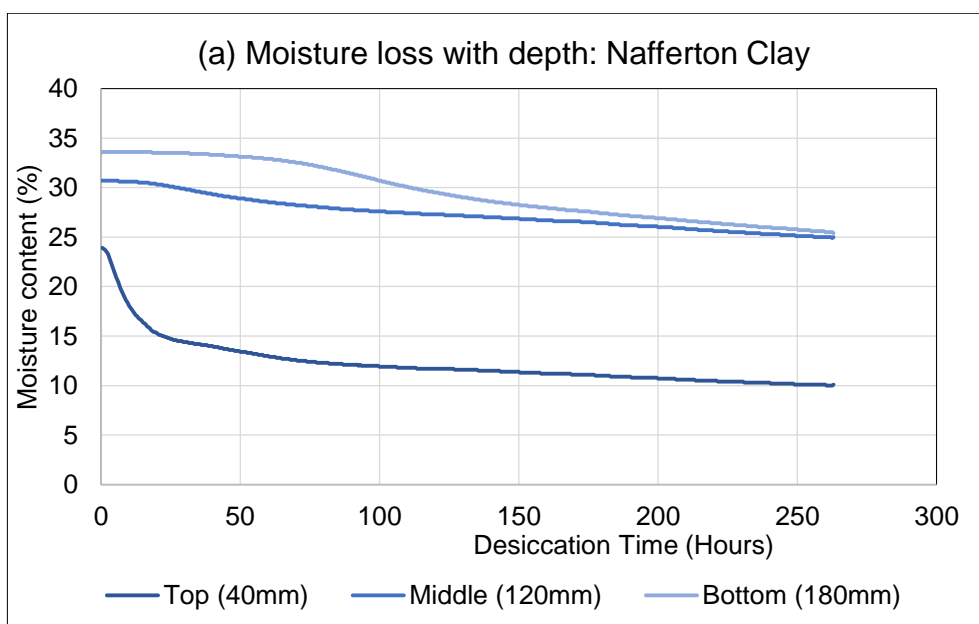


Figure 5.2: The relationship between soil plasticity and the rate of desiccation in compacted plastic soils

The above material responses can be attributed to typical moisture characteristics in fine-grained soils measured by Atterberg limits. The

increasing plasticity would result in a net higher water-retention due to increased hydrophilicity, a phenomenon which is associated with the amount and type of clay in the soil. The stronger affinity to soil water therefore likely in the VH plastic soil and this would slow the rate of moisture diffusion and hence the amount of moisture loss. The literature indicates that a high proportion of montmorillonite dominates in samples of very high plastic London and Gault Clays (Gasparre, 2005; Bell, 2013). Both materials also contain clay in the range of 36 – 60% (Gault Clay) and 40 – 70% (London Clay), depending on weathering condition. Although the clay content was not measured in the simulated VH plasticity clay specimen, the addition of Bentonite, a type of montmorillonite clay was expected to significantly increase the baseline clay content of the original Nafferton material. It is essential to consider this characteristic when selecting material type for earthwork construction in order to moderate the natural response to moisture changes. Expansive soils which have high content of hydrophilic clay are prone to high shrink-swell, hence a greater potential for plastic deformation (Jones and Holtz, 1973; Bell, 2013; Pritchard *et al.*, 2013).

Apart from the overall moisture changes presented above, the soil materials also displayed pronounced moisture gradient behaviour with depth. Figure 5.3 indicates greater moisture loss in the top soil layers (40mm), which gradually decreases to the bottom as recorded by the moisture probes (ML2x Theta probe).



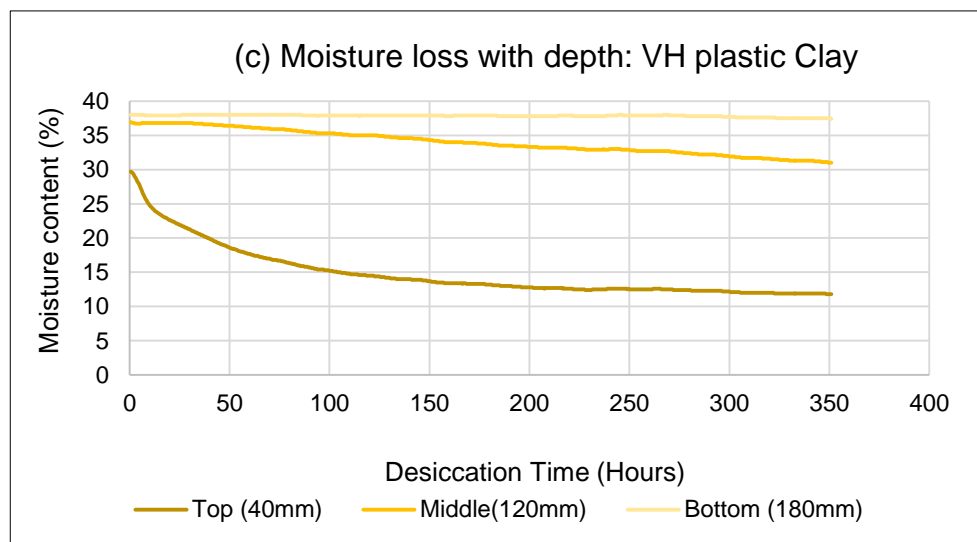
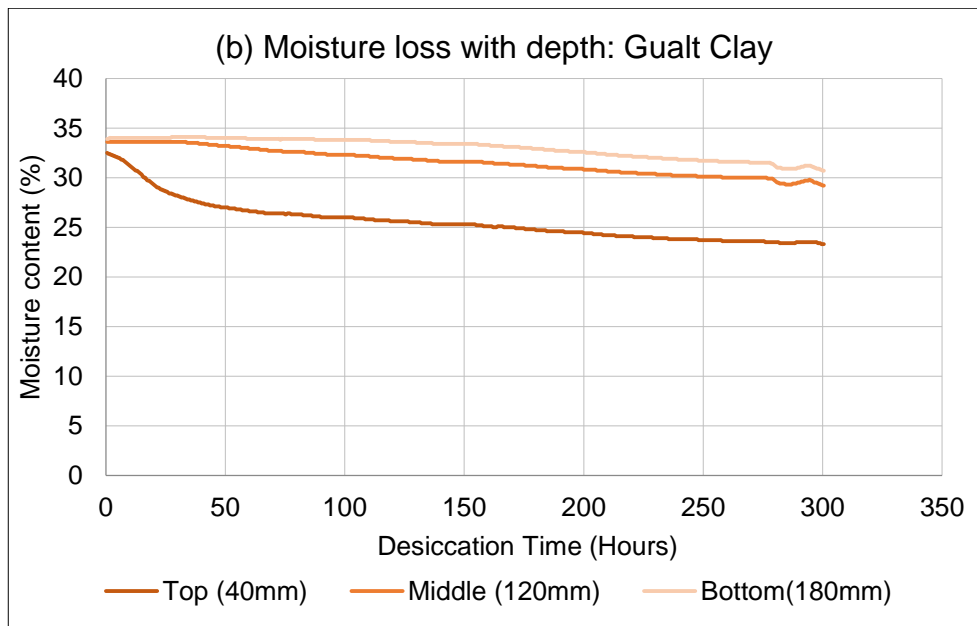


Figure 5.3: Profiles of moisture loss with depth in the plastic soils

Below the top profile, moisture change becomes less pronounced in the higher plasticity materials. This can be seen from the nearly horizontal moisture profiles of the bottom layer in Figure 5.3c. The trend supports the fact that moisture diffusion is relatively slower in plastic materials because of strong interactive forces in the clay layers. The vertical changes in moisture profile also suggest a corresponding suction gradient with important implications for soil profile mechanical variation and crack propagation. Following the dynamics of soil suction changes and cracking discussed in section 4.2.2, a more severe suction gradient over shallow depth e.g. extreme surface drying in dense soil, is likely to result in shallow cracking with a pronounced width and length. In contrast, a gradual suction change over greater depth e.g. pervasive drying in low density soil, may

give rise to increase cracking depth. This is important in the response of unsaturated fills as the hydrology fluctuates.

### 5.2.1 *The role of plasticity in soil-water retention during desiccation*

The movement of moisture in soil is affected by the energy with which the water is held in the pores or bound to solid surfaces. Clay minerals present a physio-chemical and molecular structure that enables them to retain very large amounts of water (Holtz and Kovacs, 1981).

Fundamentally, water in a clay matrix is affected by strong capillary tension and adsorptive force due to their active double layer (large specific surface area) and the exchangeable cations potentials. These forces bind water in the clay soils and can lead to porewater pressure potential falling below atmospheric pressure i.e. a “negative” matrix potential (or matrix suction). Matrix suction therefore defines the energy state of the water held in the pore spaces within the soil. In another sense, the suction can be understood as the equivalent energy required to extract a unit volume of water bound in the soil (Fredlund and Rahardjo, 1993). A difference in suction potential across the drying soil essentially influences water movement in the soil, usually from lower to higher potential. The graphical relationship between soil water content and suction is known as the soil water-retention curve (SWRC). The curve was experimentally determined as presented in Figure 3.19 and Figure 3.20 respectively. The fitted curves are re-presented together in Figure 5.4 to further evaluate the hydrodynamic response of the soils during drying and cracking.

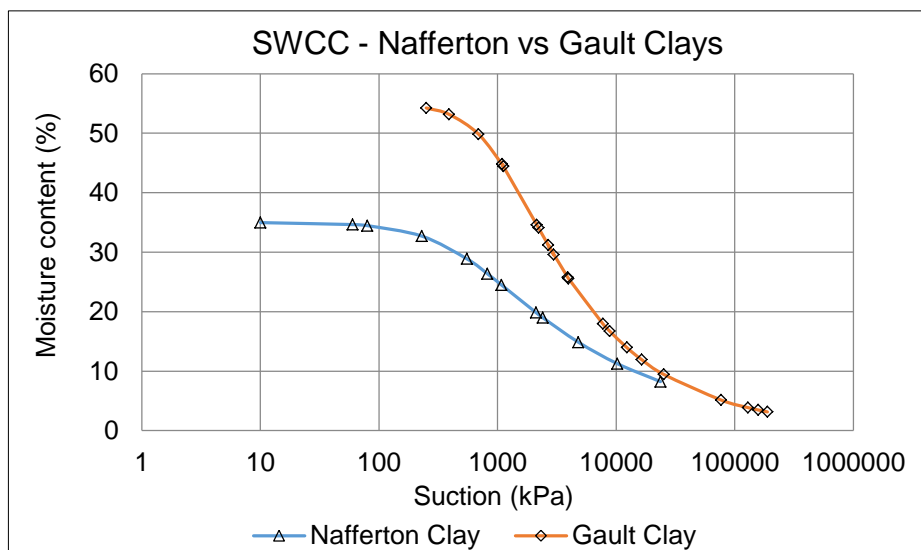


Figure 5.4: Soil water-retention behaviour of the plastic soils

An important engineering implication captured by the soil water retention behaviour of soils is that the amount of water existing in the soil for an equilibrium state is a function of the soil suction. Comparing the two curves above, the high plasticity Gault Clay shows higher moisture retention for any given value of soil suction compared to the intermediate plasticity Nafferton Clay. Following this trend, it is reasonable to assume that the VH plasticity specimen would have the highest water retention among the three soils. Generally, as the amount and type of fines increases in soil, the matrix suction would increase due to an increased potential of specific surfaces for soil water to interact. It implies that a given amount of water is held by large suction in high plasticity soils structure. Accordingly, clay soils have higher moisture affinity than sand and silt while montmorillonite clay is more hydrophilic than kaolinite clay. Similarly, Bell (2013) noted that a poorly crystalline kaolinite clay with small particle size can result in higher plasticity than a relatively coarse and well-organised particles. This also means that higher potential energy is required to mobilize or release the interparticle water with implications on the restriction of moisture movement as plasticity increases.

### **5.2.2 Suction development in drying plastic soils**

The development of soil suction during drying can be considered as an increasing hydrological stress state with a net effect on the soil skeleton. Among the different compaction conditions presented earlier in section 4.2.2, soil suction increased in the drying soil specimens of the well compacted soil as a result of higher density achieved. This also produced a net mechanical effect in terms of higher crack intensity than in the low-density poorly compacted soil. In the present Chapter, initial density remains constant. Therefore, the crack mechanism is characterised in terms of the effect of soil plasticity. Using volumetric moisture content probe records and suction values estimated from the respective SWRC, the suction develop with depth is presented in Figure 5.5.

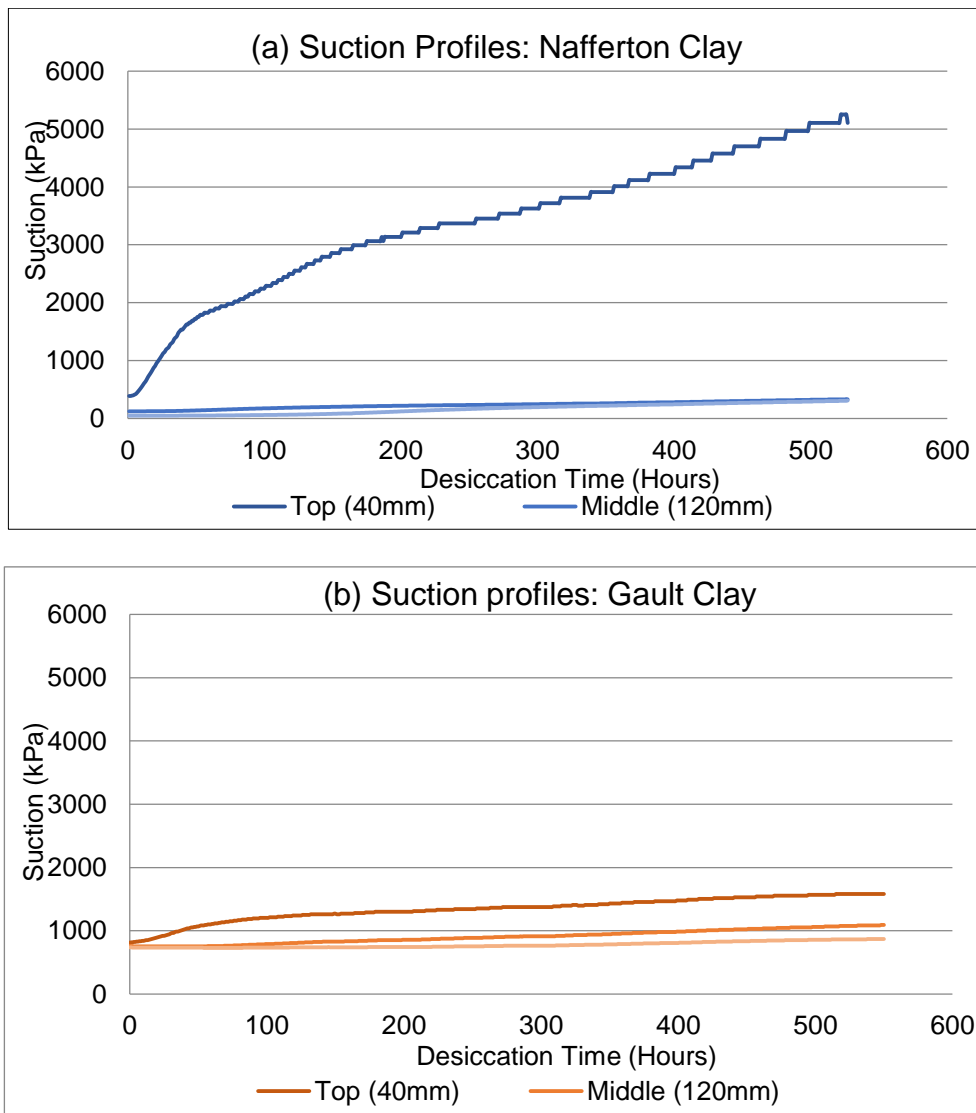


Figure 5.5: Profiles of suction with depth (a) Nafferton Clay (b) Gault Clay

The suction profiles characteristically display trends which represent a transform of the moisture loss profiles, especially in the more responsive top layer. This again is an indication of the inverse relationship that exists between soil moisture and matrix suction development. Both soils exhibit greater suctions at the topmost layer where drying is most intense and the suction response is rapid at the initial stage of desiccation, approximately between 3 to 30 hours, before gradually attaining a steady rate. A similar rapid response also exists in the moisture loss profile shown in figure 5.3, implying an important phase to consider in the desiccation behaviour of the soils, as it correspond to period of active cracking (see section 4.4.2). In the absence of external loading, this observation can be considered as an effect of interparticle arrangement in the soil-water system. As moisture is lost from the soil, the solid phase will re-adjust their interactions. The

effect of particle interaction within the spaces left behind by evaporated moisture will be more intense at this stage of rapid moisture loss. This is also considered as the normal shrinkage phase where the soil changes volume commensurate with amount of moisture loss (Haines, 1923; Tang *et al.*, 2011a). The implication of this is greater effective stress in the reduced meniscus between the grains, hence a remarkable suction development at this early stage as shown in Figure 5.5.

However, the initial suction displayed by the soils at the start of desiccation is higher in the Gault Clay material, typically due to the higher soil water retention potential. This initial value is the antecedent suction, which typically exists in unsaturated soil due to a significant capillary tension in the partially filled void (Fredlund and Rahardjo, 1993). Although the suction in the Nafferton clay test appears high, the SWRC shown in Figure 5.4 indicates that the Gault Clay material has greater suction at any given moisture state. The moisture range at 40mm depth during desiccation of the Gault Clay material was from 32% to 23% (Figure 5.3), this corresponds to an estimated suction range of 800kPa to 1,620kPa. Whereas, at the same depth, the Nafferton material desiccates from 23% to 14% corresponding to an estimated suction range of 380kPa to 5,000kPa. Although the range of moisture content in both soils vary, suction in the Gault Clay at 23% moisture content after desiccation is approximately 4 orders of magnitude greater than in the Nafferton Clay at the corresponding moisture content. Considering the trend, it can be assumed that the Gault Clay material would reach suction in the range of 20,000kPa if desiccated to 14% residual moisture content as the Nafferton clay. Similarly, a much higher suction could be reached in the VH plastic Clay under the same drying condition. Consequently, soil texture (fine vs. coarse grained) and structure (clay layers) can have a fundamental influence on soil suction development. Kim *et al.* (2011) showed that matrix suction in compacted fine-grained soil increases with the dry unit weight and compaction water content, which is in agreement with the present findings.

The trend of estimated suction within different depths appears to be more uniform in the high plasticity Gault Clay than in the intermediate plasticity

Nafferton Clay. The intermediate plasticity soil with its lower range of suction would require less energy to mobilize the porewater for evaporation. Coupled with the accelerated evaporation from the bottom through the cracks and shrunken sides of the soil, the moisture range in the 120mm and 180mm are close and significantly higher than moisture the range in the 40mm level. Therefore, two significant suction regimes tend to exist between the depth of 40mm and 180mm (Figure 5.5a). In contrast, increased moisture-clay adhesion due to increase plasticity is likely to restrict moisture movement in the Gault Clay. Consequently, the later shows a significant layering of moisture and suction as depicted in Figure 5.3(b and c) and Figure 5.5b. Following the hydro-mechanical coupling established in the soil-water system during desiccation, the disparate moisture and suction layers would create varied mechanical gradient in the drying soil profile. The variability in the strength parameter with depth would depend on the magnitude of suction changes interdependent with rate of moisture loss. Accordingly, for a soil characterised by significant plasticity, the potential for greater inhomogeneity in vertical hydrologic conditions is high. This suggests a potential for complex stress condition in such soil. Expansive soils commonly experience cyclic shrink-swell action associated with fluctuations in the porewater pressure, this have enormous impacts on infrastructure in the UK (Farewell *et al.*, 2012; Pritchard *et al.*, 2013). Soil settlement and cracking results from this behaviour, depending on dominant direction of fabric-controlled movement. Under the influence of lateral restraint in the soil shrinkage brought about by factors such as inhomogeneous moisture distribution, vegetation presence, buried utilities etc., cracking is likely to result in response to the enhanced stress condition.

### **5.3 Desiccation cracking behavior of compacted plastic soils**

Crack characteristics of natural soil and slurry are common in geotechnical literature. However, the construction of infrastructure embankment presents entirely different sets of interactive conditions in the soil mostly arising from engineering consideration. The effects of this man-made earthwork including the level of compaction, slope geometry, aspects etc.

on desiccation cracking behavior are not well understood. In this section, time-lapse photograph images of surface cracks recorded during the desiccation experiment were employed to analyze the cracking characteristics of representative embankments in the modern UK. The well compacted panel of the embankment was created in accordance to the modern highway specifications, particularly the good compaction technique.

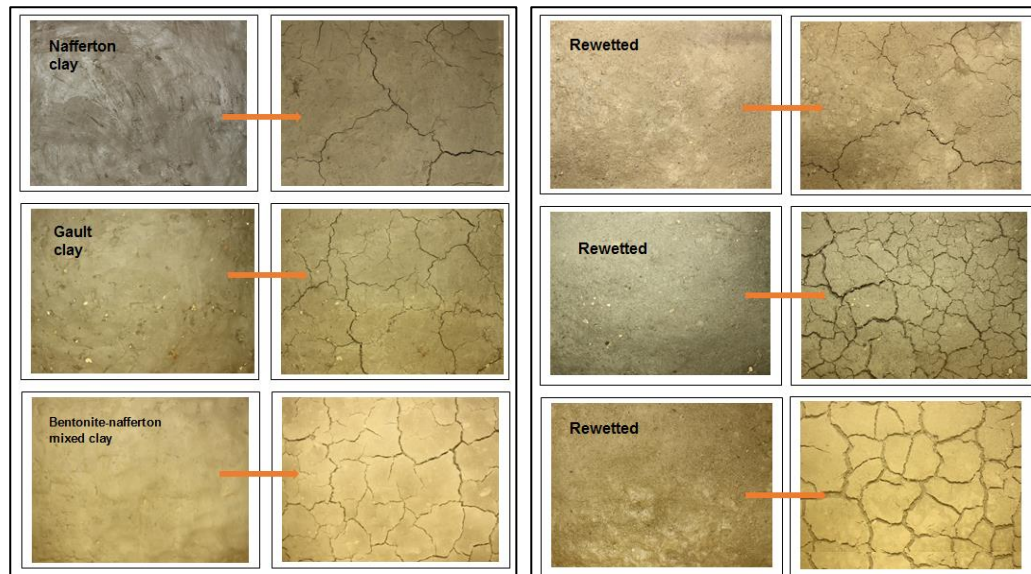
### **5.3.1 Comparison of cracking moisture and suction in three plastic soils**

The prominent antecedent suction developed in the partially saturated condition of the soils led to a near instantaneous cracking as desiccation commences. Despite this behavior, close monitoring of the laboratory experiments showed that the time of appearance of first cracks (crack initiation time) slightly differ in each compacted plastic soil specimen. The crack initiation in the intermediate, high and very high plastic soil materials occurred at 55, 40 and 33 minutes respectively. These time intervals correspond to estimated cracking suction of about 800kPa and 380kPa for the high plasticity Gault Clay material and intermediate plasticity Nafferton Clay counterpart respectively as extrapolated from the suction profiles in Figure 5.5. These values approximate the antecedent suction in the soils indicated at beginning of profiles. The short time for cracks initiation is because net moisture remains close to the molding moisture content. In slurry soils, Tang *et al.* (2016) showed that a slight change in moisture can be accompanied by a reasonable suction development near full saturation. On the other hand, a significant net negative pore water pressure (or high suction) is commonly recorded in embankments after construction. This is because of a significant suction that compaction of the fill in unsaturated condition generates in the soil, and usually favours the stability of slopes immediately after construction. This also implies that after the construction, if the drying condition is exacerbated e.g. extensive hot weather condition, the suction could increase significantly. Under such a rather accelerated condition, the critical hydrologic boundary identified in this study can be attained, which would favor the development of cracks in the embankment soil against the stable stage of the embankment history. With extreme climate conditions gradually becoming a reality, primary concern among

stakeholders is how the net condition of hotter summer and wetter winter would affect the behavior of predominantly clay slope in the UK. Some researchers have argued that the intense rainfall of short duration during a hot summer would be balanced by a net higher evaporation (Rouainia *et al.*, 2009). Others envisaged the net condition in terms of increased shrink-swell action, which presents greater potential for slope deformation. In any case, the role of critical hydrologic conditions established in section 4.4.4 of this study suggests that the magnitude of antecedent moisture and resulting suction in such slopes would influence the potential for crack formation and this feature if present, would significantly modify the net condition. Increase in the future summer temperatures predicted for the UK would likely lead to higher soil moisture loss. From experimental results, this is likely to increase the potential for cracking particularly in historic embankments constructed at lower density. The embankments constructed wet of optimum would dry considerably with potential for sustained critical moisture for cracking. Under same drying condition, cracking can be expected to occur instantaneously in slopes constructed at or near optimum. However, the cracks, in this case, may not develop considerably as the critical moisture boundary observed for active cracking would be potentially restricted.

### **5.3.2 Crack intensity in the compacted plastic soils**

In the 2-cycle of wetting and drying test, each of the tested plastic soils displayed different cracking intensity and characteristics which are examined in this section. Digital images of the soils at start and end of desiccation are shown in Figure 5.6. From a smooth, un-cracked soil surface before desiccation, the soils dried and attained networks of crack as indicated by arrow (Figure 5.6a). Between the extremes i.e. start and end of desiccation), the cracks developed systematically, increasing both in total number, intersections as well as geometry (width, length and depth) which resulted in different CIF. Cracking also intensified during the second cycle (figure 5.6b). Summary of the crack parameters obtained from image analysis is shown in Table 5.3.



(a) 1<sup>st</sup> cycle desiccation

(b) 2<sup>nd</sup> cycle desiccation

Figure 5.6: Photographs of cracks in plastic soils (a) Before 1<sup>st</sup> cycle desiccation (Left column) and end of 1<sup>st</sup> cycle desiccation (right column), (b) After rewetting for 2<sup>nd</sup> desiccation cycle (right column) and at end of 2<sup>nd</sup> drying (left column)

Table 5.3: Summary of crack properties for three compacted plastics soil after desiccation

	Nafferton Clay (PI = 20.1%)		Gault Clay (PI = 39%)		VH Plastic Clay (PI = 51.3)	
	1 <sup>st</sup> cycle	2 <sup>nd</sup> cycle	1 <sup>st</sup> cycle	2 <sup>nd</sup> cycle	1 <sup>st</sup> cycle	2 <sup>nd</sup> cycle
CIF	3.05	4.55	5.97	10.9	10.11	19
Total no. of cracks	23	31	40	64	76	64
No of intersections	7	19	27	70	59	55
Total crack length (pixel)*	20807	38824	38236	56286	54835	52110
Average crack width (pixel)*	17.65	18.74	22.3	27.7	27.7	47.7

\*1 pixel represents 0.118mm

Interestingly, the increments in most of the quantified crack parameters are nearly double in magnitude as plasticity increases. The summary generally indicates that crack width and length appear to exercise a consistent influence throughout the period. In addition, for the very high plasticity soil, total crack length is less in the second cycle implying that crack width is the most significant factor in the CIF obtained during the cycles.

Within the period of significant development, the intensity of cracking for the three plastic soils are presented in Figure 5.7 (moisture data not available for simulated very high plastic clay due to unforeseen fault that occurred in the logger).

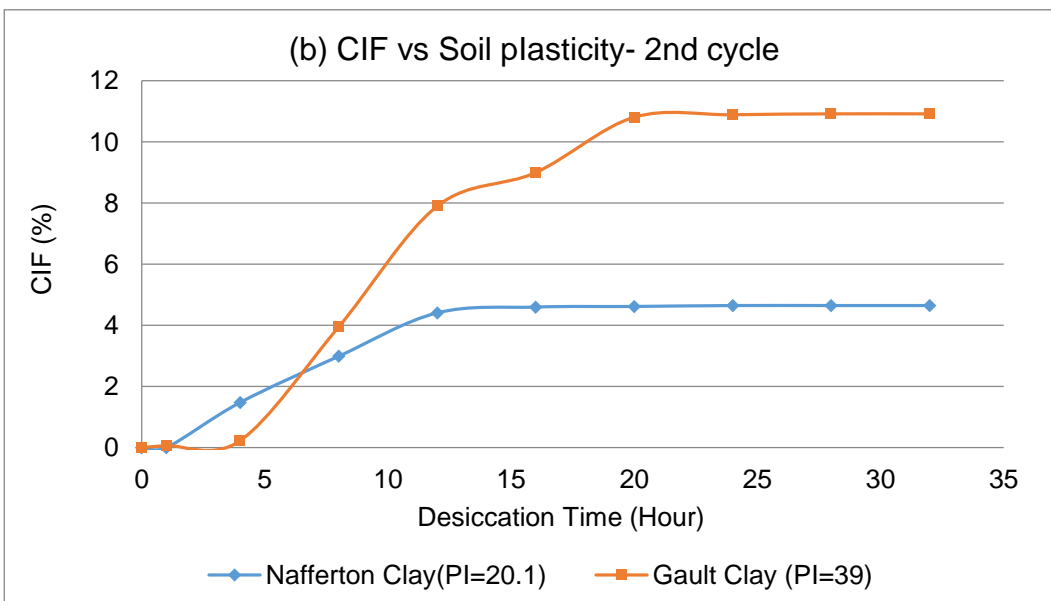
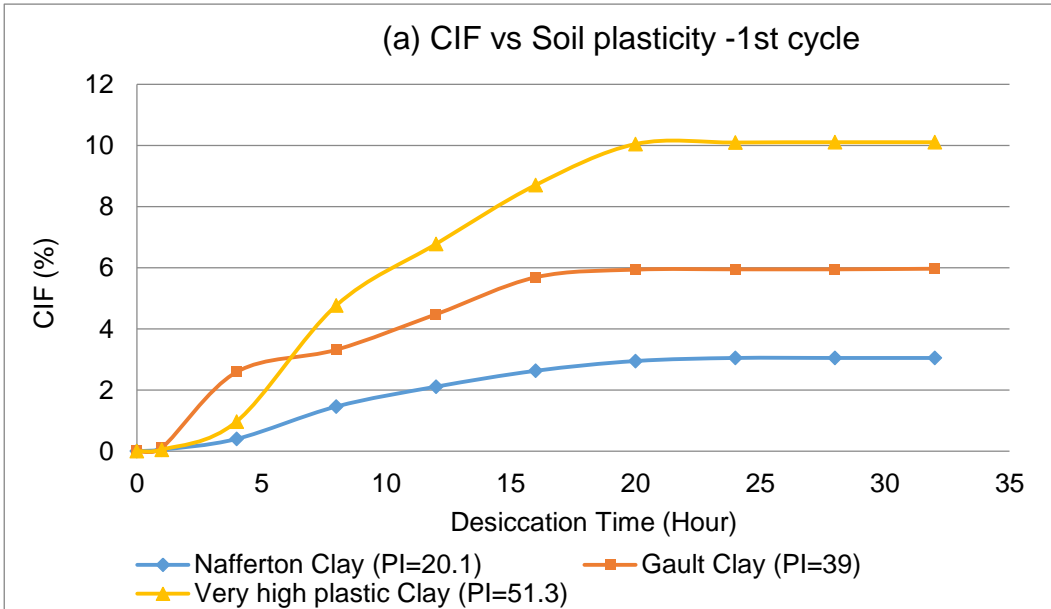


Figure 5.7: Time series crack evolution (a) 1<sup>st</sup> drying cycle (b) 2<sup>nd</sup> drying cycle.

The profiles exhibit exponential growth trend until equilibrium state began to emerge. However, there appears to be a uniform gradation in the crack intensity profile of the least plastic soil while the much higher plastic soils exhibit complex gradient with two or three tangents. It is thought that this possibly has to do with the restricted rate of moisture movement as plasticity increases. Such conditions could result in distinct stages in the soil micro structural arrangement as the soil desiccate, with each stage

acting as a new phase of stiffness that has to be compromise for the cracking to perpetuate. Hence, the rate of cracking intensifies as successively higher tensile forces compromise each of these stages with a much drier condition. This situation ultimately suggests that under a given drying condition surrounding a clay soil, microstructural balances arising from the ease of moisture movement influences the soil response. Therefore, flooded sediments, clods and peds can display different cracking characteristics during drying. As noted by Towner (1987), each of these moisture conditions presents entirely different structural stress condition under shrinkage. In the case where moisture diffusion in the soil media is restricted and prolonged as presented here for the higher plasticity clays (Figure 5.1 and Figure 5.2), the stress history may be progressive as the soil structure continuously adjusts to attain different levels of equilibrium under non-uniform drying. Therefore, the stress intensity can be increase significantly including cracking. Such multiple stress conditions may be less in soils where pore water moves relatively faster leading to a uniform pattern of stresses in the soil media, including reducing pressure potential. On this premise, it is reasonable to expect complex failure situation in very high plastic fills.

Generally, the results of laboratory hydrology and crack development in this study shows that cracks initiated in suction less than 500kPa and did not developed beyond suction in the range of 1,500kPa, which is recorded in the well-compacted specimens. A similar range of suction during cracking was reported by Miller *et al.* (1998) and Yesiller *et al.* (2000) for compacted soils and much lower ranges was reported for slurry clay by Tang *et al.* (2016). This consistency shows the method of estimation of suction introduced by Fredlund *et al.* (2011) is reliable. However, it is worthy of note that suction ranges obtained from the laboratory experiments are far greater than the field measurements. It is recognise here that embankment soils do not dry to the extent obtained in the laboratory experiment to result in very large suction. However, the actual range of suction within which the crack development occurred in the laboratory specimens reasonably approximate what was obtain on the embankment in the active dry period of 2014. Maximum suction in the well

compacted and poorly compacted panels of the South slope were 210kPa and 350kPa respectively (Figure 4.9). It is challenging to measure matric suction in the field due to a variety of limitations including instrument cavitation, laborious procedures and cost. The limitations do further widen the gap between the field and laboratory measurements.

### 5.3.3 Assessment of the potential of soil cracking across the UK

The clay materials selected for this study represents common embankment materials derived from important geology in Northern and Southern England. In section 2.4.3 it was shown that high plastic materials are prevalent in the South, and the London Clay Formation and Gault Clay Formation are among sources of unstable slope in this region. This effect is due to the high to very high plasticity of these materials. To properly understand the rate of weather-related deterioration process in infrastructure slopes, it is important to understand the potentials of cracking in the soil materials they are constructed with.

The CIF of the plastic materials were estimated under cyclic climatic condition. Figure 5.8 shows the cracking intensity increased with the soil plasticity. The relationship has a strong linear regression both in the first and second cycle. It implies that the higher plasticity soil is more susceptible to cracking than the low plasticity soil under the same environmental effects.

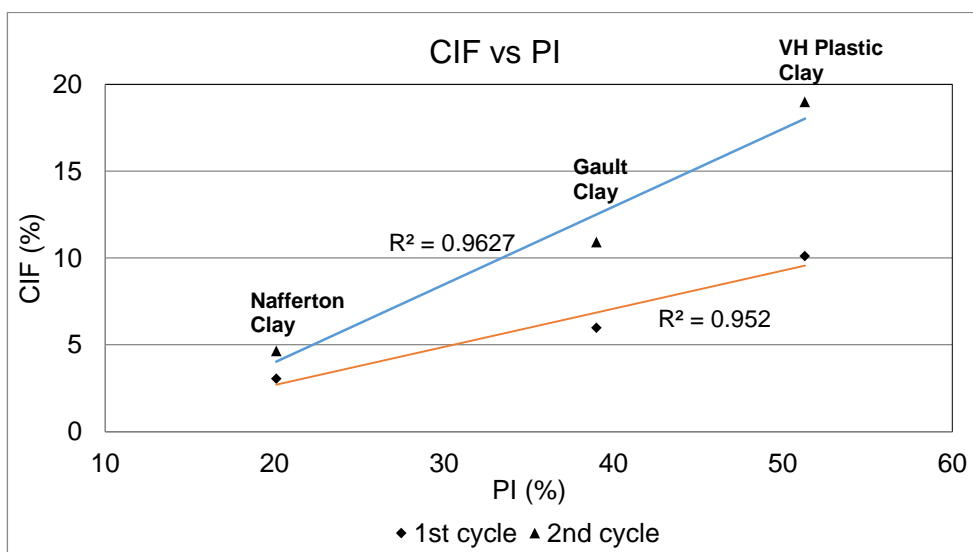


Figure 5.8: Change in cracking intensity with soil plasticity and cyclic wetting and drying

As may be expected, the cracking behavior depicted here would relate to the water retention behavior and volume change (or shrink-swell) potential of the materials, which of course depends strongly on the soil plasticity index and amount and type of clay minerals (Table 2.1). Therefore, the VH plasticity Clay shows the highest cracking respond among the three. Dyer et al., 2007 reported similar relationship between cracking and plasticity. High plasticity soil resulted in a low critical cracking ratio, a geometric factor, which inversely relates to propensity of cracking.

Cyclic condition significantly intensifies cracking with the CIF nearly doubled in the 2<sup>nd</sup> cycle in each of the plasticity condition. Considering the geographical spread of plastic materials in England, this trend of climate-related process reasonable suggests that cyclic environmental condition characterized by alternate wetting and drying has greater implication for cracking in embankments created from very high plasticity soils prevalent in the south. The higher  $R^2$  in the 2<sup>nd</sup> cycle couple with the increasing geometric sequence means the effect is likely to be exacerbated with increased seasonality in future climate.

#### **5.4 Factors influencing crack propagation and formation of network pattern in engineered soil**

From the discussion so far, it is likely that notwithstanding the quality of construction, clay-based embankments can undergo cracking when critical hydrologic conditions are reached during desiccation. In the literature, this has been shown to occur when the soil strength is compromised by the imposed hydrologic stress (Kodikara et al 2000). Apart from the controls of the basic engineering and natural properties of the soil on the cracking behaviour, syntheses of the field and laboratory results have also revealed a range of other factors affecting particularly crack propagation and topology, which are also essential to characterize the phenomena. In the field, cracks occurred mostly single while in the laboratory, single cracks propagated through the soil and interact with each other. This suggests that crack formation in the two settings varies and the process involves a stage of initiation followed by propagation and intersection. It is important to understand the controls of this behavior. Essentially, after their initiation, the cracks increase in geometry (i.e. length, width and depth) and

progressively intersect with each to form a complex but systematic crack pattern with progressive drying. For example, Figure 5.9 shows the dynamic progression of a typical crack development and network in the soil during desiccation.

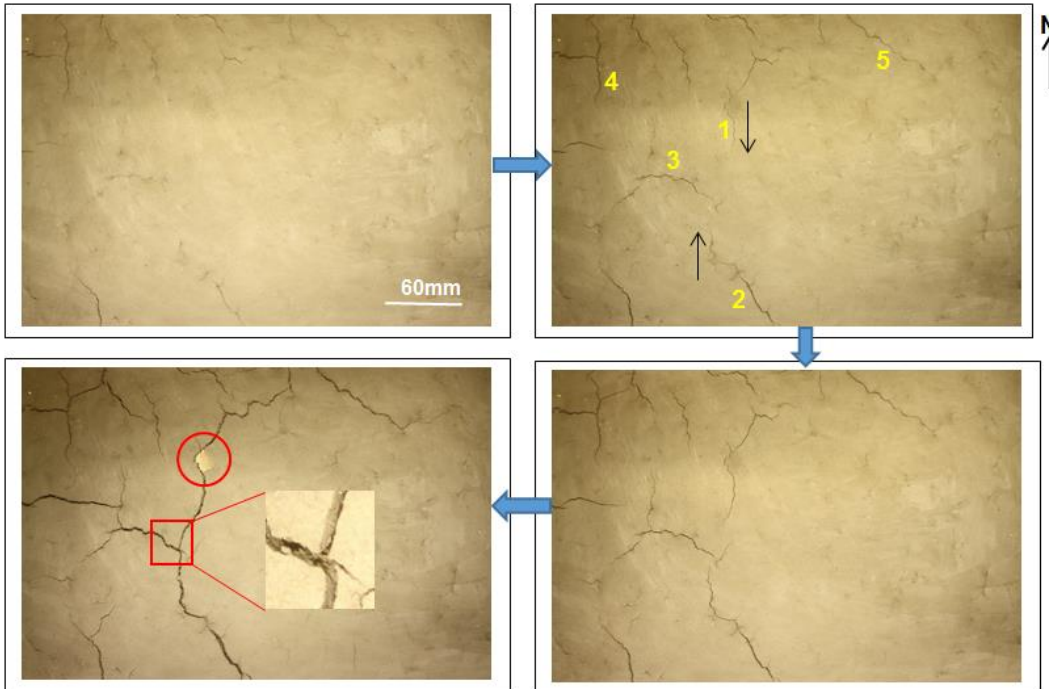


Figure 5.9: Example of progressive development and interaction of cracks in the Nafferton Clay

A referenced smooth soil surface starts to crack randomly with an average crack width of about 1mm. The cracks gradually propagate by widening and lengthening as desiccation progresses. Interestingly, some of the original cracks showed significant propagation lengthwise (e.g. crack 1 and 2 in Figure 5.9) and either intersect or join other advancing cracks. However, under the same soil condition, some of the cracks do not show any significant development after initiation (e.g. crack 3). The controls of such behavior are examined in the following subsections.

#### 5.4.1 *Moisture changes and crack propagation in soil*

In order to explain the dynamics of crack development presented in the preceding section, the pattern of moisture in the soils are examined here. Heterogeneity in soil composition can lead to a non-uniform drying, a condition which set up moisture gradient in soil. Since porewater and capillary tension in the soil are related, the non-uniform moisture distribution can ultimately give rise to complex pattern of suction stress in the soil. It is well established that depending on the soil structure and

mineral content, the stress induced by drying shrinkage can differ (Towner, 1987; Bell, 2013). The crack network therefore ultimately reflects the complex interaction of stresses with an orientation suggesting the direction of resultant principal stress propagating against the varying strength of the material as moisture changes.

As shown in Figure 5.9, short micro-cracks advances across the soil surface after initiations. This is very significant with the cracks labelled 1 and 2, which increased from initial length <50mm to a maximum of approximately 130mm each. The propagating crack tip is narrow, indicating the direction of propagation (south and north for crack 1 and 2 respectively). The two major cracks eventually join crack 3, transversely oriented across their path (intersection point insert: x10). The red circle shows a local flaw (clay clods) eventually revealed as drying advances in the soil. In recognizing the influence of flaws in crack initiation in a soil, this can be regarded as a likely origin of crack 1.

To explain further this dynamic, it is important to consider the existing soil mechanics principle on soil cracking; shrinkage restraint. In an embankment, non-uniform moisture pattern commonly constitutes such restraint. Generally, soils are anisotropic due mainly to mix pattern of structural elements e.g. grain sizes and particle orientation, mineralogy etc. Consequently, drying is non-uniform coupled with the influence of disparate climate intensity. Multi-directional drying fronts would exist with corresponding directional moisture gradient hence complex stress patterns result as the soil shrinks. Figure 5.10 shows different crack orientations in a soil surface with different drying intensity at a certain stage in this study.

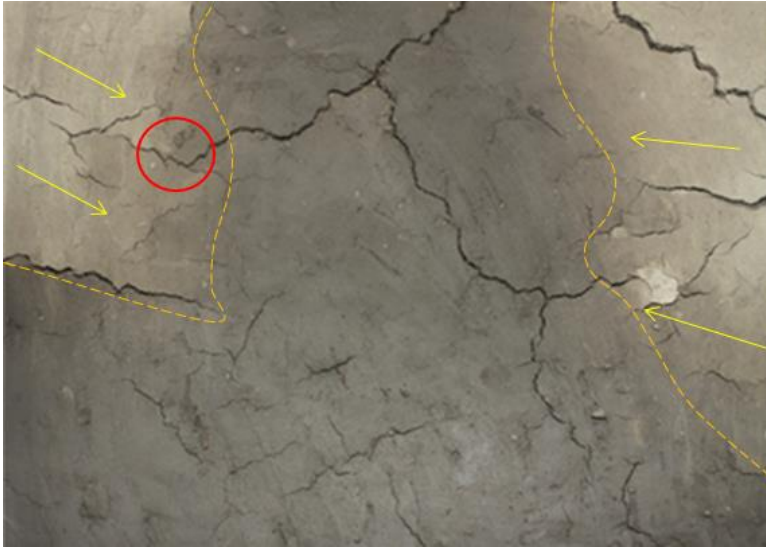


Figure 5.10: Direction of cracking in Nafferton Clay soil influenced by orientation of the drying (dashed lines).

The drying area on the soil is lighter color compare to darker color defining less drying area. This appearance enabled a delineation of the approximate boundary of the drying front on the soil surface as indicated by yellow dash lines. The cracks tend to propagate in the direction of the drying, lengthening and widening. The less dry areas are apparently weaker and the cracks propagate relatively faster within this area with enhanced width. The red circle indicates a slowing of northwest-bound crack with a reducing width at the boundary of opposing drying front. The preferred orientation of cracks in the direction of drying moisture gradient has also been studied by some authors notably Shorlin *et al.* (2000) and DeCarlo and Shokri (2014). In this study, the 2-dimensional imprint of drying front is thought to continue in the subsurface soil. In one of the laboratory test, moisture probes were inserted in two alternate sides of the soil box. The desiccation profiles did not only revealed a vertical variation in moisture but also a higher rate of desiccation trend particularly at layer of the windward side B (Figure 5.11).

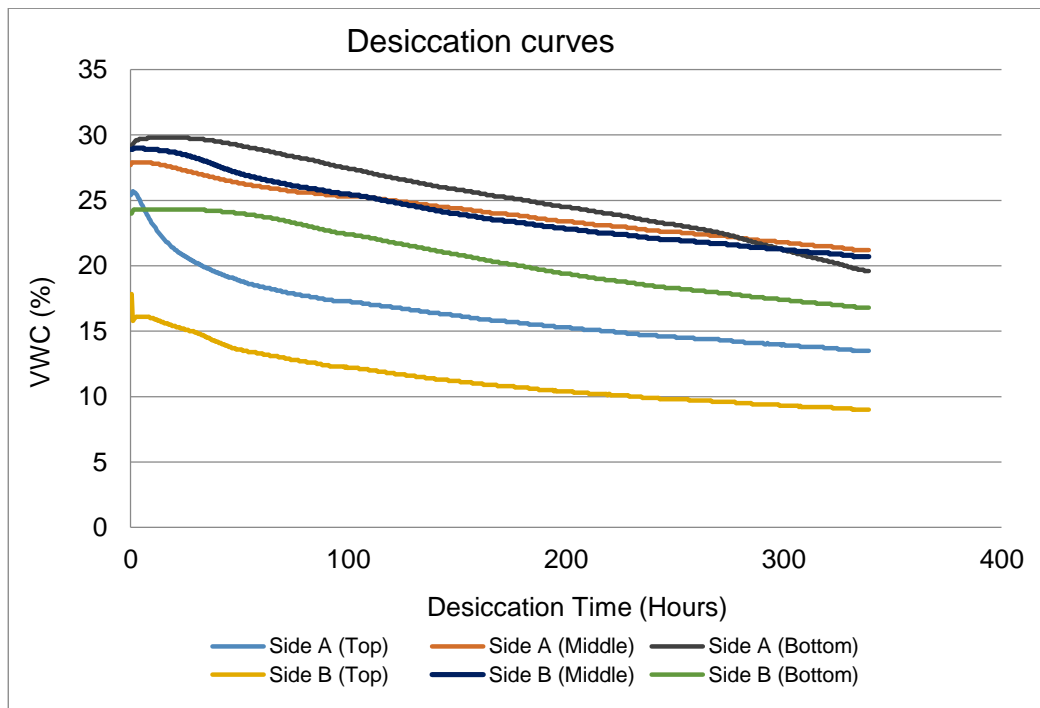


Figure 5.11: Profiles of desiccation from 2 opposite sides of a rectangular soil block similar in effect to difference in moisture loss with slope aspect in the embankment

This trend can be attributed to the impact of air from the axial fan attached at side A. The warm climate air issued his side indirectly incident at the opposite side B to cause greater drying as indicated in Figure 5.11. This in a way simulates the difference in aspects climate condition on the embankment, which led to different moisture conditions recorded on the slope. The different sides of the soil box here represent the slope aspects. Fracture mechanics principles suggest that crack propagates in a plane normal to greatest tension and in a way that generates the least energy to break the material. By simple elliptical outline commonly assumed for analysis of forces around a crack body, a normal continuous line of forces at equilibrium in an elastic material would bend at the presence of any void or crack as shown in Figure 5.12. This produces infinite lines of forces with maximum stress concentration exiting at the crack tip.

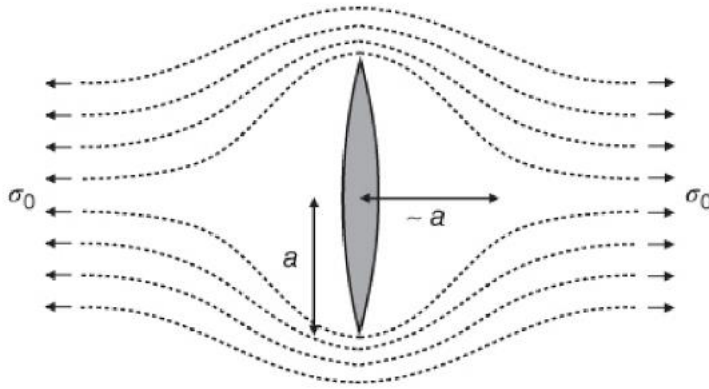


Figure 5.12: Illustration of stress field around a crack. From Goehring (2013)

Generally, crack is thought to propagate when a critical stress factor is reached in the media, and the propagation is essentially a release of the stress against the material fracture toughness. This can also be conceptualized in terms of the balance between the strain energy of the crack and bond strength in the soil. Therefore, for a crack of length  $2a$  as illustrated in Figure 5.13, Goehring (2013) shows that the stress is effectively released in the region of width,  $a$  to either side of the crack as the crack front travel in the soil. The stress is, therefore, release for the crack opening.

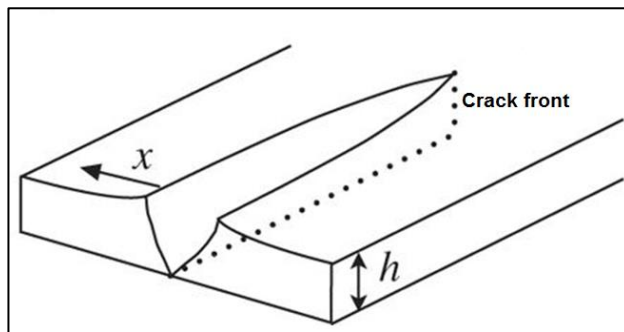


Figure 5.13: Schematic of cracking in thin soil of height,  $h$ . The crack releases stress preferentially in the direction,  $x$  perpendicular to its growth. From Goehring (2013)

A similar stress dynamics explained above can apply to the drying soil studied here. The propagating crack tip essentially advances in the direction of the drying front to elongate the crack in a relatively wetter region. From the foregoing mechanical principles, the crack will continue to propagate along this path until the stored energy gradually dissipates below the increasing soil tensile strength in order to resist the movement. This can be due to moisture equilibration as the evaporation rate slows either at the instance of a vapor pressure balance between the drying soil

and the surrounding environment or significantly dry soil surface which would reduce the ability for evaporation. In the latter case, the greater suction in the drying soil surface can increase aggregate stability. The particles essentially rearranged to increase the soil tensile strength against the stress intensity factor of an advancing crack.

Fracture mechanics principles suggest that that intensity of stress at crack tip depends on crack size, orientation and the available matrix energy around the vicinity of each crack (Anderson and Anderson, 2005). This can account for the difference in propagation velocity of individual cracks observed here as the crack sizes and moisture in their local surrounding differs. The relatively larger cracks at the time of initiation were observed to propagate faster through the soil than smaller cracks. Moisture gradient and pore geometry in a drying soil are therefore important factors in the dynamics of crack propagation. During the field survey, cracks lengths were observed to propagate mostly in the downslope direction in the soil, through both the thin topsoil layer and the underlying Nafferton Clay, which is the material, causing the shrink-swell response. Since there was no mass movement in the slope, the crack orientations are dictated by the stress field arising from the developing moisture gradients.

#### **5.4.2 Soil texture and desiccation cracks network characteristics**

An open crack in a soil surface shows outlines that are likely associated with the processes of formation. Both in field and laboratory study, the crack outlines were observed to be nonlinear with rough apertures. A review of common crack images in literature indicates that the surface crack in this study are comparable to what is obtained in compacted fills and different from crack outlines formed in slurry and muds sediment (Figure 5.14). The latter are mostly characterized by relatively straight cracks with smooth edges (Figure 5.14 a and b). In Figure 5.14c, where the cracks show roughen and tortuous outline, Yesiller *et al.* (2000) conducted the desiccation experiment using compacted clay fills.

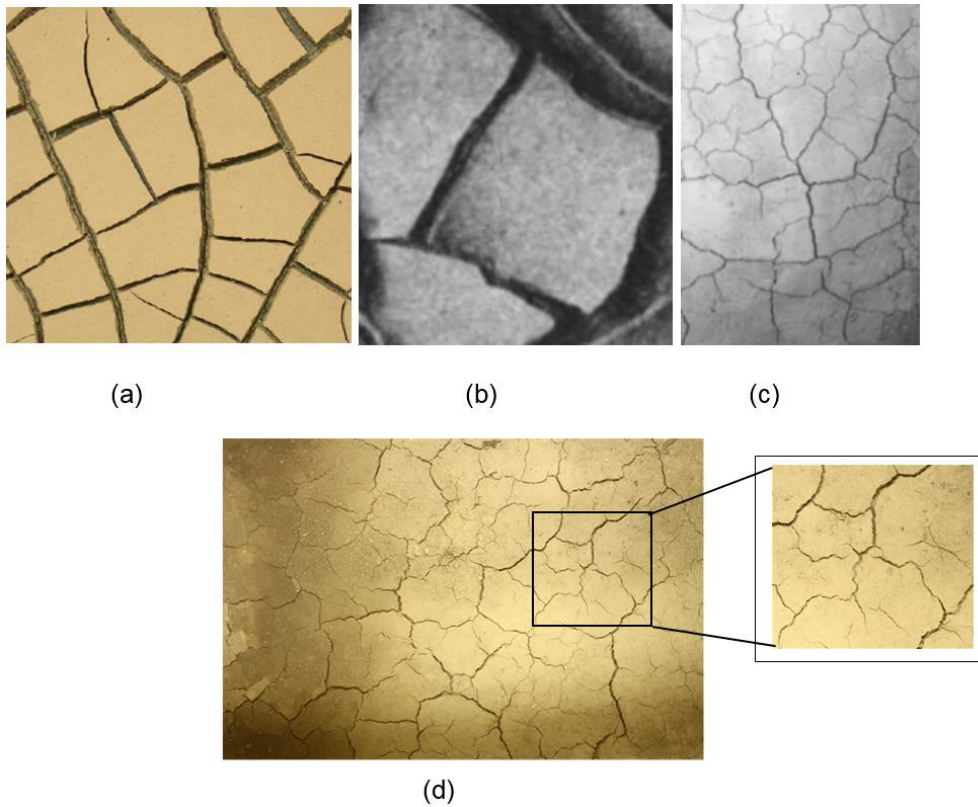


Figure 5.14: Comparison of crack outlines in different soil textures (a) Tang *et al.* (2011a):clay slurry (b) Kindle (1917): mudcrack (c) Yesiller *et al.* (2000): clay liner fill and (d) This study

From Figure 5.14, it is clear that texture of the substrate is important in appearance of crack outline. Muds are fine particulates while slurries, such as used by Tang *et al.* (2011a), are refined by significant removal of the coarse contents. On the other hand, clay fills used in this study were prepared to reflect in situ texture similar in approach to Yesiller *et al.* (2000). Grain analysis of the clay fills shows 10 to 15% by mass retained in the 5mm sieve while the Gault material is sandy and slightly gravelly. The difference in crack outlines between slurry and compacted materials, therefore, discriminates the use of crack characteristics from a slurry experiment in an application involving engineered soil. This was one of the research gaps identified in this subject. Hence, the impetus to simulate laboratory conditions that closely represent the embankment fill for rational comparison.

Apart from influence of varying soil water gradient on the general direction and extent of cracking, surface defects including solid particles, clods, surface curvatures, roots etc., was also observed to influence crack propagation routes. Throughout the tests, crack paths were commonly

deflect at sites of defects leading to local curvatures in the pattern. Textural features can, therefore, be regarded as physical interfaces, which locally acts against the normal path of hydrodynamic cracking. Material resistance would counteract stress intensity of advancing crack tip. Since crack propagation explores the most effective route for strain energy release, they would tend to deflect from such local zones of fracture toughness relative to the soil strength. This would lead to a tortuous outline along the receding moisture diffusion path. Several workers have shown that graded structures and the space defects between the grains influences crack path selection (Koh and Wong, 2006; Shin and Santamarina, 2011; Goehring, 2013). At a microscopic level, cracking in particulate materials is represented as a displacement of the bonded atomic structure. In an isotropic drying experiment, DeCarlo and Shokri (2014) showed that a uniform substrate exhibit a more or less straight line cracking but when sand impurities were added, the cracks showed significant directional preference away from the sand grains. Therefore, the textural composition of soil presents a system dynamics that significantly affect cracking behavior in drying soil. Overall, the textural defects influence the degree of orderliness in the cracking system. For a uniform fine-textured soil e.g. slurry clay, cracks will initiate and propagate in a relatively homogenous substrate following the order of drying gradient with less secondary influence. Although the cracks in such substrate may initiate at one or two random places influenced by occluded air, as showed in Figure 5.14 (a and b), they commonly set off in a straight line, and possibly changed course to reflect the direction of disparate moisture diffusion. On the other hand, the crack system in this study begins with a highly disordered orientation mostly influenced by flaws. The corners of flaws can further influence the orientation due to high stress intensity possible at the edges, especially angular stones and other sharp-edged particulate impurities. Once initiated, the microcracks were seen coalescing or propagating to merge with each other away from the flaws to eventually follow a pattern reflecting a much larger moisture stress field prevalent in the drying soil. This dynamics can be view in the series of crack development presented in Figure 5.15.

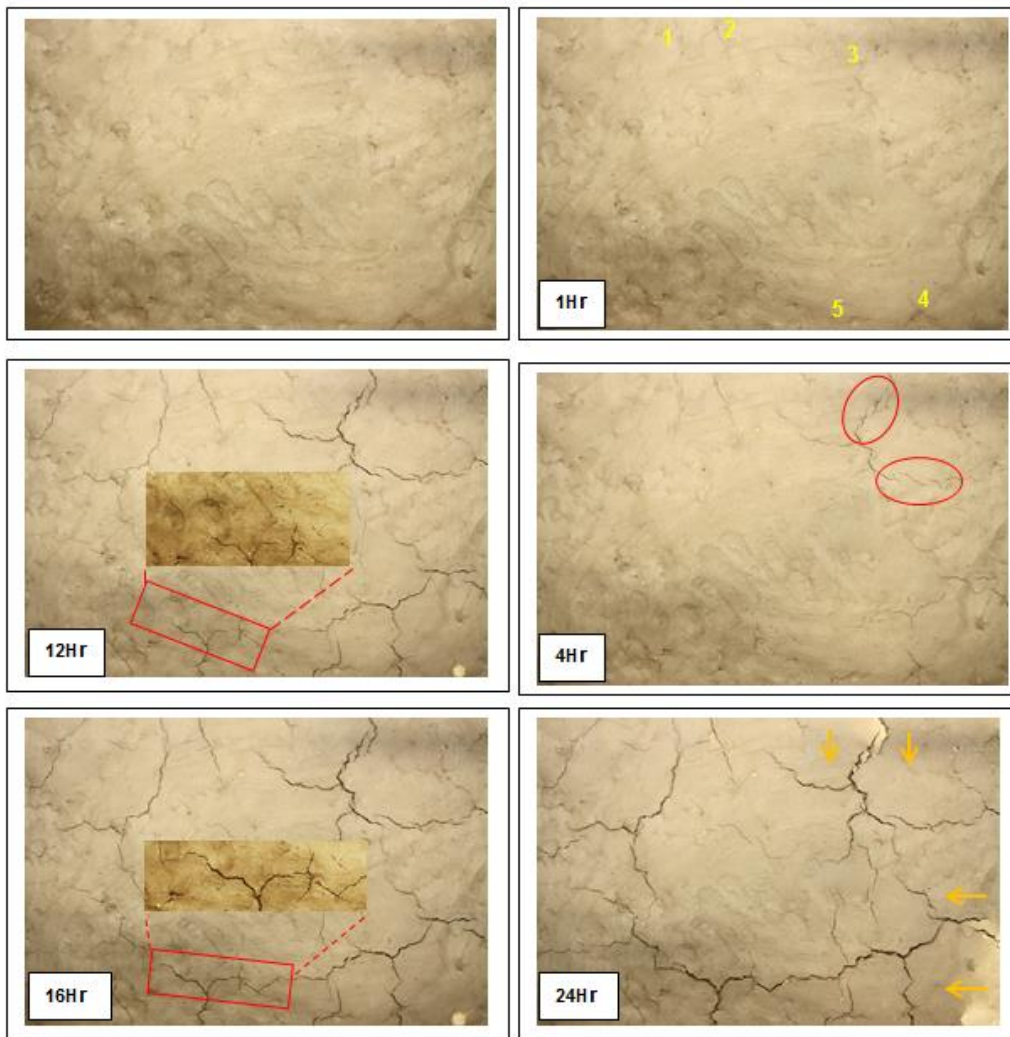


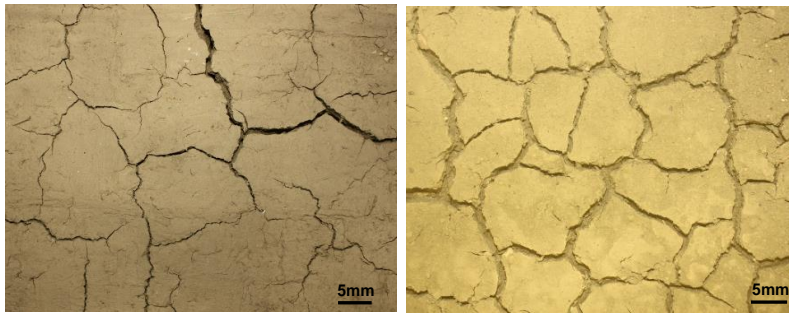
Figure 5.15: Crack network affected by texture in a compacted clay fill

As drying commenced, the cracks in the soil developed at five random locations after 1 hour. Initiation of the few random cracks does not present any clue of the underlying influence except they seem to appear predominantly in the northeast and southeast corners of the soil. After 4 hours of drying, the cracks around location 3 (red cycle) aligned together. This suggests a common stress field in their formation. More of such preferred alignments are seen as desiccation progresses, and the trend appears to advance towards the west end of the soil surface. After 16 hours of desiccation, joining of separate cracks with the common orientation shown earlier in the 12 hours image appeared as insert. Eventually, the disjointed cracks are connected together to form a network after 24 hours of desiccation. At this stage, the drying front becomes obvious as marked by the arrows. Stones and undulations in the soil clearly influenced the crack topology. This is further examined in section 5.4.4.

The rough edges of cracks seen here can be regarded as effect of outburst of energy during stress relief. Stored energy in such dry soil can be release with high intensity causing rupture and displacement of soil wedges at the drying surface. Such mechanism is also capable of either simultaneously initiating a side cracks or create weak zones for secondary cracks to develop later under the right condition. In terms of aperture characteristics, cracks in the loosely compacted soil exhibited loose particles along its aperture compared to the firmly divided soil of the denser specimen. Therefore, soil density can affect the crack surface outline with greater susceptibility to secondary modification by surface processes in loose soil. The textural characteristics are necessary to recognize in order to fully understand and adequately model the overall influence of cracking in the deformation process of a desiccating clay slope.

#### **5.4.3 *Influence of vegetation in crack network formation***

A remarkable difference exists in crack pattern in a vegetated soil surface and a soil surface with little or no vegetation. The complex but systematic polygonal networks of cracks resulting from the laboratory experimentations in mostly ordinary soils were observed in the embankment in few areas with significant exposure of the top soil (figure 5.16a). Cracks on the grass-covered embankment occurred mostly as single features with straight to slightly curved outlines (Figure 5.16b). Since the experimental soils and the embankment fills were reasonably similar in nature, it is justified to consider the difference as due to influence vegetation.



(a)



(b)

Figure 5.16: Characteristics crack patterns (a) Laboratory and (b) Field

Vegetation and soil naturally relates. In a broad sense, vegetation grows in soil and therefore constitutes the soil flora. As a habitat, vegetation plays significant role in soil development and modification. This primarily is because of moisture usage and the roots zone in the soil. Transpiration significantly contributes to moisture loss in soils. A study of global partitioning of evapotranspiration components conducted by Jasechko *et al.* (2013) showed that transpiration is by far the largest water flux from Earth's continents, representing 80 to 90% of the terrestrial evapotranspiration.

Analyses of hydrologic recordings from the embankment, showed that the presence or absence of vegetation affected the ET on the slope (section 4.3.1). This led to a significant moisture disparity as well as differences in the cracking intensity between 2014 when vegetation were cleared on the embankment and 2015 with abundant vegetation. Transpiration, especially by large trees, is significant in drawing soil moisture from a deeper layer.

However, it seems more fundamental that the absence of vegetation cover during this period exposed the embankment soil to intense drying, which directly increased the rate of desiccation. As shown in this study, the rate of desiccation is very important in the cracking process and can explain the difference in crack intensity in the vegetated and un-vegetated area of the embankment. Cracks in the scantily vegetated area formed network pattern. In the environment of alternate rain and sunshine, while the exposed soil area cracked easily under an intense rate of drying by direct insolation, the dry condition is transient as it is compromise after sunshine hours or rainfall event. Therefore, there is greater potential for shrink-swell action in the soil with implication for cracking. In addition, the intense drying leads to the formation of simultaneous cracks and forms a system of polygon influenced by the location of flaws. On the other hand, vegetation cover prevents direct insolation on the soil surface which results in a slow rate of desiccation. In addition, evaporation of soil water can be restricted and/or delayed through vegetation cover. Therefore, except for effective transpiration through the leave system, there exists a greater potential for higher desiccation rate in exposed soil than vegetated soil. However, while the condition of drying in exposed soil areas lead to simultaneous polygons of cracks, the thickly vegetated areas had cracks that are geometrically more developed. It is believed here that unlike in exposed soil area, soil temperature under vegetation cover can persevere leading to a sustain condition for crack development, i.e. drying suction.

Apart from its effect in the slope hydrodynamics, vegetation roots in particular bind soil particles together and can compress the soil by a surcharge load (Stokes et al., 2008). The mechanical benefit of vegetation root in soil has been explored in practice for the establishment of selected plant species in slope stabilization. Planned vegetation is, therefore, a common feature of transport infrastructure slopes. The mechanical anchorage provided by root zone would essentially increase soil cohesion and bind shear planes, which is a positive condition which could affect crack behavior in soil. Therefore, the influence of roots in the crack propagation is important to understand. The development of crack in this study relates to couple atmosphere-hydro-mechanical dynamics mainly arising from changes in soil water and the development of suction stress.

After crack initiation by suction related tension stress, the propagation followed a preferred path of least resistant in the soil media. To this extent, therefore, the presence of physical boundaries in the soil such as root structure can constitute restraint interface or local resistance that could preferentially dictate the crack pattern (see section 5.4.2). This could further explain the restriction in the crack pattern in the vegetated area of the embankment.

An exposed soil profile in a test pit shows roots in the embankment were typically fibrous with slender strands of about 1mm in average thickness (Figure 5.17).



Figure 5.17: Fibrous grass roots in a test pit section on the embankment

The mechanical benefits of such fragile root type will, therefore, be a network factor arising from the combined root system. Soil cohesion by fibrous grass roots has been showed to come from the composite strength of the individual strands (Abernethy and Rutherford, 2000). This has led to some experimentation in soil stability using synthetic fibers to improve the mechanical properties of soil, including shear strength, bearing capacity, toughness index etc.

Another significant feature of the vegetation on the embankment was their occurrence in clusters. The clusters formed a large stock with the fibrous root spreading radially and vertically underneath the soil. In an old experimental lysimeter used in a previous research, the fibrous roots reached an average depth of 350mm in a soil. A washout of one of the stocks in the lysimeter shows a fibrous root composition of averagely 100g per 100 cubic centimeter of the bulk soil. Most of the cracks found in the

embankment were observed to meander around the cluster of grasses with the curvature of the crack occurring near such location assuming a geometry, which describes part of the circumference of the grass stock. This suggests a possible influence of the grass stock on the crack propagation route. It is believed here as the cracks propagate in the embankment soil, their paths are deflected by the cluster of grasses which are thought to form local material resistant to crack propagation. The stock of grasses in the embankment essentially creates a local zone of lateral mechanical influence. Cracks propagating towards this zone of material toughness are therefore resisted and cause to take the next effective course as shown in Figure 5.18. In the illustration, the crack line (yellow dash lines) meanders between three neighboring grass clusters (circled). The actual strength properties of the soil were not considered in the scope of this study, however, the deflection of cracks around grass points to additional strength by the grass roots, which would be greater than stresses at the propagating crack tip.



Figure 5.18: Vegetation influence on crack orientation in the embankment

The field trend was further simulated in the laboratory for in-depth analysis. Modelling of an engineered vegetated soil in the laboratory was quite challenging. However, a reasonable model was created using a soil block from an old experimental lysimeter with grass and soil modelled after

the embankment. A large chunk of compacted lysimeter soil block containing two prominent stocks of fibrous grasses was carefully lifted into the desiccation soil box. The remaining space was filled with soil aggregates and lightly compacted together to form a whole unit. In the 2-cycle of wetting and drying test, desiccation cracks developed in the specimen is shown in Figure 5.19.



Figure 5.19: Crack pattern in experimental rooted soil (a) 1<sup>st</sup> cycle (b) 2<sup>nd</sup> cycle

Even though the crack patterns in this model do not significantly compare to field result except in the case of un-vegetated part of the embankment, there are reasonable features in the images that can be linked to the presence of the grasses. Firstly, the cracks tend to deflect away from the grass stocks judging from large cracks rounding the circumference. Furthermore, advancing cracks towards the grass stocks have reduced width except for boundary effect toward the top right corners. Secondly, the intensity of cracking in the 1<sup>st</sup> and 2<sup>nd</sup> cycle images does not show any significant difference. This suggests a limiting effect of repeated wetting and drying, which commonly intensify cracking in the 2<sup>nd</sup> cycle. Such response indicates that there is enhanced apparent cohesion and an increase in the soil tensile strength caused by the composite mechanism of network of roots. After the experiment, the soil section was dissected where it was observed that the fibrous root network from the two prominent grass stocks had grown into the fresh soil fill despite compaction. The grass leaves that were initially pruned to allow visual inspection of cracking also grew inside the box as can be seen in Figure 5.19a. Images of earlier stages of the crack development also showed enhanced drying proceeding from the grass stocks. These factors signify

that the vegetation was active in the soil with implication for increasing mechanical effect.

Occasionally, burrow organisms e.g. worms were seen crawling out on the soil surface to leave sticky marks and faeces. The soil flora and fauna, therefore, led to a remarkable effect on the moisture recording of this particular test. For instance, the gravimetric moisture record was haphazard with anomalous readings. The activities of microorganisms living in the soil are the reason for this behavior. However, the volumetric moisture recordings from inserted probes were unaffected as shown in Figure 5.20 for discussion of the moisture behavior of the rooted soil specimen.

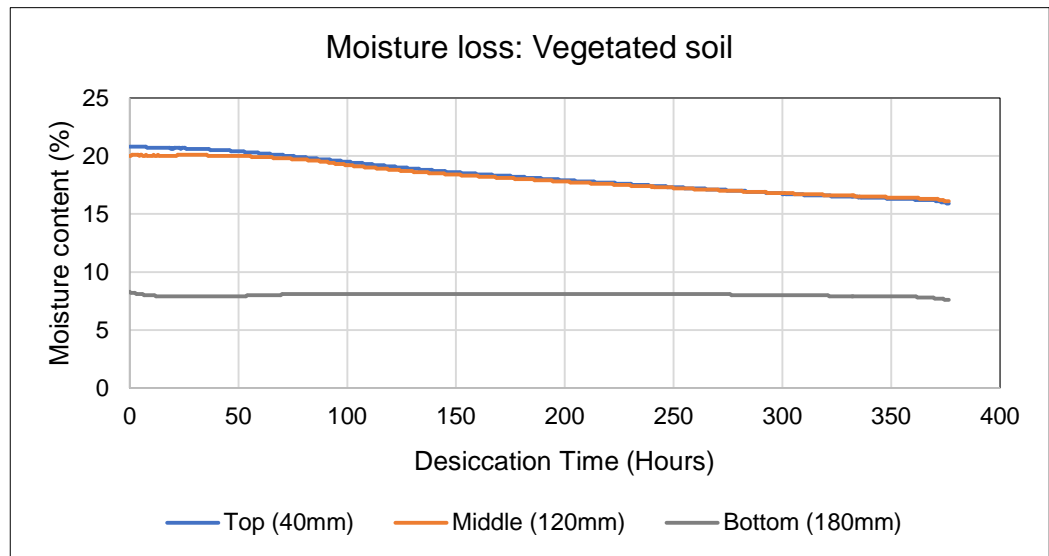


Figure 5.20: Profile of moisture loss with depth in the vegetated soil mass

The moisture loss profiles show distinction from other Nafferton clay specimens, and this can be attributed to the vegetation present. For instance, there is a large disparity in the moisture records between the top and bottom horizons in this bespoke soil specimen. In addition, desiccation at the top and middle layers is closed while the bottom profile shows no significant change with time. This agrees with other moisture loss profiles, which commonly exhibits a decreasing effects with depth. However, the close trend between the top and middle profiles can be attributed to a balance brought about by activities soil flora and fauna in the soil. Their individual moisture intake at different depths significantly draws water and accelerates moisture loss from the soil. In a dissected block of the vegetated soil at end of desiccation, the presence of intruding

vegetation roots and burrowing organisms were observed to be significant in the middle soil layer. This is probably because the living organisms tend to exploit moisture in deeper layers away from the drying surface. Their moisture uptake mainly below the drying soil surface is believed to give rise to the similarity in the trend of moisture loss in the middle and upper soil layers after approximately 50 hours of desiccation (Figure 20). A dissection of the vegetated soil block at the end of desiccation showed the bottom layer remained relatively unaffected by moisture loss. Since shrinkage was sufficiently restricted in the rooted soil block, there was no bypassed route for evaporation from the bottom layer as was observed in the other Nafferton Clay. Therefore, soil flora and fauna can induce a significant moisture gradient in top soil layers. Studies have shown that such invasive exploitation of soil moisture can significantly advance the drying front in soil with implication for generation of condition with increasing depth of cracking.

#### **5.4.4 *Mechanisms of crack intersection and orientation in soil materials***

Desiccation cracking often forms network pattern. When seen after formation, the pattern can look complex but as shown in this study, they evolved systematically with changes in the soil moisture. Important features of the crack pattern are the orientation of the crack lines, nature of crack outline as well as their intersection angle. These features combined to define the different crack topology described in nature with a polygonal arrangement being the most common. Typical cracks found in fine-grained materials intersect at an angle of  $90^\circ$ . In this study, although the cracks predominantly meet at a right angle, however, across the various test conditions, minor but intricate differences exist in the pattern with a good number of intersections occurring at variance with the common perpendicular meeting points. Figure 5.21 shows typical patterns of crack intersection in this study. The square and circle boxes represent majority of intersections at  $90^\circ$  and other variations respectively.

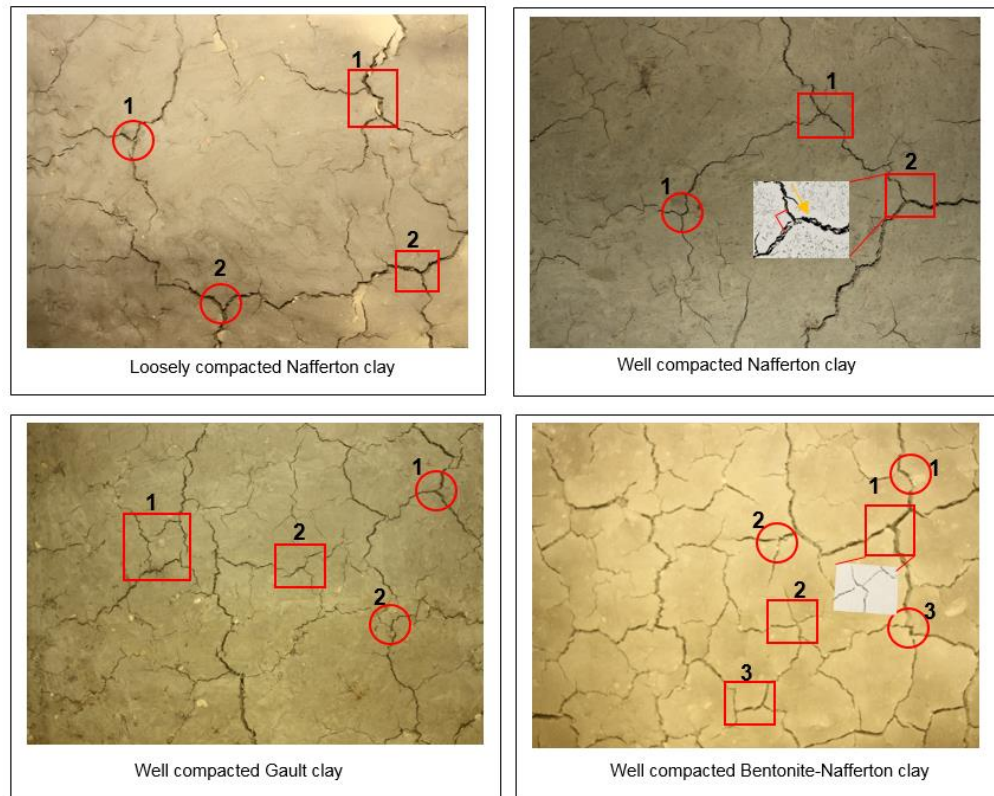


Figure 5.21: Crack patterns in compacted soils

Despite the slight curvatures in the outlines of some of the cracks identified in the square box, their final intersection is approximately perpendicular. This can be seen in a magnified image of the square box marked “2” in the image of the well-compacted Nafferton clay. The advancing crack is the north oriented arm which is seen curving to make contact with the basal crack perpendicularly. The geometry of the intersection point can also be re-engineered as the cracks developed. Going back on the sequence of development for the square box marked as 1 in the image of VH plastic clay (bottom right) reveals the dynamics involved in such change in geometry. The extract is expanded in Figure 5.22 below.

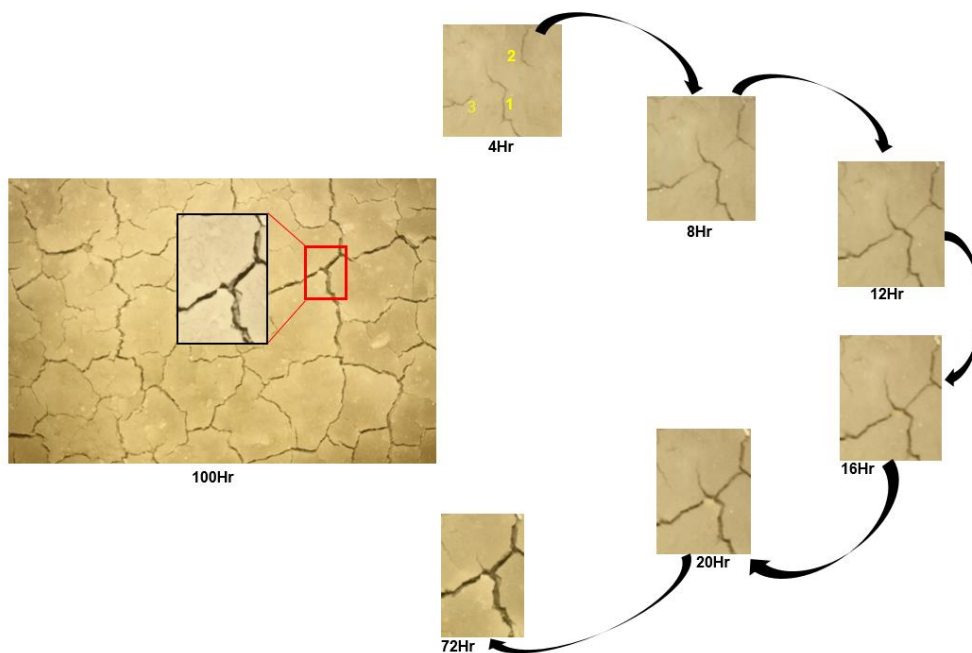


Figure 5.22: Time series changes in crack orientation and intersection (1<sup>st</sup> cycle)

The illustration shows that this particular intersection point resulted from the interaction of three individual cracks identified after 4 hours of desiccation; namely, an inactive crack labelled “1” and two advancing cracks labelled “2” and “3”. As desiccation progresses, the two advancing cracks are seen intersecting the transversally oriented inactive crack in the 12<sup>th</sup> hour (crack 2) and 16<sup>th</sup> hour (crack 3) respectively. The different times of intersection imply the two cracks are travelling at different speed. The intersection initially formed a cross junction, although with a slight offset in their individual contact points. In the final image, the geometry of the intersection point is seen changing into a “T-junction”. A curious observation shows this transformation occur primarily as the individual cracks expand with the northerly crack 2 seeming to bend eastward along the path of the older crack. The inactive old crack and the different times of intersection of the two advancing cracks imply that some cracks are more active than others in the same hydrous media. This condition can relate to the magnitude of tensile stress possess by individual crack tips, which ultimately affect their energy release rate for propagation. Hence, cracks in soils travel with different energy and a crack with greater energy release rate can overshadow a lesser crack (Gauthier *et al.*, 2007; DeCarlo and Shokri, 2014). As may be expected, propagation of the lead crack would slow or cease when it eventually dissipates its energy below the threshold of the soil-water-suction system. On the other hand,

rearward and newer cracks gather more energy to reach the propagation threshold and subsequently dominate the activities. Crack 1 shown above became inactive after early propagation while the other two cracks are still advancing. The northerly-located crack 2, which was the first to intersect the older crack can be said to be the most active between the two advancing cracks. However, the movement of crack 3 is obstructed by a relatively dry clay lump occurring just before the intersection with crack 1. This also caused a slight offset at the contact with the transverse crack as the propagation of crack 2 continues to dominate by bending into the pathway of the redundant crack. This exhibits a cut-off action similar to the formation of ox-bow Lake. The energy efficiency gained by the newer cracks, especially the northerly crack enables not only a re-engineering of the geometry of intersection point but also a realignment of the cracks along the pre-existing path of crack 1. With this development, the upper portion of the failed crack gradually closes possibly by compression at the upper axis between the two re-oriented cracks.

It is acknowledged in the literature that propagation of cracks in a direction perpendicular to the plane of principal stress is influential in the perpendicular intersection of cracks. In other words, since the stress around a crack is parallel to its body, other cracks with less energy will tend to approach it at a right angle. Walker (1986) illustrated such dynamics and identified the large horizontal stress along the crack tip as the controlling force of this interaction (Figure 2.2 repeated below).

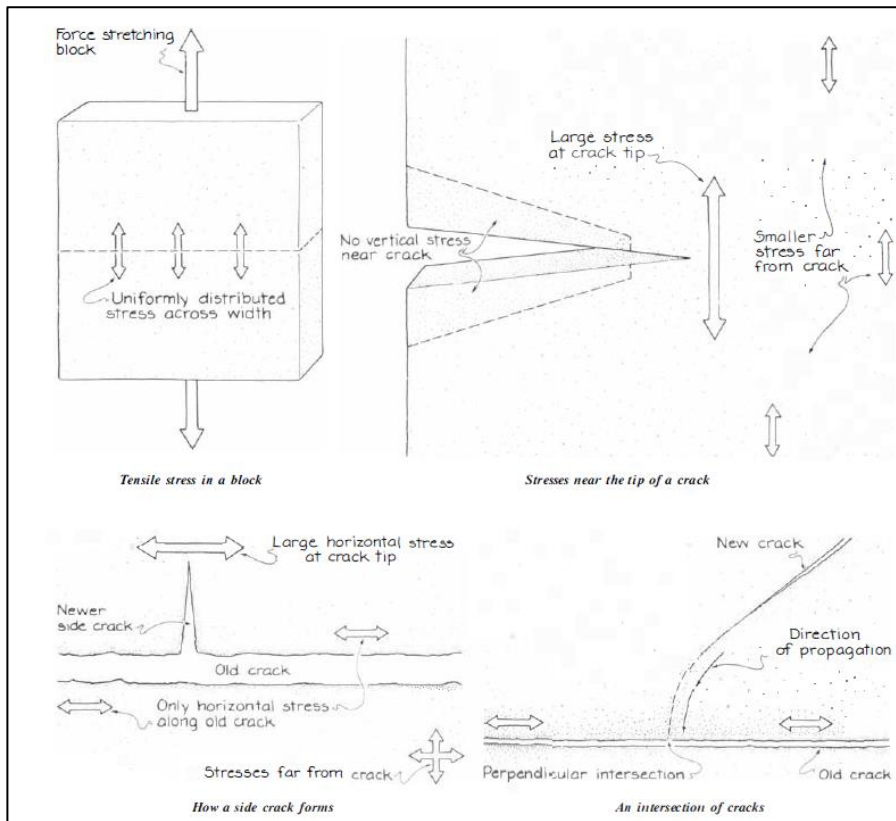


Figure 5.23: Stress concentration and crack intersection model (from Walker 1986)

From this consideration, smaller new cracks with relatively less stress concentration are bent into the larger force field around the bigger older cracks. Similarly, side cracks open and propagate perpendicularly from the intensely dried side walls of the major cracks. Although monitoring the complete sequence of cracking in still camera images can be quite challenging, as most cracks tend to appear and intersect simultaneously, however, important stages of the development were captured in this study through close monitoring.

A good number of cracks in the images intersect in a “Y”-fashion, with intersection angles of more or less than  $90^\circ$ . Such variations in intersection angle of cracks have been reported in the literature. Hexagonal crack is described as cracks forming at  $120^\circ$  and its derivatives (Kodikara *et al.*, 2000). Reports of field studies show they are rare in nature and are associated with fast rate of desiccation resulting in simultaneous cracking. In laboratory study, Shorlin *et al.* (2000) and DeCarlo and Shokri (2014) also reported intersection of cracks at angles averagely  $120^\circ$  and  $83^\circ$  respectively, which they attributed to nucleation of two or more cracks

simultaneously at the same point. Important inference can be drawn from the existing findings. Firstly, simultaneous cracking is common with crack intersection outside angle  $90^\circ$  but not necessarily restricted to angle  $120^\circ$ . In the current study, a common characteristic of crack orientation and intersections outside  $90^\circ$  was observed to be associated with textural flaws in the soil. Earlier in section 5.4.2 and 5.4.3, textural and vegetation control of crack topology were discussed. Extract of features of some cracks network recorded in the laboratory study is presented in figure 5.24 to support the current fact. Interaction of cracks around these flaws clearly shows an angle of intersection inconsistent with the traditional perpendicular angle. A similar feature was also observed in the field in an area with little or no vegetation cover (Figure 5.25).

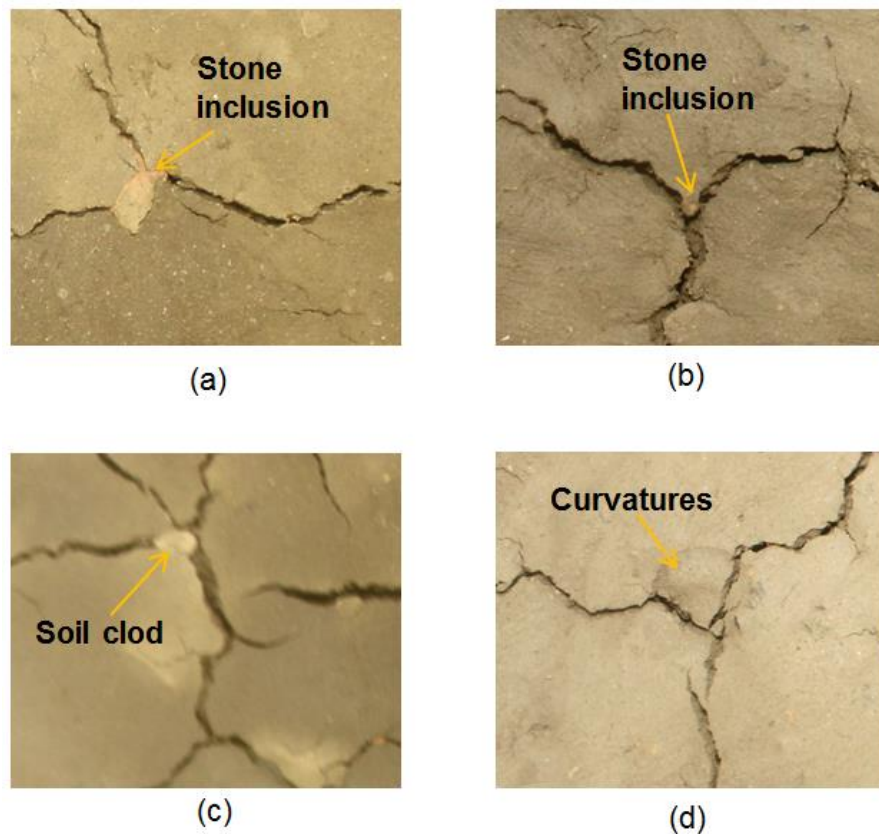


Figure 5.24: Textural control of crack orientation and intersections in soils



Figure 5.25: Polygonal cracks formed around stones and clods in exposed soil surfaces of the embankment

From the foregoing, it is reasonable to regard the existing understanding of the influence of moisture stress field on the dynamics of a perpendicular crack intersection as an ideal case in a uniform fine grained soil e.g. mud, clay slurries etc. In reality, the stresses in engineered clay fill are complicated by textural inhomogeneity including inorganic matters, coarse inclusions, large clods etc. These features are sources of local resistance in the soil, and depending on their curvatures and radius, can exert a great influence on crack topology and intensity. The present study associates the formation of simultaneous cracking with textural flaws, which gives rise to cracks intersection at variance with a perpendicular angle, depending on the curvature and size. However, the dynamics of intensified stress around these non-plastic elements in the soil can agree with accelerated rate of desiccation, which workers have suggested as influencing hexagonal crack intersection.

Among the various pattern of crack intersection recorded in the experimented soil materials, the Gault Clay specimen with the highest amount of coarse materials exhibited the greatest disorderliness in crack orientation. Cracking in the Nafferton Clay material showed relatively straight outlines. The result underscores the importance of good compaction to densify and homogenize the fills.

#### 5.4.5 ***Effect of wetting and drying cycle on cracks outline***

The intensity of cracking in the soils was showed to significantly increase by cyclic wetting and drying. A common feature in the cyclic experiment was repeatability of old cracks. Most of the cracks formed in the first cycle were closed during rewetting but subsequently re-opened as the rewetted

soil dries. Examples of crack intensity and repeatability between the first and second cycle are shown in Figure 5.26.

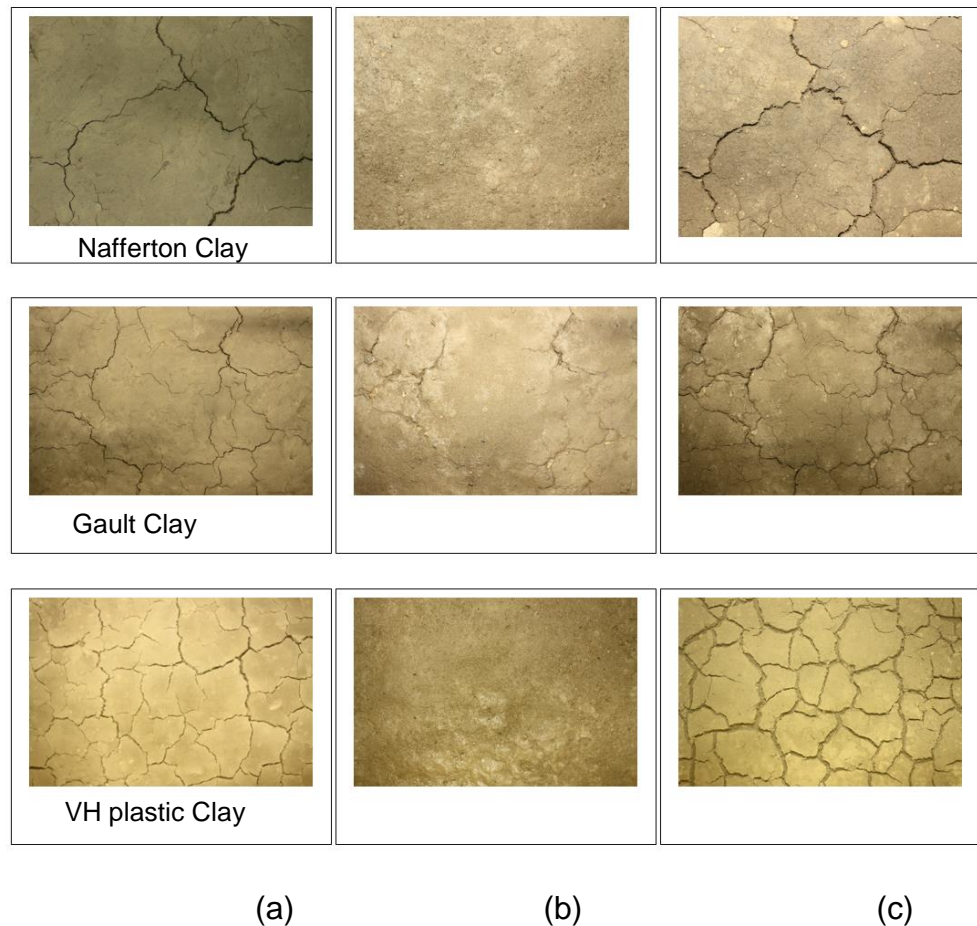


Figure 5.26: Crack repetition during wetting and drying of Nafferton, Gault and VH plastic Clays soils (a) End of 1<sup>st</sup> drying cycle, (b) Rewetting and (c) End of 2<sup>nd</sup> cycle drying cycle.

In some cases, the cracks do not close completely and simply expand geometrically in the next drying cycle as depicted in the middle row. As discussed in section 4.4.5, wetting of soil breaks particles bond and locations of old cracks in the soil are relatively weaker in bonding which become more susceptible to new fracturing. Apart from repeatability, the crack topology was also affected by cyclic wetting and drying with a common shift in orientation and intersection of the cracks. Analysis of the time lapse images of the crack morphological development reveals that the final appearance of most of the crack intersections appeared to have changed during repeated wetting and drying. The trend appears to be controlled by changes in the cracks orientation and width. To illustrate this observation, extracts of typical iterated crack intersections in 2-cycle of

wetting and drying are presented in Figure 5.27. The selected images represent the final stage of development in each cycle.

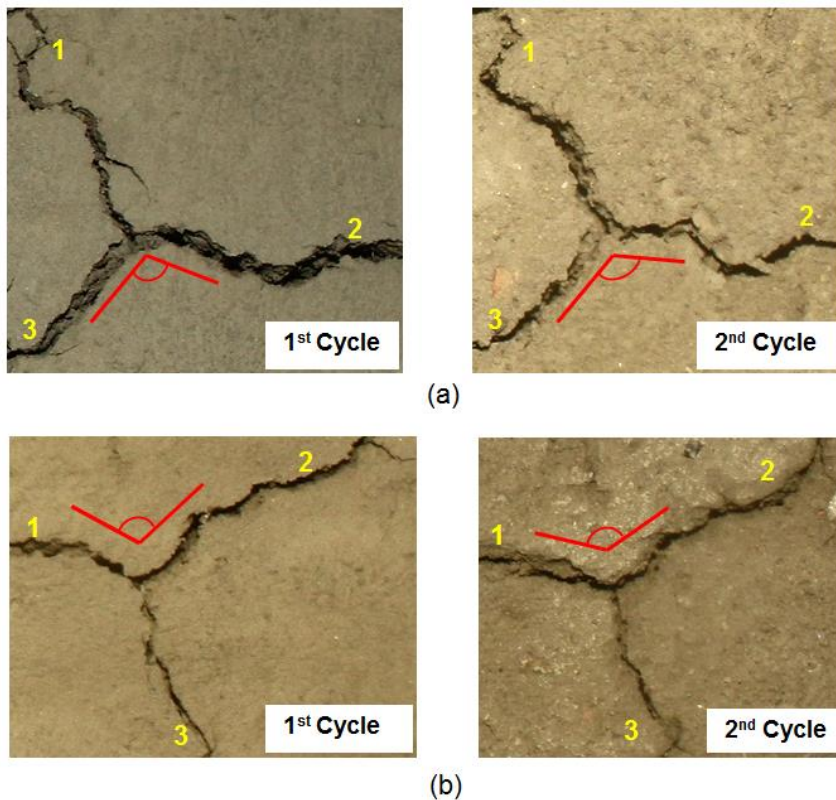


Figure 5.27: Illustration of changes in crack orientation and intersection in 2-cycle of wetting and drying

Prominent in images of the 2<sup>nd</sup> cycle are changes in the orientation of individual cracks resulting in a wider angle of intersection. The initial perpendicular angle of intersection in the first cycle is changed to an acute angle in the second cycle as arm 2 in Figure 5.27a and arm 1 in Figure 5.27b becomes straighten close to the point of intersection. The new crack orientations seem to be influenced by increased in individual crack width in the second cycle. The increased crack geometry apparently leads to new crack architecture essentially by the tension taking place within the cracks. In another extract from 6 cycles of wetting and drying (Figure 5.28), the re-orientation of cracks at the points of intersections is seen to progress gradually through successive cycles. In the outline case marked A, an initial obtuse intersection changes to a right angle while in the outline case marked B, a near perpendicular intersection is transformed gradually into an obtuse angle.

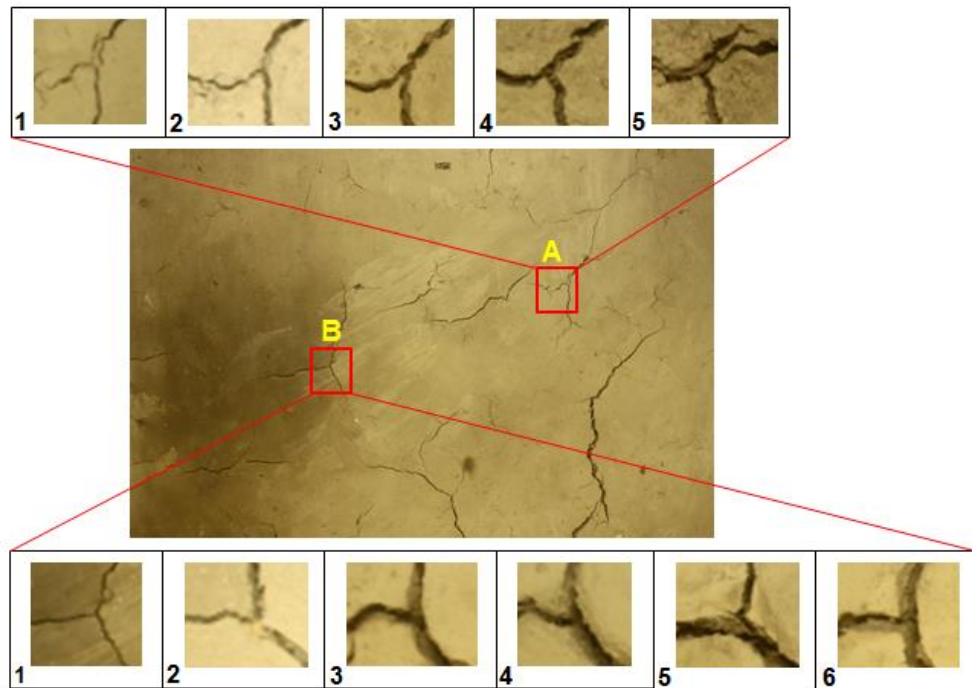


Figure 5.28: Changes in crack orientation and intersection in multiple wetting and drying. Cycle number at bottom left corner

From these traces, crack re-orientation can be said to take place at the point of intersection as their geometry increases. The orientation of the intersection in the 6th cycle in box B approximates the orientation in cycle 1. This is another possible indication of aggregate stability or equilibrium attainable by soil structure with increasing cycle of wetting and drying discussed earlier in section 4.4.5.

A change in inter-aggregate arrangement can likely bring about the increase in crack geometry hence, a re-orientation and intersection. It is considered here that as the soil dries after rewetting, the drying stress would realign to a new system of interparticle arrangement in the soil, which would be pronounced along old cracks outlines. Wetting of the soil practically results in particle disaggregation with the fines mostly dispersed in the solution. Sediments would, therefore, accumulate prominently along existing cracks, which form local troughs. Mainly, the suspended fines with a few coarse-particles from the loose edge, are mobilized into the cracks by flooded water. This resultant geometry essentially commands the propagation of cracks which commonly explores the path of effective energy release. With washed up fines prominently settling in sites of old

cracks, their re-opening dominate the new crack system as shown Figure 5.29.

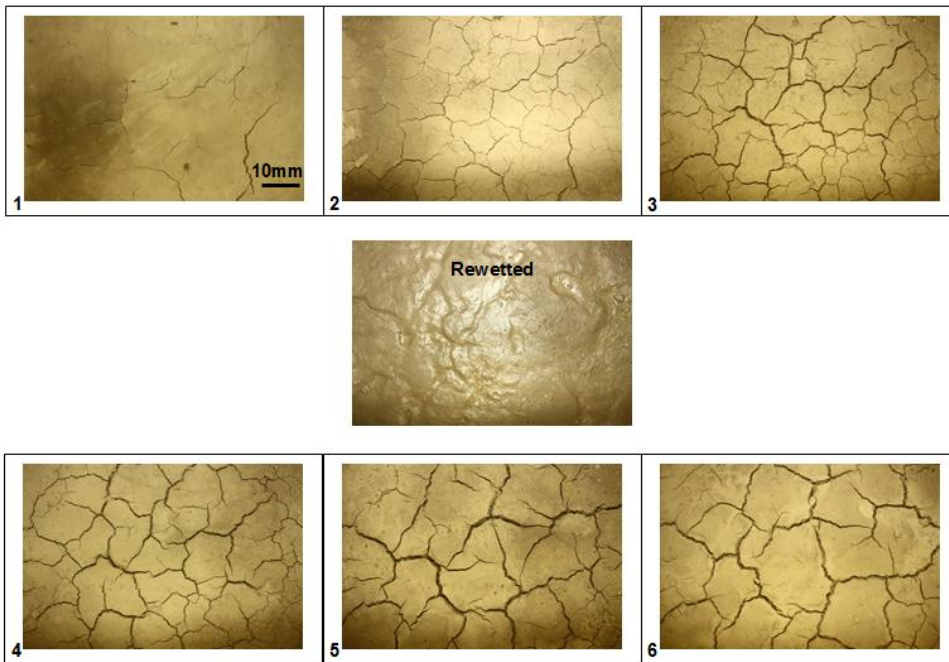


Figure 5.29: Progression of desiccation crack pattern in compacted clay soil subjected to 6 cycles of wetting and drying. Center image shows prominent fines cloaking old crack surface after rewetting

In addition, a more complex accumulation of the washed out particles can be expected at junctions of a crack intersection, being a much larger geometry with an interaction of variance particles. The gap-graded dynamics then plays a defining role in the selection of the path of a propagating crack. As depicted in Figure 5.29 above, major cracks trending at the central area in the image of the 5<sup>th</sup> cycle are reoriented in the 6<sup>th</sup> cycle mainly at intersections.

Generally, increased cracking, and multiple wetting and drying cycles can exacerbate the reduction of shear strength in slopes. Cracks preserved across alternate dry and wet seasons is one of the acknowledged factors responsible for accelerated pore water pressure degradation and the occurrence of anomalous pore water pressure zones in slopes (Anderson et al 2001). In addition, crack orientation can influence water catchment, runoff and erodibility on the slope face. Therefore, monitoring of seasonal and diurnal architectural changes in crack is important to update the effect on slope.

#### 5.4.6 **Cross-section of cracks**

A cast of the soil crack was prepared using high viscous mold cast substances, namely epoxy resin and silicon rubber (3.4.8). The silicon rubber material did not cure very well inside the soil due perhaps to insufficient aeration. Therefore, the full crack cast could not be recovered. The epoxy resin, on the other hand, cured into a hard plastic material with a reasonable imprint of the subsurface cracks. However, part of the cast was lost to breakage during the recovery process from the soil. Although both materials did not produce a full cast, however, the reasonable part of epoxy resin crack cast recovered gave useful insight for a preliminary understanding of true three-dimensional crack morphology. A part of the crack cast made from epoxy resin is shown in Figure 5.30.



Figure 5.30: Crack cast

The cast shows that the surface cracks and their intersections continue in the soil subsurface. This clearly demonstrates that cracking in soil is a 3-dimensional process. As depicted by figure 5.30a, the cracks boundary observed at the surface continue below the ground as indicated by the dominant perpendicular intersection (Figure 5.30a). Within the thin soil (50mm) used for the crack cast, the vertical cracks penetrated the entire soil thickness. Crack width measured at the surface and bottom of the soil block was 5mm and 3mm respectively, indicating a decreasing crack width with depth. Although the vertical extent of this change was restricted by the soil thickness, a similar crack geometrical trend was measured in the embankment. The inverse trend between crack width and depth coupled with the dynamic moisture gradient found associated with cracking in this study reasonably support a triangular cross section as a valid crack shape. However, a rectangular cross section has been suggested for large penetrative cracks common in Vertisols. Apart from the consistent width possible in large cracks at shallow depth, the change in hydrologic

property with crack development showed in this study does not support the rectangular crack hypothesis in any way.

Horizontal cracking was revealed in the crack cast. This is indicated by the miniature outgrowth of the epoxy material (Figure 5.30). Such lateral flow could only have taken place within an existing crack space. Since this feature associate with a relatively large crack branch, it is believed here that it represents a developing horizontal crack. As the soil dries, the parent crack surface continues to enlarge and can provide conditions of significant moisture gradient along its exposed vertical walls. Moisture gradient between layers and flaws lodging at the exposed cracked surface presents anisotropic condition capable of initiating a horizontal crack. The former condition is illustrated in Figure 5.31.

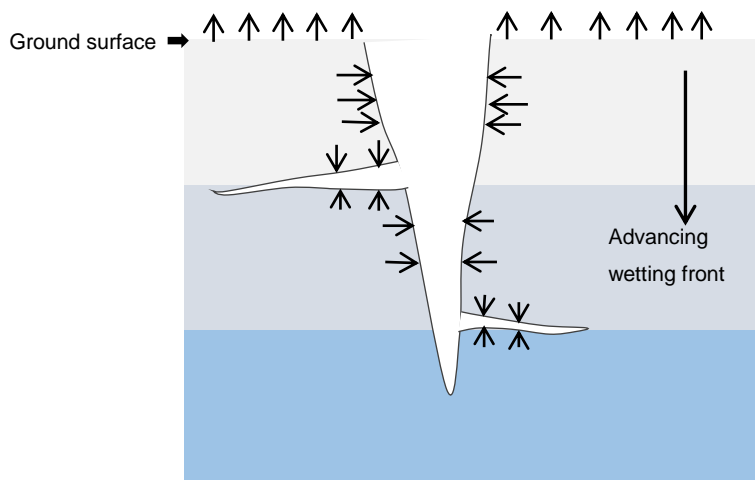


Figure 5.31: Schematic of vertical moisture gradient and the development of horizontal cracking in soil. Open crack walls enable secondary evaporation.

The propagation of horizontal cracks will generally increase the potential of soil mass degradation and can increase the extent of rainwater distribution in slopes.

#### 5.4.7 **Surface processes and the modification of cracks geometry**

In this study, crack outlines mainly the aperture, appeared significantly modified after their formation. Loose soil particles around the dry crack surface were eroded by wind. Also during rainfall, the surface materials were either wash into the cracks or eroded away by runoff. The secondary processes greatly affected the crack aperture, commonly leaving behind an irregular outline. As a result, the affected cracks displayed anomalously large width at some section. In addition, the loose soil in-fillings also

considerably contributed to the crack closure. Figure 5.32 shows wedges of in-filling soils in the crack.



Figure 5.32: Loose and wetted soil particles (arrowed) swells within a crack. The fallen soil particles either directly filled up the crack by mass or swell in volume and fill the cracks when wetted. The process of crack closure through filling and swelling of expansive soil particles is illustrated in Figure 5.33.

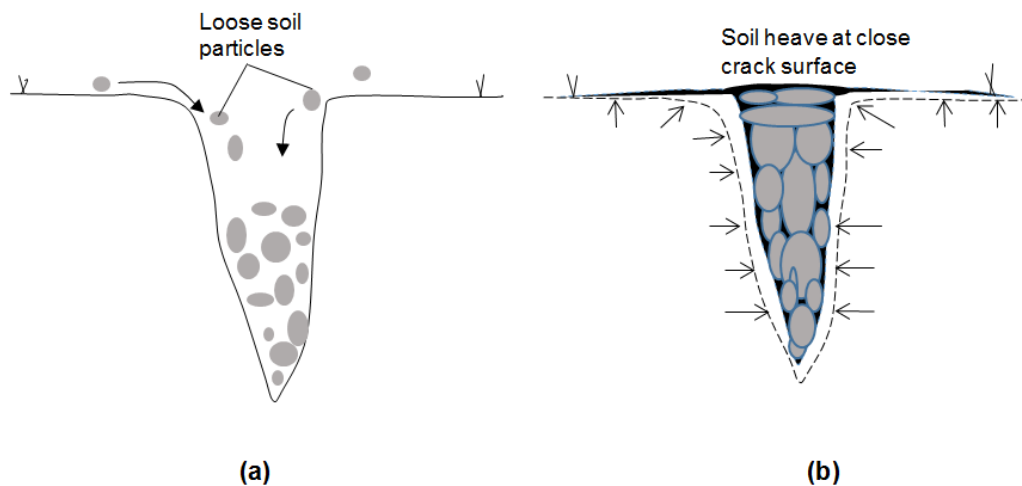


Figure 5.33: Illustration of the process of crack closure (a) Loose material fallen into cracks during dry period (b) crack closing both by swelling of wetted soil block and particles in the crack

Swelling of soil mass in open crack spaces can contribute to soil heaving and reversal of soil profiles. When dry soil particles, which fell into cracks during the dry season (Figure 5.33a) are rewetted, the cracks close both by swelling pressure likely exerted on the soil block on either side of the crack and by swelling of the infilling materials (Figure 5.33b). In the former,

the pressures are exerted on the crack walls tend to push them together by compression. The wetter materials at the bottom layer of the crack can also contribute to the swelling pressure. This can force soil material at the upper part of the crack towards the surface. With time, the soil profile is inverted with materials originally occurring in the subsoil moving up to become surface soil and vice versa. Such a reworked soil profile within the closed cracks can have a strong influence on their re-opening. With an entirely new composition, the old crack site would exhibit structural arrangement that more or less creates ineffective hydrologic characteristics against the crack reopening. During the field study, many of the closed cracks affected by this kind of process showed loosed soil texture with no subsequent cracking.

Apart from the effect of water and the wind on crack outline modification, biological activities such as animal burrow were also found to affect the morphology of cracks on the embankment. Small rodents were frequently seen digging at crack sites. Animals usually burrow in search for food or shelter, and rodents are very common in grass cover slopes. Apparently, the cracks constitute weak zones for this activity. An important effect of the burrowing was that loosed soil particles are displaced around the cracks with the burrow portion being wider and deeper than other sections of the affected cracks (Figure 5.34).

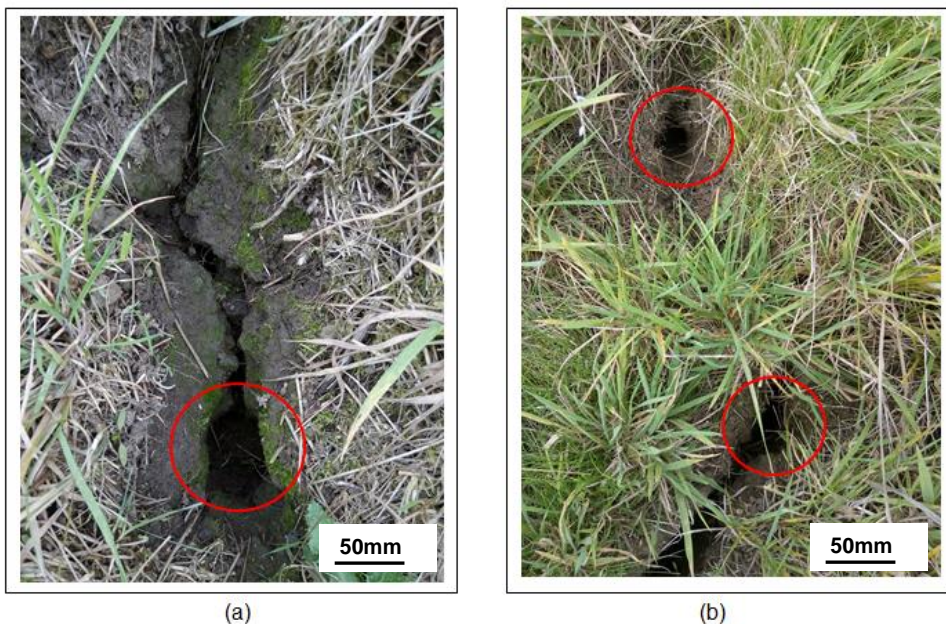


Figure 5.34: Rodent burrows (circled) enhancing crack aperture

The dynamics of burrowing can also lead to soil reversal as surface particles are pushed further into the burrow while excavated materials are heaped on the surface.

Other types of burrowers prominently affecting the cracks in the embankment are earthworms and slugs (Figure 5.35 a and b). The activity of these animals involves break the soil clods to form a soil mulched over the cracks (Figure 5.35c and d). The soil mulch provides a large surface area for effective wetting and swelling.

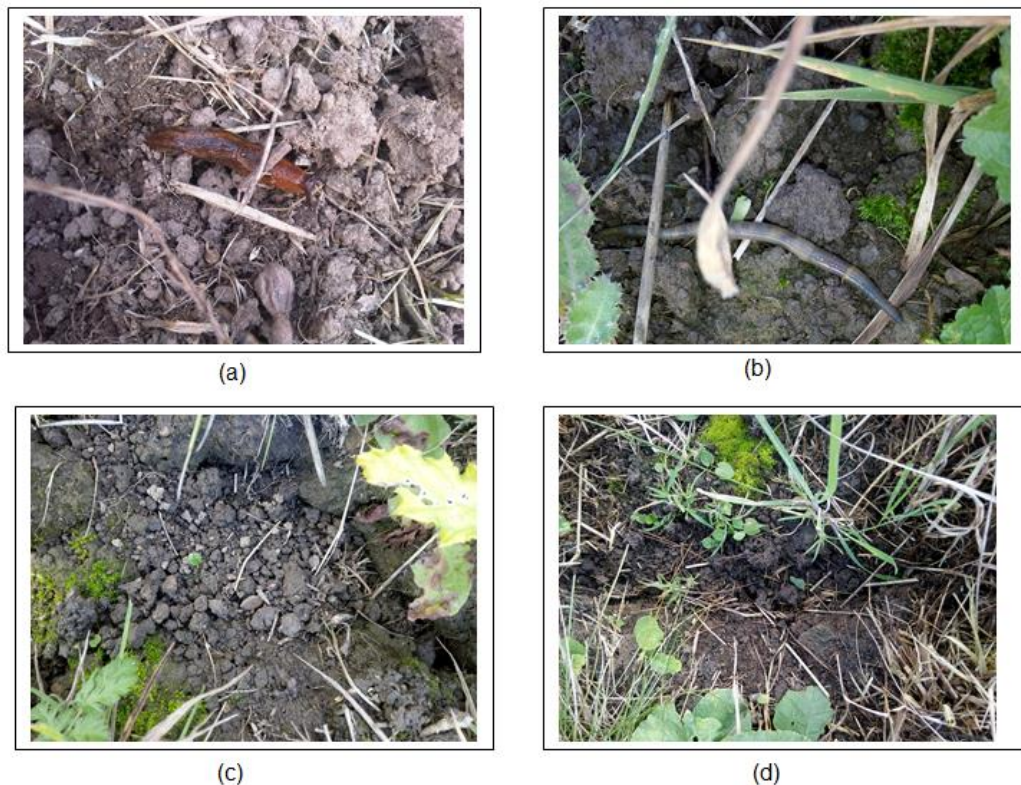


Figure 5.35: Effect of bioturbation on surface cracks: (a) and (b) common worm species in the embankment, (c) and (d) worms-generated mulch swells over cracks outline

The prominent effects of animal activities on crack's architecture require recognition, especially when considering the potential of crack sizes. Bioturbation is generally recognized as a key geomorphological factor in many landscapes. According to Gabet *et al.* (2003), their role in disrupting the integrity of stored hazardous wastes has informed many barrier designs to include normal ecological processes. Likewise, the potential effect of ecological processes is worth consideration in the stability analysis and management of infrastructure slopes, especially in aspect of effect of cracks on the slope hydrology. In order to account for the irregularities in the crack aperture, crack width was averaged from

measurement at different reference points along its length including burrows.

#### 5.4.8 *Relationship between crack geometry properties*

Measurement of crack geometry in the field can be challenging for several reasons including harsh weather, accuracy, spatial distribution etc. Cracks are generally non-linear. The dimensions of the geometric property of the cracks were relatively different. The lengths and depths of the cracks were several magnitude greater than the widths as depicted in Figure 5.36. This suggests that crack geometry is different in magnitude and direction of propagation. This section seeks to establish the relationship between the crack geometry for practical application.



Figure 5.36: Surface crack geometry. Crack length, **L** is  $\gg$  width, **W**.

Generally, geometric features can exhibit directional difference in magnitude depending on the influencing factor of their formation. In literature, the forces acting at the crack tip has been illustrated as shown in Figure 5.37 (Frost *et al.*, 1974; Atkinson, 1987).

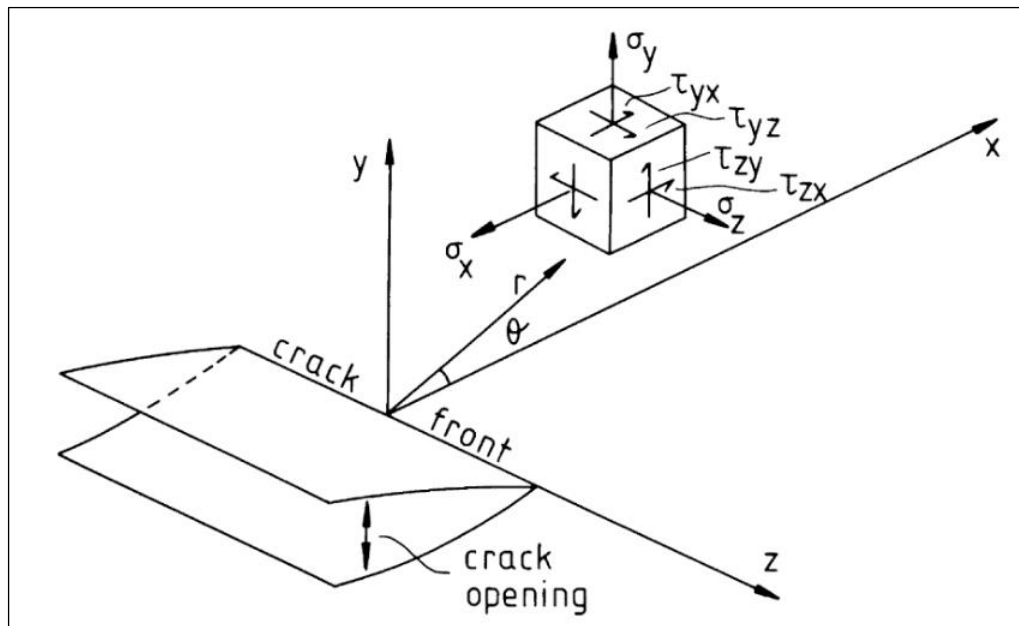


Figure 5.37: Notation for stresses at the crack tip. The point on the crack tip is the origin of the coordinate system and the z-axis lies along the crack tip. Displacements of points within the crack body when the body is loaded are  $u$ ,  $v$ , and  $w$  in the  $x$ ,  $y$ , and  $z$  directions. From Frost *et al.* (1974) and Atkinson (1987)

Considering an elliptical outline typically assumed stress around crack, maximum stress is, therefore, considered to occur at the crack tip. As this part of the crack propagates in the direction of receding moisture gradient in a drying soil, it is fundamental to understand that greater work is done in the propagation of crack front leading to crack elongation and deepening. Less stress intensity occurs around the central part of the crack, which defines the width (Figure 5.12). This part of crack would, therefore, propagate with minimum stress against a higher stress field in the predominantly drier surrounding left behind by advancing crack front. Consequently, crack width is small compared to its depths and length.

To further examine the strength of the relationship among the crack geometric properties, linear regression analysis was carried out on the field recordings. Syntheses of the results showed a strong correlation between the crack width and depth with  $R^2 = 0.77$  and  $0.75$  for the poorly compacted and well-compacted embankment respectively (Figure 5.38). The  $R^2$  for width - length correlation was consistently less than  $0.05$ , meaning a weak relationship.

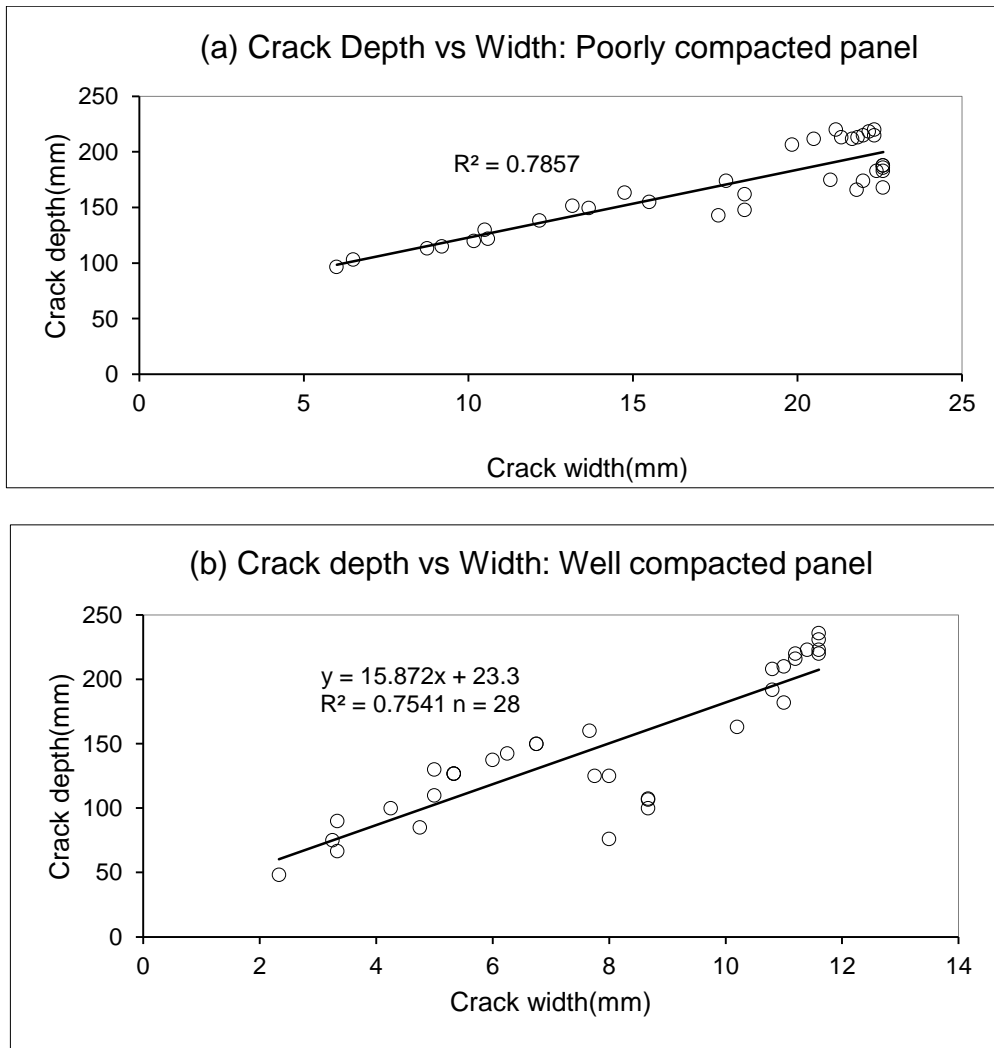


Figure 5.38: Correlation between crack width and depth in the embankment (a) Poorly compacted panel (b) Well compacted panel

The values of correlation coefficient obtained from the laboratory measurement in Nafferton Clay material reasonable compare to the field result. The  $R^2$  was 0.70 (figure 3.39a). For the Gault Clay and VH plasticity clay specimens,  $R^2$  was also positive with 0.74 and 0.94 respectively (Figure 5.39 a and b). The higher value obtained in the VH plasticity specimen signifies a relatively stronger relationship. This can be attributed to higher intensity of cracking in this specimen due to prominent geometry, which strengthens the relationship.

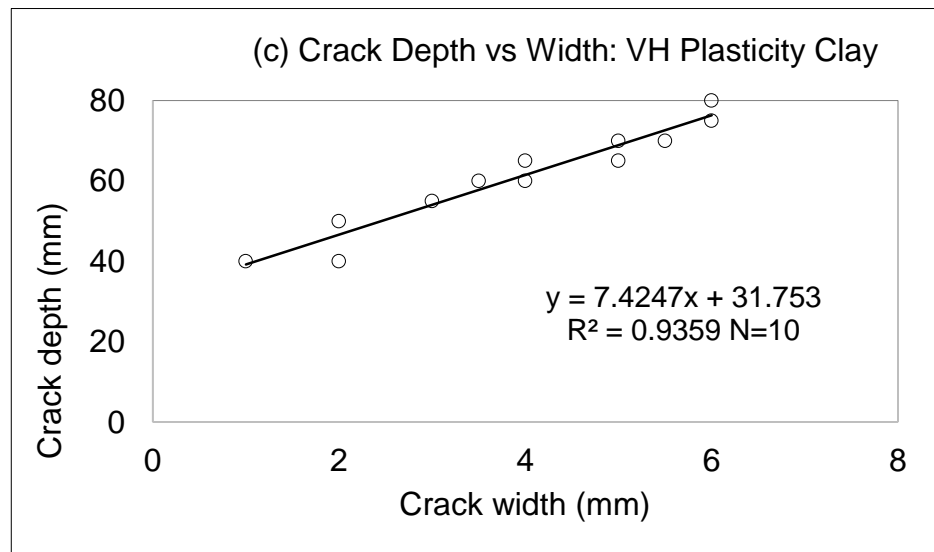
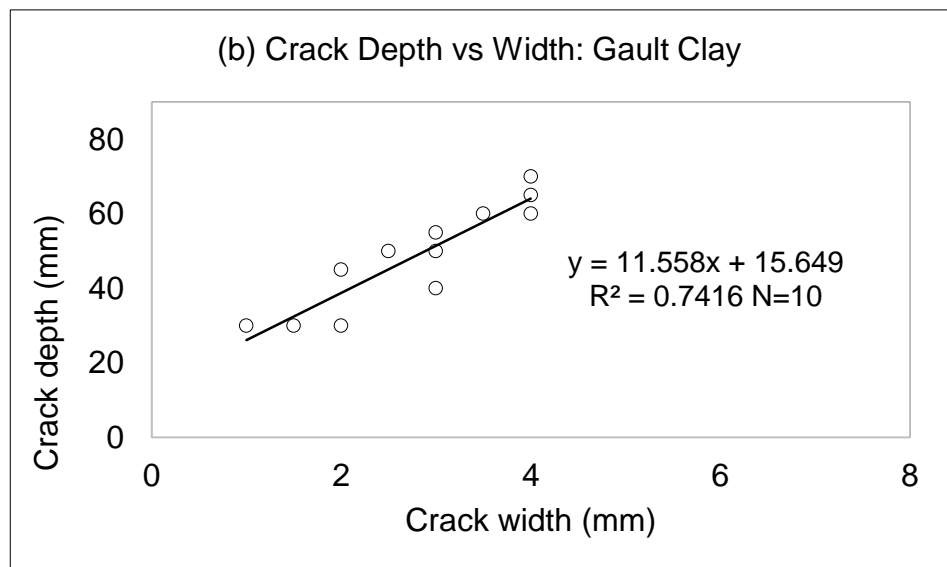
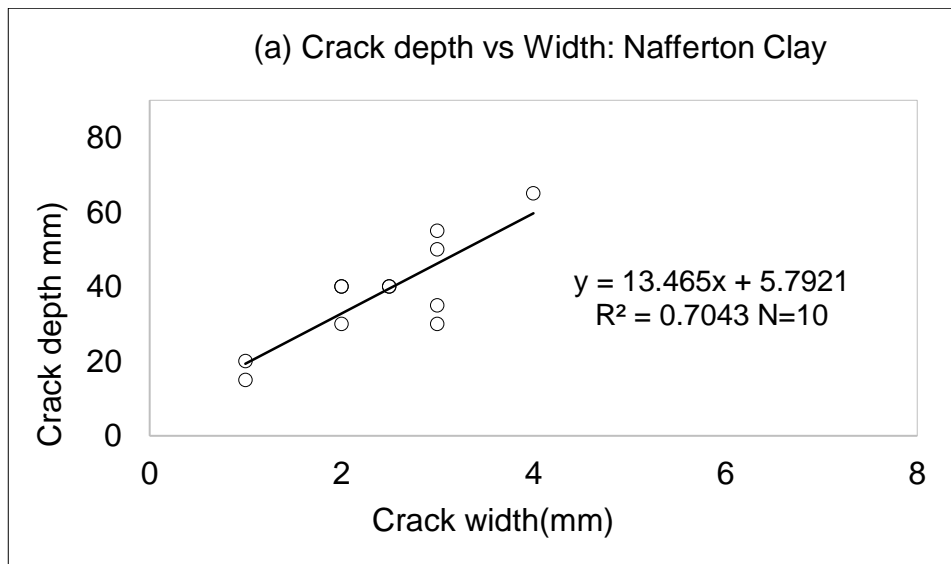


Figure 5.39: Correlation of cracks depths and widths in plastic soils  
 The value of  $R^2$  obtained in the VH plasticity material, however, is  
 inconsistency with what is reported in the literature for Vertisols (average

$R^2 = 0.5$ ) by Bandyopadhyay *et al.* (2003) and Kishné *et al.* (2009). This is in view of the fact that Vertisols are similarly very high plasticity soils and are recognized for the occurrence of very deep cracks. This statistical difference could be caused by the fact that the measurement in the Vertisols was carried out on micro-topography features, which characterize this type of soil. However, from the present study, the general increase in  $R^2$  of crack width vs. depth as the soil plasticity increases is consistent with the trend of crack intensity presented in sections 5.3.2. The trend also supports triangular cross sections for three-dimensional crack morphology (section 5.4.6). This is important for adequate representation of cracks shape in analytical and numerical procedures. In addition, the relationship can serve as a rule of thumb to estimate crack depth when the surface width is known. Therefore with regard to field measurements, crack width is much easier to be measured than crack depth.

However, crack depth is commonly emphasized in slope stability and hydrology analysis. This is because of its potential of affecting the length of slip surfaces as well as contributing to unstable pore water pressure at deeper soil layer. In section 5.4.1, it was showed that vertical changes in moisture are important in predicting the depth of propagation of cracks. The rate of changes of the drying stress field in the highly varied hydrologic condition is likely to affect the depth that can be reached by a propagating crack in a soil. Based on this condition, Aubeny and Long (2007) derived a moisture diffusion-suction relationship for prediction of crack depth. This was specifically for a uniform, homogeneous soil mass. Considering the complex hillside processes in an engineered slope leading to a transient hydro-mechanical soil profile, this derivation requires modification in order to realistically predict the depth of cracks in this type of condition.

## 5.5 Summary

The cracking characteristics of three common embankment construction soil materials in the UK were presented and comprehensively discussed including their desiccation rates, soil water retention, suction profiles etc. Under the impact of a cyclic wetting and drying to mimic alternating warm and dry climate conditions in natural environment, the plastic materials

displayed different moisture loss behavior related to their water retention properties. Moisture loss was greatest in the intermediate plastic soil (Nafferton Clay). The higher plastic materials (i.e. Gault and VH plastic Clays) on the other hand significantly inhibit moisture diffusion with only a small amount of water lost over time. The distinctive moisture loss behaviors are accompanied by corresponding soil suction characteristics developed as the pore geometry changes under capillary tension. Crack initiation was almost instantaneous as the soils begin to dry. The moisture condition at this period approximates the plastic limits which form the initial state of the soils. Couple with common observation of stable cracking behavior near the soil shrinkage limit in the literature, this led to the assumption that soil consistency may define a critical soil water suction boundaries for crack development in engineered clay fills.

Plasticity behavior is imparted in soils by the presence and amount of clay minerals and their degree of moisture affinity. Potentially, the more plastic soils are composed of very high hydrophilic clays e.g. montmorillonites, characterizes by overall properties, which enable the development of very large meniscus between their small pores during dehydration.

Consequently, moisture change in such soils leads to significant volume change influenced by suction. Suction profiles presented for Nafferton and Gault Clays materials shows the later exhibits higher ranges for any given moisture content as desiccation proceeded. Although suction record was not available for the Bentonite-Nafferton clay material, this VH plasticity clay representative exhibited more volumetric shrinkage than the rest pointing to a greater suction. In addition, the results of estimated suctions from the Nafferton and Gault Clays materials reasonably suggest the VH plastic soil created from Bentonite additive would have a higher suction estimate. Shrinkage in soil induces tensile stresses under restraint. Since cracking is a tensile feature, the intensity of cracking in the soils generally increased as the soil plasticity increases. Interestingly, the increase in CIF was nearly double for an equivalent increase in plasticity, the soil density remaining constant.

The influencing factors in crack propagation in the soil materials were studied. Vegetation affects soil moisture content through increased

evapotranspiration. However, the absence of vegetation led to increase desiccation and formation of network of cracks mainly due to direct exposure to climate intensity and lack of mechanical effect of root to restricting cracking. Crack orientations and intersections are generally influence by the direction of the diffusing moisture gradient, and this suggests the resultant stress field developed in the soil during drying. Textural defects in the soil act as mechanical interfaces and greatly the crack orderliness. Therefore, the stress field appears nonlinear as the cracks are initiated and oriented randomly at sites of defects. However, the net pattern ultimately reflects the overall pattern of the moisture front. From a mould cast of crack prepared in the study, it was showed that crack is a three-dimensional geometry, and the width decreases with depth. Therefore, the cross section approximates a triangle. Crack repeatability was recognized as a structural phenomenon related to cyclic wetting and drying in the soils. The cracks were commonly repeated along the location of old cracks. Crack intersections also undergo a gradual angular transformation during multiple wetting and drying. This was influenced by re-engineering of the geometry of cracks intersections by the cyclic condition.

Finally, surface processes e.g. the wind, water, as well as activity of bioturbation substantially modify the crack morphology after formation. These common ecological processes are important to consider in the analysis of slope stability and hydrology because of the potentials of crack depth and water catchment. Ultimately these dynamics suggest that cracking is a nonlinear process which is important to understand to improve solution slopes involving them.

## 5.6 Conclusion

The analytical results show that crack intensity has a strong correlation with soil plasticity. This relationship is down to the rate of moisture movement and the magnitude of inter-particle forces generated during drying in the materials. The finding reasonably suggests that infrastructure embankment constructed with high plasticity soil materials would experience greater cracking under the same desiccation condition and time. The crack features is further affected by textural characteristics of the soils while cyclic wetting and drying lead to complex hydromechanical profile, which significantly exacerbates the cracking behavior in the soils. Overall, the cracking potential of the plastic materials suggests a geographical implication in the UK with respect to local materials used in embankment construction.

## **Chapter 6 General summary, conclusions and recommendations**

### **6.1 Introduction**

The primary purpose of this study was to characterise desiccation cracking and moisture movement in the near surface soil in engineered clay embankments. The study originates from problems facing transport infrastructure slopes exposed to temporal changes in their surrounding environment, particularly climate condition. In several hypotheses advanced to explain the likely responses of slopes to environmental impact, surface cracking is a key factor. Cracks have both mechanical and hydrological effects on slope performance. As structural discontinuities, they directly reduce the mechanical strength of the soil block. Cracks acts as secondary permeability pathways, which reduce runoff and accelerate rainwater infiltration into the soil. The implications are increases in soil water content, increases in pore water pressure and a reduction in the shear resistance. These conditions are crucial in slope stability problems. Despite this significance, the factors controlling soil cracking in engineered slopes still represent a poorly understood area. A majority of studies on soil cracking deals with the qualitative behaviour and the studies are conducted in a material condition that is unrepresentative of the engineered soil. Hence, the impetus for the present study to quantify desiccation cracking and their behaviour specifically in engineered soil condition.

#### **6.1.1 *Research approach and methods of analysis***

In this study, specific objectives were considered based on critical factors in the embankment construction and performance in the UK. Accordingly, soil density, layer thickness, soil consistency, embankment aspects, cyclic wetting and drying, soil water content etc., were selected as control variables. A wide field and laboratory study program was developed and implemented to actualise the objectives. The study approach involved innovative research facilities. The field study was conducted on a well-instrumented clay embankment while the laboratory study was carried out in a bespoke climate control system designed to simulate, as close as

possible, the relevant environmental factors surrounding in situ embankments during crack development.

After a comprehensive test program, robust, high-quality data for analysis were obtained. The data were processed and analysed using various computer aided tools including Microsoft excel, digital image techniques etc. Relevant empirical relations for the estimation of other classification parameters, e.g. volume of a crack, evapotranspiration, soil suction etc. were also employed. The results were discussed in appropriate themes and sub-themes to arrive at valid conclusions in this study. Presented in this chapter are a summary of the discussions and findings. The study outcomes according to the respective study objectives. Finally outlined are the conclusions and recommendations for further work.

## **6.2 Hydromechanical response in engineered clay embankment**

The dynamics of water movement can significantly affects the behaviour of expansive soil. The process can be complicated in unsaturated condition. As a result, matrix suction is prominent and fluctuate in the partially saturated soils. Ultimately, variations in the near surface hydrologic conditions observed in this study relates to impact of weather condition of the surrounding atmosphere. Coupled with the characteristic geometric and engineered condition of the embankment, the hydrologic response showed distinctive behavior bordering on changes in the soil suction as the solid particles interact during the volume change in the impacted expansive material. In this study, the cracks developed significantly by opening and closing as soil moisture changes. Since cracks are tensile features, their development under this condition depicts a coupled hydro-mechanical process. Consequently, the trend of hydrologic changes in the different soil condition was analysed and used to characterise the desiccation cracks.

### **6.2.1 *Moisture behaviour in engineered clay embankment***

The construction of the embankments used in this study involved both materials, environmental and engineering considerations. The main soil property characterizing embankment fills in the UK is plasticity, a crucial factor in the shrink-swell behaviour of clay materials, with well-known

slope stability problems arising from many of them. The engineering variables of the embankments considered in the hydrologic process include the level of compaction (density), soil layer thickness, aspect etc. These factors were studied under cyclic wetting and drying conditions representing alternate rainfall and sunshine. In all the tests, moisture loss were characteristically different. The profiles of moisture enabled the quantification of rate of desiccation, a critical parameter that defines the moisture behaviour of the soils. The desiccation rate was found to decrease with increased in soil density, with the poorly compacted embankment soil showing greater moisture loss than the well-compacted counterpart. This pattern is ascribed to the higher propensity of moisture movement in loosely packed soil structure. A faster moisture decay was also observed in the thin compacted soil specimen as well as in the soil compacted in one layer. The former is because of the short distance of moisture travel for evaporation at the surface while the latter relates to the inefficient distribution of compaction effort resulting in a relatively loose soil compared to a similar thin soil specimen compacted in two layers.

Under a given environmental and engineered condition, a distinction exists in moisture characteristics of the slope aspect. The results indicate that this difference relates to intensity of climate impact leading to higher evapotranspiration in the exposed South facing slope of the embankment. Three typical embankment construction materials in the UK were tested, ranging from intermediate to very high plasticity. The materials also displayed unique moisture profiles with the highest moisture loss recorded in the low plasticity soil. The rate of moisture diffusion in these materials was the primary factor responsible for this behavior as the specimens were compacted to approximately the same density. Due to potentials for a stronger affinity to water, evaporation moisture loss was slower in the very high plasticity soil. This behavior relates to high porewater potentials associated with both the increased clay particle surfaces with increase in the amount of clay and increased potential for water affinity with presence of hydrophilic type of clay minerals.

Trends of moisture movement in each of the simulated soil conditions changed during repeated wetting and drying. In the 2-cycle test, the rate of

moisture loss was generally slower in the second cycle. However, in the multiple cycle test this moisture loss trend tend to reverse between the 3<sup>rd</sup> and 4<sup>th</sup> cycle. Since during rewetting, approximately the same amount of moisture lost during drying was used, the observed differences in the rates of desiccation between two alternating cycle directly associate with structural changes likely in the volume changing soil. Wetting and drying event can disaggregate an initial homogeneous soil. The resulting inhomogeneous structure, including presence of cracks, can segment moisture distribution in the soil leading to a significant change in the profiles as the cycle increases.

Overall, moisture loss in the soils displayed exponential behavior with characteristic gradients. This trend fundamentally depicts a changing relationship in the soil's phase relation during desiccation leading to the quantifiable responses in the soils e.g. suction, shrinkage and cracking. It follows that the greater the interparticle interactions, the more significant this measurable effects would be, with a stable state capable of resulting when the moisture loss profile approaches equilibrium.

#### **6.2.2 *Suction profiles in the near surface clay layer***

A significant development of soil suction were found to associate with the near surface moisture movement in the soil. Fundamentally, soil water movement relate to the pressure potential in the voids. The two parameters displayed close trends in the embankment soil in a clear response to changes in climate events, i.e. dry and wet spells. The well-compacted panel of the embankment showed the largest suction apparently due to increased capillarity as densification decrease the effective pore size. Moisture change was also slow in the dense soil, corresponding to the high suction state and by implication a low permeability.

Analysis of the hydrologic trends in the plastic soils reveals that suction increased as the plasticity increases. Therefore, the high plasticity Gault Clay material displayed greater suction than the intermediate plasticity Nafferton Clay. This trend mostly arises from the dependence of suction on water affinity in clay minerals (adsorption). Practically, water retention

in soil is strongly affected by soil structure and texture. Following this background, the very high plasticity soil created with Bentonite additive would have the highest range of suction among the three plastic soils tested.

Quantitatively, a small amount of moisture loss in the soil was found to be accompanied by a significant change in suction. The results showed that the cracking suction conditions were much wider than similar moisture condition with implication for intensive cracking within a short change in the drying condition. Increased in suction beyond the threshold cracking moisture conditions did not lead to any significant crack development in the soil suggesting a limit condition.

### **6.2.3 *Desiccation cracking and hydrologic changes in clay embankment***

To quantify the development of cracks and near surface changes in hydrology, the volumes of cracks estimated with an empirical equation, was used. The volume estimation involved the geometric properties measured on the cracks and is therefore considered as a holistic parameter to quantify the morphological development. Analyses of field recordings showed that the crack morphological changes trend closely with profiles of moisture and suction in the embankment over the period of the survey. Maximum volume of cracks estimated in the embankment corresponds with the period of highest suction and lowest soil moisture and vice versa with minimum volume of cracks. Transient increase and decrease in the volume also correspond temporal change between dry and wet spells respectively, suggesting that soil hydrology has significant influence in the mechanism of cracking.

Analysis of laboratory results further revealed other factors that contributes to the dynamics of cracking as the hydrologic condition in the soil changes. The cracks occurred within a restricted range of moisture change in the soil. This led to a recognition of critical hydrologic conditions for active crack development, which relates to the moisture content in the soils. A common observation was a near instantaneous commencement of cracking at moisture state close to the plastic limits. Similarly, some workers have attributed the later stable stage of crack development with

the approach to the shrinkage limits. Ultimately, the difference in the crack intensity between any two opposing test variables, e.g. low and high density, north and south aspect, first and second cycle etc., was mainly influenced by the rate of moisture loss. The high level of moisture fluctuation in the low density soil significantly caused interaction of the solid particles and flaws. Multiple stress conditions may result leading to increased potential for cracking. These suggest that analysis of moisture conditions on slopes including the plastic limits, antecedent moisture content, optimum moisture content etc., can be useful to predict cracking in the soil.

### **6.3 Influencing factors of cracking in engineered clay embankment**

Embankment constructions involve important engineering considerations for optimum performance. As shown in this study, the engineered conditions associated with the embankment structure influenced its response to the environmental changes. In this section, the crack characteristics related to the embankment geometry, engineered condition and climate are summarized.

#### **6.3.1 Influence of soil density**

The cracks developed in the well compacted and poorly compacted panels were quantified and compared. Cracking occurred at different intensities in the two engineered soil conditions. Nearly 80% of the cracks found in the embankment occurred in the loose fills of the poorly compacted panels. The morphology of cracks in this panel also developed prominently resulting in larger crack cross sectional volumes. This behavior is an evidence of the strong relationship between soil strength and suction-related tensile stress. Although greater suction was recorded in the dense soil of the well compacted panel, the loose soil structure of the poorly compacted panel will offer less material resistant to fracture due to overall low strength. This implies that under the same drying intensity, cracking would occur at a different rate in a given soil compacted at different densities. In the laboratory simulations, the time taken for the first crack to initiate tends to increase as the soil density decreases among the three compacted specimens of the Nafferton Clay. This suggests that historic railway embankments in the UK, constructed at low density have greater

implication for cracking than the modern highway embankments. However, results from this study show cracks also occurred in the well-compacted soil. Although in this case, the cracks were relatively fewer in number and small in sizes, meaning a limited cracking, repeated wetting and drying, however, significantly increased the intensity. Proliferation of cracking in slopes means greater potentials for infrastructure deterioration and likely, the failure mechanisms may change as these features redefine the soil structure. This calls for improvement of the construction techniques, particularly good compaction and drainage control against environmental degradation of infrastructure slopes.

### **6.3.2 Effect of embankment geometry**

The geometric factors of infrastructure embankment investigated in this study included aspect, soil layer thickness and layers of compaction. These factors also affected the crack development mainly by the extent of moisture changes in each. The moisture behavior was evaluated by the rate of moisture loss. Ignoring in the first instance the slight difference in the densities of the specimens, CIF was higher in the thick soil block (195mm) than the thin soil specimen with nearly half this thickness (100mm). This was attributed to the slow rate of moisture loss occurring in the thick soil, which leads to significant suction gradient. If the soil's densities are considered, the thick soil can be regarded as the loosest, which suggest a higher propensity for cracking, considering the low strength likely. However, between the two thin specimens, the 1-lift thin specimen displayed more cracking than the counterpart constructed in 2-lift. Since the two specimens had the same thickness, the difference in crack intensity attributes to their density differences, which were  $1.63\text{Mg/m}^3$  for the 1-lift and  $1.65\text{Mg/m}^3$  for the 2-lift specimen. In this case, the thin specimen with 1-lift is less dense, and because of strength, is more prone to cracking. Density is an important factor in the soil mechanical behavior. Since soil structure is complex, it is likely that slight difference in density can reflect significant mechanical response. Overall, the soil with two lifts is densest ( $1.65\text{Mg/m}^3$ ) follow by the soil with one lift ( $1.63\text{Mg/m}^3$ ) and lastly, the thick soil ( $1.62\text{Mg/m}^3$ ). The CIF results, therefore, suggest a trend of increasing cracking with decreasing density.

Regarding aspect, the east-west orientation of the embankment result in a south and north facing slope. More cracks were found on the South slope. The cracks on this face of the slope were also geometrically larger than the few cracks found on the North slope. Analysis of the slope hydrology and meteorological variables reasonably suggests that this development relates to the predominant southwesterly inclination of the elements. This imposed a variable climatic condition with the net effect on more significant moisture loss on the south slope. Similarly, a majority of the cracks occurred on the middle and upper section of the south slope. The influence of aspects on the crack development ultimately relates to the rate of moisture movement characterising the amount of insolation incident on each part.

### **6.3.3 *Effect of soil plasticity***

The intensity of cracks resulting from the three plastic soils were quantified. The results showed that intensity of cracking increased linearly with plasticity. The mechanism was discussed regarding water retention properties in the plastic soils. The VH plasticity Clay showed substantial limitation in moisture diffusion with time leading to a slow rate of moisture loss. However, the little moisture loss resulted in a relatively larger shrinkage volume (a summary of laboratory measurements can be found in Appendix III). Correspondingly, a higher cracking intensity occurred. Although suction in this specimen was not measured due to unforeseen issue with the equipment, the greater linear shrinkage occurring in this soil specimen suggests a relatively high suction state to significantly pull the soil solids closer together. Conversely, moisture variations in the intermediate plasticity Nafferton Clay was high at the same density. The desiccation of this sample showed less shrinkage, low suction and less cracking. The high plastic Gault Clay displayed cracking intensity between these extremes. This trend reasonably suggests a geographic implication in the potential of crack occurrence in fill across the UK. Very high plasticity fill materials dominate the Southern part of the country. The relatively warmer weather and more rainfall prevalent in this region can further exacerbate this potential by greater shrink-swell as climate becomes extreme.

#### 6.3.4 ***Role of vegetation in cracking of clay embankment***

The mechanical and hydrological importance of vegetation in the performance of slopes has been recognised in geotechnical practice. Under these two factors, the possible influence, which the vegetation presence on a slope can have on cracking, was investigated as part of the objectives of this study. The field study indicates that cracks significantly developed in the embankment in 2014, particularly between May and July when the vegetation was mowed. In 2015 on the other hand, the vegetation was not cut down, and throughout the year, no prominent cracking was observed on the embankment, especially reopening of the closed cracks. Syntheses of ground condition and meteorological events revealed that the embankment was relatively drier in 2014 with a considerable increase in the rate of desiccations in the period when the vegetation was cut. Without the leaves, the transpiration component of this record is minimal. This means that a greater part of the estimated evapotranspiration came from direct evaporation from the exposed soil surface. Therefore, the absence of vegetation practically exposed the embankment surface to direct insolation and accelerated moisture loss by increasing the rate of desiccation from the soil surface.

The root system in the soil was study for their influence in the crack development. It was seen that the cracks propagated in a preferred path around the grasses on the embankment. In addition, a few areas on the embankment with little or no vegetation displayed network of cracks compared to the single cracks, which occurred in the entire grass covered area. The difference in cracking behaviour, therefore, suggests a possible influence of vegetation root, particularly the restriction of crack propagation by a mechanical implication. The field survey shows that the grasses have clustered fibrous roots. The literature indicates that fibrous root system can increase the apparent cohesion of the soil mass, hence tensile strength. Therefore, a localised material stiffness is likely around the cluster of grasses, which affects crack paths and pattern development. In the laboratory, the intensity of crack in the simulated vegetated soil did not change between 1<sup>st</sup> and 2<sup>nd</sup> cycle. This is despite the common trend of crack intensification associated with cyclic wetting and drying. Overall, the

material resistance by randomly distributed vegetation roots significantly controlled the crack propagation in the embankment. This shows a promising condition that can control cracking in infrastructure slopes. However, this benefit weighs against the potential of by-pass drying by invasive roots, especially by large water absorbing trees, which can exacerbate conditions for sub-aerial cracking.

#### **6.3.5 *Crack intensity under cyclic wetting and drying***

As presented in the results, cyclic wetting and drying intensified cracking in the soils. Practically, cyclic wetting and drying produced crack repeatability and increase in the geometry. The reopened old cracks commonly increased geometrically resulting in significant increase in the crack intensity. This indicates that alternate wet and dry conditions could change the initial soil state of the soil, particularly the mechanical properties, which the cracks indirectly represent. Eventually, the development of crack approaches a consistent intensity as cycles of wetting and drying increases beyond a threshold. This suggests with time, a state of stability can be reached by the soil mass under this condition that can prevent further cracking. This is a promising characteristic when considering the effect of cracking on slopes in the long term.

### **6.4 Mechanisms of cracks orientation and modification**

After their formation under influence of soil water suction, the cracks propagated and interacted systematically. In this section, important factors observed in crack topology are summarised.

#### **6.4.1 *Influence of soil texture***

The texture of soil includes grain size, curvature, flaws etc. Both in the field and laboratory, the cracks prominently developed at sites of stone defects. The flaws significantly influenced their orientation and interactions, hence contributed to crack intensity and morphologic changes. Commonly, two or more cracks start-off at varied angles around sites of flaws in the soil while the path of an advancing crack deflects on approach to such features. These effects bordered on high-stress concentration expected around defects relative to the overall moisture laden soil matrix. The high stress field primarily acts to modify the general

moisture stress pattern with which the cracks propagate in the soil. Therefore, textural characteristics in soil can control the degree of the orderliness of cracking, hence their direction and spacing. The direction of crack orientation is important in water capture and runoff potential. A transversely oriented crack relative to the slope face would affect water capture while a longitudinally oriented crack would tend to promote runoff and decrease infiltration. The influence of texture can guide the selection of graded materials for embankment placement against conditions of increase cracking. The presence of large particle size materials in the near surface layer of the slope should therefore be minimised. Practically, good compaction can achieve homogenisation of fills. Ultimately, monitoring changes in crack topology is essential in updating the slopes hydrology for better understanding of the processes of deterioration.

#### **6.4.2 *Surface processes and crack morphology changes in a grass covered embankment***

Physical and biological activities acting on the surface of the embankment affected the morphological features of the cracks. These include erosion and bioturbation. Wind and rainwater caused considerably loss of soil material around crack aperture in the embankment. Because of these factors, crack widths were commonly non-uniform and significantly widened. Some eroded materials were deposit in the cracks, which contributed to their closure. Worms and rodents were other prominent modifiers of the cracks morphology. Bioturbation did not only increase crack width randomly but sometimes obliterated the aperture. The engineering significance of these processes is increased capacity of rainwater capture and infiltration as the crack width increases.

### **6.5 Conclusions**

Specific objectives were outline to achieve the purpose of this undertaking. These related to the key factors characterising transport embankment and their performance, especially environmental moisture condition, nature of fill material and construction techniques. Accordingly, the objectives included:

- I. To characterise near surface moisture movement, crack initiation and propagation in engineered clay embankment

- II. To quantify desiccation cracking in clay base infrastructure embankment with different construction methods and materials
- III. To establish the influencing factors in crack orientation and intersection in compacted clay fills
- IV. To determine the influence of vegetation in crack network pattern
- V. To understand the effect of slope geometry in cracking

The first objective has to do with understanding the relationship between environmental-driven hydrologic changes and cracking in the slope while the remaining involved the influencing factors related to embankment constructions and cracking. The conclusions of this study are given in two categories to address these objectives.

#### **6.5.1 *Soil moisture movement and crack development***

The cracks were studied under environmentally driven soil moisture changes. From syntheses of seasonal and diurnal recordings, the following conclusions were drawn on the first objective:

- I. A positive linear correlation exists between changes in the soil water-suction and crack development. This suggests a strong coupling between weather condition and desiccation crack mechanism
- II. During crack development, critical hydrologic boundary exists within which the cracks initiated and intensified in the soil. The boundary condition relates to the extent of drying and soil consistency limits, and can help to understand condition for incipient cracking on a desiccating clay slope
- III. After initiation, crack propagation is primarily influenced by the stress field generated by the diffusing moisture gradients in the soil. The effect of gravity on moisture movement can also influence this behavior.

#### **6.5.2 *Factors affecting intensity of cracking in engineered clay slope***

Critical analysis of the field and laboratory results revealed that crack intensity is affected by the following general and specific embankment construction conditions:

- I. The geometry of the slope mainly soil thickness, the number of compacted layer and aspect. Crack intensified in thick soil layer and in the slope face with greater insolation
- II. Material properties including density, permeability, plasticity etc. A loose soil structure enhances cracking due to low strength and greater fluctuation in hydrologic condition while increase soil plasticity leads to prominent cracking through greater shrinkage and higher suction developed.
- III. Environmental factors including humidity, repeated wetting and drying cycles. Low humidity condition characterised by a warm, dry atmosphere favors desiccation hence the condition for increase cracking compare to a wet condition, which rather causes cracks to close. Repeated wetting and drying exacerbates cracking. However, this role may become insignificant in later cycles as soils tend to attain stability against deformation after reaching a threshold structural re-arrangement, a factor which is considered to be soil specific.
- IV. Vegetation presence, particularly the root system influences the path of crack propagation by increasing mechanical resistant in the top soil. Therefore, crack network is common in the area with little or no vegetation cover. Soil moisture extraction by roots is capable of causing sub-aerial cracking due to increased drying suction around the root zone.
- V. Soil texture influences the degree of the orderliness of cracking, hence their orientation and interaction.
- VI. The response to cracking mainly relates to the rate of moisture movement and the soil strength as affected by the texture and density.

In summary, the above findings ultimately suggest that crack development in an engineered slope has implication for (1) construction techniques, particularly the old embankments constructed to lower densities, (2) climatic changes as drying/wetting cycles exacerbate crack development, and may lead to more rapid infiltration and (3) geographical locations of infrastructure related to locally sourced fills and their plasticity property.

## 6.6 Recommendations for further study

The broad theme of weather processes in infrastructure slopes covered in this study has revealed other aspects that can further be investigated.

These include:

1. Investigation of micro-structural changes during cracking (optical and X-ray micro-tomography studies) to understand the magnitude of hydrologic stress affecting the soil skeleton as well as verify if soil structures attain stability under multiple wetting and drying.
2. The intensity of cracking showed decreasing potential under certain conditions, which mostly moderate the rate of moisture loss, as well as reduces shrinkage volume change. The conditions include fibrous root system, soil shading, soil densification (compaction), suction in root zone etc. These can be studied details for crack control in clay slopes.
3. This study has generated specific experimental results and conditions that are crucial in cracking mechanism. It would be useful to constitute the results in analytical model to validate the realistic behaviour of embankments with cracks.

## References

- Abernethy, B. and Rutherford, I.D. (2000) 'The effect of riparian tree roots on the mass-stability of riverbanks', *Earth Surface Processes and Landforms*, 25(9), pp. 921-937.
- Abu-Hejleh, A.N. and Znidarčić, D. (1995) 'Desiccation theory for soft cohesive soils', *Journal of Geotechnical Engineering*, 121(6), pp. 493-502.
- Aitchison, G.D. and Woodburn, J.A. (1969) *Proceedings of the 7th International Conference on Soil Mechanics and Foundation Engineering*.
- Al-Homoud, A.S., Basma, A.A., Husein Malkawi, A.I. and Al Bashabsheh, M.A. (1995) 'Cyclic swelling behavior of clays', *Journal of geotechnical engineering*, 121(7), pp. 562-565.
- Al Wahab, R.M. and El-Kedrah, M.A. (1995) 'Using fibers to reduce tension cracks and shrink/swell in a compacted clay', *Geoenvironment 2000: Characterization, Containment, Remediation, and Performance in Environmental Geotechnics*. ASCE, pp. 791-805
- Albrecht, B.A. and Benson, C.H. (2001) 'Effect of desiccation on compacted natural clays', *Journal of Geotechnical and Geoenvironmental Engineering*, 127(1), pp. 67-75.
- Allen, R.G., Pereira, L.S., Raes, D. and Smith, M. (1998) 'Crop evapotranspiration-Guidelines for computing crop water requirements-FAO Irrigation and drainage paper 56', *FAO, Rome*, 300(9), p. D05109.
- Alonso, E.E., Romero, E., Hoffmann, C. and García-Escudero, E. (2005) 'Expansive bentonite–sand mixtures in cyclic controlled-suction drying and wetting', *Engineering geology*, 81(3), pp. 213-226.
- Amarasiri, A.L., Kodikara, J.K. and Costa, S. (2011) 'Numerical modelling of desiccation cracking', *International Journal for Numerical and Analytical Methods in Geomechanics*, 35(1), pp. 82-96.
- Anderson, M.G., Hubbard, M.G. and Kneale, P.E. (1982) 'The influence of shrinkage cracks on pore-water pressures within a clay embankment',

*Quarterly Journal of Engineering Geology and Hydrogeology*, 15(1), pp. 9-14.

Anderson, M.G. and Richards, K.S. (1987) *Slope stability: geotechnical engineering and geomorphology*. John Wiley & Sons.

Anderson, T.L. and Anderson, T.L. (2005) *Fracture mechanics: fundamentals and applications*. 3rd edn. CRC press.

Atkinson, B.K. (1987) 'Introduction to fracture mechanics and its geophysical applications', *Fracture mechanics of rock*, pp. 1-26.

Aubeny, C. and Long, X. (2007) 'Moisture diffusion in shallow clay masses', *Journal of Geotechnical and Geoenvironmental engineering*, 133(10), pp. 1241-1248.

Baker, R. (1981) 'Tensile strength, tension cracks, and stability of slopes', *Soils and foundations*, 21(2), pp. 1-17.

Bandyopadhyay, K.K., Mohanty, M., Painuli, D.K., Misra, A.K., Hati, K.M., Mandal, K.G., Ghosh, P.K., Chaudhary, R.S. and Acharya, C.L. (2003) 'Influence of tillage practices and nutrient management on crack parameters in a Vertisol of central India', *Soil and Tillage Research*, 71(2), pp. 133-142.

Bell, F.G. (2013) *Engineering properties of soils and rocks*. Elsevier.

Bell, F.J. (2003) *Geological Hazards: their assessment, avoidance and mitigation*. London etc: E & FN Spon.

Bensallam, S., Bahi, L., Ejjaouani, H. and Shakhirev, V. (2012) 'Shrinkage curve: experimental study and modelling', *International Journal of Engineering*, 25(3), pp. 203-210.

BGS (2017) 'Rainfall and landslide data for the UK' *Montly*. 20 February 2017. Online. Available at:  
<http://www.bgs.ac.uk/research/engineeringGeology/shallowGeohazardsAndRisks/landslides/LandslidesandRainfall.html>.

- Bishop, A.W. (1959) 'The principle of effective stress', *Teknisk ukeblad*, 106, pp. 859-863.
- Blight, G.E. (2005) 'Desiccation of a clay by grass, bushes and trees', *Geotechnical & Geological Engineering*, 23(6), pp. 697-720.
- Bradley, C., Mosugu, M. and Gerrard, J. (2007) 'Seasonal dynamics of soil–water pressure in a cracking clay soil', *Catena*, 69(3), pp. 253-263.
- Briggs, K.M., Loveridge, F.A. and Glendinning, S. (2016) 'Failures in transport infrastructure embankments', *Engineering Geology*.
- Brink , A., Partridge, T.C. and AAB, W. (1982) *Soil survey for engineering*. Oxford University Press.
- Brinker, C.J. and Scherer, G.W. (2013) *Sol-gel science: the physics and chemistry of sol-gel processing*. Academic press.
- Broomhead, E. N., 1999. *The stability of slopes*. CRC Press.
- Bronswijk, J.J.B. (1989) 'Prediction of actual cracking and subsidence in clay soils', *Soil Science*, 148(2), pp. 87-93.
- Bronswijk, J.J.B. (1990) 'Shrinkage geometry of a heavy clay soil at various stresses', *Soil Science Society of America Journal*, 54(5), pp. 1500-1502.
- Charles, J.A. (1993) '*Engineered fills*', *proceedings of the conference 'engineered fills '93'* Newcastle Upon Tyne.
- Cheng, Y.M. and Lau, C.K. (2014) *Slope stability analysis and stabilization: new methods and insight*. CRC Press.
- Chenu, C., Le Bissonnais, Y. and Arrouays, D. (2000) 'Organic matter influence on clay wettability and soil aggregate stability', *Soil Science Society of America Journal*, 64(4), pp. 1479-1486.
- Chertkov, V.Y. (2000) 'Using Surface Crack Spacing to Predict Crack Network Geometry in Swelling Soils', *Soil Science Society of American Journal*, 64(6), pp. 1918-1921.

- Chertkov, V.Y. (2013) 'Shrinkage anisotropy characteristics from soil structure and initial sample/layer size', *Geoderma*, 200, pp. 1-8.
- Chirico, G.B., Borga, M., Tarolli, P., Rigon, R. and Preti, F. (2013) 'Role of Vegetation on Slope Stability under Transient Unsaturated Conditions', *Procedia Environmental Sciences*, 19, pp. 932-941.
- Chok, Y., Kaggwa, G., Jaksa, M. and Griffiths, D. (2004) 'Modelling the effects of vegetation on stability of slopes', *9th Australia New Zealand conference on Geomechanics*. Auckland.
- Chok, Y.H. (2008) *Modelling the effects of soil variability and vegetation on the stability of natural slopes*. The University of Adelaide.
- Churchill, R.R. (1982) 'Aspect-induced differences in hillslope processes', *Earth Surface Processes and Landforms*, 7(2), pp. 171-182.
- Clarke, D. and Smethurst, J. (2007) 'Embankment and cut slope monitoring and analysis', 3rd Climate impact forecasting for slopes (CLIFFS) workshop.
- Collison, A., Wade, S., Griffiths, J. and Dehn, M. (2000) 'Modelling the impact of predicted climate change on landslide frequency and magnitude in SE England', *Engineering Geology*, 55(3), pp. 205-218.
- Colmenares Montanez, J.E. (2002) *Suction and volume changes of compacted sand-bentonite mixtures*. PhD Thesis thesis. Imperial College London (University of London).
- Cordero, J., Cuadrado, A., Prat, P. and Ledesma, A. (2016) *E3S Web of Conferences*. EDP Sciences.
- Corte, A. and Higashi, A. (1960) *Experimental Research on Desiccation Cracks in Soil-Research Report 66*. Wilmette, Illinois: US Army Snow Ice and Permafrost Research Establishment.
- Corte, A. and Higashi, A. (1964) 'Experimental research on desiccation cracks in soil', In Kodikara, J. K. Barbour, S. L. Fredlund, D. G. 2004,

'Desiccation cracking of soil layer', *Unsaturated soil for Asia*, 90(5809), pp. 139.

Costa, S., Kodikara, J. and Shannon, B. (2013) 'Salient factors controlling desiccation cracking of clay in laboratory experiments', *Geotechnique*, 63(1), pp. 18-29.

Croney, D. and Coleman, J.D. (1953) 'Soil moisture suction properties and their bearing on the moisture distribution in soils', *Proceedings of the 3rd International Conference of Soil Mechanics and Foundation Engineering*.

Cutts, A.R. (2014) 'The effect of varying meteorological parameters on slope pore water pressures', MSc Thesis, Newcastle University.

Dasog, G.S., Acton, D.F., Mermut, A.R. and Jong, E.D. (1988) 'Shrink-swell potential and cracking in clay soils of Saskatchewan', *Canadian Journal of Soil Science*, 68(2), pp. 251-260.

Davies, O., Rouainia, M., Glendinning, S. and Birkinshaw, S.J. (2008) 'Assessing the influence of climate change on the progressive failure of a railway embankment', *Young*, 2500, p. 100.

DeCarlo, K.F. and Shokri, N. (2014) 'Effects of substrate on cracking patterns and dynamics in desiccating clay layers', *Water Resources Research*, 50(4), pp. 3039-3051.

Dijkstra, T.A. and Dixon, N. (2010) 'Climate change and slope stability in the UK: challenges and approaches', *Quarterly Journal of Engineering Geology and Hydrogeology*, 43(4), pp. 371-385.

Dyer, M., Utiy, S. and Zielinski, M. (2009) 'Field survey of desiccation fissuring of flood embankments', *Water management*, 162(3), pp. 221-232.

Dyer, M., Utiy, S. and Zielinski, M. (2007) 'The influence of desiccation fine fissuring on the stability of flood embankments'. FRMRC Research Report UR11.

El Abedine, A.Z. and Robinson, G.H. (1971) 'A study on cracking in some vertisols of the Sudan', *Geoderma*, 5(3), pp. 229-241.

- Fan, P., Liu, Q., Li, J. and Sun, J. (2005) 'Numerical analysis of rainfall in filtration in the slope with a fracture', *Science in China Series E Engineering & Materials Science*, 48(1), pp. 107-120.
- Fang, H.-Y. and Daniels, J.L. (2006) *Introductory geotechnical engineering: an environmental perspective*. CRC Press.
- Farewell, T.S., Hallett, S.H., Hannam, J.A. and Jones, R.J.A. (2012) 'Soil impacts on national infrastructure in the United Kingdom', *NSRI, Cranfield University, UK*.
- Favre, F., Boivin, P. and Wopereis, M.C.S. (1997) 'Water movement and soil swelling in a dry, cracked Vertisol', *Geoderma*, 78(1–2), pp. 113-123.
- Fredlund, D.G. (2006) 'Unsaturated soil mechanics in engineering practice', *Journal of geotechnical and geoenvironmental engineering*, 132(3), pp. 286-321.
- Fredlund, D.G. and Morgenstern, N.R. (1976) 'Constitutive relations for volume change in unsaturated soils', *Canadian Geotechnical Journal*, 13(3), pp. 261-276.
- Fredlund, D.G. and Rahardjo, H. (1993) *Soil mechanics for unsaturated soils*. John Wiley & Sons.
- Fredlund, D.G., Rahardjo, H. and Fredlund, M.D. (2012) *Unsaturated soil mechanics in engineering practice*. John Wiley & Sons.
- Fredlund, D.G., Sheng, D. and Zhao, J. (2011) 'Estimation of soil suction from the soil-water characteristic curve', *Canadian Geotechnical Journal*, 48(2), pp. 186-198.
- Fredlund, D.G., Xing, A., Fredlund, M.D. and Barbour, S.L. (1996) 'The relationship of the unsaturated soil shear to the soil-water characteristic curve', *Canadian Geotechnical Journal*, 33(3), pp. 440-448.
- Frost, N.E., Marsh, K.J. and Pook, L.P. (1974) '*Metal fatigue: What It Is, Why It Matters*', *Solid Mechanics and Its Applications*, Courier Corporation, 145(1525), pp. 135-158

Gabet, E.J., Reichman, O.J. and Seabloom, E.W. (2003) 'The effects of bioturbation on soil processes and sediment transport', *Annual Review of Earth and Planetary Sciences*, 31, pp. 249-273.

Gasparre, A. (2005) *Advance laboratory characterization of London clay*. Imperial College London (University of London).

Gauthier, G., Lazarus, V. and Pauchard, L. (2007) 'Alternating crack propagation during directional drying', *Langmuir*, 23(9), pp. 4715-4718.

Glendinning, S., Hughes, P., Helm, P., Chambers, J., Mendes, J., Gunn, D., Wilkinson, P. and Uhlemann, S. (2014) 'Construction, management and maintenance of embankments used for road and rail infrastructure: implications of weather induced pore water pressures', *Acta Geotechnica*, pp. 1-18.

Glendinning, S., Loveridge, F., Starr-Kedde, R.E., Bransby, M.F. and Hughes, P.N. (2009) 'Role of vegetation in sustainability of infrastructure slopes', *Proceedings of the ICE-Engineering Sustainability*, 162(2), pp. 101-110.

Goehring, L. (2013) 'Evolving fracture patterns: columnar joints, mud cracks and polygonal terrain', *Philosophical Transaction of Royal Society of America*, 371(2004), p. 20120353.

Gokhale, K. and Anandakrishnan, M. (1970) 'Role of active clay in the shrinkage behaviour in multicomponent clay-sand systems', *Soils and Foundations*, 10(3), pp. 92-94.

Gomboš, M. (2012) 'The Impact of Clay Minerals on Soil Hydrological Processes', In *Clay Minerals in Nature-Their Characterization, Modification and Application*, Chapter 7, Intech.

Griffith, A.A. (1921) 'The phenomena of rupture and flow in solids', *Philosophical transactions of the royal society of london. Series A, containing papers of a mathematical or physical character*, 221, pp. 163-198.

- Haines, W.B. (1923) 'The volume-changes associated with variations of water content in soil', *The Journal of Agricultural Science*, 13(03), pp. 296-310.
- Hallett, P.D., Gordon, D.C. and Bengough, A.G. (2003) 'Plant influence on rhizosphere hydraulic properties: direct measurements using a miniaturized infiltrometer', *New Phytologist*, 157(3), pp. 597-603.
- Hallett, P.D. and Newson, T.A. (2005) 'Describing soil crack formation using elastic–plastic fracture mechanics', *European Journal of Soil Science*, 56(1), pp. 31-38.
- Hamza, O. and Bellis, A. (2008) *Advances in Transportation Geotechnics: Proceedings of the International Conference held in Nottingham, UK, 25-27 August 2008*. CRC Press.
- Harrison, A.M., Plim, J.F.M., Harrison, M., Jones, L.D. and Culshaw, M.G. (2012) 'The relationship between shrink–swell occurrence and climate in south-east England', *Proceedings of the Geologists' Association*, 123(4), pp. 556-575.
- Hassan, A. and Toll, D.G. (2013) 'Electrical resistivity tomography for characterizing cracking of soils', *Geo-Congress 2013: Stability and Performance of Slopes and Embankments III*. ASCE, pp. 818-827.
- Hassan, A.A. and Nsaif, M.D. (2016) 'Application of 2D Electrical Resistivity Imaging Technique for Detecting Soil Cracks: Laboratory Study', *Iraqi Journal of Science*, 67(2A), pp. 930-937.
- Hassan, M., Woche, S.K. and Bachmann, J. (2014) 'How the root zone modifies soil wettability: Model experiments with alfalfa and wheat', *Journal of Plant Nutrition and Soil Science*, 177(3), pp. 449-458.
- Herrera, M.C., Lizcano, A. and Santamarina, J.C. (2007) 'Colombian volcanic ash soils', *Characterization and engineering properties of natural soils*, pp. 2385-2409.
- Hillel, D. (2003) *Introduction to environmental soil physics*. Academic press.

- Holgate, T.F. (1901) *Elementary Geometry, Plane and Solid: For Use in High Schools and Academies*. New York: Macmillian Company.
- Holmes, D.M., Vasant Kumar, R. and Clegg, W.J. (2006) 'Cracking during lateral drying of alumina suspensions', *Journal of the American Ceramic Society*, 89(6), pp. 1908-1913.
- Holtz, R.D. and Kovacs, W.D. (1981) *An introduction to geotechnical engineering*. Prentice-Hall.
- Hu, L., Péron, H., Hueckel, T. and Laloui, L. (2006) *Numerical and phenomenological study of desiccation of soil* In *Advances in Unsaturated Soil, Seepage, and Environmental Geotechnics*
- Hueckel, T. (1992) 'On effective stress concepts and deformation in clays subjected to environmental loads: Discussion', *Canadian Geotechnical Journal*, 29(6), pp. 1120-1125.
- Hughes, P.N., Glendinning, S., Mendes, J., Parkin, G., Toll, D.G., Gallipoli, D. and Miller, P.E. (2009) 'Full-scale testing to assess climate effects on embankments', *Proceedings of the ICE-Engineering Sustainability*, 162(2), pp. 67-79.
- Irwin, G.R. (1997) 'Analysis of stresses and strains near the end of a crack traversing a plate', *Spie milestone series MS*, 137, pp. 167-170.
- Jasechko, S., Sharp, Z.D., Gibson, J.J., Birks, S.J., Yi, Y. and Fawcett, P.J. (2013) 'Terrestrial water fluxes dominated by transpiration', *Nature*, 496(7445), pp. 347-350.
- Jones, D.E. and Holtz, W.G. (1973) 'Expansive soils - The hidden disaster', *Civil Engineering ASCE*, 43(8), pp. 49-51.
- Jones, L.D. and Jefferson, I. (2012) *Expansive soils*. London: ICE.
- Juárez-Luna, G. and Ayala, G. (2014) 'Application of Fracture Mechanics to Cracking Problems in Soils', *Open Construction and Building Technology Journal*, 8, pp. 1-8.

Khan, F.S. and Azam, S. (2017) 'Determination of the desiccation behavior of clay slurries', *International Journal of Mining Science and Technology*, 26 (2), pp. 277-283.

Kilsby, C., Glendinning, S., Hughes, P.N., Parkin, G. and Bransby, M.F. (2009) 'Climate-change impacts on long-term performance of slopes', *Proceedings of the ICE-Engineering Sustainability*, 162(2), pp. 59-66.

Kim, T.-H., Kim, T.-H., Kang, G.-C. and Ge, L. (2011) 'Factors influencing crack-induced tensile strength of compacted soil', *Journal of Materials in Civil Engineering*, 24(3), pp. 315-320.

Kindle, E.M. (1917) 'Some Factors Affecting the Development of Mud-Cracks', *Journal of Geology*, 25, pp. 135-144.

Kirkham, M.B. (2014) *Principles of soil and plant water relations*. Academic Press.

Kishné, A.S., Morgan, C.L.S. and Miller, W.L. (2009) 'Vertisol crack extent associated with gilgai and soil moisture in the Texas Gulf Coast Prairie', *Soil Science Society of America Journal*, 73(4), pp. 1221-1230.

Kleppe, J.H. and Olson, R.E. (1985) 'Desiccation cracking of soil barriers', *Hydraulic barriers in soil and rock, ASTM STP*, 874, pp. 263-275.

Knappett, J. and Craig, F. (2012) *Craig's soil mechanics*. Oxon: Spon press.

Kodikara, J., Barbour, S. and Fredlund, D.G. (2002) 'Structure development in surficial heavy clay soils: a synthesis of mechanisms', *Australian Geomechanics: Journal and News of the Australian Geomechanics Society*, 37(3), p. 25.

Kodikara, J., Barbour, S.L. and Fredlund, D.G. (1999), 'Changes in clay structure and behaviour due to wetting and drying', *Proceedings 8th Australia New Zealand Conference on Geomechanics: Consolidating Knowledge*. Australian Geomechanics Society.

- Kodikara, J. and Costa, S. (2013) 'Desiccation Cracking in Clayey Soils: Mechanisms and Modelling', in *Multiphysical Testing of Soils and Shales*. Springer, pp. 21-32.
- Kodikara, J.K., Barbour, S.L. and Fredlund, D.G. (2000) 'Desiccation cracking of soil layers', *Unsaturated Soils for Asia*, 90(5809), p. 139.
- Kodikara, J.K., Nahlawi, H. and Bouazza, A. (2004) 'Modelling of curling in desiccating clay', *Canadian geotechnical journal*, 41(3), pp. 560-566.
- Kodikara, J.K. and Choi, X. (2006) 'A simplified analytical model for desiccation cracking of clay layers in laboratory tests', *In Unsaturated Soils 2006* pp. 2558-2569.
- Koh, Y.K. and Wong, C.C. (2006) *Monitoring Defect Formation in Colloidal Self Assembly using Photonic Bandgap Variations, Advanced Materials for Micro- and Nano-Systems*.
- Konrad, J.M. and Ayad, R. (1997a) 'Desiccation of a sensitive clay: field experimental observations', *Canadian Geotechnical Journal*, 34(6), pp. 929-942.
- Konrad, J.M. and Ayad, R. (1997b) 'A idealized framework for the analysis of cohesive soils undergoing desiccation', *Canadian Geotechnical Journal*, 34(4), pp. 477-488.
- Lachenbruch, A.H. (1961) 'Depth and spacing of tension cracks', *Journal of Geophysical Research*, 66(12), pp. 4273-4292.
- Lakshmikantha, M.R., Prat, P.C. and Ledesma, A. (2012) 'Experimental evidence of size effect in soil cracking', *Canadian Geotechnical Journal*, 49(3), pp. 264-284.
- Laloui, L. and Nuth, M. (2009) 'On the use of the generalised effective stress in the constitutive modelling of unsaturated soils', *Computers and Geotechnics*, 36(1), pp. 20-23.
- Lambe, T.W. (1958) 'The structure of compacted clay', *Journal of the Soil Mechanics and Foundation. Division of ASCE*, 84, pp. 10-34.

- Lees, A.S., MacDonald, G.J., Sheerman-Chase, A. and Schmidt, F. (2013) 'Seasonal slope movements in an old clay fill embankment dam', *Canadian Geotechnical Journal*, 50(5), pp. 503-520.
- Leshchinsky, B. (2013), 'Comparison of limit equilibrium and limit analysis for complex slopes', *Geo-Congress 2013: Stability and Performance of Slopes and Embankments III*.
- Li, A.G., Yue, Z.Q., Tham, L.G., Lee, C.F. and Law, K.T. (2005) 'Field-monitored variations of soil moisture and matric suction in a saprolite slope', *Canadian Geotechnical Journal*, 42(1), pp. 13-26.
- Li, J.H. and Zhang, L.M. (2010) 'Geometric parameters and REV of a crack network in soil', *Computers and Geotechnics*, 37(4), pp. 466-475.
- Li, J.H. and Zhang, L.M. (2011) 'Study of desiccation crack initiation and development at ground surface', *Engineering Geology*, 123(4), pp. 347-358.
- Lim, T.T., Rahardjo, H., Chang, M.F. and Fredlund, D.G. (1996) 'Effect of rainfall on matric suctions in a residual soil slope', *Canadian Geotechnical Journal*, 33(2), pp. 618-628.
- Lourenço, S.D.N., Wang, G.H. and Kamai, T. (2015) 'Water repellent soils for slope stability', In European Conference on Soil Mechanics and Geotechnical Engineering (ECSMGE) Soil Mechanics. British Geotechnical Association/ICE Publishing.
- Loveridge, F.A., Spink, T.W., O'Brien, A.S., Briggs, K.M. and Butcher, D. (2010) 'The impact of climate and climate change on infrastructure slopes, with particular reference to southern England', *Quarterly Journal of Engineering Geology and Hydrogeology*, 43(4), pp. 461-472.
- Lozada, C. (2013) 'Review of factors affecting formation of cracks in clay layers', *Advances in Unsaturated Soils; Caicedo B., Murillo C., Hoyos L., Esteban J., Eds., CRC Press: London*, pp. 365-370.
- Michalowski, R.L. (2013) 'Stability assessment of slopes with cracks using limit analysis', *Canadian geotechnical journal*, 50(10), pp. 1011-1021.

- Miller, C.J., Mi, H. and Yesiller, N. (1998) 'Experimental analysis of desiccation crack propagation in clay liners1', *JAWRA Journal of the American Water Resources Association*, 34(3), pp. 677-686.
- Miller, G.A., Hassanikhah, A. and Varsei, M. (2015) *Unsaturated Soil Mechanics-from Theory to Practice: Proceedings of the 6th Asia Pacific Conference on Unsaturated Soils (Guilin, China, 23-26 October 2015)*. CRC Press.
- Miller, J.D. and Gaskin, G.J. (1999) 'ThetaProbe ML2x', *Principles of operation and applications. MLURI Technical Note*.
- Mitchell, J.K. (1993) '1993, *Fundamentals of Soil Behavior*, John Wiley and Sons, Inc., New York'.
- Mizuguchi, T., Nishimoto, A., Kitsunozaki, S., Yamazaki, Y. and Aoki, I. (2005) 'Directional crack propagation of granular water systems', *Physical Review E*, 71(5), p. 056122.
- Mokhtari, M. and Dehghani, M. (2012) 'Swell-shrink behavior of expansive soils, damage and control', *Electronic Journal of Geotechnical Engineering*, 17, pp. 2673-2682.
- Morris, P.H., Graham, J. and Williams, D.J. (1992) 'Cracking in drying soils', *Canadian Geotechnical Journal*, 29(2), pp. 263-277.
- Nahlawi, H. and Kodikara, J.K. (2006) 'Laboratory experiments on desiccation cracking of thin soil layers', *Geotechnical & Geological Engineering*, 24(6), pp. 1641-1664.
- Nelder, L., Gunn, D. and Reeves, H. (2006) 'Assessment of railway embankment stiffness using continuous surface waves', *Proceeding of 1st International Conference of Railway Foundation*. Birmingham.
- Nisbet, T. (2005) *Water use by trees*. Edinburgh: Forestry Commission.
- Novak, V., Simunek, J. and van Genuchten, M. (2000) 'Infiltration of Water into Soil with Cracks', *Journal of Irrigation and drainage engineering ASCE*, 126(1), pp. 41-47.

Omidi, G.H., Thomas, J.C. and Brown, K.W. (1996) 'Effect of desiccation cracking on the hydraulic conductivity of a compacted clay liner', *Water, air, and soil pollution*, 89(1-2), pp. 91-103.

ORR (2013) 'Annual Efficiency Assessment of Network Rail' [News and Media]. September 12th. Office of rail and road. Available at: <http://orr.gov.uk/news-and-media/press-releases/2013/annual-efficiency-assessment-of-network-railRegional> (Accessed: February 26th, 2017).

Péron, H., Hueckel, T., Laloui, L. and Hu, L. (2009a) 'Fundamentals of desiccation cracking of fine-grained soils: experimental characterisation and mechanisms identification', *Canadian Geotechnical Journal*, 46(10), pp. 1177-1201.

Peron, H., Laloui, L., Hu, L.-B. and Hueckel, T. (2013) 'Formation of drying crack patterns in soils: a deterministic approach', *Acta Geotechnica*, 8(2), pp. 215-221.

Péron, H., Laloui, L., Hueckel, T. and Hu, L.B. (2009b) 'Desiccation cracking of soils', *European Journal of Environmental and Civil Engineering*, 13(7-8), pp. 869-888.

Perry, J., Pedley, M. and Reid, M. (2003) *Infrastructure embankments: condition appraisal and remedial treatment*. CIRIA London.

Pook, L. (2007) *Why Metal Fatigue Matters*. Netherland: Springer.

Potts, D.M., Kovacevic, N. and Vaughan, P.R. (1997) 'Delayed collapse of cut slopes in stiff clay', *Géotechnique*, 47(5), pp. 953-982.

Prat, P.C., Ledesma, A., Lakshmikantha, M.R., Levatti, H. and Tapia, J. (2008) 'Fracture mechanics for crack propagation in drying soils', *In Proceedings of the 12th International Conference of the International Association for Computer Methods and Advances in Geomechanics (IACMAG), Goa, India*. Citeseer.

Pritchard, O.G., Hallett, S.H. and Farewell, T.S. (2013) *Soil movement in the UK – Impacts on critical infrastructure*. Cranfield University NSRI.

Rahardjo, H., Leong, E.C. and Rezaur, R.B. (2008) 'Effect of antecedent rainfall on pore-water pressure distribution characteristics in residual soil slopes under tropical rainfall', *Hydrological Processes*, 22(4), pp. 506-523.

Rahardjo, H., Li, X.W., Toll, D.G. and Leong, E.C. (2001) 'The effect of antecedent rainfall on slope stability', in *Unsaturated Soil Concepts and Their Application in Geotechnical Practice*. Springer, pp. 371-399.

Rao, S.M. and Revanasiddappa, K. (2006) 'Influence of cyclic wetting drying on collapse behaviour of compacted residual soil', *Geotechnical & Geological Engineering*, 24(3), pp. 725-734.

Ridley, A., McGinnity, B. and Vaughan, P. (2004a) 'Role of pore water pressures in embankment stability', *Proceedings of the ICE-Geotechnical Engineering*, 157(4), pp. 193-198.

Ridley, A.M., Vaughan, P.R., McGinnity, B. and Brady, K. (2004b) *Advances in geotechnical engineering: The Skempton conference: Proceedings of a three day conference on advances in geotechnical engineering, organised by the Institution of Civil Engineers and held at the Royal Geographical Society, London, UK, on 29–31 March 2004*. Thomas Telford Publishing.

Ringrose-Voase, A.J. and Sanidad, W.B. (1996) 'A method for measuring the development of surface cracks in soils: application to crack development after lowland rice', *Geoderma*, 71(3–4), pp. 245-261.

Rivera, L.D. (2008) *Comparing methods of estimating crack volume in shrink-swell soils*. Department of Biological and Agricultural Engineering, Texas A&M.

Rogers, C. and Glendinning, S. (1993) *Engineered fills. proceedings of the conference engineered fills '93'*. Newcastle Upon Tyne.

Roldane, S. (2010) 'Laboratory assessment of cracking in soils. MSc dissertation', MSc thesis, Newcastle University.

- Rouainia, M., Davies, O., O'Brien, T. and Glendinning, S. (2009) 'Numerical modelling of climate effects on slope stability', *Proceedings of the ICE-Engineering Sustainability*, 162(2), pp. 81-89.
- Samouëlian, A., Cousin, I., Richard, G., Tabbagh, A. and Bruand, A. (2003) 'Electrical resistivity imaging for detecting soil cracking at the centimetric scale', *Soil Science Society of America Journal*, 67(5), pp. 1319-1326.
- Samouëlian, A., Cousin, I., Tabbagh, A., Bruand, A. and Richard, G. (2005) 'Electrical resistivity survey in soil science: a review', *Soil and Tillage Research*, 83(2), pp. 173-193.
- Samouëlian, A., Richard, G., Cousin, I., Guerin, R., Bruand, A. and Tabbagh, A. (2004) 'Three-dimensional crack monitoring by electrical resistivity measurement', *European Journal of Soil Science*, 55(4), pp. 751-762.
- Sanchez, M., Atique, A., Kim, S., Romero, E. and Zielinski, M. (2013) 'Exploring desiccation cracks in soils using a 2D profile laser device', *Acta Geotechnica*, 8(6), pp. 583-596.
- Sánchez, M., Manzoli, O.L. and Guimarães, L.J.N. (2014) 'Modeling 3-D desiccation soil crack networks using a mesh fragmentation technique', *Computers and Geotechnics*, 62, pp. 27-39.
- Sasekaran, M. (2011) '*Impact of permeability and surface cracks on soil slopes*', MSc Thesis. University of Manchester
- Sepehrnia, N., Hajabbasi, M.A., Afyuni, M. and Lichner, L. (2017) 'Soil water repellency changes with depth and relationship to physical properties within wettable and repellent soil profiles', *Journal of Hydrology and Hydromechanics*, 65(1), pp. 99-104.
- Sheng, D., Zhang, S. and Yu, Z. (2013) 'Unanswered questions in unsaturated soil mechanics', *Science China Technological Sciences*, 56(5), pp. 1257-1272.

Shin, H. and Santamarina, J.C. (2011) 'Desiccation cracks in saturated fine-grained soils: particle-level phenomena and effective-stress analysis', *Géotechnique*, 61(11), pp. 961-972.

Shorlin, K.A., de Bruyn, J.R., Graham, M. and Morris, S.W. (2000) 'Development and geometry of isotropic and directional shrinkage-crack patterns', *Physical Review E*, 61(6), p. 6950.

Sima, J., Jiang, M. and Zhou, C. (2013) 'Modelling desiccation cracking in thin clay layer using three-dimensional discrete element method', *AIP Conference Proceedings*. AIP 1542, pp. 245-248.

Simoni, A., Berti, M., Generali, M., Elmi, C. and Ghirotti, M. (2004) 'Preliminary result from pore pressure monitoring on an unstable clay slope', *Engineering geology*, 73, pp. 117-127.

Smethurst, J.A., Clarke, D. and Powrie, W. (2006) 'Seasonal changes in pore water pressure in a grass-covered cut slope in London Clay', *Geotechnique*, 56(8), pp. 523-538.

Smith, A., Dixon, N. and Fowmes, G.J. (2017) 'Early detection of first-time slope failures using acoustic emission measurements: large-scale physical modelling', *Géotechnique*, 67(2), pp. 138-152.

Smith, G. N., and Smith, I. G. N., 1989. *Elements of soil mechanics*. Blackwell Science, London.

Song, W. (2014) *Experimental investigation of water evaporation from sand and clay using an environmental chamber*. Doctoral dissertation, Université, Paris Est.

Spencer, E. (1968) 'Effect of tension on the stability of embankments', *ASCE*, 94(SM 5), pp. 1159-1173.

Stewart, R.D., Rupp, D.E., Abou Najm, M.R. and Selker, J.S. (2016) 'A unified model for soil shrinkage, subsidence, and cracking', *Vadose Zone Journal*, 15(3).

- Stirk, G.B. (1954) 'Some aspects of soil shrinkage and the effect of cracking upon water entry into the soil', *Crop and Pasture Science*, 5(2), pp. 279-296.
- Stirling, R.A. (2014) *Multiphase modelling of desiccation cracking in compacted soils*. PhD Thesis thesis. Newcastle University, UK.
- Stirling, R.A., Davie, C.T. and Glendinning, S. (2013) 'Numerical modelling of desiccation crack induced permeability', *18th International Conference on Soil Mechanics and Geotechnical Engineering*.
- Stirling, R.A., Glendinning, S. and Davie, C.T. (2017) 'Modelling the deterioration of the near surface caused by drying induced cracking', *Applied Clay Science*, 146, pp. 176-185.
- Stokes, A., Norris, J., Beek, L.P.H., Bogaard, T., Cammeraat, E., Mickovski, S., Jenner, A., Iorio, A. and Fourcaud, T. (2008) 'How Vegetation Reinforces Soil on Slopes', in Norris, J., Stokes, A., Mickovski, S., Cammeraat, E., Beek, R., Nicoll, B. and Achim, A. (eds.) *Slope Stability and Erosion Control: Ecotechnological Solutions*. Springer Netherlands, pp. 65-118.
- Take, W.A. and Bolton, M.D. (2002) 'An atmospheric chamber for the investigation of the effect of seasonal moisture changes on clay slopes', *Proceeding of International Conference on Physical Modeling in Geotechnics*. Balkema Rotterdam, The Netherlands.
- Take, W.A. and Bolton, M.D. (2011) 'Seasonal ratcheting and softening in clay slopes, leading to first-time failure', *Géotechnique*, 61(9), pp. 757-769.
- Tang, C.-S., Cui, Y.-J., Shi, B., Tang, A.-M. and Liu, C. (2011a) 'Desiccation and cracking behaviour of clay layer from slurry state under wetting–drying cycles', *Geoderma*, 166(1), pp. 111-118.
- Tang, C.-S., Cui, Y.-J., Tang, A.-M. and Shi, B. (2010) 'Experiment evidence on the temperature dependence of desiccation cracking behavior of clayey soils', *Engineering Geology*, 114(3–4), pp. 261-266.

Tang, C.-S., Shi, B., Liu, C., Suo, W.-B. and Gao, L. (2011b) 'Experimental characterization of shrinkage and desiccation cracking in thin clay layer', *Applied Clay Science*, 52(1–2), pp. 69-77.

Tang, C.-S., Wang, D.-Y., Shi, B. and Li, J. (2016) 'Effect of wetting–drying cycles on profile mechanical behavior of soils with different initial conditions', *Catena*, 139, pp. 105-116.

Tang, C., Shi, B., Liu, C., Zhao, L. and Wang, B. (2008) 'Influencing factors of geometrical structure of surface shrinkage cracks in clayey soils', *Engineering Geology*, 101(3–4), pp. 204-217.

Taylor, D. (1948) *Fundamentals of soil mechanics*. Chapman And Hall, Limited.; New York.

Terzaghi, K. (1943) *Theoretical soil mechanics*. Chapman And Hall, Limited John Wiler And Sons, Inc; New York.

Toll, D.G. (2001) *Unsaturated soil concepts and their application in geotechnical practice*. Springer.

Toll, D.G., Mendes, J., Hughes, P.N., Glendinning, S. and Gallipoli, D. (2012) 'Climate change and the role of unsaturated soil mechanics', *Geotechnical Engineering (SEAGS)*, 43(1), pp. 76-82.

Towner, G.D. (1987) 'The mechanics of cracking of drying clay', *Journal of Agricultural Engineering Research*, 36(2), pp. 115-124.

Trabelsi, H., Jamei, M., Zenzri, H. and Olivella, S. (2012) 'Crack patterns in clayey soils: Experiments and modeling', *International Journal for Numerical and Analytical Methods in Geomechanics*, 36(11), pp. 1410-1433.

Uday, K.V. and Singh, D.N. (2013) 'Investigation on cracking characteristics of fine-grained soils under varied environmental conditions', *Drying technology*, 31(11), pp. 1255-1266.

Umana, U. (2016) *Investigation of shrinkage and cracking in clay soils under wetting and drying cycles*. MSc thesis. Newcastle University.

- Utili, S. (2013) 'Investigation by limit analysis on the stability of slopes with cracks', *Geotechnique*, 63(2), p. 140.
- Utili, S., Castellanza, R., Galli, A. and Sentenac, P. (2015) 'Novel approach for health monitoring of earthen embankments', *Journal of geotechnical and geoenvironmental engineering*, 141(3), p. 04014111.
- Van Genuchten, M.T. (1980) 'A closed-form equation for predicting the hydraulic conductivity of unsaturated soils', *Soil science society of America journal*, 44(5), pp. 892-898.
- Varsei, M., Bourasset, C.M. and Miller, G.A. (2014) 'Laboratory Investigation of Desiccation Cracking', In *Geo-Congress 2014*.
- Walker, J. (1986) 'Cracks in a surface look intricately random but actually develop rather systematically', *Scientific American*, 255(4), pp. 204-209.
- Wang, J.J., Zhu, J.G., Chiu, C.F. and Zhang, H. (2007) 'Experimental study on fracture toughness and tensile strength of a clay', *Engineering Geology*, 94(1), pp. 65-75.
- Wang, Z.F., Li, J.H. and Zhang, L.M. (2011) *Proc., 5th Asia-Pacific Conf. on Unsaturated Soils (AP-UNSAT 2011)*.
- Wilks, J.H. (2010) 'Forecasting transportation infrastructure slope failures in a changing climate', *11th Young Geotechnical Engineers Symp., University of Bristol, Bristol, Australia*.
- Wilks, J.H. (2015) *Transport infrastructure slope failures in a changing climate*. Doctoral thesis, Loughborough University.
- Wu, T.H., McKinnell III, W.P. and Swanston, D.N. (1979) 'Strength of tree roots and landslides on Prince of Wales Island, Alaska', *Canadian Geotechnical Journal*, 16(1), pp. 19-33.
- Yesiller, N., Miller, C.J., Inci, G. and Yaldo, K. (2000) 'Desiccation and cracking behavior of three compacted landfill liner soils', *Engineering Geology*, 57(1), pp. 105-121.

Yong, R.N. and Warkentin, B.P. (1975) '*Soil Properties and Soil Behavior*'. Elsevier, Amsterdam.

Yu, H.S., Salgado, R., Sloan, S.W. and Kim, J.M. (1998) 'Limit analysis versus limit equilibrium for slope stability', *Journal of Geotechnical and Geoenvironmental Engineering*, 124(1), pp. 1-11.

Zarzycki, J., Prassas, M. and Phalippou, J. (1982) 'Synthesis of glasses from gels: the problem of monolithic gels', *Journal of materials science*, 17(11), pp. 3371-3379.

Zeh, R.M. and Witt, K.J. (2007) 'The tensile strength of compacted clays as affected by suction and soil structure', *Experimental unsaturated soil mechanics*, pp. 219-226.

Zhan, L.T., Ng, C.W.W. and Fredlund, D.G. (2006) 'Instrumentation of an unsaturated expansive soil slope', *Geotechnical Test Journal*, 30(2), pp. 1-11.

Zhang, Z., Tao, M. and Morvant, M. (2005) 'Cohesive slope surface failure and evaluation', *Journal of geotechnical and geoenvironmental engineering*, 131(7), pp. 898-906.

Zieliński, M. (2009) *Influence of desiccation fissuring on the stability of flood embankments*. PhD thesis, University of Strathclyde.

Zielinski, M., Sánchez, M., Romero, E. and Atique, A. (2014) 'Precise observation of soil surface curling', *Geoderma*, 226, pp. 85-93.

## Appendix

## List of Notations

$Z_0$	- Thickness of an intensive-cracking layer
$S_0$	- Crack spacing
$G_s$	- Strain energy during cracking of material
$\Delta\omega$	- Change in soil moisture
$\alpha$	- Hydraulic constant
$W$	- Maximum crack width at the surface
$\omega$	- Crack width at any discrete depth
$D$	- Maximum crack depth
$d$	- Crack depth at any point in the ground
$\sigma'_{ij}$	- Effective normal stress
$\sigma_{ij}$	- Total normal stress
$\delta_{ij}$	- Kroenecker's delta
$u_w$	- Pore water pressure
$u_a$	- Pore air pressure
$S_s(\varphi)$	- Matrix suction
$\chi =$	- Soil parameter related to degree of saturation
$U$	- Displacement between the clay and the base interface
$U_p$	- Peak value of interface displacement during cracking
$AEV$	- Air entry value
$E$	- Young's modulus
$G_c$	- Material resistant to failure
$\sigma_f$	- Failure stress
$K_{IC}$	- Stress intensity factor
$K_I$	- Driving force for failure
$\sigma_t$	- Tensile stress
$w$	- Soil water content at desiccation time, t
$w_r$	- Residual water content
$w_i$	- Initial water content
$V$	- Volume
$\Delta V$	- Change in volume
$r$	- Dimensionless geometric factor for shrinkage anisotropy
$C_R$	- Apparent cohesion factor of roots in the soil
$C$	- Cohesion

$C'$	- Effective cohesion
$\phi'$	- Effective angle of internal friction
$R_n$	- Net radiation at the crop surface
$G$	- Soil heat flux density
$T$	- Mean daily air temperature at 2m height
$U_2$	- Wind speed at 2m height
$e_s$	- Saturation vapour pressure
$e_a$	- Actual vapour pressure
$\Delta$	- Slope vapour pressure
$\gamma$	- Psychometric constant
$w$	- Saturated water content
$a, n$ and $m$	- Soil parameters related to for deriving soil water –suction
$\xi$	- Percentage lateral shift
$a_d$	- Point of inflexion on drying curve
$a_w$	- Point of inflexion on wetting curve
$\phi_{ad}$	- Suction at the point of inflexion, $a_d$ , on the drying curve
$\phi_{aw}$	- Suction at the point of inflexion, $a_w$ , on the wetting curve
$y$	- Dependent variable of exponential curve
$x$	- Independent variable of exponential curve
$a$	- Initial value of exponential curve
$-r(w)$	- Desiccation coefficient
$Z_t$	- Depth of tension crack
$\phi'$	- Effective angle of internal friction
$C_u$	- Undrained shear strength
$\gamma$	- Unit weight of the soil

## APPENDIX 1

### Newcastle University

#### Fieldwork Risk Assessment (2014 – 2015)

<b>Title of project or activity</b>	Crack Development Mechanisms in Clay Embankments		
<b>Responsible Person / Manager</b>	Oboho Eminue		
<b>School</b>	School of Civil Engineering and Geosciences		
<b>Date of assessment</b>	28/02/2014		
<b>Location of work (Buildings and room numbers)</b>	BIONICS Embankment, Nafferton Farm, Northumberland (~13 Miles West of Newcastle City Centre), UK		
<b>Introduction</b>			
The following risk assessment and guidance has been developed to assess the hazardous activities, risks and identify appropriate prevention and control measures. A simple implementation check is provided to assist schools in demonstrating that the control measures are being implemented. Please identify when they have been implemented.			
<b>Activities with Hazardous Potential and Significant Risks</b>			
These are contained within the shaded area. The first shaded area in the assessment identifies the hazard or hazardous activity and the second identifies the risks imposed by that activity.			
<b>Preventative and Protective Measures to Avoid or Reduce Risks to an Acceptable Level</b>			
These are contained within the un-shaded areas. This section identifies the control measures required and may require schools to choose options or carry out additional risk assessments.			
<b>Help and Support</b>			
<u>Safety Office</u>	Schools must visit the University Safety Office website. The website contains a wide range of guidance to assist schools to manage health and safety effectively including University Safety Policies and Supplements, Safety Guidance, Training, Forms, etc.		
<u>Occupational Health Service</u>			
<b>Hazard 1</b>	Steep and Slippery Slope	<b>Implemented</b>	<b>Date</b>

Risks	Slip, Trip and Fall		
Control Measures	Use safety boot with good grips and safety helmet Exercise adequate care when climbing and sampling slope		
Hazard 2	Weather Conditions	Implemented	Date 2014/15
Risks	Health		
Control Measures	Check daily weather forecast and avoid fieldwork during severe weather Put on adequate weather protection clothing/reflector jackets during fieldwork		
Hazard 3	Allergies, Insect Bites, Animal attack	Implemented	Date 2014/15
Risks	Health		
Control Measures	Wear protective clothing/safety wares Watch and avoid contact with Farm Animals, raise alarm in case of sudden attack Identify with nearby GP to field location		
Hazard 4	Soil sampling/Trenching, Equipment use	Implemented	Date 2014/152015
Risks	Health and weight Accident		
Control Measures	Care will be exercise when digging ground. Get technical assistant Samples shall be carried in light weight quantity Electronic equipment/devices will be checked for radiation/transmission effect and manufacturer's safety rule adhered were such is applicable		
Hazard 5	Working Away from School/Lone working	Implemented	Date 2014/15

Risks	Getting Lost/Lack of Rescue			
Control Measures	<p>The BIONICS mobile phone will always be used to maintain contacts with the school</p> <p>Adhere to the Nafferton Farm visit sign-in/sign-out rules</p> <p>Inform Supervisor/Necessary Officials before and after fieldwork</p> <p>Get field assistant from related colleagues or technical staff</p>			
Hazard 6	Transportation	Implemented	Date	
Risks	Road Accident/Lack of Accessibility to Site			
Control Measures	<p>University pool vehicle will be used driven by a certify staff</p> <p>Road safety regulations shall be observed and strictly adhered to</p> <p>Bus route to the Farm shall be explore in case of unavailability of pool vehicle</p>			
	<b>Emergency Procedures</b>	implemented	Date	
Risks	Accidents			
Control Measures	<p>Call 911 for Police or Ambulance service</p> <p>Always carry First aids kits</p> <p>Contact Supervisor in case of any challenge</p> <p>Avoid working late, during unofficial hours and alone working</p>			
Hazards	<b>Additional Control Measures Required</b> <b>(List and Implement)</b>	implemented	Date	N/A <input type="checkbox"/>
Risks				
Control Measures	<p>Concise fieldwork plan specifying days, nature and duration has been prepared</p> <p>Fieldwork will be restricted to official time (9am to 4pm)</p>			

	Ethical conducts shall be adhere to.	
Assessor		
<b>Name</b>	<b>Signature</b>	<b>Date</b>
Dr Colin Davie	Dr Colin Davie	06/03/2014
Responsible Person / Manager		
<b>Name</b>	<b>Signature</b>	<b>Date</b>
Oboho Eminue	Oboho Eminue	06/03/2014

## Appendix II Summary of Laboratory Results

TEST CONDITION	SOIL TYPE								
	NAFFERTON CLAY							GAULT	VH PI
	<i>High density</i>	<i>Mod. density</i>	<i>Low density</i>	<i>Thin Soil (2-Lift)</i>	<i>Thin Soil (1-Lift)</i>	<i>Multipl e Cycles</i>	<i>Root soil</i>		
Plastic Index (%)	20.1	20.1	20.1	20.1	20.1	20.1	20.1	39	51.3
Soil Layer Thickness (mm)	195	198	200	100	100	195	220	195	195
Density (Mg/m <sup>3</sup> )	1.62	1.51	1.34	1.65	1.63	1.64	1.3	1.62	1.62
Moulding Moisture Cycle (%)	22.8	22.5	22.8	22.8	22.8	22.8	20.1	25	23
Residual moisture 1 <sup>st</sup> Cycle (%)	14.3	14.4	13.5	11.8	9.3	na	na	18.9	17.9
Percentage moisture loss 1 <sup>st</sup> Cycle (%)	38	36	40.6	50.4	60.1	na	na	24.3	21
Time for Crack Initiation 1 <sup>st</sup> Cycle (min)	55	50	45	50	52	na	50	40	33
Cracking initiation moisture 1st Cycle (%)	22.7	22.4	22.8	22.7	22.7	na	na	24.7	22.8
Residual crack moisture 1 <sup>st</sup> C cycle (%)	21.5	21.3	21.8	na	na	na	na	na	na
Crack initiation Suction 1 <sup>st</sup> Cycle (kPa)	393	304	165	na	na	na	na	800	na
Residual crack Suction 1 <sup>st</sup> Cycle (kPa)	580	400	222	na	na	na	na	900	na
Final CIF 1 <sup>st</sup> /2 <sup>nd</sup> Cycle or *6 <sup>th</sup> Cycle (%)	3.1/4.65	3.2/na	4.29/5.3 3	0.84/2.36	0.8/1.24	3.05/11	na	5.9/10.9	10.1/19
Average Crack width 1st/2 <sup>nd</sup> Cycle (mm)	2/2	2.5/3	4/4	2/2	2/2	1/3	2/2	3/5	3/7
Average Crack depth 1 <sup>st</sup> /2 <sup>nd</sup> Cycle (mm)	30/40	30/40	40/50	25/30	30/30	20/40	50/40	50/70	50/70
Maximum crack width 1 <sup>st</sup> /2 <sup>nd</sup> Cycle (mm)	3/3	3/5	5/6	3/3	3/3	2/5	3/3	4/7	5/10
Maximum crack 1 <sup>st</sup> /2 <sup>nd</sup> Cycle (mm)	50/50	50/55	60/60	35/30	30/40	40/60	40/40	70/80	70/100
Settlement 1 <sup>st</sup> /2 <sup>nd</sup> cycle (mm)	8/6	8/7	9/8	6/5	5/5	na	5/5	10/9	10/10
Shrinkage 1 <sup>st</sup> /2 <sup>nd</sup> cycle (mm)	5/5	6/6	8/6	5/5	5/5	na	4/4	8/8	10/8

## Conferences

Eminue, O. O., Davie, T. C. & Stirling, R. A. 2018. Moisture Movement and Mechanisms of Desiccation Crack Development in Engineered Clay Fills. Abstract accepted. To be presented in The 7th International Conference on Unsaturated Soils (UNSAT2018): Climate change and soil-atmospheric interaction.

### ABSTRACT:

Desiccation cracking is a common phenomenon observed in clay soils subject to drying/wetting cycles. The phenomenon has potentially severe implications for infrastructure constructed from clay fills (e.g. railway embankments) as cracks can lead to rapid water infiltration and increased pore pressures at depth that can ultimately destabilise such structures. This issue may become more prevalent for UK infrastructure as climate forecasts predict warmer, drier summers and shorter but more intense periods of rainfall.

However, the precise mechanisms controlling crack evolution under cyclic drying/wetting conditions are not well understood and there are complex interactions of soil, atmosphere and vegetation to be considered.

This study combined field observations with laboratory experiments to develop a better understanding of the factors influencing the development and evolution of fractures.

Field observations consisted of regular walkover surveys carried out on a full scale embankment test site for more than a year during which measurements were taken of crack locations and dimensions. The evolution of individual cracks was tracked over the course of the changing seasons and correlated with their locations on the embankment with regards to height, aspect to the prevailing weather and material density, as well as to extensive records of environmental and soil conditions.

Concurrent laboratory experiments consisted of cyclic drying/wetting tests within a controlled environmental chamber with the time evolution of cracks monitored using digital image analysis. Variation of parameters

showed that material characteristics (plasticity, density, and permeability), geometric factors (thickness of the deposit, slope aspect) and environmental factors (humidity, number of drying/wetting cycles) were all influential.

The findings suggest that there are implications for: geographic location of infrastructure, as related to locally sourced materials; construction techniques, particularly for historic infrastructure constructed to lower densities before modern methods; and climatic changes, as drying/wetting cycles exacerbate crack development, and may lead to more rapid infiltration.

**Eminue, O. O., Colin, D. J. & Stirling, R. A., 2016. Crack Development Mechanisms in Clay Embankments. In: 14th BGA Young Geotechnical Engineers' Symposium. University of Strathclyde, UK.**

O. O. Eminue, C. T. Colin, and R. Stirling  
School of Civil Engineering and Geosciences, Newcastle University, UK

**Abstract**

An extensive study of desiccation cracking involving widespread embankment construction conditions and materials in the UK was undertaken both in the field and using a bespoke soil-climate interaction system. Crack development was closely associated with moisture changes in the near surface embankment soil and the intensity was affected by soil properties, engineered conditions, vegetation presence and repeated wetting and drying.

**Introduction**

The occurrence of desiccation cracks can significantly degrade slope stability and compromise impermeable barriers (Fig. 1a & b). The phenomenon is envisaged as a likely factor in the deformation of clay slopes due to the impact of climate change (Hughes et al, 2009). Despite this significance and much research, the essential mechanism of cracking in the field is not well understood.



Fig. 1: The problem – slope failure like this can be activated by occurrence of cracks

This study seeks to characterise crack development in engineered fill. The results will contribute to understanding of the phenomenon and facilitate efficient earthwork slope management and adaptation against the effects of climate change.

**Materials and Methodology**

Naturally occurring cracks and the influencing factors are studied on a research embankment with engineered conditions representing historic railway and modern highway embankment (Fig. 2).



Fig. 2: The study site: instrumented embankment with distinctive well compacted and poorly compacted panels (b)

Common soils and construction conditions involved in embankment creation across the UK are used to simulate wet-dry laboratory desiccation experiments in a bespoke climate-soil interaction system (Fig. 3).

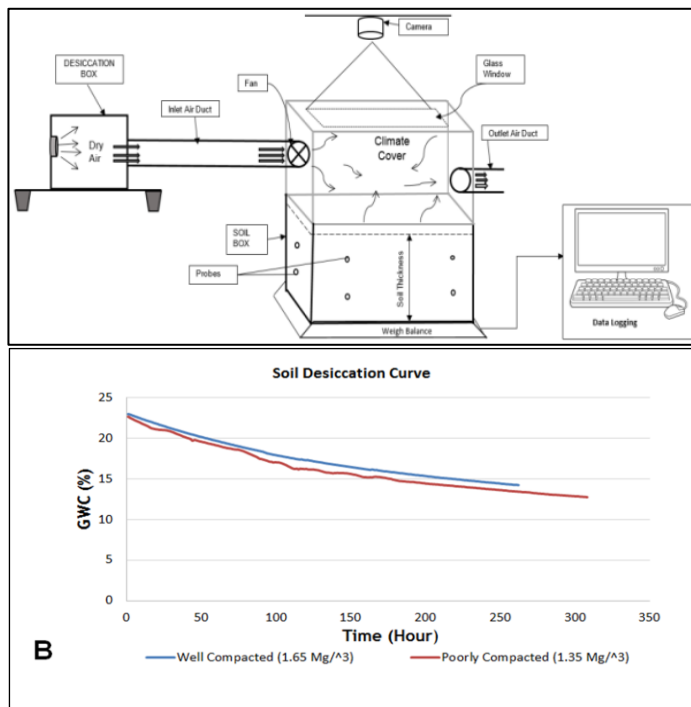


Fig. 3: Schematic of laboratory experiment set-up and (b) typical desiccation curve

## Results and Discussion

Moisture varied in the near surface embankment layer (1 – 2m) with greatest fluctuation observed in the poorly compacted embankment fill (Fig. 3b & 4a) apparently due to resultant loosely packed soil structure which mobilise greater tension. Computed crack development time series reasonably trend with near surface suction profile (Figure 4b) indicating a functional hydro-mechanical process underlying crack development (Kodikara et al 2000, Peron et al, 2009).

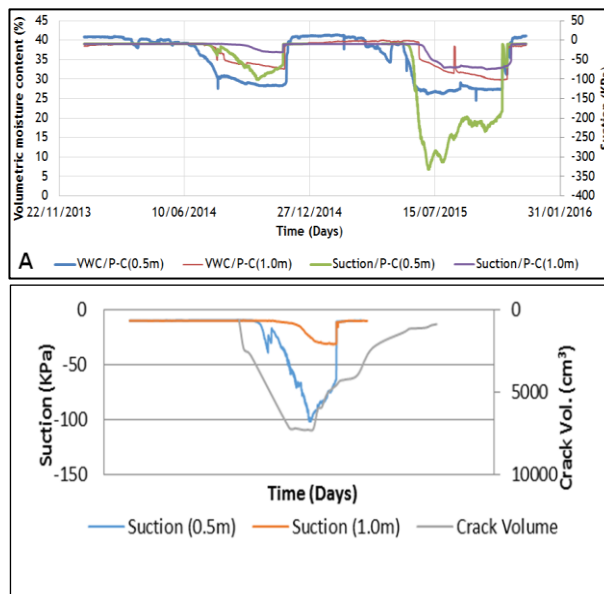


Fig. 4: (a) Moisture changes in poorly compacted BIONICS embankment panel, (b) Crack development and measured suction

Consequently, there were more cracks in the loosely compacted fill and on the south facing slope impact more by the dominant south westerly wind (Fig. 5a). The higher plasticity of Gault clay compared to the intermediate plasticity of the embankment fill, together with cyclic wetting and drying, intensifies cracking while vegetation presence was observed to significantly influenced crack pattern (Figure 4b).

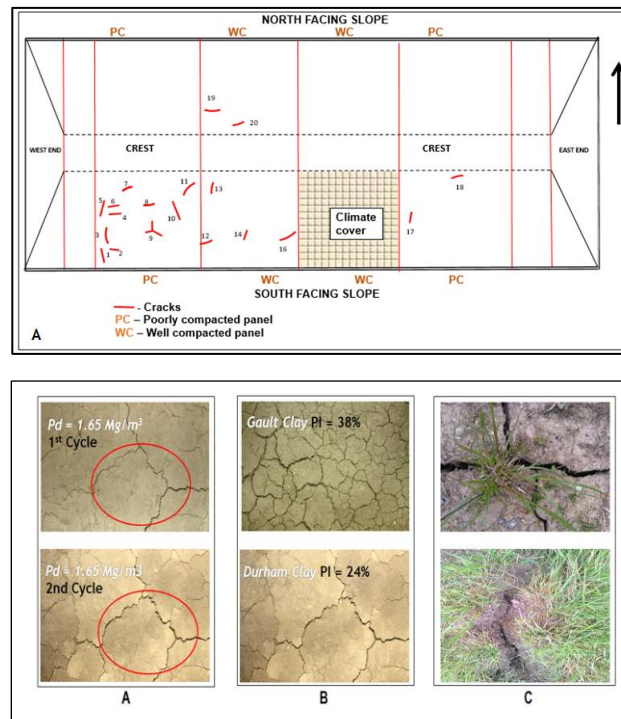


Fig. 5: (a) Crack distribution on BIONICS embankment, (b) Crack Intensity in laboratory simulated embankment conditions

### Preliminary Conclusion

Preliminary result suggest cracking in soil is related to hydro-mechanical process largely due to evapotranspiration moisture loss. Vegetation cover, construction conditions, and soil properties affected cracking with greater susceptibility exhibited on the fill conditions representing historic embankments. Further studies include quantification of cracking suction and time lapse images of crack morphology for more detail conclusions.

### References

- Péron, H., Hueckel, T., Laloui, L. & Hu, L. 2009a. Fundamentals of desiccation cracking of fine-grained soils: experimental characterisation and mechanisms identification. *Can. Geotech. Journal*, 46, 1177-1201.
- Hughes, P. N., Glendinning, S., Mendes, J., Parkin, G., Toll, D. G., Gallipoli, D. & Miller, P. E. 2009. Full-scale testing to assess climate effects on embankments. *Proceedings of the ICE-Engineering Sustainability*, 162, 67-79.
- Kodikara, J. K., Barbour, S. L. & Fredlund, D. G. 2000. Desiccation cracking of soil layers. *Unsaturated Soils for Asia*, 90, 139.

